



Università
Ca' Foscari
Venezia

**Scuola Dottorale di Ateneo
Graduate School**

**Dottorato di ricerca
in Scienze Chimiche
Ciclo XXIX
Anno di discussione 2016**

***Archaeometric Studies of Historical Ceramic
Materials***

SETTORE SCIENTIFICO DISCIPLINARE DI AFFERENZA: CHIM/12

Tesi di Dottorato di Giulia Ricci, matricola 956083

Coordinatore del Dottorato

Prof. Maurizio Selva

Supervisore del Dottorando

Prof. Elisabetta Zendri

Contents

	Page
AIM OF THE THESIS	1
1. The Archaeometric Research	2
Summary	2
1.1. Definitions and History	2
1.2. Review on Archaeometric Research Applied on Pottery	5
1.3. Diagnostic Tools in Archaeometric Studies on Potteries	9
1.4. Bibliography	17
2. Ceramic Materials	21
Summary	21
2.1. Pottery in Archaeology	21
2.2. Raw Materials	24
2.2.1. Clay minerals	24
2.2.2. Non-clay materials	26
2.3. Production Technologies	29
2.3.1. Forming, shaping and drying	30
2.3.2. Decoration	31
2.3.2.1. Glazes and enamels	31
2.3.3. Kilns and Firing procedures	35
2.4. Chemical and Physical Reactions during Ceramic Firing Processes	38
2.5. Bibliography	42
3. Materials and Methods	45
Summary	45
3.1. Investigation Strategy	45

3.2. Investigation Techniques	48
3.2.1. Fourier-Transform-Infra Red Spectroscopy (FT-IR)	48
3.2.2. Micro-Raman Spectroscopy (μ -Raman)	48
3.2.3. Laser Induced Spectroscopy (LIF)	49
3.2.4. UV-Vis Spectrophotometry	50
3.2.5. X-ray Fluorescence analyses (XRF)	51
3.2.6. Laser Induced Breakdown Spectroscopy (LIBS)	51
3.2.7. X-ray Diffractometry (XRD)	52
3.2.8. Optical Microscopy (OM)	53
3.2.9. Petrographic analysis and Image acquisition	53
3.2.10. Scanning Electron Microscopy coupled with Energy Dispersive X-ray Probe (SEM-EDX)	53
3.2.11. Mercury Intrusion Porosimetry (MIP)	54
3.2.12. Micro Computed X-ray Tomography (μ -CT)	54
3.3. The Ceramic Samples	56
3.3.1. Raw ceramic specimens made in laboratory	56
3.3.2. Ceramic from the Venetian Lagoon	57
3.3.2.1. Archaeological Excavation in Torcello	59
3.3.2.2. Archaeological sherds	60
3.3.3. German potteries	64
3.3.3.1. Central-Eastern German ceramic production sites	65
3.3.3.2. Central-Eastern German sherds	68
1.1. Bibliography	74
4. Results and Discussion	78
Summary	78
4.1. Analyses and Characterization of Raw ceramic specimens made in Laboratory	78
4.1.1. Raw Material Characterization	78
4.1.2. Chemical, Mineralogical and Microstructural Changes of the Raw Ceramic samples after Firing	83

4.1.3.	Brief Conclusions on the Chemical, Mineralogical and Microstructural Changes of the Raw Ceramic samples after Firing	102
4.2.	Characterization of Ceramics from Torcello	103
4.2.1.	Chemical and Mineralogical Characterization. Results and Discussion	103
4.2.2.	Petrographic and Mineralogical Results and Discussion	113
4.2.3.	SEM-EDX Analyses. Results and Discussion	115
4.2.4.	Microstructural and Porosimetry Results and Discussion	122
4.2.5.	Brief Conclusions on the Archaeometric study on Archaeological Potteries from the Venetian Lagoon	127
4.3.	Characterization of German Ceramic Sherds	128
4.3.1.	FT-IR Analyses. Results and Discussion	128
4.3.2.	μ -Raman Analyses. Results and Discussion	137
4.3.3.	LIF Analyses. Results and Discussion	142
4.3.4.	UV-Vis Spectrophotometry Analyses. Results and Discussion	145
4.3.5.	XRF and LIBS Analyses. Results and Discussion	148
4.3.6.	Petrographic and Morphological Results and Discussion	158
4.3.7.	Porosimetry Analyses (MIP). Results and Discussion	176
4.3.8.	Brief Conclusions on Archaeometric study on German ceramic sherds	180
4.4.	Bibliography	182
5.	Conclusions & Future Perspectives	190
5.1.	Bibliography	196
6.	GLOSSARY	199
7.	ABSTRACT	201
	Acknowledgements	203

AIM OF THE THESIS

Ceramics are complex objects, rich source of information and constitute a large part of the staple memory of past and present human activities. Therefore, the study of this material is essential in order to thoroughly understand the materiality of historical events and their echo in the present.

Archaeometric research on potteries are focused on studying their production techniques, provenance, age, usage and conservation state. The archaeological interests regard many issues as the cultural identity of the potters, the functional aspects of the ceramics, the organisation and technology of the pottery workshops, the availability of the raw materials, the reconstruction of the far-reaching trade relationships, etc. In order to contribute in these issues, scientific material analyses, able to provide the characterisation of the chemical and morphological features of the artefacts which are connected to production aspects, are forcefully involved in this research field.

In line with the strongly archaeological interest, the aim of this research was to evaluate the incidence of the production techniques on the final features of the ceramic artefact, considering all the phases of the ceramic life cycle including selection and use of raw materials, manufacturing processes and firing conditions.

The present research was carried out by means of traditional and innovative techniques exploring their applicability in this research field encouraging the use of non-destructive techniques. The proposed innovative techniques have been only recently used in cultural heritage material investigation and their application in archaeometric research on potteries was assessed in this research work.

Furthermore, this research would highlight the relevance of complementary information obtainable by a multi-analytical approach in order to deeply understand the complexity of the ceramic objects and provide insights on production technology which has an essential role in ceramic manufacturing.

1. The Archaeometric Research

Summary

This chapter would underline how the study and awareness of cultural heritage, such as its material composition, the production technology as well as its conservation state, are fundamental for its preservation and why enable in understanding of historical events, ancient culture and usage. The art object becomes a storyteller, which is able to describe environmental, anthropological and cultural contexts. The chapter starts defining archaeometry and the archaeometric research, and their history is briefly discussed. Afterwards, it provides an overview on archaeometric research and tools used in archaeometric studies of pottery. It has to be notice that archaeological and art-historical methods provide primary information of the material heritage and scientific analyses are nowadays strongly requested. Furthermore, it is shown that cooperation between different specialists is therefore extremely important.

1.1. Definitions and History

Archaeometry is an interdisciplinary research area where complementary approaches cooperate to investigate cultural heritage materials. It can be considered a bridge between humanities, such as archaeology and art history, and natural sciences, as chemistry, physics, biology and geology.

Archaeometric research includes a wide range of studies and can be defined as the application of scientific techniques for the knowledge and characterization of artefacts and their involvement with humans and environment [1]. The age, use, production technique, provenance and environmental data are some of the achievable information as result of this investigation. Moreover, also conservation science partially overlaps with archaeometry, because the study of the conservation state provides insights on how to preserve and restore the material.

The application of natural science methods, in particular chemistry, to characterize cultural heritage objects has its origins since 18th century when the German scientist Martin Heinrich Klaproth in 1796 determined the chemical composition of some Greek and Roman metal coins. Later, other chemists were involved in scientific studies of ancient objects, and in 1842 the German chemist Dr. F.R. Göbel published all his results obtained by chemical analyses of archaeological findings. He was the first to assert that the chemical analyses should be an aid

to archaeology, by starting the cooperation between scientists and archaeologists. In fact, for the first time in 1853 chemical analysis was inserted as appendix within an archaeological report, made by the British archaeologist Austen Henry Layard [2], [3]. In the same period, Dr. Ernst Freiherr von Bibra¹, German naturalist, chemically analysed metal objects and published in 1869 the work entitled “Die Bronzen und Kupferlegierungen der alten und ältesten Völker mit Rücksichtnahme auf jene der Neuzeit” (“The Bronze and Copper Alloys of the Old and Most Ancient Peoples”) regarding more than 1000 quantitative analysis on metals as result of 82 researchers’ work [4]. Not only metals were investigated from a chemical point of view, but also ceramic materials, even earlier than mineralogical investigations. In 1829, Alphonse Buisson, personal assistant to Alexandre Brongniart, director of the Sevres factory, analysed Italian potteries measuring out silicon, aluminium, iron, calcium, magnesium and water. His work in publishing was continued by Louis-Alphonse Salvétat, chief chemist at the National Laboratory of Porcelain Manufacture in Sevres [5]–[7].

Physical methods were applied in 1896 once Wilhelm Conrad Röntgen, German engineer and physicist, discovered and applied X-rays on paintings to study pigments, such as lead pigments. Fundamental discoveries were made by Nobel Prizes in the same period: Antoine Henri Becquerel, French physicist, along with Marie Skłodowska-Curie and Pierre Curie, discovered the radioactivity; Ernest Rutherford, New Zealand physicist, demonstrated the nuclear nature of atoms; James Chadwick, English physicist, discovered the neutron. As a consequence of these important discoveries, the development of several analytical techniques based on atomic and nuclear properties was carried out and the technique of Neutron Activation Analysis (NAA) invented, by George Hevesy in 1936. This technique has an important role in the cultural heritage characterization and in 1956 Robert Oppenheimer and a group of archaeologists and chemists at the Princeton Institute of Advanced Studies (New Jersey, US) discussed the possibility of applying the method to archaeological studies [8].

Great contribution to archaeological science was given from Andrew Ellicott Douglass, American astronomer at University of Arizona (US), who discovered the relation between tree-rings and sunspot cycle and made pioneering experiments through dendrochronology² for dating analysis of archaeological findings with the support of Clark Wissler, the curator of the American Museum of Natural History between 1914 and 1916 [9]. In the ‘30s Richard Pittioni, professor of Prehistory at University of Vienna, and his group applied trace element analysis on copper and bronze objects for their characterization and provenance studies. In his work, published in 1937 [10], the authors asserted to determine “from which production area a

¹ Dr. Ernst Freiherr von Bibra published also “Concerning Old Discoveries of Iron and Silver” in 1873 (“Über alte Eisen- und Silberfunde”).

² Dendrochronology is the scientific method of dating based on the analysis of patterns of tree rings.

specific object would derive” [4]. In the ‘50s, several works in these areas have grown up and were published many papers about conservation and technology of artefacts, as well as archaeometallurgy [11].

The term “archaeometry” has its roots since 1958, when Christopher Hawkes, professor of European Archaeology at Oxford University, together with Frederick Alexander Lindemann, professor of Physics at Oxford as well as Lord Cherwell and personal adviser of Winston Churchill, coined this word as a consequence of the concept (back to 1950) to have a laboratory dedicated for applying scientific techniques, in particular physics, to archaeology and art-history [12]. Thanks to them, in 1955, Oxford University established the Research Laboratory of Archaeology and History of Art, at Oxford 6 Keble Road. Edward Thomas Hall, British scientist and PhD in Physics at Clarendon Laboratory of Oxford University, known as professor “Teddy” Hall, was the first director of the new research laboratory and he was the director for 35 years until his retirement in 1989, playing a significant role in developing archeometry [13]. He had been using X-Ray Fluorescence (XRF) throughout his studies and helped to uncover many frauds such as the best known Piltdown Man. The so-called Piltdown Man, was discovered in 1912 in Southern England and it was defined as the “missing link” in evolution. The archaeological discoveries raised doubts due to the fact that the skull of the Piltdown man seemed to be human but its jaw was more similar to that of the ape. In 1953, Professor Hall added evidences supporting that it was a forgery: using XRF technique he detected the presence of chromium in cranial fragments and he proved that the bones had been stained to make them look fossilized. Furthermore, he discovered iron filings indicating teeth of an orangutan's jawbone smoothed to make them appear more human. "Indeed, these analyses were probably the very first practical use of XRF for either academic or commercial purposes", Edward Hall [14]–[16].

The Bulletin of the Research Laboratory of Archaeology and History of Art, published by Oxford University for about 40 years, became the international journal “Archaeometry”³, which covers several topics related to science applied in cultural heritage such as dating methods, artefact studies, statistical methods, conservation science and the study of man and his environment. Furthermore, in the Research Laboratory there were annual reunions where the users discussed on different aspects of archaeometry. These reunions, now biennial, became the International Symposium on Archaeometry (ISA), the 41st of which was held this year in May (2016) in Kalamata, Greece [17][17], [18].

³ Since 2001, the journal has been published on behalf of Oxford University, in association with the Gesellschaft für Naturwissenschaftliche Archäologie Archäometrie and Society for Archaeological Sciences by Wiley-Blackwell [90].

Going on with the history of the archaeometric research throughout the 20th century, the '60s began with a Nobel Prize in Chemistry received by William Frank Libby, American physical chemist, who applied ¹⁴C dating method on archaeological findings (1960) [19], [20]. Important contributions were given in this period also by different works such as “The science in Archaeology” and “Scientists and Archaeologies”, where methodological and interdisciplinary aspects were discussed, and definition of new approaches from different fields such Archaeological Chemistry and Studies in Ancient Technologies were provided. In Italy, in 1967, the archaeologist Tiziano Mannoni and his team made a step on applying mineralogical analyses to archaeology. For this purpose, Mannoni founded the Laboratory of Mineralogy applied on Archaeology⁴ in Genova [21]. Beside few cases, archaeometry in Italy did not have as much success as in UK, in which the term “archaeological science”, instead archaeometry, became more diffuse. In fact, in the '70s, at University of Bradford was introduced Archaeological Sciences as Bachelor Degree and Scientific Methods in Archaeology as a Master. Moreover, in 1976, was established in UK a Science-based Archaeological committee which was able to support and fund research on: dating, innovative technologies applied in provenance and conservation studies, organic residues for ancient diet and DNA studies, geoarchaeology, archaeobotany and zooarchaeology.

Nowadays, archaeometry is more widespread and entire courses of studies are dedicated to archaeologists and scientists [11], [17]. The main topics in which archaeometry is involved are: dating ancient materials by thermoluminescence, ¹⁴C and dendrochronology; provenance investigations, analysing trace elements, isotopes and chemical composition; authenticity of the art-object; production techniques of the artefact through microstructure analysis; human-environment interactions; bioarchaeology; remote sensing and geophysical prospection; etc. [22]. Furthermore, new laboratories are established and they aim to answering to the archaeological questions laying the of what can now be called “conservation science”.

1.2. Review on Archaeometric Research Applied on Pottery

A. Buisson and L. A. Salvétat, in 1829, as I briefly mentioned in the previous paragraph, chemically analysed Italian ceramics [5]–[7] and later, due to industrial interests, other scientists, such as Henry Le Chatelier, French chemist, and A. Levi were involved in ceramic studies. The first scientist studied the thermal expansion of glasses and the production of Greek ceramics (1907), and the second one can be considered the first person who analysed

⁴T. Mannoni founded in Genova also the Laboratory of Architectural Archaeology, in which historical topics were connected with conservation and restoration ones.

ceramics, in particular Greek potteries found in Puglia region, determining the provenance through chemical analysis (1931) [7], [23].

In the '70s and '80s two powerful methods were used for ancient ceramic characterization: XRF and NAA. Both the methods give information about chemical composition, and were both used for provenance studies of potteries exploiting the concept that the chemical composition can be characteristic of a particular site because of the different chemical depositions of some elements such as phosphorous, strontium and barium. In that context, scientific analysis on potteries increased and widened, taking in to consideration the complementarity of other disciplines: mineralogy and petrography, able to determine compounds and minerals present [24], [25].

Potteries are found in large quantity in archaeological excavations and their study has been central to the archaeological and anthropological interpretation of a site. Archaeometric research contributes to the reconstruction of their life cycle considering production technique, distribution and usage. The investigation of pottery considers two clear attributes: its fabric and form. The former one, indicates the raw materials (clays and inclusions) used, forming and firing temperature conditions; and the latter regards the shape in general considering for instance rims and decorations. Studying these features it is possible to go back to the provenance (where?), technological production (how?), usage (why?), age (when?) and conservation state (how to preserve and restore the artefact?). These question marks in brackets represent the fundamental questions directed to archaeometry [11], [26], [27].

Provenance study was the first issue discussed in archaeometric research applied on ceramic materials. The determination of provenance means: locate a production site useful to understand how the land and sources were used; acquire information for technology research and reconstruct the ways of marketing of raw materials and artefacts, therefore the trade between ancient populations; provide information for authenticity studies. Furthermore, provenance issue can have more connotations, and different levels of provenance classification should be considered, as it shown clearly in **Fig.1**. M. Daszkiewicz in her paper makes a very detailed description about provenance studies and meanings, underlining the fact that it can be referred to raw materials used and/or to workshop/production site [23].

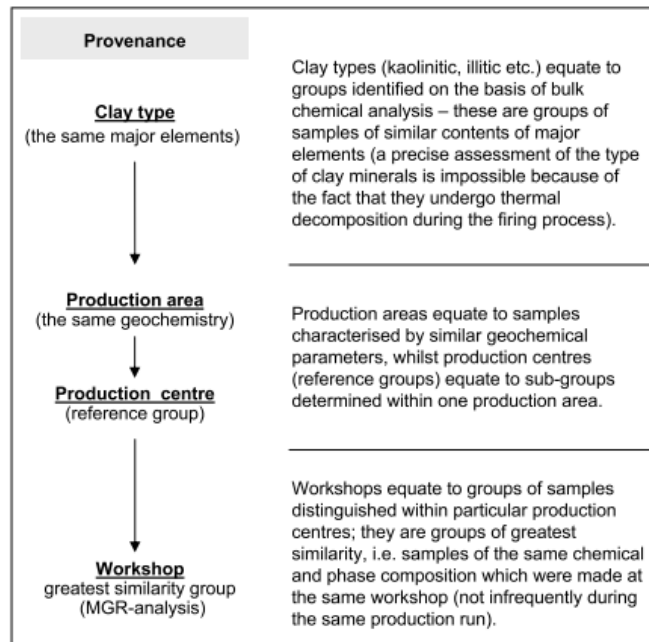


Figure.1. Levels of provenance classifications based on scientific analyses⁵.

The first scientific approach for provenance studies of ceramics was carried on through chemical composition analysis, in particular minor and trace elements detected by NAA [28]. Methods for elemental analysis, such as Optical Emission Spectroscopy (OES), Inductively Coupled Plasma Mass Spectrometry (ICP-MS), Energy-Dispersive X-ray spectroscopy (EDS, EDX) and XRF are widely applied to determine major and minor elements in the ceramic matrix and are used till the present days [29]–[33]. Elemental composition provides a chemical “fingerprint” for pottery, where numerous samples must be analysed to form pottery groups according to similarities in chemical data. These results can be linked to the clay sources, therefore allow to establish the production area or site and make consideration if the materials were locally produced or imported. However, it has to be considered the eventual prior treatment of the raw materials and the potential changes in composition during burial [34], [35]. Another methodology to determine ceramic provenance is to compare the ceramic samples with those coming from a certain production site, taking them as a reference group [36]–[39]. This comparison is done by studying both the fabric and form of the artefact.

The composition in terms of minerals and compounds present in the ceramic matrix, allows also to determine features as firing conditions and raw materials used, able to characterize a particular workshop, in terms of time-period and origin, and investigate the production technique. The knowledge of manufacturing process helps in reconstructing the history of the technology of the ancient potters evaluating their production capability and craft

⁵ Image Source: M. Daszkiewicz, (2014) “Ancient Pottery in the Laboratory-Principles of Archaeoceramological Investigations of Provenance and Technology.” *Novensia* 25; 177–198.

specialization as well as cultural exchanges [11], [27]. Ethnoarchaeology⁶, a branch of archaeology and connected to anthropology, studies people and cultures interpreting archaeological findings. In particular, it can refer to the study of the way an object was made and all the anthropological implication giving a valuable insight into the understanding of ancient and present cultures [40]–[43]. Technological studies most of the time involves the determination of firing conditions rather than forming methods, surface treatments and decorations [23], [27]. Investigation of firing conditions includes the estimation of original firing temperature and firing atmosphere. These features are related to both mineralogy and microstructure of the pottery [44]–[47]. During firing in the kiln, minerals and other compounds present in the ceramic bulk are subjected to reactions and transformations, and because of which, final properties of the ceramic products are determined. The detection of a particular mineral phase, through both mineralogical and chemical methods, allows to estimate the original firing temperature and atmosphere. The key factor to consider is that thermal transformation in clay composition is irreversible and changes in the mineral composition can be observed only firing the samples above the temperature applied by the potter. Archaeometric research were carried out in this topic and many papers have been published. New mineral phases, for instance gehlenite, wollastonite, diopside, etc., and/or carbonate minerals (calcite, dolomite, etc.), are considered as firing temperature indicators and have been extensively studied [48]–[50]. Furthermore, the detection of the iron oxides hematite and magnetite, allows to identify the firing atmosphere: oxidising or reducing atmosphere respectively [51]–[53]. Mineralogy of the pottery is usually studied by X-ray Diffraction (XRD), thin section petrography, Thermogravimetric analysis (TGA/DSC), Fourier-Transform Infrared Spectroscopy (FT-IR), Raman Spectroscopy, as well as Scanning Electron Microscope with Energy-Dispersive X-ray (SEM-EDS) [45], [48], [49], [54]–[64]. The effects of firing conditions are also observed on the morphology and microstructure of the final product. These features are investigated by means of SEM, petrographic microscopy and porosity analyses [54], [65]–[68].

Moreover, characterization of pottery paste and glaze (if present) allows to determine the age, authenticity and the use of the artefact in an indirect way. Compounds and pigments eventually present can be distinctive of a particular production period, as cobalt blue which was synthesized by Louis-Jacques Thenard in 1802; or for a particular usage, where, for examples, the presence of calcareous rich clay indicates that the ceramic is not resistant to thermal shock and therefore not suitable for fire pottery [69], [70]. The exact use of a ceramic

⁶ Ethnoarchaeology is defined as “the use of ethnographic methods and information to aid in the interpretation and explanation of archaeological data” [43].

artefact is often considered as a complex issue. Stylistic and composition features may play a role in providing clues in usage but an interdisciplinary approach is strongly needed. Recently, investigation of organic residues preserved on the sherd surface or trapped into the porous wall plays a relevant role in understanding usage, ancient diet and trade. Mostly lipids and proteins of plants and animals preserved in unglazed pottery are analysed by means of Gas Chromatography (GC) and GC/Mass Spectrometry (GCMS), isotope analysis and pyrolysis. Chemists, biochemists, specialists in food science, archaeologists and anthropologists collaborate to analyse the often small amount of the organic remains and provide, moreover, reliable information about paleodiet, nutrition and dietary changes throughout the lifetime [71]–[76].

Regarding dating methods of ceramic materials, the first one used, with its own sources of errors, was based on stylistic features and the pottery became an indicator of date in the excavation site. In 1949 Libby introduced radiocarbon methods (^{14}C), but it can be used in ceramic only if there are present organic residues on or within the sherd. The first absolute dating method applied to pottery was the thermoluminescence technique (TL), developed by physicists in the '60s. The principle is to measure the accumulated dose of radiation since the object was fired; it offers the advantages to have the age in calendar years but it has limitations due to its application practicability and in terms of precision of pottery related to Neolithic period. Another physical based method is the archaeomagnetic (AM) dating, which studies the magnetic properties of iron oxides content in the clay [71], [72], [77], [78].

A final issue is related to the conservation and restoration of the ceramic materials. An old object is marked by time, usage and burial condition. Integration of both archaeological indications about conditions of the findings in the excavation site and studies on degradation phenomena and compatibility of restoration products provides a useful conservation approach aiming at preservation and fruition of the archaeological objects. The restoration procedures must be preceded by the study of material properties and characterization.

1.3. Diagnostic Tools in Archaeometric Studies of Potteries

The ceramic findings come to the lab after a selection made by the archaeologist. The best approach may be the selection of samples by means of the cooperation between archaeologists and scientists keeping in mind: archaeological considerations on technical features of the artefacts, definition of archaeological questions, and problems facing the conservation scientist in terms of selection of the methods in light of the particular issue to be addressed. Particular requirements of analytical techniques have to be considered, because the

set of problems in analysing archaeological materials is quite different in comparison with those present in a conventional analytical laboratory. The principal issues are related to the type of the object and to the type of the method which has to be chosen, therefore respecting the CH material and extracting information able to answer to the archaeological questions. Thus, selecting samples represents the first step in the archaeometric study, and it is fundamental to achieve the objectives in the research, being focused towards obtaining specific information [70], [79].

Archaeometric research on pottery, as well as on all cultural heritage materials, exploits analytical techniques generally used in other research fields for the study of organic and inorganic materials. Once the selected objects are in the lab, in form of inter vase and/or sherd for instance, attention must be given to the sampling strategy: it can influence the scale of interpretation, can limit or expand the methods and techniques that can be applied in the study of ceramics and the representativeness of the collected samples must be discussed and considered. The analytical techniques are able to provide independent information without being influenced by archaeological context, shape and stylistic aspects used in defining pottery in archaeology. The analytical methods, used in chemistry, physics and natural sciences, can be destructive or non-destructive⁷. On the basis of the sampling availability and the aim of the research, the conservation scientist chooses the approach and techniques to apply in the archaeometric study. Because most of archaeometric analyses are destructive, sometimes a compromise between museum curators and scientific researchers should be agreed. For these reasons, in recent years, non-destructive methods have been developed and applied in archaeometry, and also in this PhD research particular attention has been given to the validation of innovative and non-destructive techniques to the study of the ceramic materials.

Analytical techniques applied in archaeometric studies of ceramic materials can be divided on the basis of: the sampling strategy (non-destructive and destructive techniques); solicitation source used to investigate the sample (photons, electrons, protons, etc.); and the information achievable able to address the archaeological issues (provenance, dating, technology and conservation state). Other factors to consider are the kind of information that can be obtained (chemical, physical, mineralogical, structural features), the economic cost of the analyses requested, the availability of the instruments, the amount of the sample needed, and the time employed to carry on the investigation in terms of duration of the analyses and researchers' work (connected also to the economic cost) [11], [70].

⁷ From a scientific point of view, a method defined as destructive means that the collected sample will be attacked by chemical products and/or treated in a way that the sample cannot be recovered and reused for other analyses. While using a non-destructive method, even if the sample will be manipulated, it can be reused for other analyses because the chemical composition and/or the structure has not changed.

In the **Fig.2** is shown a scheme which has been made taking into account the considerations mentioned above regarding the choice of the methodological approach and there are summarize the most used analytical techniques in pottery investigation. Moreover, in **Tab.1** the analytical techniques are briefly discussed more in detail, and the amount of the required sample for each analysis is specified.

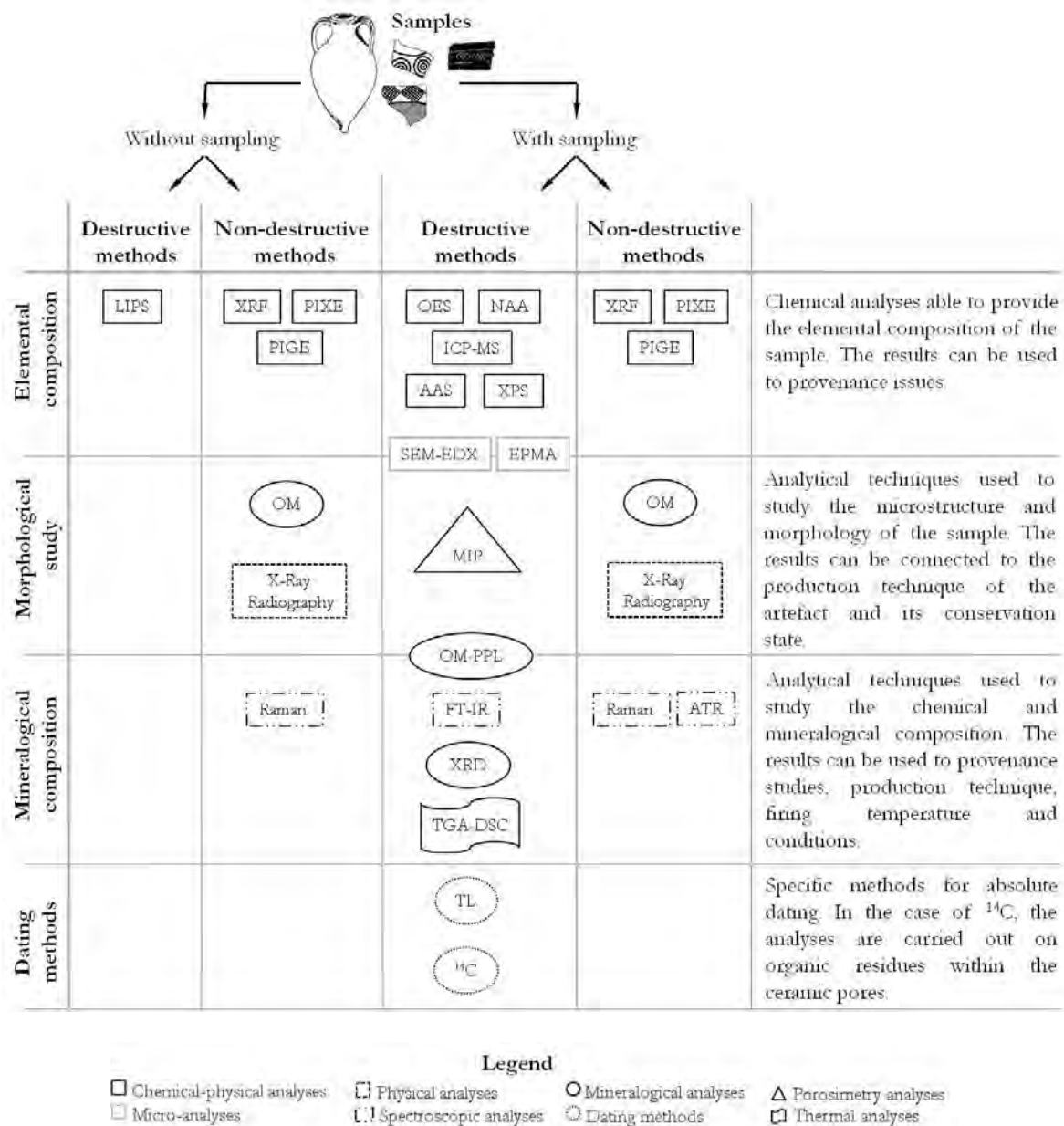


Figure.2. Scheme of the most used analytical techniques for pottery studies.

Table.1. The analytical techniques most commonly used in ceramic studies [1], [70], [80], [81].

	Acronym	Name	Principle	Sample requested
Physicochemical Analyses - Elemental Analyses	XRF	X-ray Fluorescence	Elemental qualitative and quantitative analysis which uses high energy X-ray beam to excite the sample and measures the wavelength and energy of the characteristic radiations emitted from the atoms when they are coming back to the fundamental state. It is used for chemical analysis for the surface of ceramic glaze and body; it has medium cost and offers the advantage to be portable for in situ measurements.	Sampling not required
	PIXE	Proton Induced X-ray Emission Spectroscopy	Elemental analyses where the sample is bombarded and excited by charged and accelerated particles (α -particles for PXE and protons for PIGE) and for determining the chemical composition, emitted energy throughout the energetic decay in form of X-ray for PIXE and γ -ray for PIGE is studied and it is characteristic for each atom. These methods are considered as complementary: PIXE is more sensitive for detection of element with high atomic number ($>Al$) and PIGE for light elements. Complex tools and very high cost.	Sampling not required
	PIGE	Proton Induced γ -ray Emission Spectroscopy		
	NAA	Neutron Activation Analysis	The analysis needs a nuclear reactor and it is based on neutron activation to make the sample radioactive forming radioactive isotopes. To determine the element concentrations, spectra of their well-known radioactive emissions and decay are studied. Complex and expensive equipment with security issues linked to its use.	10-30 mg in powder
	AAS	Atomic Absorption Spectroscopy	Quantitative and qualitative analytical technique capable to determine chemical elements using the absorption of optical radiation by atoms in the gaseous state, after sample nebulisation. The complex instrument implicates high cost.	Few mg – 1 g

Physicochemical Analyses - Elemental Analyses	XPS	X-ray Photoelectron Spectroscopy	Elemental analysis (qualitative and semi-quantitative) able to investigate the surface and depth-profiling (till few μm). It is capable to investigate the chemical composition and the chemical and electronic state. The sample is bombarded by high energetic X-ray beam and the method measures the kinetic energy of emitted photoelectrons allowing the identification of the energy binding and, thus, the chemical element. Relative simplicity in use and in interpreting data.	Few mg
	OES	Optical Emission Spectroscopy	Method for trace metal analysis using spark excitation to determine the chemical composition of the sample. It involves electrical energy whereby the vaporized atoms are brought to a high energy state in the discharge plasma, creating an unique emission spectrum specific to each element. The cost is medium.	200-500 mg in solution
	ICP-MS	Inductively Coupled Plasma – Mass Spectroscopy	Mass spectrometry able to detect elements in very low concentration (ppq). The sample is ionized by inductively coupled plasma (6000-10000°C) and to separate and quantify these ions is used a mass spectrometer. It is a specific technique and the cost is very high.	>100 mg in acid solution
	LIPS (LAS)	Laser Induced Plasma Spectroscopy (Laser Ablation Spectroscopy)	The highly energetic laser beam is focused on the sample surface and small quantity of mass is removed from the irradiated zone, forming a plasma which is analysed to determine the concentration of the elements present. This method is able to perform rapid chemical analysis of all the elements.	Sampling not required. Produces craters of 2r ~ 10-300 μm , depth of few μm
Mineralogical-Petrographic Analyses	OM	Optical Microscope using light reflected (Stereo microscope)	Surface analysis, provides information of the ceramic body, glaze and/or decoration layer if present. The cost is limited.	Sampling not required
	OM-PPL	Optical Petrographic Microscope – Plane Polarized Light	Thin section of the sample is needed. The analysis is able to examine the microstructure, glaze and/or decoration layer. The polarized light across the thin section allows to determine the mineralogical composition due to the optical properties of the minerals.	2-4 cm^2 for thin section preparation

	XRD	X-ray Diffraction	Qualitative and semi-quantitative analysis of the mineralogical composition. It is based constructive interference of monochromatic X-rays and a crystalline sample. Useful method to study the crystal structure and atomic spacing. High cost and specific laboratory is requested.	10-100 mg of homogenous powder
Molecular Spectroscopic Analyses	FT-IR	Fourier-Transform Infrared Spectroscopy	It is an absorption technique which can be used to identify chemical compounds and it provides information about the chemical bonding in both inorganic and organic materials. IR radiation interacts with a molecule causing vibration motion of the bonds at characteristic frequencies. FT-IR provides a fingerprint by which molecules can be identified. ATR is a sampling technique combined with FT-IR allowing to the samples to be directly analysed without any preparation. IR spectroscopy is commonly used and has low cost.	Few mg
	ATR	Attenuated Total Reflection		Sampling not required
	Raman	Raman Spectroscopy	It is an absorption technique, as FT-IR, for molecular identification based on inelastic scattering of monochromatic light. It allows to identify organic and inorganic materials and in the ceramic material studies it is used to detect minerals.	Sampling not required
Thermal Analysis	TGA-DSC	Thermogravimetric analysis - Differential scanning calorimetry	These are two complementary techniques that use the same sample and can be carried out simultaneously. The analyses identify the mineralogical composition and chemical-physical changes through measuring the Loss of Ignition (LOI) as a function of increasing temperature.	Typically 5-20 mg
Micro Analyses	SEM-EDX	Scanning Electron Microscope – Energy Dispersive X-ray Spectroscopy	Imaging technique (SEM) coupled with an analytical technique to detect the chemical composition (EDX). An electron beam is focused on the sample surface and there are produced: secondary and backscattered electrons, which are able to provide images at high magnifications and contrast; and fluorescence X-rays, allowing elemental analysis.	Few mm ² treated to for conductive surface

	EPMA	Electron Probe Microanalyzer	Very high energetic electron beam is focused on the sample surface and elemental composition is carried out analysing the fluorescence X-rays produced. It is a punctual analysis (spot of few μm^2) and has penetration power of 2-10 μm .	Few mm^2 treated to obtain polished and conductive surface
Physical Analyses	MIP	Mercury Intrusion Porosimetry	Analytical technique capable to evaluate porosity, pore size distribution, pore volume, density, and other porosity-related characteristics of a material. Application of external pressure permits mercury to be forced into the open pores. The instrument measures the progressive intrusion of mercury into a porous structure under controlled pressure.	600-800 mg
	RX	X-ray Radiography	It is able to detect defects, structural discontinuity and may be also able to identify technical production properties. X-rays pass through the sample and impress photographic film with different X-ray absorption, thus, different thickness and density.	Sampling not required
Dating Methods	TL	Thermoluminescence	The pottery absorbs radiation from its environment during its life. The older the pottery, the more radiation it has absorbed. The methods measures the TL, connected to how much radiation has been absorbed and uses this information to calculate the approximate age of the pottery. It is a complex and expensive technique.	10-20 g treated to obtain homogenous powder
	^{14}C	Radiocarbon dating	This dating method is applicable only to matter which was once living organism and presumed to be in equilibrium with the atmosphere because the method is based on the exchange between organic material and environment. It measures the ^{14}C radioactivity and calculates the time (age) elapsed since organic material death. High cost of analysis.	2-10 mg treated

Archaeometric techniques permit to collect a large amount of information and data. For these reasons, handling and modelling data are necessary and more sophisticated mathematical and statistical approaches are requested. Data management allows to organize, store and retrieve information facilitating the work and the “vision” of the collected data. In archaeometric research, multivariate data analyses are often used to analyse data that arises from more than one variable. They have shown the ability to obtain a clear picture of what is going on and offer the possibility to process the information, present for instance in tables, in a meaningful fashion. Principle Component Analysis (PCA), Cluster Analysis (CA) as well as Classification and Discriminant Analyses (DA) are statistical techniques widely used in archaeometry where they find large application in particular in provenance studies. The general aim is to identify groups of chemically similarities that could potentially be used to answer questions of provenance [82]–[86].

CA is a set of statistical techniques which represents the main method used for identifying groups and outliers. The aim is the grouping of n individuals into clusters, where those individuals in a cluster have to be similar to each other and distinct from individuals that belong to other clusters. The formed clusters are set of meaningful sub-classes which help the users understand the natural grouping or structure in a data set [3], [87]. As well as CA, PCA and DA are used to make data easy to explore and visualize, their capability is to emphasize variation and bring out strong patterns in a dataset highlighting the similarity or differences between presumed groups [85], [88], [89].

Taking into account the state of the art in archaeometric research of potteries, this work would examine in depth the connection of the obtained analytical data to the technological production aspects which strongly affect the final features of the ceramic materials. Traditional methods, as proposed in literature, and innovative techniques were employed in this research in order to establish a methodology able to investigate both chemical and morphological features of the ceramic objects encouraging the use of innovative techniques as they are non-destructive and micro-destructive techniques.

1.4. Bibliography

- [1] A. Castellano, M. Martini, and E. Sibilla, *Elementi di Archeometria. Metodi fisici per i beni culturali*, Second ed. 2007.
- [2] A. H. Layard, “Discoveries in the ruins of Nineveh and Babylon,” p. XXIII, 686 2 geog.; 22x15 cm, 1853.
- [3] P. Olivera, A. Lopez, P. Bedregal, J. Santiago, S. Petrick, J. Bravo, J. Alcalde, J. Isla, L. Vetter, and E. Baca, “Applications of Nuclear Analytical Techniques to Investigate the Authenticity of Art Objects. Chapter 11.,” *Nucl. Tech. Cult. Herit. Res.*, 2011.
- [4] B. W. Roberts and C. P. Thornton, *Archaeometallurgy in Global Perspective*. Springer New York, 2015.
- [5] J. Carbert, “Gold - Based Enamel Colours,” *Gold Bull.*, vol. 13, no. 4, pp. 144–150, 1980.
- [6] a. M. Pollard, “Letters from China: A History of the Origins of the Chemical Analysis of Ceramics,” *Ambix*, vol. 62, no. 1, pp. 50–71, 2015.
- [7] M. Maggetti, “Il contributo delle analisi chimiche alla conoscenza delle ceramiche antiche,” *Sci. Archeol. Ciclo di Leg. sulla Rievca Appl. Archeol. Certosa di Pontignano (Siena), 7-19 novembre 1988*, no. 1985, pp. 65–88, 1990.
- [8] M. D. Glascock, *Encyclopedia of Archaeology*. Elsevier, 2008.
- [9] W. H. Berger, “Discovery of the 5.7-year Douglass cycle: A pioneer’s quest for solar cycles in tree-ring records Author:,” *Berkeley Plan. J.*, vol. 26, no. 4, p. 12, 2010.
- [10] E. Preuschen and R. Pittioni, “Untersuchungen im Bergbaugebiete Keldhalpe bei Kitzbühel, Tirol,” *Mitteilungen der Prähistorischen Kommission*, vol. 3, p. 7001, 1939.
- [11] E. Gliozzo, “La ceramica e l’archeometria,” *Introduzione allo Stud. della Ceram. Archeol.*, no. 1967, pp. 47–62, 2007.
- [12] C. F. C. Hawkes, “The Research Laboratory: Its Beginning,” *Archaeometry*, vol. 28, no. 2, pp. 131–132, 1986.
- [13] “Professor Edward Hall,” *Independent*, no. 16 August, 2001.
- [14] S. A. Young, “Obituary: Edward T. Hall (1924–2001),” *Nature*, vol. 413, no. 6856, p. 588, Oct. 2001.
- [15] W. Saxon, “E. T. Hall, Archaeologist Who Debunked Piltdown Man, Dies at 77,” *The New York Times*.
- [16] E. T. Hall, “Analysis of archaeological specimens: a new method,” *Times Sci. Rev.*, no. 9, pp. 13–14, 1953.
- [17] M. Piacentini and M. Martini, *Physics Methods in Archaeometry*, IOS Press. 2004.
- [18] A. M. POLLARD, “Archaeometry 50Th Anniversary Issueeditorial,” *Archaeometry*, vol. 50, pp. 191–193, 2008.
- [19] [Http://www.nobelprize.org/nobel_prizes/chemistry/laureates/1960/libby-bio.html](http://www.nobelprize.org/nobel_prizes/chemistry/laureates/1960/libby-bio.html), “William F. Libby - Biographical.”
- [20] W. F. Libby, “Accuracy of radiocarbon dates,” *Science (80-)*, vol. 140, no. 356, p. 278-, 1963.
- [21] C. Capelli, “Tiziano Mannoni, la nascita e il futuro incerto dell’archeometria ‘per archeologi,’” *Debates Archeol. Mediev.*, vol. 1, pp. 17–22, 2011.
- [22] N. Zacharias and E. Palamara, Eds., *41st International Symposium on Archaeometry (Kalamata 15-21 May) ISA2016. Book of Abstracts*. 2016.
- [23] M. Daszkiewicz, “Ancient pottery in the laboratory-Principles of archaeoceramological investigations of provenance and technology,” *Novensia*, vol. 25, pp. 177–198, 2014.
- [24] A. O. Shepard, *Ceramics for the Archaeologist*, 5th editio. 1968.
- [25] a. L. Wilson, “Elemental analysis of pottery in the study of its provenance: A review,” *J. Archaeol. Sci.*, vol. 5, no. 3, pp. 219–236, Sep. 1978.
- [26] J. Wooding, “A Standard for Pottery Analysis in Archaeology,” 2015.
- [27] M. S. Tite, “Ceramic Production, Provenance and Use—a Review,” *Archaeometry*, vol. 50, no. 2, pp. 216–231, Apr. 2008.

- [28] V. M. Emeleus, "The technique of neutron activation analysis as applied to trace element determination in pottery and coins," *Archaeometry*, vol. 1, pp. 6–15, 1958.
- [29] C. M. Belfiore, M. F. La Russa, D. Barca, G. Galli, A. Pezzino, S. A. Ruffolo, M. Viccaro, and G. V. Fichera, "A trace element study for the provenance attribution of ceramic artefacts: the case of Dressel 1 amphorae from a late-Republican ship," *J. Archaeol. Sci.*, vol. 43, pp. 91–104, Mar. 2014.
- [30] C. M. Belfiore, M. Di Bella, M. Triscari, and M. Viccaro, "Production technology and provenance study of archaeological ceramics from relevant sites in the Alcantara River Valley (North-eastern Sicily, Italy)," *Mater. Charact.*, vol. 61, no. 4, pp. 440–451, Apr. 2010.
- [31] R. Scarpelli, A. M. De Francesco, M. Gaeta, D. Cottica, and L. Toniolo, "The provenance of the Pompeii cooking wares: Insights from LA-ICP-MS trace element analyses," *Microchem. J.*, vol. 119, pp. 93–101, Mar. 2015.
- [32] R. Z. Selden, T. K. Perttula, and D. L. Carlson, "INAA and the provenance of shell-tempered sherds in the ancestral Caddo region," *J. Archaeol. Sci.*, vol. 47, pp. 113–120, Jul. 2014.
- [33] M. T. Boulanger and M. D. Glascock, "Elemental variation in prehistoric Unionoida shell: Implications for ceramic provenance," *J. Archaeol. Sci. Reports*, vol. 1, pp. 2–7, Mar. 2015.
- [34] J. Buxeda i Garrigós, "Alteration and Contamination of Archaeological Ceramics," *J. Archaeol. Sci.*, vol. 26, pp. 295–313, 1999.
- [35] J. B. I. Garrigós, H. Mommsen, and A. Tsolakidou, "Alterations of Na, K and Rb concentrations in Mycenaean pottery and a proposed explanation using X-ray diffraction," *Archaeometry*, vol. 44, no. 2, pp. 187–198, 2002.
- [36] V. Vitali, "Archaeometric provenance studies: An expert system approach," *J. Archaeol. Sci.*, vol. 16, no. 4, pp. 383–391, Jul. 1989.
- [37] C. M. Belfiore, P. M. Day, A. Hein, V. Kilikoglou, V. La Rosa, P. Mazzoleni, and A. Pezzino, "Petrographic and chemical characterization of pottery production of the Late Minoan I kiln at Hagia Triada, Crete," *Archaeometry*, vol. 49, no. 4, pp. 621–653, 2007.
- [38] M. Tenconi, L. Maritan, G. Leonardi, B. Prosdocimi, and C. Mazzoli, "Ceramic production and distribution in North-East Italy: Study of a possible trade network between Friuli Venezia Giulia and Veneto regions during the final Bronze Age and early Iron Age through analysis of peculiar 'flared rim and flat lip' pottery," *Appl. Clay Sci.*, vol. 82, pp. 121–134, Sep. 2013.
- [39] L. Maritan, "Archaeometric study of Etruscan-Padan type pottery from the Veneto region: petrographic, mineralogical and geochemical-physical characterisation," *Eur. J. Mineral.*, vol. 16, no. 2, pp. 297–307, Mar. 2004.
- [40] W. A. Longacre and T. R. Hermes, "Rice farming and pottery production among the Kalinga: New ethnoarchaeological data from the Philippines," *J. Anthropol. Archaeol.*, vol. 38, pp. 35–45, Jun. 2015.
- [41] M. Beck, *International Encyclopedia of the Social & Behavioral Sciences*. Elsevier, 2015.
- [42] J. W. Arthur, "Pottery uniformity in a stratified society: An ethnoarchaeological perspective from the Gamo of southwest Ethiopia," *J. Anthropol. Archaeol.*, vol. 35, pp. 106–116, Sep. 2014.
- [43] D. Stiles, "Ethnoarchaeology: A Discussion of Methods and Applications," *Man, New Ser.*, vol. 12, no. 1, pp. 87–103, 1977.
- [44] A. M. Musthafa, K. Janaki, and G. Velraj, "Microscopy, porosimetry and chemical analysis to estimate the firing temperature of some archaeological pottery shreds from India," *Microchem. J.*, vol. 95, no. 2, pp. 311–314, Jul. 2010.
- [45] R. Palanivel and U. Kumar, "Thermal and Spectroscopic analysis of ancient potteries," *Rom. J. Physiol.*, vol. 56, pp. 195–208, 2011.
- [46] M. Riccardi, B. Messiga, and P. Duminuco, "An approach to the dynamics of clay firing," *Appl. Clay Sci.*, vol. 15, pp. 393–409, 1999.
- [47] M. M. Jordan, M. A. Montero, S. Meseguer, and T. Sanfeliu, "Influence of firing temperature and mineralogical composition on bending strength and porosity of ceramic tile bodies," *Appl. Clay Sci.*, vol. 42, no. 1–2, pp. 266–271, Dec. 2008.
- [48] G. Barone, V. Crupi, F. Longo, D. Majolino, P. Mazzoleni, D. Tanasi, and V. Venuti, "FT-IR spectroscopic analysis to study the firing processes of prehistoric ceramics," *J. Mol. Struct.*, vol. 993, no. 1–3, pp. 147–150, May 2011.

- [49] G. Cultrone, C. Rodríguez-Navarro, E. Sebastian, O. Cazalla, and M. J. De La Torre, "Carbonate and silicate phase reactions during ceramic firing," *Eur. J. Mineral.*, vol. 13, no. 1, pp. 621–634, 2001.
- [50] B. Fabbri, S. Gualtieri, and S. Shoval, "The presence of calcite in archeological ceramics," *J. Eur. Ceram. Soc.*, vol. 34, no. 7, pp. 1899–1911, Jul. 2014.
- [51] G. Kurap, S. Akyuz, T. Akyuz, S. Basaran, and B. Cakan, "FT-IR spectroscopic study of terra-cotta sarcophagi recently excavated in Ainos (Enez) Turkey," *J. Mol. Struct.*, vol. 976, no. 1–3, pp. 161–167, 2010.
- [52] C. Rathossi and Y. Pontikes, "Effect of firing temperature and atmosphere on ceramics made of NW Peloponnese clay sediments: Part II. Chemistry of pyrometamorphic minerals and comparison with ancient ceramics," *J. Eur. Ceram. Soc.*, vol. 30, no. 9, pp. 1853–1866, Jul. 2010.
- [53] C. Lofrumento, A. Zoppi, and E. M. Castellucci, "Micro-Raman spectroscopy of ancient ceramics: a study of Frenchsigillata wares," *J. Raman Spectrosc.*, vol. 35, no. 89, pp. 650–655, Aug. 2004.
- [54] C. Rathossi and Y. Pontikes, "Effect of firing temperature and atmosphere on ceramics made of NW Peloponnese clay sediments. Part I: Reaction paths, crystalline phases, microstructure and colour," *J. Eur. Ceram. Soc.*, vol. 30, no. 9, pp. 1841–1851, Jul. 2010.
- [55] R. García Giménez, R. Vigil de la Villa, M. D. Petit Domínguez, and M. I. Rucandio, "Application of chemical, physical and chemometric analytical techniques to the study of ancient ceramic oil lamps," *Talanta*, vol. 68, no. 4, pp. 1236–46, Feb. 2006.
- [56] M. J. Trindade, M. I. Dias, J. Coroado, and F. Rocha, "Mineralogical transformations of calcareous rich clays with firing: A comparative study between calcite and dolomite rich clays from Algarve, Portugal," *Appl. Clay Sci.*, vol. 42, no. 3–4, pp. 345–355, 2009.
- [57] P. Duminuco, B. Messiga, and M. P. Riccardi, "Firing process of natural clays. Some microtextures and related phase compositions," *Thermochim. Acta*, vol. 321, no. 1–2, pp. 185–190, Nov. 1998.
- [58] J. Froh, "Archaeological ceramics studies by scanning electron microscopy," *Hyperfine Interact.*, vol. 154, pp. 159–176, 2004.
- [59] C. Fiori, D. Vitali, E. Camurri, B. Fabbri, and S. Gualtieri, "Archaeometrical study of Celtic ceramics from Monte Bibele (Bologna, Italy)," *Appl. Clay Sci.*, vol. 53, no. 3, pp. 454–465, Sep. 2011.
- [60] S. Shoval, M. Boudeulle, and G. Panzer, "Identification of the thermal phases in firing of kaolinite to mullite by using micro-Raman spectroscopy and curve-fitting," *Opt. Mater. (Amst.)*, vol. 34, no. 2, pp. 404–409, Dec. 2011.
- [61] S. Bahçeli, G. Güleç, H. Erdogan, and B. Sogüt, "Micro-Raman and FT-IR spectroscopic studies of ceramic shards excavated from ancient Stratonikeia city at Eskişehir village in West-South Turkey," *J. Mol. Struct.*, vol. 1106, pp. 316–321, 2016.
- [62] L. Maritan, L. Nodari, C. Mazzoli, a. Milano, and U. Russo, "Influence of firing conditions on ceramic products: Experimental study on clay rich in organic matter," *Appl. Clay Sci.*, vol. 31, no. 1–2, pp. 1–15, Jan. 2006.
- [63] G. Raja Annamalai, R. Ravisankar, a Rajalakshmi, a Chandrasekaran, and K. Rajan, "Spectroscopic characterization of recently excavated archaeological potsherds from Tamilnadu, India with multi-analytical approach," *Spectrochim. Acta. A. Mol. Biomol. Spectrosc.*, vol. 133, pp. 112–8, Dec. 2014.
- [64] C. Rodríguez-Navarro, E. Ruiz-Agudo, a. Luque, a. B. Rodríguez-Navarro, and M. Ortega-Huertas, "Thermal decomposition of calcite: Mechanisms of formation and textural evolution of CaO nanocrystals," *Am. Mineral.*, vol. 94, no. 4, pp. 578–593, Apr. 2009.
- [65] P. Colomban, N. Q. Liem, G. Sagon, H. X. Tinh, and T. B. Hoành, "Microstructure, composition and processing of 15th century Vietnamese porcelains and celadons," *J. Cult. Herit.*, vol. 4, no. 3, pp. 187–197, Jul. 2003.
- [66] a. K. Marghussian, H. Fazeli, and H. Sarpoolaky, "Chemical-Mineralogical Analyses and Microstructural Studies of Prehistoric Pottery From Rahmatabad, South-West Iran*," *Archaeometry*, vol. 51, no. 5, pp. 733–747, Oct. 2009.
- [67] R. Palanivel and S. Meyvel, "Microstructural and microanalytical study - (SEM) of archaeological pottery artefacts," *Rom. Reports Phys.*, vol. 55, no. 3–4, pp. 333–341, 2010.
- [68] G. Velraj, K. Janaki, a. M. Musthafa, and R. Palanivel, "Spectroscopic and porosimetry studies to estimate the firing temperature of some archaeological pottery shreds from India," *Appl. Clay Sci.*, vol. 43, no. 3–4, pp. 303–307, Mar. 2009.

- [69] J. Wisniak, "Louis-Jacques Thenard," *Rev. CENIC. Ciencias Químicas*, vol. 33, no. 3, pp. 141–149, 2002.
- [70] N. Cuomo di Caprio, *Ceramica in Archeologia 2. Antiche tecniche di lavorazione e moderni metodi di indagine*, L'Erma di. 2007.
- [71] D. Griffiths, "The role of interdisciplinary science in the study of ancient pottery," *Interdiscip. Sci. Rev.*, vol. 24, no. 4, pp. 289–300, 1999.
- [72] G. Artioli, "Scientific methods and cultural heritage," p. 520, 2010.
- [73] C. Heron, R. P. Evershed, and L. J. Goad, "Effects of migration of soil lipids on organic residues associated with buried potsherds," *J. Archaeol. Sci.*, vol. 18, no. 6, pp. 641–659, 1991.
- [74] R. P. Evershed, "Organic residue analysis in archaeology: The archaeological biomarker revolution," *Archaeometry*, vol. 50, no. 6, pp. 895–924, 2008.
- [75] C. Heron, O. E. Craig, A. Luquin, V. J. Steele, A. Thompson, and G. Piličiauskas, "Cooking fish and drinking milk? Patterns in pottery use in the southeastern Baltic, 3300–2400 cal BC," *J. Archaeol. Sci.*, vol. 63, pp. 33–43, 2015.
- [76] T. F. M. Oudemans and J. J. Boon, "Molecular archaeology: Analysis of charred (food) remains from prehistoric pottery by pyrolysis-gas chromatography/mass spectrometry," *J. Anal. Appl. Pyrolysis*, vol. 20, no. C, pp. 197–227, 1991.
- [77] C. Bonsall, G. Cook, J. L. Manson, and D. Sanderson, "Direct dating of Neolithic pottery: progress and prospects," *Doc. Praehist.*, vol. XXIX, no. Neolithic Studies 9, pp. 47–59, 2002.
- [78] S. Khasswneh, Z. Al-Muheisen, and R. Abd-Allah, "Thermoluminescence dating of pottery objects from tell al-husn, Northern Jordan," *Mediterr. Archaeol. Archaeom.*, vol. 11, no. 1, pp. 41–49, 2011.
- [79] P. M. Rice, *Pottery Analysis: A Sourcebook*. 1987.
- [80] A. E. Kaifer, "Fundamentals of Analytical Chemistry. Sixth edition (Skoog, Douglas A.; West, Donald M.; Holler, James F.)," *J. Chem. Educ.*, vol. 69, no. 11, p. A305, 1992.
- [81] E. Ciliberto and G. Spoto, *Modern Analytical Methods in Art and Archeology*. Wiley-Interscience, 2000.
- [82] G. Vaggelli, M. Serra, R. Cossio, and A. Borghi, "A new approach for provenance studies of archaeological finds: inferences from trace elements in carbonate minerals of Alpine white marbles by a bench-to-top μ -XRF spectrometer," *Int. J. Mineral.*, vol. 2014, 2014.
- [83] C. Papadristodoulou, A. Oikonomou, K. Ioannides, and K. Gravani, "A study of ancient pottery by means of X-ray fluorescence spectroscopy, multivariate statistics and mineralogical analysis," *Anal. Chim. Acta*, vol. 573–574, pp. 347–53, Jul. 2006.
- [84] G. Barone, C. M. Belfiore, P. Mazzoleni, A. Pezzino, and M. Viccaro, "A volcanic inclusions based approach for provenance studies of archaeological ceramics: application to pottery from southern Italy," *J. Archaeol. Sci.*, vol. 37, no. 4, pp. 713–726, Apr. 2010.
- [85] M. Baxter, "Multivariate Analysis of Archaeometric Data An Introduction," 2016.
- [86] R. King, D. Rupp, and L. Sorenson, "A multivariate analysis of pottery from southwestern Cyprus using neutron activation analysis data," *J. Archaeol. Sci.*, pp. 361–374, 1986.
- [87] R. Ravisankar, G. Raja Annamalai, a Naseerutheen, a Chandrasekaran, M. V. R. Prasad, K. K. Satpathy, and C. Maheswaran, "Analytical characterization of recently excavated megalithic sarcophagi potsherds in Veeranam village, Tiruvannamalai dist., Tamilnadu, India," *Spectrochim. Acta. A. Mol. Biomol. Spectrosc.*, vol. 115, pp. 845–53, Nov. 2013.
- [88] Q. Ma, A. Yan, Z. Hu, Z. Li, and B. Fan, "Principal component analysis and artificial neural networks applied to the classification of Chinese pottery of neolithic age," *Anal. Chim. Acta*, vol. 406, no. 2, pp. 247–256, 2000.
- [89] M. Baxter, "DETECTING MULTIVARIATE OUTLIERS IN ARTEFACT COMPOSITIONAL DATA," *Archaeometry*, vol. 41, no. 2, pp. 331–338, 1999.
- [90] "<http://www.arch.ox.ac.uk/archaeometry.html>."

2. Ceramic Materials

Summary

This chapter provides an introduction on ceramic material: from its relevance in archaeology to its chemical-physical reactions during firing. Mineralogical composition of the raw materials used and chaîne opératoire, which includes selection of raw materials, modelling, decorations and firing conditions, are presented. Particular regard on the firing procedure is given. The knowledge of the heating process, where the clay paste is converted to a new consolidated material, is of particular interest in archaeometric studies on ceramic, because allows to estimate and evaluate firing condition and make consideration on the technologies applied in ancient cultures.

2.1. Pottery in Archaeology

Pottery is certainly a key element in cultural heritage field. In an archaeological site, the ceramic findings are considered as the most important set of data due to their large distribution. The constant manufacturing process, recycling of vessels and waste pieces found in the site lead to the creation an archive of testimonies which faithfully record the changes in terms of mode of time, technical functions and symbols [1]. The study of pottery is useful in defining societal roles and can be used to determine social ranking and the relationship to other societies.

Ceramic¹ is one of the most ancient industries and its invention is the learning result of two particular processes: the handling clay and its change by means of the fire. The creation of functional objects, as containers, had followed a period of experiments with trials and errors.

The first clay-fired objects found in archaeological excavation were fragments of statuettes found in Czech Republic in the Moravian Basin, where was also found the first known pottery kiln. One of those statuettes was a female sculpture almost undamaged and it was named the “Venus of Dolní Věstonice”, as the Gravettian site name (see **Fig.3**). The site has been a

¹ The term ceramic refers to an object made by firing materials extracted from the Earth. Ceramic is actually an artificial form of stone. It is defined as a non-metallic inorganic solid and it is characterized by several properties, such as high hardness and strength, very high melting points, low deformation under forces, corrosion and abrasion resistance, and good electrical and thermal insulation [1], [2]. The traditional ceramic includes bricks and tiles and in general pottery, which indicates a generic artefact made of fired clay and it refers also to lower grades of ceramic materials.

particularly abundant source of prehistoric artefacts, more than 10000 ceramic fragments, dating from 28000 to 24000 BCE² [2].



Figure.3. The Venus of Dolní Věstonice, one of the earliest examples of ceramic artefact [2]. It is around 10 cm tall and dated as far back as 23000 BCE.

The earliest archaeological evidence of pottery production dates back to about 10000 BCE, as settled communities were established and tiles were manufactured in Japan, where the oldest known pottery vessels was found³, Mesopotamia and India. Pottery is dishes, plates, cups, cooking pots, storage jars for water and food, bricks, etc. Since the Neolithic period (6500 BCE), pottery making was a well-developed craft and pots were useful objects found into all aspect of everyday life (household use, trade, religious uses). All owned pottery, rich or poor people, due to the fact that clay is cheap, widespread and it is easy to make a useful pot. Furthermore, ceramic vessels can be made very pretty and decorated for being different for each production.

The beginning of glass production is uncertain, but it seems that it has been developed for the first time in Mesopotamia (5000 BCE). Later, a new material called *faience* was developed probably in Egypt⁴, where its full development was accomplished, but it has to be considered that the glass was produced independently and not earlier than 1500 BCE [3].

Since these ancient times, the ceramic and glass technologies has continuously increased and they cover a major role in the progress of humankind. The ceramic history may be briefly

² CE (Current Era or Common Era) and BCE (Before Current Era) are abbreviations alternative to Anno Domini system, where AD (Anno Domini or Year of our Lord) and BC (Before Christ) are used.

³ The type of pottery found in Japan, near Nagasaki, is called Jomon, which in Japanese means “rope-patterned”, because of the surface patterns impressed into the day. Jomon is used also to identify the prehistoric period and culture [62].

⁴ Egyptians coated their objects with substances for making them non-porous. These substances were composed of quartz, soda and a mineral containing copper, for blue and green colouration, which when fired covered the ceramic vases with a glass-like surface [63].

showed by the scheme in **Fig.4** where, C. B. Carter and M. G. Norton, authors of the scheme, illustrated the evolution of the ceramic production of earthenware, terra cotta, stoneware, porcelain, tin-glazed ware, etc. The authors specify that the diagram has to be completed but can help in understand the timeline of the ceramic craft development [4].

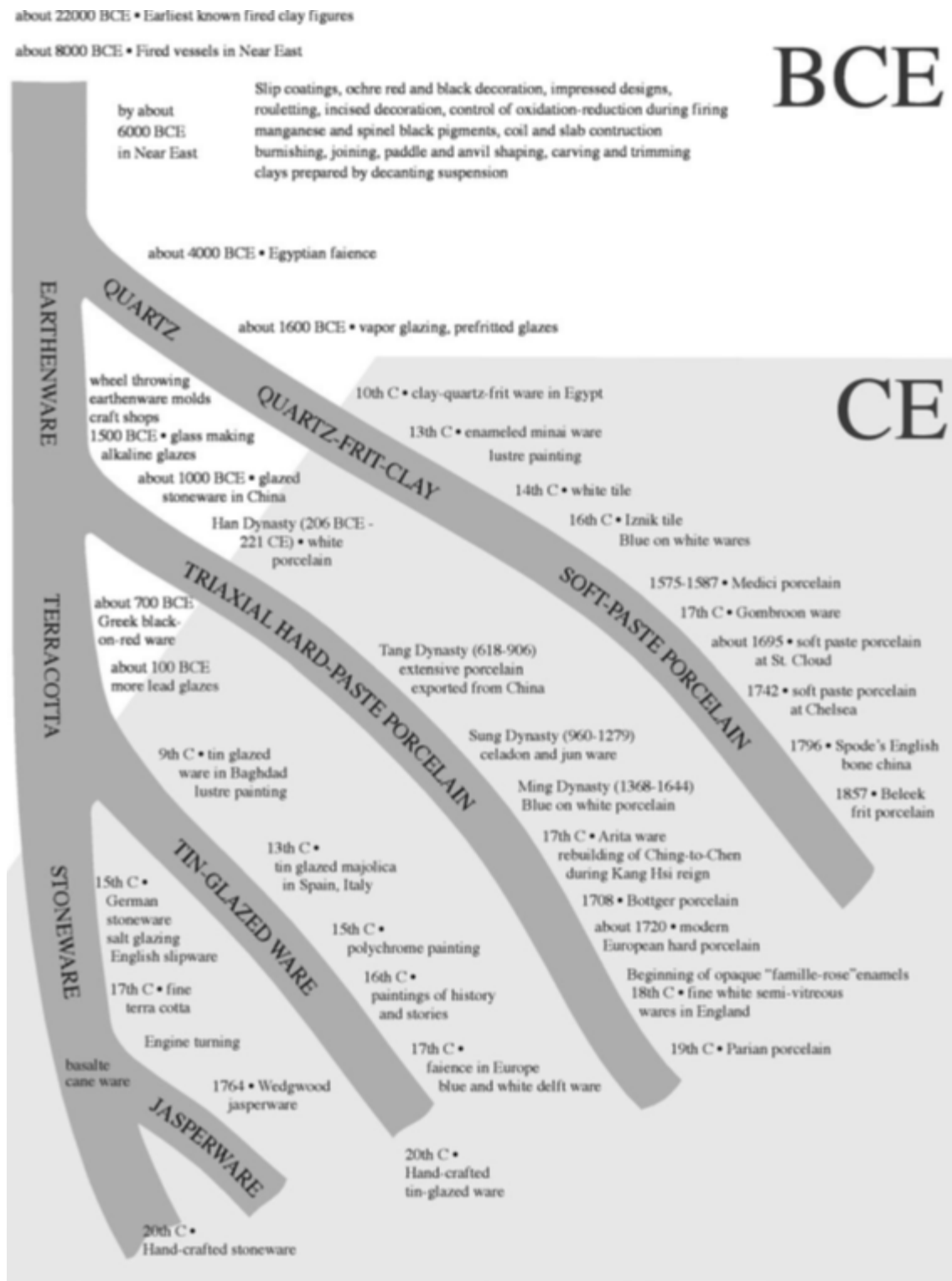


Figure.4. Diagram of timeline regarding the history of ceramic development [4].

2.2. Raw Materials

Ceramic paste⁵ is composed of naturally-occurring raw materials classified according to their functions in ceramic object and their basic properties. The two basic groups are represented by plastic (clay) and non-plastic (non-clay⁶) materials. The raw materials of pottery are: clay minerals, non-clay minerals, accidental materials (such as organic and heterogeneous compounds) and water, necessary to create and model the paste [5]–[7]. The selection of raw materials is the first step in ceramic production cycle and the features of each single component are briefly discussed in the followed paragraphs [6], [8]–[15].

2.2.1. Clay minerals

Clays represent the most important component of a ceramic body and their amount generally range 40-60 wt%. They include clay minerals and accidental materials. Clay minerals are phyllosilicates chemically constituted of the hydrous silicate of alumina based on $[(\text{Si}_2\text{O}_5)^{2-}]_n$ sheets and minor amounts of impurities such as potassium, sodium, calcium, magnesium, or iron. The clays with low content of impurities and high content of aluminium silicate (more than 30%) characterized by high plasticity⁷ are called fat, while those with only 22-24% of aluminium silicate are lean. Clays were formed by alteration through aging and weathering of primary rocks such as granite, feldspar, mica and quartz. Their properties include plasticity when wet, shrinkage under firing and air drying, fineness of grain (less than 2 μm in diameter), colour after firing, hardness and cohesion. In fact, the ideal specifications of clays are: plastic enough for shaping; dry without excessive cracking and warping; have low and wide vitrification range; low carbonate content; have a spread in particle size promoting a stronger texture; contain non-clay constituents.

These minerals have platy morphology because of the arrangement of atoms in the structure. There are two basic components to the structure: a sheet of tetrahedral corner-linked (T) and a sheet of octahedral edge-sharing (O) [13], [14]. Almost all phyllosilicates have hydroxyl (OH) ions involved in the linkages to form sheets, in addition to the oxygens, and the sheets extend laterally over many hundreds of Angstroms, as it shown in **Fig.5**. Due to the clay's crystal structure, these minerals can be classified in seven groups (the structures of five

⁵ It has to be considered that ceramic materials are also commonly classified as traditional and advanced. The first are made from natural raw materials, whereas the second ones, developed in the last 100 years, are considered engineering ceramics from artificial or chemically treated raw materials.

⁶ Non-clay materials are also named as fillers, inclusions, tempers and additives, and are added into the paste to obtain good working and drying characteristics and toughness and strength after firing [19].

⁷ Plasticity was defined as a property which permits a material to be deformed under stress without rupturing and to retain the shape produced after the stress is removed

of them are shown in **Fig.6**): i) kaolinite group; ii) clay-micas group; iii) smectite group; iv) chlorite group; v) vermiculite group; vi) allopane group; vii) sepiolite and palygorskite group [16]. For the purpose of the ceramic production, the first three groups listed above are considered and described more in details.

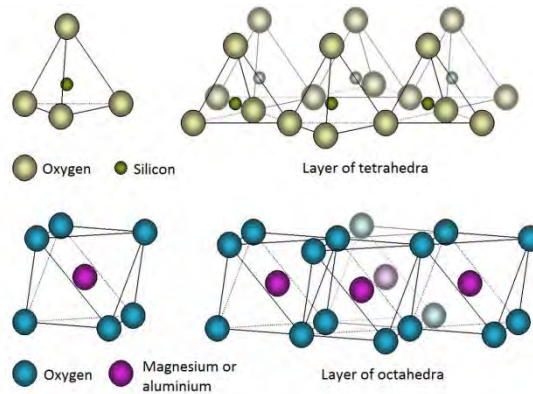


Figure.5. Tetrahedral and octahedral structures of phyllosilicates⁸.

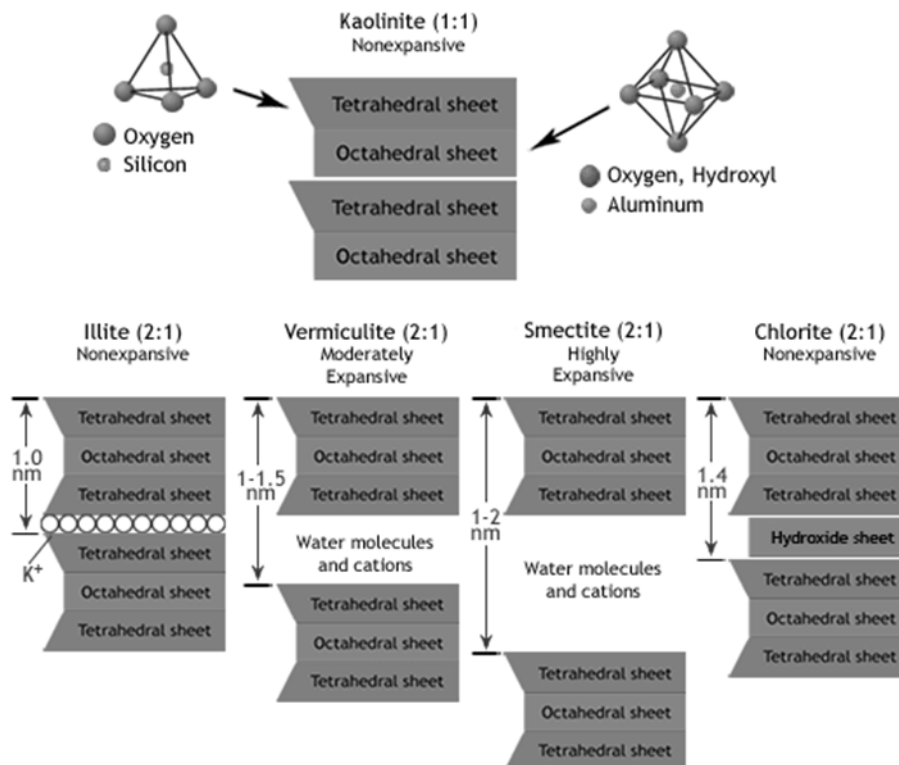


Figure.6. Structure of clays⁹.

⁸ Source of the image: <http://blogs.egu.eu/divisions/sss/tag/soil-genesis>.

⁹ Image credit: Josh Lory, <http://soilnews.feedsinews.com/day-mineralogy>.

i) Kaolinite group includes three polymorphs: kaolinite, dickite and nacrite ($\text{Al}_2\text{Si}_2\text{O}_5(\text{OH})_4$). Kaolinite is one of the most common clay minerals and it finds large use in ceramic production. Its structure consists of alternating layers T-O. Due to the weak bond between the layers and the water that cannot enter in the interlayer, kaolinite characteristics are: poor toughness and poor workability, easy to shatter, low plasticity and low drying shrinkage. For this reason the kaolinite is usually used as a base of very fine and refined paste for the production of porcelain and earthenware. Important mines of this mineral are known in England, Spain, France, Germany and China.

ii) Clay-micas or illite group, is basically a hydrated muscovite. The mineral illite ($(\text{K}, \text{H}_3\text{O})(\text{Al}, \text{Mg}, \text{Fe})_2(\text{Si}, \text{Al})_4\text{O}_{10}[(\text{OH})_2, (\text{H}_2\text{O})]$) is one of the most common clay minerals, it is a main component of shales and other argillaceous rocks. The crystal structure is T-O-T, and the space between individual clay crystals is occupied by poorly hydrated potassium cations which is responsible for the absence of swelling. Illite has good workability and plasticity. Its coloration changes from grey-greenish to brown-reddish and dark-black in depending on the content of calcite, iron oxides and pyrite, respectively, and firing process. These clays are abundant in Mediterranean region, and in particular in Italy: in Piedmont, Lombardy, Puglia and Sicily.

iii) Smectite group, also called montmorillonite group, includes several minerals, among which montmorillonite ($(\text{Na}, \text{Ca})_{0.3}(\text{Al}, \text{Mg})_2\text{Si}_4\text{O}_{10}(\text{OH})_2 \cdot n(\text{H}_2\text{O})$). It has a complex structure T-O-T with cations as Na^+ , Mg^{++} and Ca^{++} able to surrounded themselves with water molecules forming interlayer water swelling phenomena. This entails excessive plasticity, strong shrinkage and difficulty in modelling, whereby in the ceramic paste are added lean clays. It can be found in Italy in Lazio and Puglia, and in particular in France, Germany, Japan and USA [13], [14].

2.2.2. Non-clay Materials

Non-clay materials are already naturally present in clay and the potter intentionally adds more amount of them to modify the final characteristic of the artefact: for reducing high plasticity and/or shrinkage of the body when drying or firing. They include quartz, feldspar, limestone, iron hydroxides and oxides and minor compounds, and when mixed with water are not plastic. Basing on their function in the ceramic production, non-clay materials, both artificial or natural, can be divided in three main groups.

The first group includes inert tempers (grog or degreasing) able to reduce plasticity and shrinkage after drying, and providing structure to the artefact, because they do not absorb

water maintaining constant their volumes. The main components in this group are: non-clay minerals as quartz, micas, feldspars and the non-clay and artificial material chamotte.

- Quartz (SiO_2): is the principal silica mineral, constituent of igneous rocks, metamorphic rocks and sandstones. Silica is an important raw material in ceramic and it is used for glass production. A major source is sand, defined as granular rock particles that pass through a No. 4 mesh (4.75-mm aperture) by the American Society for Testing and Materials (ASTM). 20-25 wt% of silica is usually added in ceramic mixture. Shape as well as grain size, rounded or sharp edges, distinguish natural (river sand) or artificial (mechanical grinding) temper. It is defined as inert because is chemically stable and during firing process till 1000°C (common fired temperature of archaeological findings in less than 1000°C) does not react with other components and does not change the composition of the ceramic mixture. Quartz is characterized by a continuous framework of T with oxygen shared between two tetrahedral which not allow entrance of other ions giving as result a compact structure and high level of purity and hardness (Mohs scale 7). Silica presents polymorphs with different thermal stability: quartz- α stable till 573°C , quartz- β till 870°C , tridymite 1470°C and cristobalite 1710°C . These inversions are reversible and occur volume variations, that has to be considered during firing and cooling processes [17].
- Micas are phyllosilicates and muscovite (white) and biotite (black) are the most important minerals in this group. The crystal structure is well defined, the bonds within the layers are very strong while those between the layers are weak, hence they are very rigid and cleave easily along the plane. They are also characterized by vitreous brightness, visible by naked eyes and used by archaeologist to classify ceramic findings.
- Feldspars are the most common minerals in the Earth's crust (around 60%) and are present in sedimentary deposits, igneous and metamorphic rocks. The minerals belonging this group are tectosilicates and on the basis of the chemical composition the endmembers of feldspars are: K-feldspar (KAlSi_3O_8); albite ($\text{NaAlSi}_3\text{O}_8$) and anorthite ($\text{CaAl}_2\text{Si}_2\text{O}_8$). Alkali feldspars (orthoclase, sanidine, microcline and anorthoclase) are the solid solution between K-feldspar and albite; and between albite and anorthite are called plagioclase. Their functions in ceramic mixture are similar to those of silica and micas as tempers. Furthermore, feldspars is used as a flux in modern ceramic fired at high temperature (above 1000°C). The flux action is given by their bond strength which improves mechanical properties, scratch resistance and ability to withstand thermal shock decreasing the melting point of clays.

- Chamotte is the artificial temper added intentionally from the potter. It is terracotta and/or pottery finely ground and it works as a good degreasing. Potters used to have this material available in their workshop as waste material and thus easy to obtain and extremely cheap. Chamotte is used in terracotta and laterizio production but not for fine ceramic products due to its necessity to be ground very fine.

The second group of non-clay materials consists of fluxes and binders, as calcite and oxides, which throughout the firing process melt, and chemical-physical transformations occur. As a result, new mineral phases as complex silicates can be formed with lower melting point. Furthermore, flux melting joins other particles together involving sintering process which reinforces and stabilizes the ceramic paste increasing the mechanical strength.

- Calcite (CaCO_3) is an inorganic salt often associated with dolomite ($\text{CaMg}(\text{CO}_3)_2$). Calcite is a common component to sedimentary rocks, limestone and metamorphic marble. Ceramic mixture with low content of calcite, less than 2%, is defined non-calcareous, while Ca-rich clays may have till 20% of CaCO_3 and form calcareous ceramics. The thermal decomposition of calcium carbonate occurs at relatively low temperature (around 800°C) forming CO_2 and CaO . The last one is very reactive and reacts with clay particles the ceramic mixture. Analysing potteries, carbonates are considered thermal indicators because provide information about firing temperature.
- Iron oxides and hydroxides, hematite (Fe_2O_3), magnetite (Fe_3O_4) and limonite ($\text{FeO}(\text{OH})\cdot n\text{H}_2\text{O}$), are responsible of the clay colour and can be present in large amount in clays. Iron oxides are reactive forms as CaO and are influenced also by furnace conditions, whether oxidizing or reducing.

The potter could add other materials with the function of fluxes, as alkali compounds which have low melting point at around $750\text{-}850^\circ\text{C}$ and they have important role in glaze and glass manufacturing.

The third and last group of non-clay materials are represented by accidental materials: organic compounds, fossils, flint fragments, heterogeneous materials, pyrite, etc. These materials could be incorporated in sedimentary rocks, deliberately added from potters or accidentally present in sands retrieved from rivers or other natural sources. Organic materials could be added intentionally because the putrefaction process produces organic colloids increasing plasticity and workability. Pyrite (FeS_2) can be found in fine grains in clays if not well depurated and its thermal decomposition at 400°C releases sulfuric anhydride (SO_3) which reacts with CaO forming CaSO_4 stable till 1000°C , however, in atmospheric conditions

the sulphate absorbs water and forms gypsum ($\text{CaSO}_4 \cdot 2\text{H}_2\text{O}$) with volume increasing and forming whitish spots on the ceramic surface.

2.3. Production Technology

Ceramic production involves the following basic steps:

- Procuring and selection the raw materials (clay and non-clay materials);
- Preparing the clay paste mixing the raw materials with water;
- Shaping and modelling the paste into object;
- Drying the object;
- Surface treatments;
- Firing the object in to a kiln.

Each step has its procedure and is able to modify chemically and physically the final properties of the artefact. Techniques, *chaîne opératoire* and technology¹⁰ are extremely important in studying archaeological pottery. Actually the study of technology, meant as a broad framework, allows to approach the society and is the key issue of archaeology [18].

The ceramic production begins once the raw materials are collected, transported and stored at the manufacturing facility or workshop. They come from natural deposits in mine and/or deposited clay along river courses. In the workshop the collected impure clay goes under beneficiation process to obtain pure powder to be used in pottery production. In this process purification, comminution (reduction of the particle size of the raw material by crushing and fine grinding) and classification are carried on. The clay is reduced to fine particles to liberate impurities removed by washing with water and filtering, and modify morphology and size distribution facilitating the forming procedures. The purpose of mixing is to combine the raw materials to produce a homogenous paste. Potters can add particular tempers altering the original properties of the clay and determining the chemical, mineralogical and morphological features of the artefacts. This choice is related to the particular interaction between potter, clays and tempers available [19]. The powdered clay and tempers are then mixed with water and a uniform paste is formed and kneaded.

¹⁰ Techniques are able to encode the technological process and represent the link between people, craft and materiality. They are a set of procedures used by people in making objects in craftworks with the aim to fulfil a numbers of needs.

Chaîne opératoire is a French term used in archaeology and sociocultural anthropology. It means “operational sequences” and regards the reconstruction of organization and technological system of an archaeological site. It has been defined by Perlès as a “succession of mental operation and technical gestures, in order to satisfy a need (immediate or not), according to a pre-existing project).

Technology is a broad issue where theoretical and methodological development of techniques is reflected in its concept becoming the social dimension of techniques [18].

2.3.1. Forming, shaping and drying

The plastic clay paste is shaped in the desired object through different manual and partly mechanised techniques. The common hand-building potteries are made by pinching, coiling and slabbing methods [6], [20], [21]. The first one is a simple methods which begins taking a lump of clay; the potter pinches a hollow in the centre forming a vessel shape using thumb and fingers of one hand while slowly rotates the lump in the palm of the other hand. Due to the building technique's limitations, most pinch pots are small and very simple objects.

The coiling methods is one of the most ancient methods for pottery production. It is used to create vessels and sculptures and nowadays is still used by primitive cultures to preserve their cultural heritage [22]. Coiling pots are made by rolling clay on a flat surface or between the palms and then stacking and adding the coils one on top of another. Coils may be pressed with the fingers or a tool on both the inside and outside to create the artefact. The coiling method can be also combined with turntable or other rotational device to better smooth the walls of the vessel [23].

The slabbing method allows to build large scale objects. Potters use a rolling pin to make flat clay slabs of a certain thickness. Pieces of different shapes are cut out and are then joined with thick pasting slip and/or coils.

The use of moulds (or molds), of particular dimensions and shapes, to form ceramic object is also widespread at many periods. A hollow object or a leather mould can be used to hold and shape the clay during hand-forming. Particular vessel can be made by means of sophisticated moulds where surface decoration on the inner face is incised or impressed.

Partly mechanised techniques include the use of wheel, very common in pottery production process since 5000 BCE in Egypt, Middle East and Asia [20]. The potter's wheel is created for making round forms of different thickness. Pottery which has been made on a potter's wheel has a continuous spiral all the way up its body and horizontal and parallel striations (rillings) [24], [25]. Despite the evidence of the use of this method, archaeological findings of potter's wheel are fragmentary at all periods and it is easy to confound them with other rotary devices. Wheel-throwing pots are more symmetric because the pots are centred and shaped on the turntable [26]. Wheel-throwing method includes several tools and sub-methods distinct by the use of hands, feet, sticks, etc., and are well explained by N. Cuomo Di Caprio [6].

The plastic clay is shaped and while is still wet, surface of the artefacts is usually smoothed in order to improve its appearance and fill out the pores with fine particles of clay.

Before firing, the clay object has to be dry. The drying process is a simple but at the same time very important operation where the absorbed water that has combined physically with the clay, which makes the clay plastic, flexible and provides lubrication for modelling, starts to

evaporate. During drying, the clay undergoes a volume contraction: the clay particles slip close together and the object shrinks in size, the structure is more compacted, as a result of consolidation action, and the holes left by the water produce pores. This process is reversible and the water can be re-combined with clay making it plastic again. All water has to evaporate before firing the artefact and not too quickly, because in this case differential shrinkage can occur between the inner and external surfaces and as a consequence, cracks and fractures can be generated by mechanical stress [19], [23].

2.3.2. Decoration

Decoration of the surface is an optional procedure that can be made before firing process when the clay object is leather-hard. After drying, mixture of clay and water (as fluid suspension) can be applied on the unfired object surface to form a thin non-vitreous coating, call *slip* or *engobe*. The purpose is to smooth the surface, correct defects, decorate the pot and/or produce a good substrate for painting. Also pigments, organic compounds and/or copper and iron oxides can be added to change the colour of the artefact. The mixture applied is rich of alkali often used by Romans in *terra sigillata*¹¹ pottery. Actually, in antiquity, very beautiful slips were made by Greek and Romans using fine textured illite clays [27]. If the paste is macro-porous, the infiltration of the slip through the pores can be higher, facilitating the adherence with the substrate. Slips can be applied generally by brush and dipping into the slip and the thickness can range between 30 and 80 μm . The use of slips, even if rich of iron oxides for red, reddish and brown coloration, does not influence the thermal expansion of the body because they have similar thermal behaviour [18], [26]. Afterwards, a second drying process is necessary before firing.

Pot surface, can be also carved, incised and perforated by removing clay material with several kind of tools, as fingernails, reeds and stamp-seals. Examples of incising are combing and graffito and can be performed above the slip layer [28].

2.3.2.1. Glazes and enamels

A separate paragraph must be devoted to ceramic coverings, as glazes and enamels. These kinds of decorations are usually applied after the first firing process: the ceramic body becomes more robust and manageable and afterwards it is fired for the second time (biscuit or bisque). The fired pottery surface is porous and can absorb water and moisture, therefore

¹¹ *Terra sigillata* may be defined as a “fine-quality red ware with a glossy red-slipped surface” [64] but, as specified by the authors, there is no a common agreement of its definition.

cannot be used for the transport of beverages. To make pottery impermeable to water and other liquids, many ceramic artefacts are covered with a thin layer of glaze, by means of glazing process. Furthermore, the covering is used to mask imperfections and decorate the surface with the use of pigments and other compounds [15], [19]. The glaze coating mainly differs from slips for the high firing condition and complexity in chemical composition, as well as for the fact to make completely impermeable surface [27].

Glaze and enamel are forms of glass for coating ceramics and/or other materials as metals and alloys. They have similar chemical composition and can be referred to vitreous materials¹². However, glass and glaze differ on their proportion of chemical composition, and the differences are observed in their different light absorption and in the particular properties of the glaze to be attached on the pottery surface [26]. Glaze coatings should have lower melting point than glass, long plastic time during cooling and expansion coefficient similar to the under body to avoid cracks and crazing [29].

Distinction between glaze and enamel is given by their aspect: glaze is transparent and enamel is opaque, usually applied on metals or on top of glazes; both are bright and during firing process they become integral part of the artefact by soldering to the under pottery surface. Furthermore, glazes normally contain high content of lead (Pb, as PbO) to decrease the melting point and if it is present a thin layer of silver and/or copper, the glaze is called *lustre*. Enamel is commonly defined as a coloured glaze, generally stanniferous¹³, fired at low temperature (around 800°C) [30]–[32].

The chemical composition of glassy coatings includes quartz as a principle component, metal oxides and lime as fluxes and/or opacifiers. Quartz, available in silica sand, if heated until its melting point (1710°C) and cooled down rapidly turns into silica glass having the same chemical composition but it lacks crystalline structure. In order to decrease the melting temperature of silica, fluxes are added and the mixture can be melted at around 1000°C, temperature reached from ancient kilns at which it becomes viscous [19], [33].

Glazes and enamels always contain soda (Na₂O) and/or potash (K₂O) as modifiers of silica network altering its viscosity. Their function is that to be fluxes. The ashes of plants provides rich source of sodium and Na₂O is obtained by thermal decomposition of sodium carbonate (Na₂CO₃). Sodium feldspar, as albite, can be also used to obtain soda, but adding this mineral are added also alumina and silica. Potash source are: orthoclase, tartar (KAlC₄H₄O₆) and

¹² Glassy or vitreous materials are amorphous solids, or supercooled liquids, which at ambient temperature they are hard, rigid and impermeable. The internal structure is not crystalline and the atoms are organized and arranged in the space in a short-range order without periodicity and symmetry characteristics like crystalline solids [19].

¹³ Luca Della Robbia is considered the inventor of stanniferous glaze due to his development of the method of creating tin-glaze terracotta sculptures [31].

potassium alum ($\text{KAl}(\text{SO}_4)_2 \cdot 12\text{H}_2\text{O}$). Other modifiers as stabilizers added to the glaze composition are alkaline earth oxides such as lime (CaO) and magnesium (MgO), obtained from calcination of their carbonates and silicates. CaO improves the durability and the chemical stability of the glaze preventing crystallization during the cooling step. Alumina (Al_2O_3), phosphorous pentoxide (P_2O_5) and iron oxide (Fe_xO_y) are minor components usually in the glaze often as impurity of raw materials. They are intermediate oxides having low solubility, therefore they improve the resistance to dissolution by immobilizing free alkali ions not anymore able to move in the silica network; for example alumina forms aluminium silicates preventing the separation of silica crystals [15], [32]. Furthermore, aluminium oxide, as a refractory, stabilizes the melt glass and helps in keeping it in vertical on the pot surface because increases the viscosity [33]. The proportion and the amount of these added components has to be under control, because large amount of those and small of silica create a fragile glaze. Actually, difference in composition of glaze, as well as glass, is the reason of different deterioration [32].

As mentioned above, glaze composition includes Pb, introduced as lead oxides, litharge (PbO) or minio (red lead, Pb_3O_4) obtained after calcification of galena (PbS) or white lead ($2\text{PbCO}_3 \cdot \text{Pb}(\text{OH})_2$). Lead oxides have high melting power, they chemically react with quartz forming low-melting silicates which can contain till 92% of Pb expressed as PbO . Due to the high refractive index, lead provides brilliance and spectral colours to the glaze. Moreover, PbO content increases the glaze density and encourages colouring effects [6], [15], [32].

Enamel composition includes Sn, obtained from cassiterite mineral (SnO_2). The metal is used together with lead during calcification process in order to reach a complete oxidation. Tin-oxides has low solubility in the glaze solution and the particles remain un-melted (colloids) within the glaze making it non-transparent and then acting as opacifier¹⁴. Majolica enamel is made with a white tin-enamel, and the white colour of it depends on the amount and grain size of the stanniferous oxide [27], [32]. In reducing conditions, tin oxide loses its opacifying power forming a rough and grey surface [33].

Salt-glaze is another kind of glaze which is worth to describe briefly. It is a once-fired alkali glaze made by throwing salt (NaCl) into the kiln at high temperature ($1100\text{-}1250^\circ\text{C}$). The salt decomposes and forms Na_2O , which, acting as a flux, reacts with silica and forms a soda-rich glaze coating on the surface of the pottery. The chlorine in the salt reacts with the steam in the kiln and produces acidic hydrogen chloride gas. This is what is known as a Grès de Flandre, and this procedure was particular used in Germany, as well as Holland [15], [26], [27], [31].

¹⁴ Titania (TiO_2) and zirconium oxide (ZrO_2) are other oxides used as opacifiers often found in ceramic coatings. Furthermore, they are used to accentuate and stabilize colours respectively [33].

Actually, the first salt-glaze pottery appeared in Germany at the end of the 13th century, in Rhineland [34].

Glaze coatings also include colourants. The colour of the glass and glaze depends on the absorption of the visible light through interaction with colourant agents and the reflected wavelengths in the visible spectrum [26]. Colourant oxides are the oxides of the so-called transition-metal elements and they include: chromium, manganese, iron, cobalt, nickel and copper; their oxides are seldom pure because of impurities which can be contained [33]. Some of these oxides come in form of carbonates, and in order to obtain the same colour intensity like adding the metal oxide, more amount of carbonates it is needed [27]. Low temperatures of firing (<1100°C) may provide a broad range of colours because at higher temperature many of these elements are unstable and can volatilize, such as chromium, tin and copper do. In the **Tab.2** are reported the colourant agents and their description, considering also firing conditions, since oxidizing and reducing atmosphere can influence the final colour [15], [26]. Colorants are added in finely ground oxides from their carbonates or salts and combination of them are also used with the aim to change and/or intensify the colouration.

Table.2. Glaze and glass colourants [20], [26], [27], [32], [33].

Colourant	Oxides/ compounds	Colouration		Needed amount
		Oxidizing atm.	Reducing atm.	
Cobalt Co ²⁺ ; Co ³⁺	CoO; Co ₂ O ₃ ; Co ₃ O ₄ ; CoCO ₃	It is unaffected by atmospheric conditions. Blue. Zn intensifies the blue colour; purple with Mg oxide; reddish with boric oxide.		It is the strongest colourant. 0,5-1% gives medium blue; 2-4% midnight blue.
Iron Fe ²⁺ ; Fe ³⁺	FeO; Fe ₂ O ₃ ; Fe ₃ O ₄ ; Fe ₂ O ₃ ·H ₂ O	Yellow, amber, brown. Green with Cu.	Rusty red, reddish brown	Black glass ^a was made using an excess of iron oxide, more than 10% of the glass batch.
Manganese Mn ²⁺ ; Mn ³⁺	MnO; MnO ₂ ; MnCO ₃	Purple, black	Brown	Small amount (2-10%) of manganese dissolves in the glaze but if more forms crystallized surface. Furthermore, MnO ₂ at high temperature (>1000°C) decomposes in MnO causing bubbling in the glaze.
Copper Cu ²⁺ ; Cu ⁺	CuO; Cu ₂ O; Cu ₄ O; CuCO ₃	Green or blue	Red in heavy reduction atm.	It disperses well in the glaze. 3-6% for green colouration in lead glaze, turquoise without Sn and Pb; 0,5-2% for red in alkaline glaze base.

Nickel Ni ²⁺	NiO; NiO ₂ ; Ni ₂ O ₃ ; Ni ₃ O ₄	Grey or brown	Grey-brown	Strong colourant, 0,5-1% may be enough to colour. It produces nice colours if coupled with other oxides.
Chromium Cr ³⁺ ; Cr ⁶⁺	Cr ₂ O ₃	It is unaffected by atmospheric conditions. Strong green. Pink with tin oxide; brown with zinc oxide; yellow/green in sodium glaze.		Bright green powder derived from iron chromate. Very powerful colourant: 0,5% gives an intense colouration.

^aA case of black glass was produced in Britain in the 17th century were a combination of iron, manganese and sulphur in reducing atmosphere. However, an excess of any colourant oxide will produce a black glass [32].

Other elements can be used as colourants: antimony, titanium, vanadium, gold, cadmium, selenium, etc., although, some of them may give undesirable reactions and disadvantages: cadmium and selenium are toxic, antimony is unstable at high temperature (1100°C) and gold is pretty expensive [27].

Glazed wares may be also coloured by underglaze drawing and pigments. In this case, the pot (biscuit) is decorated with a paint layer made by mixing oxides, carbonate, sulfate, etc., an opacifier and a flux to make it adhere better to the pot. Underglaze layer represents the first coating, and afterwards, the artefact is coated with a proper glaze and fired, forming an in-glaze decoration [27], [35].

2.3.3. Kilns and Firing Procedures

Firing process is a critical step in production technology of pottery. The clay object undergoes to heating process at high temperature, where chemical and physical transformations take place changing characteristics of pottery which becomes hard, robust and durable. The necessary changes in order that firing process becomes irreversible, start at temperature above 550-600°C; actually, above 700°C the artefact is considered fired and many simple potteries are fired at that temperature [19], [21], [26]. Several reactions occur in this process and new mineral phases can be formed from those which decomposed. Hence, secondary minerals provides indication about firing temperature and they can be considered as firing indicators. All the successive reactions which occur during firing process can be divided in three phases: oxidation (100-400°C), dehydration (450-600°C) and incipit of vitrification, including baking and burning (above 600°C). In the next paragraph (2.4.), chemical and physical reactions will be developed and discussed in details.

A key element to create a ceramic object is the kiln, and throughout the archaeological history, two primary types of firing procedure can be recognized: open firings and kiln firings (**Fig.7**). The former ones are primitive forms largely used in North America and Middle East. They refer to bonfire, pit and clamp firings (**Fig.7 (a)**), in which pots and fuels are in direct contact in a stack. Open firings can reach relatively low temperatures (minimum 600°C and maximum 800°-900°C) and the procedure cannot be well controlled, in terms of firing temperature as well as atmospheric conditions (oxidizing or reducing). Potters place the objects to be fired up on a bed of fuel and more fuel is added on the top of those. All is ignited and the firing process ends when the firing is over. Problematics related to this first type of firing procedure are encountered in the fact that it is not contained and not controlled: i) the fuel burns and can shift causing damage to the potteries; ii) due to the direct contact between fuel and potteries, those are submitted to inconstant and variable temperature which can cause cracks on them; iii) lot of heat can be lost to the atmosphere by means of radiation and convection; iv) the rate of heating is not proportional and inhomogeneous, because open firings reach the maximum temperature very fast and for a short range of time, afterwards decline rapidly to low temperature (around 500°C) and end slowly.

In order to reach higher temperature and to better control the firing process (temperature and atmosphere), kilns were constructed, usually made by bricks and/or stones. Kiln firings are containers in which pots and fuel are separate and the pots are fired by flames and gases from the fuel. These kilns can be simplified as a structure which includes two chambers: one for the fuel combustion and the other for the pot firing. Oxidizing and reducing atmosphere is managed through an opening, chimney, which allowed the adjustment of the air flow. There are mainly two types: *updraft* and *downdraft* kilns, consisted of two vertical and in plan chambers respectively. Updraft kilns were widely used during Roman period in the Mediterranean Basin and they are able to reach 1000°C but with irregular distribution of the heat (**Fig.7 (b)**). Instead, downdraft kilns allow to reach temperature till 1300°C with a better management of heating time and atmosphere, with the chimney at the opposite side of the combustion chamber (**Fig.7 (c)**) [15], [19], [21], [26], [36].

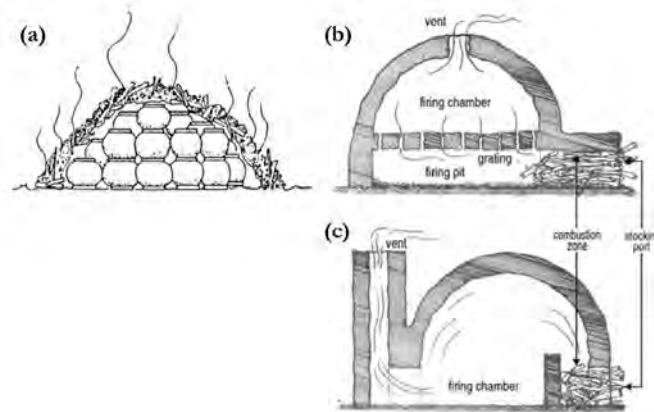


Figure.7. Pottery kilns. The picture shows the three main types of kilns: **(a)** an open firing – bonfire firing; **(b)** and **(c)** kiln firings, downdraft and updraft respectively [19].

Important factors to consider when studying ceramics and technological production are connected with firing process: firing temperature, firing atmosphere and length of firing. These complex parameters are not direct connected with each other and the combination of them is reflected in the final product [37]. To better study the behaviour and features of the potteries under firing process, all the reachable data by means of complementary analytical techniques are requested [18].

Firing temperatures reached in the kiln are able to distinguish, together with chemical and mineralogical composition, different types of fired ceramics¹⁵: terracotta ($T < 900^{\circ}\text{C}$); earthenware ($900 < T < 1200^{\circ}\text{C}$); stoneware ($1200 < T < 1350^{\circ}\text{C}$) and porcelain ($T > 1300^{\circ}\text{C}$). In fact, the chemical and physical transformations are dependent on temperatures and mineralogy of the raw materials.

Firing atmosphere depends on the presence of oxygen managed regulating air circulation in the firing chamber: oxidizing or reducing atmosphere, if oxygen or little oxygen is present respectively. This factor influences especially the final colour of the artefact. Generally, in oxidizing atmosphere, carbon present is completely consumed and the ceramic object appears light in colour. Instead, reducing atmosphere promotes dark brown colour due to the deposition of carbon on the pottery surface [38].

Length of firing is not often taken in to consideration when studying ceramic technologies and it refers both to the total time from the initial heating to the final cooling and the time related to the maximum temperature maintained into the kiln. Firing duration can range between 15 minutes to several days, and it has to be considered that heating potteries should be gradual and not too rapid reducing the risk of damage due to a too fast water evaporation and organic compound volatilization. As well as firing duration, rate of cooling influences the

¹⁵ A detailed description of fired ceramics classification is given in the section Glossary of this thesis.

final characteristic of the pottery: if it is carried on rapidly may cause cracks and fractures [18], [38].

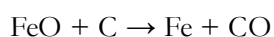
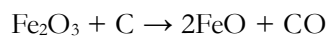
2.4. Chemical and Physical Reactions during Ceramic Firing Processes

Firing clay objects is a irreversible process which produce ceramic materials characterized by new chemical-mineralogical composition and different physical and microstructural features. The changes involved in the clay matrix during firing depend on the firing strategies adopted by the potter, intended as a combination of the factors as firing temperature, atmosphere conditions, firing duration and fuels. The firing temperature plays a fundamental role in the dynamic aspect of the process, thus in developing new mineral phases (secondary phases) depending also on the raw material composition [39]. Chemical and mineralogical changes are strictly connected to morphological and structural adjustments, and in this paragraph are discussed the main chemical and physical reactions occurring throughout firing clay paste divided in particular range of temperatures.

50°C – 200°C. Water physically absorbed in the clay paste evaporates: the dehydration process, started during drying procedures, continues. The water trapped in the micro pores and that one absorbed in the lamellar structure of the clay (interlayer water) is eliminated in form of steam. Water evaporation produces porous microstructure. Heating rate should be slow because the steam has to escape from the clay particles avoiding high pressure into the pores which may cause cracks and explosion [6], [15], [18], [40].

Heating process increases the thermic energy and ensues a dilatation of the material which depends on the chemical composition into the matrix [15].

200°C – 700°C. The organic matter in the paste (present as humus in clay and/or intentionally added by the potter) can be completely combusted through the firing process increasing the porosity of the ceramic material. In oxidizing atmosphere there are produced CO₂ and steam; instead, in reducing condition are produced carbon particles. An increase of the amount of carbon influences the colour and the quality of the pottery. Carbon can act as reducing agent and may react with iron oxides:



The decomposition of organic compounds generates an exothermic phase related to its oxidation and involves a low decrease of weight which is not considered dangerous and able to damage the structure of the pottery [15], [18], [41].

Firing above 450°C causes the removal of chemically bond water¹⁶ of clay minerals. The crystalline lattice is destroyed and the reaction is irreversible. The broad range of temperature in which the dehydroxilation occurs depends on the type of the mineral and the firing condition. This reaction provokes significant shrinkage of the pottery walls and during this process non-clay minerals act as a skeleton, improving also heat distribution minimising the generation of cracks [6], [18], [42], [43]. Kaolinite, montmorillonite and illite, as already mentioned in the paragraph 2.2.1., are the most used clay minerals in ceramic paste. Their dehydroxilation reactions were widely studied and because they occur at particular temperatures, these clay minerals are also used in archaeometric studies as indicators of firing temperature of ceramic artefacts [44]–[48]. Between 450 and 650°C, kaolinite dehydroxilates and loses hydroxyl until it decomposes completely in metakaolinite (at 950°-1000°C); montmorillonite dehydroxylates below 600°C and form a stable dehydroxylated phase that preserves some of the crystal structure of the original clay mineral until its structure collapses (at around 800°C); illite starts loosing hydroxyl at low temperature, as montmorillonite mineral, and its skeleton persists still it breaks down between 700 and 850°C. Once the crystal structure collapses at higher temperature, reactive oxides are formed and may react in the matrix creating new mineral phases and compounds [43], [49]–[51].

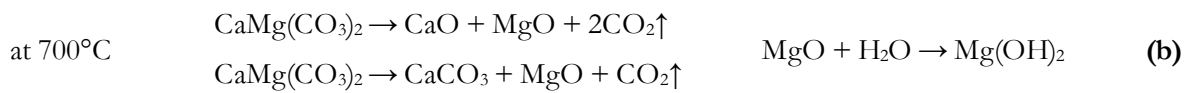
At 500-700°C, the temperature is high enough to avoid the rehydration of the clay mineral structures which become a-plastic: the ceramic body has certain hardness, mechanical properties and resistance to water immersion. Furthermore, shrinkage is reduced and clay particles are permanent bonded [18].

573°C is the temperature in which quartz undergoes to a reversible phase transition (α to β) accompanied by a 7 vol% change causing fractures if the heating process goes to fast [15], [30], [35], [52].

700°C – 900°C. This range of temperature is characterized by the decomposition of carbonates, which starts at around 650°C and ends at around 800-850°C. Calcite, the most common pure calcium carbonate (CaCO_3), decomposes in calcium oxide (CaO) and release CO_2 increasing the porosity (see below reaction **(a)**). The formation of CaO may cause stress in the structure generating fractures. Furthermore, this oxide is reactive: it can form new phases reacting with other compounds and absorb water from atmospheric moisture producing its hydrated form (Ca(OH)_2). This hydration increases the volume of the crystals and it may cause the collapse of the ceramic structure. Actually, the production of Ca-rich ceramics requires technological skills and knowledge able to control firing temperature,

¹⁶ It refers to the hydroxyls from the inner and inner-surfaces of the minerals which migrate outside [65].

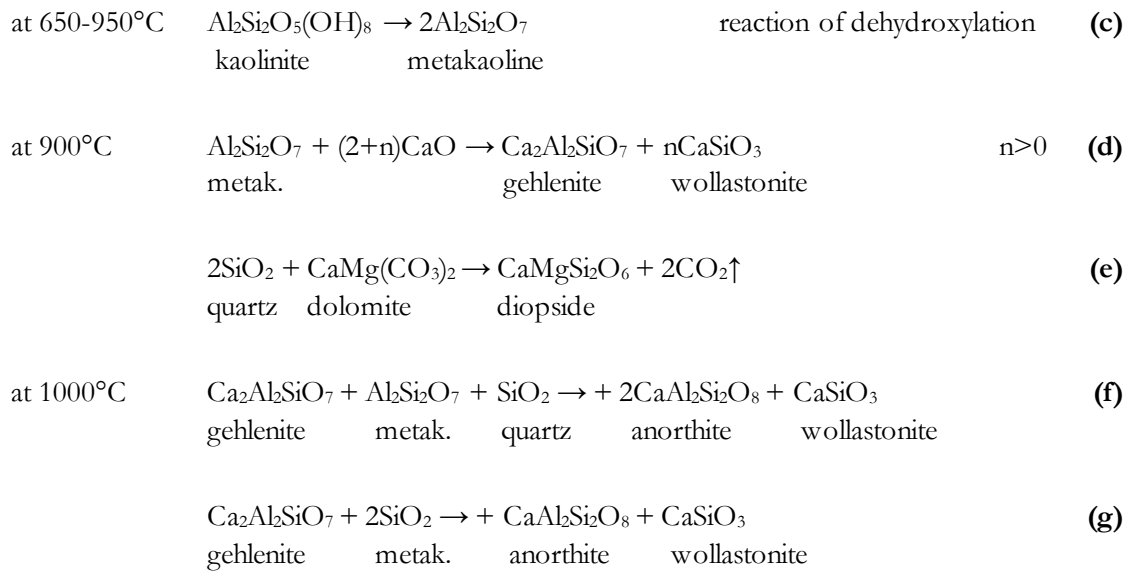
duration and atmosphere in order to avoid the destruction of the artefact. Other parameters which influence the reactivity of the carbonates are the particle size and the degree of crystallinity, explaining why the range of temperature related to the decarbonation reactions is so broad. At lower temperature (around 700°C) dolomite ($\text{CaMg}(\text{CO}_3)_2$) decomposes in CaO, periclase MgO and CO_2 (see reaction **(b)**). Magnesium oxide, in contrast to calcium oxide, does not react so fast with water, but may react very slowly forming brucite ($\text{Mg}(\text{OH})_2$) and limiting the problem related to the structure collapse. However, calcium oxides react with acid oxides resulting by decomposition of silicates, as clay minerals, and they form calcium-silicates and alumina-silicates at high temperature (above 900°C), the so-called high-temperature crystalline phases [44].



Moreover, calcareous components affects, as well as other parameters as iron oxides, the colour of the final product. In oxidizing condition the colour tends to creamy and light pink and in reducing atmosphere turns into grey-white colour, that happens because calcite influences the redox reaction of iron oxides [6], [18], [39], [41], [53], [54].

At 870°C the second change of quartz takes place: from β -quartz to tridymite; it does not affect the structure during heating procedure but may provoke structural tensions during cooling [15].

900°C – 1100°C. At this range of temperature the crystalline lattice of clay minerals is destroyed and new phases are formed. High-temperature crystalline phases are the result of the reactions involving carbonates, calcium oxides and silicates (see reaction **(c)**, **(d)**, **(e)**, **(f)** and **(g)**). These secondary minerals include gehlenite ($\text{Ca}_2\text{Al}_2\text{SiO}_7$), diopside ($\text{CaMgSi}_2\text{O}_6$), wollastonite (CaSiO_3) and anorthite ($\text{CaAl}_2\text{Si}_2\text{O}_8$). Aluminium minerals, as spinel (MgAl_2O_4), mullite ($\text{Al}_6\text{Si}_2\text{O}_{13}$) or γ -alumina ($\gamma\text{-Al}_2\text{O}_3$), tend to form at 1100°C as a result of illite and carbonate decomposition and reaction [15], [55]–[57]. Mullite appears with a needle-shape and plays the role of a skeleton increasing the strength and reducing deformation during formation of the glassy phase [18], [58], [59].



When the temperature is high enough, the sintering and vitrification processes begin. There is a development of a partial fusion and fusion of the grains and the consequences are related to porosity, colour, hardness and heat resistance. The porosity is reduced also because of the grain growth at the expense of small grains [26]. Compounds, such as potassium oxides present in illite clay mineral or calcium oxides, act as fluxes in the paste encouraging sintering process. In this process particle surfaces begin to fuse and stick to others, pores become more spherical till they are eliminated increasing the density. The extension of sintering is the vitrification process as heating continues and the glassy phase is formed. Glass formation usually begins at around 1100°C, and physical changes as shrinkage due to the loss of open porosity and the development of close porosity occur [18], [26], [36], [60]. The microstructure of the matrix appears more consolidated and the gain of volume due to new phases balances the shrinkage occurred at lower temperatures [15].

Furthermore, anatase (TiO_2), present as impurities in clay or added to obtain lighter colouring, is stable at room-temperature and when potteries is fired at 1000°C it is converted to the high-temperature phase, rutile [35], [61].

New crystalline phases, presence or absence of determined minerals and/or compounds, porosity and microstructure, as a consequenc of chemical and physical transformations throughout firing potteries, are some of the features used as indicators of firing conditions. The study of those, by means of diagnostic analyses, may allow to evaluate the firing temperature and atmosphere conditions able to investigate the production technique and, hopefully, characterize a particular workshop.

2.5. Bibliography

- [1] M. Vidale, *Ceramica e Archeologia*. Carocci, 2007.
- [2] P. B. Vandiver, O. Soffer, B. Klima, and J. Svoboda, “The origins of ceramic technology at dolni vecaronstonice, czechoslovakia,” *Science*, vol. 246, no. 4933, pp. 1002–1008, 1989.
- [3] S. C. Rasmussen, “Origins of Glass: Myth and Known History,” in *How Glass Changed the World*, vol. 3, Springer Science & Business Media, 2012, pp. 8–11.
- [4] C. B. Carter and M. G. Norton, “Some History,” in *Ceramic Materials: Science and Engineering*, New York, NY: Springer New York, 2007, pp. 15–32.
- [5] C. B. Carter and M. G. Norton, “Ceramic Materials,” no. 1, 2013.
- [6] N. Cuomo di Caprio, *Ceramica in Archeologia 2. Antiche tecniche di lavorazione e moderni metodi di indagine*, L’Erma di. 2007.
- [7] E. Giannichedda and N. Volante, “Materiali e tecniche di fabbricazione,” *Introduzione allo Stud. della Ceram. Archeol.*, pp. 3–32, 2007.
- [8] M. Valášková, “Clay, Clay Minerals and Cordierite Ceramics - A Review,” *Ceram. - Silikaty*, vol. 59, no. 4, pp. 331–340, 2015.
- [9] B. Velde and I. C. Druć, *Archaeological Ceramic Materials: Origin and Utilization*. Springer Science & Business Media, 2012.
- [10] C. J. C. Reeves George M, Sims Ian, *Clay Materials Used in Construction*, no. 21. 2006.
- [11] T. W. Smoot, “Clay Minerals in the Ceramic Industries,” *Clays Clay Miner.*, vol. 10, no. 1, pp. 309–317, 1961.
- [12] M. Gorea and M. Benea, “Characterization of some days used for whiteware ceramics ii. technological characterization,” *Ceramics*, pp. 77–84, 2002.
- [13] C. Klein and C. S. Hurlbut Jr, *Manual of mineralogy*. 1993.
- [14] B. Mason and L. G. Berry, *Elements of Mineralogy*. W. H. Freeman and Company, 1968.
- [15] L. Campanella, *Chimica per l’Arte*. Zanichelli, 2007.
- [16] R. C. Mackenzie, “The classification and nomenclature of clay minerals,” *Clay Miner. Bull*, vol. 4.21, pp. 52–66, 1959.
- [17] D. M. Roy and R. Roy, “Tridymite-cristobalite relations and stable solid solutions,” *Am. Mineral.*, vol. 49, pp. 952–962, 1964.
- [18] D. A. Santacreu, *Materiality, Techniques and Society in Pottery Production: The Technological Study of Archaeological Ceramics through Paste Analysis*. Walter de Gruyter GmbH & Co KG, 2014.
- [19] Z. Goffer, *Archaeological Chemistry: Second Edition*. 2006.
- [20] S. Peterson and J. Peterson, *The Craft and Art of Clay: A Complete Potter’s Handbook*. Laurence King Publishing, 2003.
- [21] C. Orton, M. Hughes, and M. Hughes, *Pottery in Archaeology*. Cambridge University Press, 2013.
- [22] K. Muller, *Potter’s Studio Handbook: A Start-to-Finish Guide to Hand-Built and Wheel-Thrown Ceramics*. Quarry Books, 2007.
- [23] H. D. G. Maschner and C. Chippindale, *Handbook of Archaeological Methods*. Rowman Altamira, 2005.
- [24] M. a. Courty and V. Roux, “Identification of wheel throwing on the basis of ceramic surface features and microfibrils,” *J. Archaeol. Sci.*, vol. 22, no. 1, pp. 17–50, Jan. 1995.
- [25] E. Gandon, R. Casanova, P. Sainton, T. Coyle, V. Roux, B. Bril, and R. J. Bootsma, “A proxy of potters’ throwing skill: Ceramic vessels considered in terms of mechanical stress,” *J. Archaeol. Sci.*, vol. 38, no. 5, pp. 1080–1089, 2011.
- [26] J. Henderson, *The Science and Archaeology of Materials: An Investigation of Inorganic Materials*. Routledge, 2013.
- [27] P. M. Rice, *Pottery Analysis: A Sourcebook*. 1987.

- [28] S. McCarter, *Neolithic*. Routledge, 2012.
- [29] NIIR Board of Consultants & Engineers, *The Complete Book on Glass and Ceramics Technology*. ASIA PACIFIC BUSINESS PRESS Inc, 2005.
- [30] G. Artioli, “Scientific methods and cultural heritage,” p. 520, 2010.
- [31] C. W. Elliott, *Pottery and Porcelain: From Early Times Down to the Philadelphia Exhibition of 1876*. Library of Alexandria, 2015.
- [32] S. Davison, *Conservation and Restoration of Glass*. 2003.
- [33] J. Britt, *The Complete Guide to High-Fire Glazes textures this popular medium makes possible*. Sterling Publishing Company, Inc, 2007.
- [34] P. Rogers, *Salt Glazing*. University of Pennsylvania Press, 2002.
- [35] C. B. Carter and M. G. Norton, “Ceramic Materials,” 2013.
- [36] G. B. Remmey, *Firing Ceramics*. World Scientific, 1994.
- [37] S. Weiner, *Microarchaeology: Beyond the Visible Archaeological Record*. 2010.
- [38] C. M. Sinopoli, *Approaches to Archaeological Ceramics*. Springer Science & Business Media, 2013.
- [39] M. Riccardi, B. Messiga, and P. Duminuco, “An approach to the dynamics of day firing,” *Appl. Clay Sci.*, vol. 15, pp. 393–409, 1999.
- [40] K. Şerifakia, H. Bökea, Ş. Yalçın, and B. İpekoğlu, “Characterization of materials used in the execution of historic oil paintings by XRD, SEM-EDS, TGA and LIBS analysis,” *Mater. Charact.*, vol. 60, no. 4, pp. 303–311, 2009.
- [41] L. Maritan, L. Nodari, C. Mazzoli, a. Milano, and U. Russo, “Influence of firing conditions on ceramic products: Experimental study on day rich in organic matter,” *Appl. Clay Sci.*, vol. 31, no. 1–2, pp. 1–15, Jan. 2006.
- [42] R. King, “Provenance of day material used in the manufacture of archaeological pottery from Cyprus,” *Appl. Clay Sci.*, vol. 2, no. 3, pp. 199–213, Aug. 1987.
- [43] C. M. Stevenson and M. Gurnick, “Structural collapse in kaolinite, montmorillonite and illite day and its role in the ceramic rehydroxylation dating of low-fired earthenware,” *J. Archaeol. Sci.*, vol. 69, pp. 54–63, May 2016.
- [44] R. Ravisankar, S. Kiruba, P. Eswaran, G. Senthilkumar, and a. Chandrasekaran, “Mineralogical Characterization Studies of Ancient Potteries of Tamilnadu, India by FT-IR Spectroscopic Technique,” *E-Journal Chem.*, vol. 7, no. s1, pp. S185–S190, 2010.
- [45] R. Palanivel and U. R. Kumar, “The mineralogical and fabric analysis of ancient pottery artifacts (Análise mineralógica de fragmentos de peças cerâmicas antigas),” vol. 57, pp. 56–62, 2011.
- [46] A. Mangone, L. C. Giannossa, G. Colafemmina, R. Laviano, and A. Traini, “Use of various spectroscopy techniques to investigate raw materials and define processes in the overpainting of Apulian red figured pottery (4th century BC) from southern Italy,” *Microchem. J.*, vol. 92, no. 1, pp. 97–102, May 2009.
- [47] S. Shoval, “Using FT-IR spectroscopy for study of calcareous ancient ceramics,” *Opt. Mater. (Amst)*, vol. 24, no. 1–2, pp. 117–122, Oct. 2003.
- [48] D. Yeskis, A. F. K. Van Groos, and S. Guggenheim, “The dehydroxylation of kaolinite,” *Am. Mineral.*, vol. 70, no. 1–2, pp. 159–164, 1985.
- [49] M. A. Legodi and D. de Waal, “Raman spectroscopic study of ancient South African domestic day pottery,” *Spectrochim. Acta. A. Mol. Biomol. Spectrosc.*, vol. 66, no. 1, pp. 135–42, Jan. 2007.
- [50] C. Ionescu, L. Ghergari, M. Horga, and G. Rădulescu, “Early Medieval ceramics from the Viile Teii archaeological site (Romania): an optical and XRD study,” *Nucl. Instruments Methods*, vol. 52, no. 2, pp. 29–35, 2007.
- [51] I. Allegretta, D. Pinto, and G. Eramo, “Effects of grain size on the reactivity of limestone temper in a kaolinitic day,” *Appl. Clay Sci.*, vol. 126, pp. 223–234, 2016.
- [52] N. S. Müller, V. Kilikoglou, P. M. Day, and G. Vekinis, “The influence of temper shape on the mechanical properties of archaeological ceramics,” *J. Eur. Ceram. Soc.*, vol. 30, no. 12, pp. 2457–2465,

- Sep. 2010.
- [53] J. Molera and T. Pradell, "The colours of Ca-rich ceramic pastes : origin and characterization," 1998.
- [54] G. Cultrone, E. Sebastián, K. Elert, M. J. de la Torre, O. Cazalla, and C. Rodríguez-Navarro, "Influence of mineralogy and firing temperature on the porosity of bricks," *J. Eur. Ceram. Soc.*, vol. 24, no. 3, pp. 547–564, Mar. 2004.
- [55] M. Jordán, T. Sanfeliu, and C. D. la Fuente, "Firing transformations of Tertiary days used in the manufacturing of ceramic tile bodies," *Appl. Clay Sci.*, pp. 87–95, 2001.
- [56] M. J. Trindade, M. I. Dias, J. Coroado, and F. Rocha, "Mineralogical transformations of calcareous rich days with firing: A comparative study between calcite and dolomite rich days from Algarve, Portugal," *Appl. Clay Sci.*, vol. 42, no. 3–4, pp. 345–355, 2009.
- [57] A. İssi, A. Kara, and A. O. Alp, "An investigation of Hellenistic period pottery production technology from Harabebezikan/Turkey," *Ceram. Int.*, vol. 37, no. 7, pp. 2575–2582, Sep. 2011.
- [58] P. Colomban, N. Q. Liem, G. Sagon, H. X. Tinh, and T. B. Hoành, "Microstructure, composition and processing of 15th century Vietnamese porcelains and celadons," *J. Cult. Herit.*, vol. 4, no. 3, pp. 187–197, Jul. 2003.
- [59] M. Maggetti, J. Rosen, C. Neururer, and V. Serneels, "Paul-Louis Cyfflé's (1724-1806) terre de lorraine: A technological study," *Archaeometry*, vol. 52, no. 5, pp. 707–732, 2010.
- [60] R. Palanivel and S. Meyvel, "Microstructural and microanalytical study - (SEM) of archaeological pottery artefacts," *Rom. Reports Phys.*, vol. 55, no. 3–4, pp. 333–341, 2010.
- [61] D. de Waal, "Raman investigation of ceramics from 16th and 17th century Portuguese shipwrecks," *J. Raman Spectrosc.*, vol. 35, no. 89, pp. 646–649, Aug. 2004.
- [62] D. M. Kenrick, *Jomon of Japan: The World's Oldest Pottery*. Kegan Paul International, 1995.
- [63] P. T. Nicholson and I. Shaw, *Ancient Egyptian Materials and Technology*. Cambridge University Press, 2000.
- [64] A. Rathje, M. Nielsen, and B. B. Rasmussen, *Pots for the Living, Pots for the Dead*. Museum Tusulanum Press, 2002.
- [65] C. M. Stevenson and M. Gurnick, "Structural collapse in kaolinite, montmorillonite and illite day and its role in the ceramic rehydroxylation dating of low-fired earthenware," *J. Archaeol. Sci.*, vol. 69, pp. 54–63, 2016.

3. Methods and Materials

Summary

This chapter is focused on materials and methods employed. It is discussed the investigation strategy adopted in order to investigate the relationship between chemical-microstructural changes and the final features of the artefacts. It gives a summary of the diagnostic techniques applied and what kind of information these techniques are able to provide when applied in ceramic material investigation. Details of experimental set-ups and conditions are also provided. Furthermore, there are presented and described the ceramic samples investigated which are: raw ceramic materials laboratory made, archaeological sherds excavated at Torcello (in the Venetian Lagoon) and historical potsherds from German sites.

3.1. Investigation Strategy

It was developed an investigation strategy in order to provide information related to archaeological questions in the domain of composition and production techniques of the selected ceramic sherds. The research was carried out encouraging interdisciplinary connections and having collaboration with national and international institutions, such as ENEA Research Centre in Rome, Saint-Petersburg University and Senckenberg Museum in Dresden.

Several diagnostic techniques were used in this research work to characterize ceramic materials in order to establish a scientific method able to evaluate the impact of different production techniques on the final ceramic product and define the membership of a potsherd to a certain production site.

The investigations started analysing and defining the relationship between chemical and microstructural changes of the ceramic objects considering known samples. It was set up an innovative and systematic procedure in order to better study the morphological and chemical-mineralogical changes in depending on firing temperature. Therefore, raw ceramic materials were made in laboratory following traditional recipes and they were submitted to different thermal treatments (between 400° and 1000°C).

Subsequently, real case studies were investigated by a reverse procedure: from the analysis and study of the final features of the artefacts to the identification of the production techniques used. Different kind of samples, as historical and archaeological ceramic fragments from the Venetian Lagoon and sites of Germany, were taken in to consideration.

Chemical, physical and petrological features were studied by the joint use of traditional and

non-traditional analytical methods in order to evaluate the best scientific approach able to investigate pottery production techniques. The methods were chosen on the base of the information required and the data reported in literature. About innovative methods, they were chosen because promising tools in cultural heritage investigation and may be suitable in archaeometric research on pottery. So, the application of innovative techniques exploiting their advantages were explored in this field.

A multi-analytical approach was applied and chemical composition, mineral phases, microstructure as well as morphology of potteries were investigated, due to the fact that these features depend on the native material composition, technology, and conservation state in particular for the samples from archaeological excavation.

Optical and morphological studies by Polarizing Microscopy (OM) and Scanning Electron Microscopy (SEM); chemical characterization by X-ray Diffraction (XRD), Fourier-Transform Infrared Spectroscopy (FT-IR), micro-Raman spectroscopy (μ -Raman) and X-ray Fluorescence (XRF); and microstructural analysis by Mercury Intrusion Porosimetry (MIP) were performed. Encouraging the use of non-destructive techniques, UV-Vis spectrophotometry, Laser Induced Fluorescence (LIF) and the micro-destructive Laser Induced Breakdown Spectroscopy (LIBS) were applied to deepen the chemical characterization and the production techniques of the ceramic glaze. Moreover, complementary microstructural investigation of the ceramic pastes respecting the integrity of the artefact was carried out by X-ray micro-Computed Tomography (μ -CT). These techniques are new tools only recently applied within conservation science, but not yet widely employed within archaeology.

The investigation strategy adopted is reported in **Fig.8**, where the diagram shows the analysed sample typologies and the choice of the diagnostic techniques. 15 laboratory-made raw ceramics; 15 archaeological ceramic fragments from Torcello excavation; and more than 70 (73) German sherds were analysed in this research work.

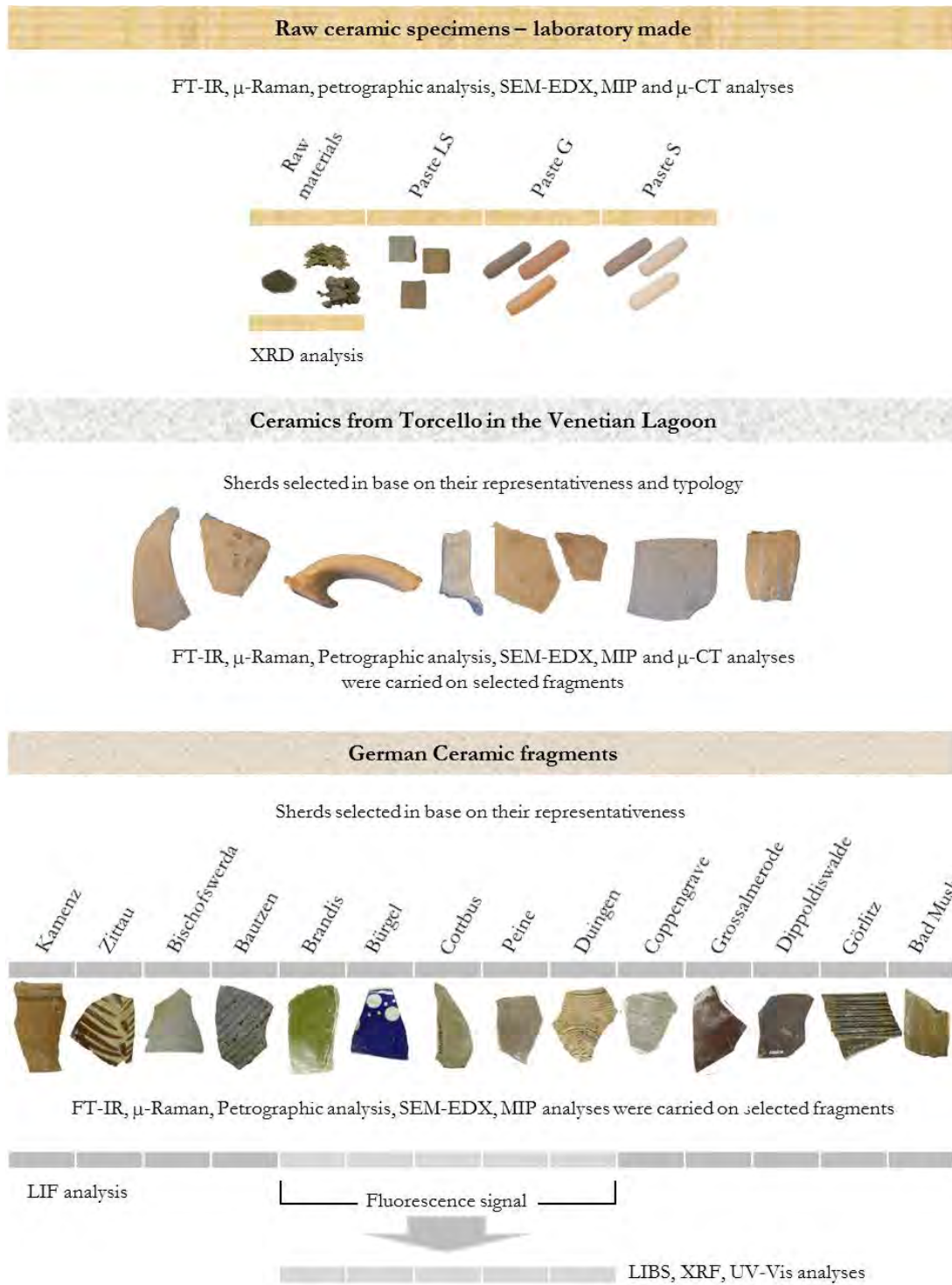


Figure.8. Diagram representing the investigation strategy. There are indicated the diagnostic techniques used and the typology of the samples along with some representative pictures.

3.2. Investigation Techniques

In line with the aim of the research and its investigation strategy, in these paragraphs are reported the analytical techniques used with a brief explanation of the principles and tool descriptions.

3.2.1. Fourier-Transform Infrared Spectroscopy (FT-IR)

Infrared spectroscopy was used to analyse the chemical composition of ceramic samples in terms of molecular species present. The obtained spectra were compared with data reported in literature, which allowed the attribution of the vibration bands to mineral species [1]–[4]. The measurements were carried out by means of FT-IR Nicolet Nexus 750 spectrometer in transmission configuration using mixture of sample powder and KBr to form pellets (1:100-wt.% sample/KBr). Spectra were recorded in the mid-infrared range 4000–400 cm^{-1} as a ratio of 64 single-beam scans at 4 cm^{-1} resolution. Baseline subtraction, when necessary, were performed using Omnic 6.0 and OriginPro9 software. All the ceramic samples were analysed by this technique.

3.2.2. Micro-Raman Spectroscopy (μ -Raman)¹

Potsherds were cut to obtain body-glaze cross-sections, embedded in polyester resin and then polished in order to have flat surface. The system is a custom-made micro-Raman, based on a single 320 mm focal length imaging spectrograph (Triax - 320 Horiba Jobin Yvon), equipped with a holographic 1800 g/mm grating and a liquid nitrogen cooled CCD detector. The excitation source was a Spectra Physics Ar⁺ ion laser (Stabilite 2017) operating at 514.5 nm. An optical microscope (Olympus BX40) equipped with three objectives, 20 \times /0.35, 50 \times /0.75 and 100 \times /0.90, was optically coupled to the spectrograph. Microscope objective 50 \times was employed to focus on the samples and the visual camera attached to the microscope allowed the selection of different points from which to collect Raman spectra, obtained by averaging 10 scans and with 1.5–2.0 cm^{-1} spectral resolution. The laser power was set at 8 mW and recording time at 10 s. Peak at 520 cm^{-1} of the silicon standard was used for calibration. Baseline subtraction, when necessary, were performed using OriginPro9 software. Selected samples were analysed by this technique.

¹ Micro-Raman analyses were carried out at the Department of Chemical Sciences of University of Padua in collaboration with Prof. Danilo Pedron, who is kindly acknowledged.

3.2.3. Laser Induced Fluorescence Spectroscopy (LIF)

It could be considered an innovative technique applied in the characterization of archaeological artworks which provides non-destructive and non-invasive qualitative analyses. In this research, the potentiality of LIF applied in the study of ceramic artefacts is explored and evaluated. This technique offers the advantages to be sensitive, non-destructive, remote, portable, and has been used as a diagnostic tool for artworks with successful results [5]–[8]. Despite great performances of this technique, only a few studies regarding LIF applied on archaeometric research on pottery were found in literature [9], [10]. The fluorescence in minerals is sensitive to activator elements, impurity ions, defects, as well as chemical composition and crystal lattice [11], [12]. Actually, LIF analyses may be useful to detect trace elements in minerals [13], [14]. In the present study LIF was applied to obtain indication of both ceramic glaze and matrix composition.

LIF analyses were performed at ENEA Research Centre in Frascati (Rome)². The experiments were carried on using a radiation source Thomson DIVA diode pulsed Nd:YAG laser with excitation wavelength of 266 nm, a repetition rate of 20 Hz with a pulse duration of 8 ns, and a laser fluence of 0.9 mJ/cm². The LIF apparatus was made at the ENEA laboratory (**Fig.9**) and it is described with more details in the references [7], [15]. The spectrometer was an Ocean Optics USB 4000, its working range is 200–900 nm and appropriate filters were placed at its entrance in order to avoid the backscattered radiation and the second order of the emissions at lower wavelengths. No optical elements were used to collimate the laser beam and the resolution was approximately 1 to 2 nm, inferred from the spot size on the target. The digitized spectrum is transferred to a portable computer where a LabView programme allowed the user to set experimental parameters, control data acquisition and perform a preliminary data analysis.

LIF analyses were performed on selected German sherds.

² Thanks to the collaboration with Dr. Luisa Caneve, who is kindly acknowledged.

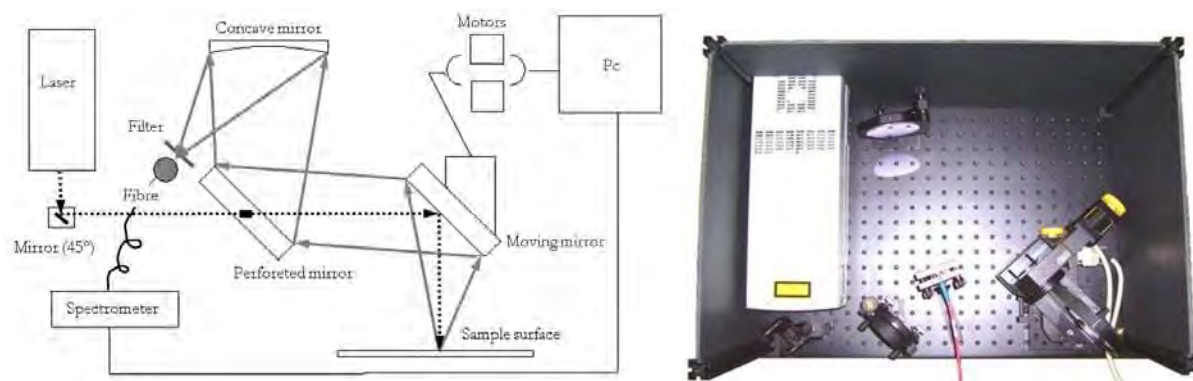


Figure.9. Schematic LIF set-up³ on the left, and on the right picture of the system in the portable box (60x115x45 cm³). LIF set-up includes: laser, mirror at 45°, perforated mirror, optical fibre connected with the spectrometer, concave mirror and moving mirror driven by small motors controlled by the operator from the Pc.

3.2.4. UV-Vis Spectroscopy

Reflectance spectrophotometry in the UV-Vis range was used as powerful and non-invasive tool to obtain spectroscopic information. It is by now widely applied in cultural heritage investigation of paintings, pigments and recently on ancient glass characterization allowing to obtain information regarding used materials, fabrication techniques and originality of the glass pieces [16]–[20]. In this research reflectance analysis was used in order to evaluate its potentiality to be a beneficial tool in glaze studies as it was for ancient glass materials. It was employed with the aim to investigate the coloured glazes present in order to provide as much as possible information on the colouring agents, without sampling operation. These analyses were performed at TU Bergakademie Freiberg, at the Department of Mineralogy⁴. Reflectance spectra were recorded by UV-Vis Specord*50 spectrometer with double-beam mode made by Analytik-Jena. The spectra were recorded from 200 to 1100 nm using an internal integrating-sphere system (Ulbricht sphere), where only diffuse reflected light is measured. Analyses were performed by placing the sample in front of the incident light window, and concentrating the light reflected from the sample on the detector. Furthermore, to control the spectrometer and record the data, WinASPECT* software was used. The UV-Vis spectrophotometry was applied on selected German sherds.

³ The presented system was developed and patented by the Diagnostics and Metrology laboratory of ENEA Research Centre, Frascati, Rome.

⁴ Thanks to the collaboration and cooperation of Prof. Gerhard Heide and Margitta Hengst.

3.2.5. X-ray Fluorescence Analyses (XRF)

Philips MiniPal X-ray fluorescence spectrometer was employed in this study on selected German sherds. It was used to detect the chemical composition in the ceramic body and glaze in terms of major, minor and some trace elements. Pottery sherds were placed in the holder samples with their surface perpendicular to the detector axis. The analyses were carried out in He atmosphere, without filter, at 18 kV and in the range of 50–100 μ A.

3.2.6. Laser Induced Breakdown Spectroscopy (LIBS)

LIBS is a laser-based atomic emission spectroscopy which provides information about elemental composition. It is a micro-destructive multi-elemental technique which is able to provide highly sensitive qualitative data. Application of LIBS for chemical characterization of art materials, such as paintings, pigments and metals, provided great results. In the last decades LIBS spectroscopy has been increasingly applied to CH characterization and it is often used in combination with complementary laser techniques as LIF and Raman spectroscopy [6], [15], [21]. Data reported in literature showed its application also in characterization of ceramic materials as an alternative method to other spectroscopic techniques considering its advantages to be rapid, remote, applicable in situ and avoiding sampling preparation [9], [22]–[25].

The energetic laser pulses are focused on the sample surface⁵ and produce a micro-plasma of ionized matter. Plasma emission from atomic species can be spectrally resolved and recorded, and it represents a spectral signature of the chemical composition [26]–[28]. LIBS allows to carry out measurements in laboratory or in situ conditions⁶ with a minimal loss of material. It is considered a micro-destructive technique due to the atom ablation which produces a crater of 200-400 μ m of diameter, as it shown in **Fig.10 (b)** [6], [21]. The experimental apparatus for LIBS measurements used in this research and shown in **Fig.10 (a)** includes a solid state laser source (Nd:YAG Handy Quanta System) operating at 1064 nm. The analyses were carried out at ENEA Research Centre laboratory in Frascati (Rome)⁷ at atmospheric temperature and pressure. Some tests were carried on in order to optimize the experimental conditions. The pulse duration was 8 ns, the repetition rate was set at 10 Hz and the energy at 50 mJ, which yields a fluence of about 40 J/cm². The laser beam is focalized onto the target surface by a lens. The plasma emission is collected by an optical system and focused by an optical fibre to the entrance of high-resolution monochromator (Jobin Yvon model TRIAX550) coupled to an intensified CCD

⁵ LIBS is able to investigate samples in the form of gases, liquids and solids [28].

⁶ Working conditions of LIBS technique include space, undersea and Antarctic conditions [66].

⁷ Thanks to the collaboration with Dr. Luisa Caneve, who is kindly acknowledged.

detector with a spectral range⁸ of 200-1000 nm. The TRIAX550 is equipped with three different gratings and in this experiments the grating of 1200 grooves/mm was chosen. Furthermore, for the detection of the plasma, a delay of signal acquisition between the laser pulse and the time of the registration was 1,5 μ s and the width of the acquisition temporal window was 5 μ s. There is no need of sample preparation and the potsherds were directly placed out of the laser focal plane. Pottery fragments were analysed by single and multiple pulses. Glaze ceramic fragments were investigated by successive LIBS measurements on the same spot, in order to provide a stratigraphic analysis able to identify the elemental composition at different depths. Further advantages of this diagnostic tool are to provide fast and remote measurements with reasonable costs.

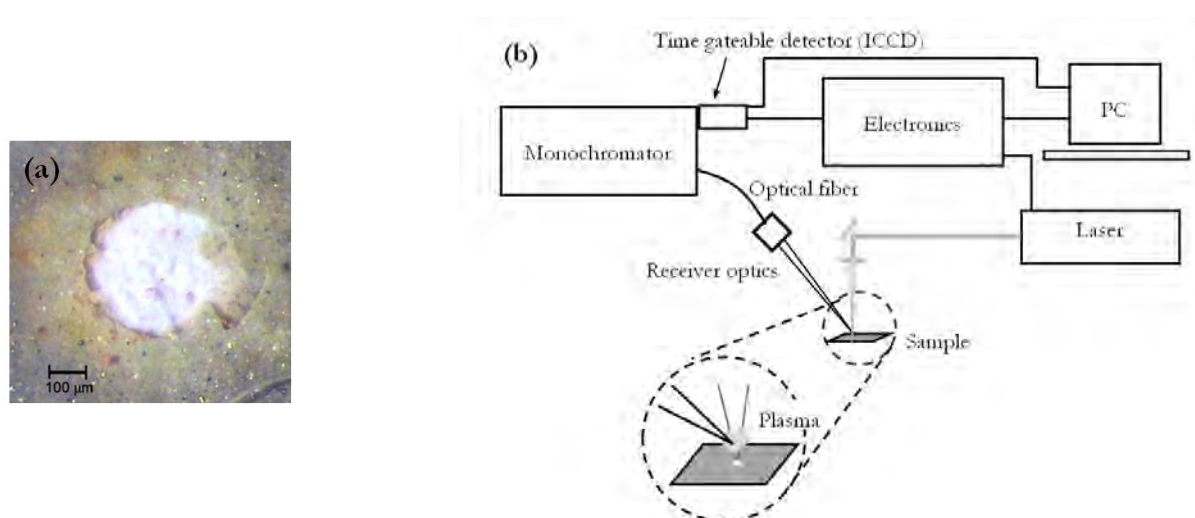


Figure.10. (a) Optical microscope picture of a crater by a single laser shot on the sample surface⁹. (b) Typical experimental LIBS set-up.

3.2.7. X-ray Diffractometry (XRD)

X-ray powder diffraction was used to define the mineralogical composition of the raw ceramic materials used to prepare laboratory-made samples¹⁰. Qualitative analyses were performed on dried and ground samples and XRD patterns were obtained by a Philips PW1050 diffractometer and a generator Philips PW1830 using Cu-K α radiation at 40 kV and 30 mA. Diffractograms were obtained by continuous scanning from 5 to 70° 2 θ with a step size of 0.02° 2 θ .

⁸ The spectral range was selected on the base of the main spectral emissions of the detected elements in ceramics and glazes.

⁹ The crater picture is shown in order to demonstrate the minimal invasiveness of LIBS technique. The picture refers to a study carried out by Caneve et.al., which published results regarding LIBS application on the characterization of Roman wall paintings from Pompeii archaeological site [21].

¹⁰ Thanks to Prof. Pietro Riello and his collaborators from the Department of Molecular Sciences and Nanosystems of Ca' Foscari University in Venice.

3.2.8. Optical Microscope (OM)

Light observations of the samples were performed on selected samples by an Olympus SZX16 optical microscope on polished cross-sections¹¹, which were obtained by embedding the samples in polyester resin and further polished by abrasive papers. Observation with the stereomicroscope allowed to collect information about the ceramic body and its main characteristics, such as mass background and presence of inclusions, and the cover layer, the presence/absence of engobe, colour and thickness of the glaze layer.

3.2.9. Petrographic Analysis and Image Acquisition

Selected ceramic sherds were petrographically analysed by means of Optical Polarising Microscopy (Olympus BX41) via observing thin-sections of those samples. Petrographic analyses allowed identification of the fabric defining: mineralogical composition, percentage, shape, size distribution, non-plastic inclusions and pores. Thin-sections of potsherds were realized at Petrography Department in the Museum für Mineralogie und Geologie of Senckenberg Naturhistorische Sammlungen in Dresden (Germany)¹². Furthermore, at the TU Bergakademie Freiberg (Germany)¹³, digitalization of thin-sections was performed both in plane and cross polarised light by a digital camera connected to the microscope in transmitted light. A ZEISS Axio Skop.A1 petrographic microscope equipped with a AxioCam ICc 1 Rev.4 (O) digital camera, 60N-C 2/3" 0,5x camera-adapter, N-Achroplan 5x/0,15 Pol M27 objectives and AxioVision Rel.4.8 software were used for the image acquisitions.

3.2.10. Scanning Electron Microscope coupled with Energy Dispersive X-ray Probe (SEM-EDX)

SEM-EDX analysis is able to recognize crystal structures and investigate the microstructure, morphology and elemental composition of the material. In this research, polished cross-sectioned samples were metalized with carbon or Au-Pt coatings for working in high vacuum conditions at 20 kV of accelerating voltage. The measurements were performed at Senckenberg Naturhistorische Sammlungen in Dresden (Germany)¹⁴, by means of ZEISS EVO50 microscope and Bruker XFlash 6/10 EDX detector.

¹¹ Afterwards, the same sections were also used for Scanning Electron Microscopy analysis.

¹² Thanks to the collaboration with Dr. Jan-Michael Lange and Martin Kaden which are kindly acknowledge.

¹³ Thanks to the collaboration with Prof. Gerhard Heide, head of the Institut für Mineralogie, and Susanne Eberspächer, researcher at Geowissenschaftliche Sammlungen of TU Bergakademie Freiberg, which are kindly acknowledge.

¹⁴ Thanks to the collaboration with Dr. Jan-Michael Lange of Petrography Department in the Museum für Mineralogie und Geologie, who is kindly acknowledge.

3.2.11. Mercury Intrusion Porosimetry (MIP)

Porosimetry analysis was used to investigate the microstructure, bulk density, total open porosity and pore size distribution of all raw ceramics made in laboratory and selected archaeological and historical ceramic samples. MIP technique provides information about the volumetric distribution of open pores depending on their dimension, considering the diameter of a circular pore. Meso and macropores¹⁵ in the pore size range between 0,003 – 20 μm (even >20 μm) were measured. The analysis is destructive and was carried on dried samples at 50°C of about 0,30 g; the measurements were repeated three times¹⁶ for each fragment in according to the rule Normal 4/80. Pascal 140 and Pascal 240 Thermo Nicolet instruments were employed. The volume of mercury (mm^3/g) intruded at a given pressure (kg/cm^2) provides the pore volume value, and the relation between intrusion pressure and pore radius is given by Washburn's equation:

$$r = (2\gamma \cos\theta) / P$$

where r is the pore radius (μm), γ is the mercury surface tension ($486,5 \text{ mN}/\text{m}^{-1}$), θ is the mercury/solid contact angle and P (MPa) is the absolute applied pressure [29].

3.2.12. Micro-Computed X-ray Tomography (μ -CT)

The X-ray Tomography is a non-destructive technique used with the aim to carry on 3D inspection of the ceramic samples providing morphological and physical information about their inner structure and preserving the integrity of the object [30]–[33].

Recently, due to these capabilities, μ -CT was used as diagnostic tool in cultural heritage materials (paintings, sculptures, jewellery, etc.) in order to obtain information about manufacturing process, presence of defects and conservation state [34]–[37]. The investigation by means of μ -CT of micro-structural characteristics of ancient ceramics is of particular interest in archaeometry and a few works were found in literature aiming at determining production technology and use of pottery by studying the present inclusions [37], [38]. The application of this non-destructive method allows to inspect the inner part of the ceramic object and in this research particular regard was given to the porosity of ceramic mixture, which was proved to have a key role to understand its structural parameters and the related material composition and firing temperature [39]–[41]. It was possible to evaluate and calculate through imaging elaboration total porosity (closed and open porosity) in terms of cumulative volume and pore size

¹⁵ IUPAC (International Union of Pure Applied Chemistry) defines the pore size according to the diameter size as micro ($<2 \text{ nm}$), meso (between $2\text{--}50 \text{ nm}$) and macropores ($>50 \text{ nm}$) [67].

¹⁶ The analyses were repeated using three different fragments of the same sample due to the destructiveness of the technique which involves the use of mercury.

distribution. The results are complementary to those obtained by MIP.

In order to obtain high spatial resolution, raw ceramic samples laboratory made and selected archaeological fragments excavated at Torcello were analysed with μ -CT system: SkyScan 2011 (see **Fig.11**), which allowed to investigate pores with diameter of 1-2 μm analysing cylindrical samples with diameter of 1 mm and height 5 mm. The SkyScan 2011 is a laboratory nano-CT scanner with spatial resolution in the range of hundreds of nanometres. The measurements were carried out at Geomodel Research Centrum of Saint-Petersburg State University (Russia)¹⁷ using a voltage of 50 kV, a current of 200 μA and performing a 180° rotation with a step size of 0,25°. Elaboration and visualization of images were performed by CTvox and CTan programs, and the percentage of the voids of the analysed samples was calculated.



Figure.11. X-ray μ -CT set-up SkyScan 2011 used at Geomodel Research Centrum of Saint-Petersburg State University.

¹⁷ Thanks to the collaboration with Alexander Kulkov of the Geomodel Research Centrum and Prof. Marianna Kulkova of Herzen State University of Russia, which are kindly acknowledge.



















3.3. The Ceramic Samples

3.3.1. Raw ceramic specimens made in laboratory

Three ceramic pastes were made in laboratory using different clays mixed with sand (20 wt%) and water, as the traditional methods [42]. The sand used is common to the three pastes and is the typical carbonate-silicate river sand with grain size between 150 and 250 μm , supplied by San Marco Laterizi s.r.l., Venice. The three different clay materials used are: a local Ca-rich clay, also provided by San Marco Laterizi s.r.l., used for the paste named **LS**; and two German kaolin-rich clays, one from Triebel in Saxony and the other from Frohnsdorf in Thuringia, used for the pastes named **S** and **G** respectively, both supplied by Landesamt für Archäologie Sachsen in Dresden¹⁸. These raw materials were chosen due to their similarity with the chemical-mineralogical composition of the historical samples of the case studies.

The pastes were shaped as prisms ($4 \times 4 \times 1,5 \text{ cm}^3$) and cylinders ($r=1 \text{ cm}$, $h=5 \text{ cm}$) and were left to dry at room temperature (23°C) for 7 days. Afterwards, the raw pastes were submitted to thermal treatments at different temperatures from 400°C to 1000°C for 8 hours each. The temperatures were selected depending on the main transformations which occur into ceramic materials during firing, as reported in the previous chapter 2.4. Pictures of the raw materials used and the samples fired at different temperatures are reported in **Tab.3**.

Table.3. Raw materials used to form the ceramic pastes made in lab and the raw ceramics after each thermal treatment.

Raw Materials		Firing Temperature				
		T0 (23°C)	T1 (400°C)	T4 (700°C)	T6 (900°C)	T7 (1000°C)
Sand	Local clay LS 					
	German clay S 					
	German clay G 					

¹⁸ Thanks to the collaboration with Dr. Stefan Krabath from Landesamt für Archäologie Sachsen in Dresden, and Nadine Holesch of Max-Planck-Institut für ethnologische Forschung in Halle/Saale, which are kindly acknowledge.

3.3.2. Ceramics from the Venetian Lagoon

Selected ceramic samples from Late Antique and Early Medieval contexts have been considered in this study. Those were uncovered during the archaeological excavation carried out in the 2012-2013 within the Interreg Project “Share Culture” at Torcello, Venice Lagoon [43]. Considering the overall stratigraphic sequence, the findings have been classified on the basis of the age, type, and morphological characteristics [43]. The selected sherds can be attributed to three main groups related to three distinct chronological phases of the site: Late Antiquity (5th-7th centuries), Early Middle Ages (8th-10th century), Middle Age (10th- 11th centuries). During these phases the site of Torcello could be described as a trade centre (an emporium) with warehouses, piers, docks, embankments, living and artisanal quarters. Actually, the selected fragments found in Torcello site are part of a significant group of findings that testifies and illustrates the commercial contact with North Africa, Southern Mediterranean, East Mediterranean and Black Sea. The imported goods are mainly typified by amphora-type vessels imported in Torcello in the framework of oil, wine, and spice trade. According to the archaeological sequences, the most intense period of the exchange activities may be ascribed between the 7th and the 10th centuries.

The three ceramic groups (see **Tab.4**) considered in this study are the following:

a) Late Antique Amphora are mostly produced in North African, in particular in the Eastern Mediterranean as Egypt, Syrian-Palestinian Region, Turkey, Asia Minor and Aegean area. The fragments found in Torcello are part of the most widespread types defined Late Roman (LR). The LR1 form evolved considerably through the 4th to 7th centuries, and in the early to mid-5th century AD the LR1 was first exported en masse to western ports. 6th century examples differ by having a more cylindrical body. The walls are characteristically “turned” to create stepped wide flat sections separated by a narrow ridge. LR1 were mainly produced in the Roman provinces of *Cilicia* and Cyprus, and both wine and oil have been suggested as contents. LR2 is a globular amphora with a short conical neck. However, this type was produced for some three hundred years and shows a development of form over that period: by the middle of the 6th century the form is more oval in shape and the neck sharply conical. At this time the basal knob has shrunk to a basal wort. Production is attested in Aegean area, and there are evidence for both wine and olive oil [43], [44].

b) Early Medieval Global Amphora, from the South-Eastern Mediterranean; were defined as globular after the Aegean LR2 amphorae, which are quite morphologically distinguishable but the variety of ceramic bodies suggests different productions and provenances. In the 7th century different productions from the centre of Italy, Northern Aegean and coasts of Black Sea, where globular amphorae were particularly widespread, appeared in the Venetian Lagoon [45]. Actually,

previous excavations in Torcello and San Francesco del Deserto¹⁹ show ceramic fragments very similar to those found during the excavation in 2012-2013, confirming the circulation of amphorae as a consequence of commercial trade in that historical period [43], [45], [46]. In some cases, preliminary analysis did not allow a certain classification of the finds as part of globular amphorae and further investigation should be made in this regard. Furthermore, although the literature shows documentation on the facilities used to make ceramics in the Mediterranean area, scholars are not still able to define accurate manufacturing sites and their production. The consistent occurrence of those amphorae in every important excavations undertaken in the north Adriatic region (Ravenna, Classe, Venice, Comacchio, Torcello, Grado) suggests a pivotal role of the emerging trade hubs located in the lagoons for the commercial contact between the Mediterranean and western Europe. Cyprus, Crete, the northern Aegean, the Southern Italy (Apulia, Calabria), and probably the Black Sea are possible locations of imports, some were transported by way of Constantinople or Alexandria, due to the instance that in the excavated sites there were not found traces of kilns able to provide ceramic productions of amphorae²⁰ [43], [47]. These aspects complicate the study of technological aspects and the identification of artefact provenance. For this reason, archaeometric analyses of excavated pottery fragments at Torcello were carried out. The aim is to characterize the artefacts and provide further information on production techniques, useful to enlarge the knowledge of this ancient production. This type of amphora is not properly standardized and there are a variety of subclasses. It is difficult to distinguish globular amphorae into classes and also to other globular containers of late antique tradition, especially those widely disseminated during the 7th century. As for the contents, both wine and oil have been suggested and found in content analysis. Analysis undertaken in similar vessels uncovered in Comacchio, showed that the amphorae were used for the transport of oil and probably for solids, such as grains or minerals [43], [48].

c) Single-glazed pottery, probably manufactured regionally or at least in North Italy. In this study, two single-fired glazed ceramic fragments were analysed. They are characterized by a sandwich-cooking with a glossy coating of yellow-green and brown colour (goldenrod-amber colour). Single-fired glazed ceramics, known also as *forum ware*, appeared at the end of the 8th century and became common in the 9th-10th centuries. Those potteries, known as *Ceramica a Vetrina Pesante*, are very similar to Lazio Dorum ware. The forms are closed, sometimes decorated with reliefs petals, and they were probably used for domestic activities. Petrological analysis and macroscopic elements in similar fragments collected in Comacchio excluded a provenance from central Italy [49]. This kind of pottery have been traditionally considered as an archaeological

¹⁹ San Francesco del Deserto is another island in Venice archipelago, close to Sant'Erasmus.

²⁰ Thanks to Dr. Calzon for the insight information and considerations.

indicator of trade due to its Mediterranean exportation, but in the case of Torcello, as it has been suggested for Comacchio, it can suggest a local production connected with the economic activities of the Adriatic Emporia [50], [51].

The three groups of ceramic selected for the analysis describe quite well the complexity of the import goods and the distribution of ceramic containers in the Early Medieval emporia in the Adriatic area during the early middle age. The analysis were undertaken in order to better evaluate the technological characteristics of those vessels, as well as to contribute to the debate around some crucial archaeological and historic questions, such as: how to define the technical characteristics of the different types; how to understanding the technological shifts occurred between Late Antiquity and Early Middle age in the production of amphorae; how to verify if those possible different production techniques could help in a more precise grouping of the archaeological sherds.

3.3.2.1. Archaeological Excavation in Torcello

The archaeological excavation was carried out under the direction of Dr. Diego Calao, archaeologist from Ca' Foscari University of Venice. Ca' Foscari team in co-operation with the municipality of Venice and the Veneto Region have selected areas of Torcello archaeologically unstudied yet but believed extremely important for the archaeological potentiality of the Island. Torcello is one of the first settled island on the northern Venetian Lagoon (see **Fig.12**). It represents the historical memory of Venice and the aim of the excavation was to investigate the late antique origins of the Serenissima, looking at the settlement sequences and object productions in order to understand the history of ancient activities characterized by a complicated sequence of events²¹.

The excavated areas (named as 1000, 5000, 6000 and 7000), today re-covered with grass, are very close to the basilica of Santa Maria Assunta in the heart of Torcello, except for the area 6000 located more in the South-West side, as it is shown in **Fig.13**. The stratigraphy of the main areas covered the chronology of the Torcello history: from the Late Antiquity to Early and Modern Middle Age and up to the present days. In **Fig.14** it is shown the area 5000 during the excavation for providing a picture as an example of the archaeological site.

²¹ For further information about archaeological studies on Torcello see references [68]–[70].



Figure.12. Geographical location of Torcello island in the Venetian Lagoon²².



Figure.13. Location of the excavated areas, Torcello⁴.



Figure.14. Area 5000 during the excavation in 2012-2013 at Torcello⁴.

3.3.2.2. Archaeological Sherds





The archaeological sherds taken from excavations were treated in order to remove soil and deposits before subjecting them to diagnostic analyses. The applied cleaning methodology involved the use of water vapour at low pressure and temperature [43].

Ceramic sherds were selected in the areas: 1000, 5000, 6000. The fragments are ascribable to the three groups aforementioned: a) Late Antique Amphorae, b) Early Medieval globular amphorae, and c) Single-fired glazed. Few fragments have a not clear identification from a macroscopic point of view, defined as group d).

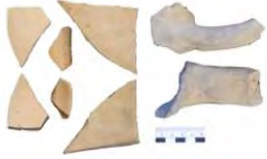





²² Picture by Dr. Diego Calaon, in *Torcello scavata. Patrimonio Condiviso* [43].




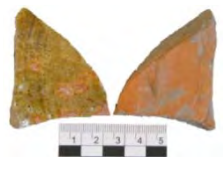

In **Tab.4** are reported pictures of the sherds and a brief macroscopic description, thanks to the help of the archaeologist Dr. Calaon.

Table.4. Pottery sherds from Torcello excavation: both sides pictures of each sample and macroscopic and archaeological²³ description.

GROUP A – Late Antique Amphora	
Samples and code*	Description and Archaeological attribution
<p>Tor_1151_4</p> 	<p>LR1, Part of the wall of LR1 amphora with cylindrical body.</p>
<p>Tor_1151_5</p> 	<p>LR1, Fragments of the wall with the characteristic presence of the stepped wide flat sections separated by a narrow ridge.</p>
<p>Tor_5157</p> 	<p>LR1, Fragments of the wall with the characteristic presence of the stepped wide flat sections separated by a narrow ridge.</p>
<p>Tor_6001_1</p> 	<p>LR2 Fragments of the ovoidal-section handle of a LR2 amphora.</p>

²³ Thanks to Dr. Diego Calaon and Prof. Claudio Negrelli of Ca'Foscari University of Venice for the archaeological information and the description of the ceramic sherds.

GROUP B – Early Medieval Globular Amphora	
Samples and code*	Description and Archaeological attribution
<p>Tor_1154_8</p> 	<p>Early Medieval globular amphora, Micaceous fabric, probably Aegean provenance.</p>
<p>Tor_1154_10</p> 	<p>Early Medieval globular amphora, light brown-greyish body. Micaceous fabric, probably Aegean provenance.</p>
<p>Tor_1159_2</p> 	<p>Early Medieval globular amphora, bottom side, light brown-cream body. Calcareous Fabric, Apulian (Otranto) possible area of production. Possible 10th century production</p>
<p>Tor_1167_1</p> 	<p>Early Medieval globular amphora, light brown body. Similar to the 9th-10th cent. Amphorae from Mljet Shipwreck, probable east Mediterranean or Black Sea Production.</p>
<p>Tor_1188_4</p> 	<p>Early Medieval globular amphora, light brown body. Micaceous fabric, probably Aegean provenance.</p>
<p>Tor_1210_1</p> 	<p>Early Medieval globular amphora, bottom part. Macroscopically is not possible to define or suppose any provenance area.</p>

<p style="text-align: center;">Tor_1224_2</p> 	<p>Early Medieval globular amphora, light brown body. Fragments of a wall of the first globular amphorae, 8th-9th cent.</p>
<p style="text-align: center;">Tor_5155_23</p> 	<p>Early Medieval Globular, light brownish-reddish body, decorated by parallel engraved lines over the entire surface. Probable Aegean production, with the distinctive decorations of parallel engraved lines, probably 7th- 8th century.</p>
<p style="text-align: center;">Tor_1155_1</p> 	<p>Early Medieval globular amphora, Aegean production. Dubious chronology, or 9th century or end of 10th century.</p>
GROUP C – Single-glazed Potteries	
Samples and code*	Description and Archaeological attribution
<p style="text-align: center;">Tor_1078_2</p> 	<p>Single-glazed pottery, reddish-greyish body. Goldenrod-amber glazed layer with dots. Probably locally produced and used in domestic setting. Closed form. Similar to S. Alberto Types, Emilia Romagna, 11th – 12th cent.</p>
<p style="text-align: center;">Tor_1151_1</p> 	<p>Single-glazed pottery, reddish-greyish body. Goldenrod-amber glazed layer with dots. Probably locally produced and used in domestic setting. Closed form. Similar to S. Alberto Types, Emilia Romagna, 11th – 12th cent.</p>

* The sample code is related to the area of excavation.

3.3.3. German Potteries

The historical ceramic fragments examined in this research, dating from the late 13th to 19th century, come from several sites located in the Central and Eastern Germany, and they include: stoneware, near-stoneware, unglazed earthenware and glazed earthenware (see glossary for further information).

In this study 14 different provenance sites were considered (Bad Muskau, Bautzen, Bischofswerda, Brandis, Bürgel, Coppengrave, Cottbus, Dippoldiswalde, Duingen, Görlitz, Grossalmerode, Kamenz, Peine and Zittau, as showed in **Fig.15**) and more than 200 sherds were provided from Landesamt für Archäologie Sachsen in Dresden²⁴. Due to the large amount of ceramic materials, a first selection of the samples to be analysed was made on the basis of macroscopic features which allowed a selection of 73 German sherds as the most representative fragments for each site. All the sherds considered in this archaeometric research are presented along with a brief description of the site in the **Tab.5**.



Figure.15. German map where there are indicated the Central and Eastern German provenance sites of the potteries analysed in this research.

Several ceramic types with incomplete sintered body, proto- and near-stoneware, can be considered as a preliminary stage of the development of ceramic production technique. The

²⁴ Thanks to the collaboration with Dr. Stefan Krabath from Landesamt für Archäologie Sachsen in Dresden, and Nadine Holesch of Max-Planck-Institut für ethnologische Forschung in Halle/Saale, which are kindly acknowledge.

emergence of a dense sintered ceramic body can be traced in Germany since around 1250 and a huge number of production sites were established in the subsequent periods [52]. The majority of these workshops had traded their products primarily in Central and North Europe and some of them reached the New World as well as the Far East [53]. These unique manufacturing conditions for ceramic materials outstanding in medieval Central Europe, are comparable only to China, where the development of stoneware began in the middle of the second millennium BC [53]. D. Gaimster and other collaborators [53] underlined very well the historical and stylistic relevance of the German stoneware production between 1200 and 1900. Actually, the German stoneware was a production model for the neighbouring and economic orbit regions, representing commercial and cultural exchange material over international boundaries due to their properties as extremely hard body, completely water-repellent and suitable for drinking, storage and trade purposes. During the late Middle Ages the stoneware produced in Germany was its main mass-products and international exports.

Stoneware technology as well as glazing process are the main issues of archaeological and historical interest of the German ceramic production.

Most of the information available from archaeological and historical sources about the German ceramic production regard only some of the provenance sites mentioned in this work and a very few scientific research were carried out in this field²⁵. Therefore, archaeometric analyses offer a new possibility to find out more about the applied technology and the distribution of the ceramic products.

3.3.3.1. Central-Eastern German ceramic production sites

A synthetic description of the ceramic production sites is given in this paragraph underlining the relevance of these productions which raise international interest.

In the area known as *Pottland*, along the rivers Weser and Werra in the south of Lower Saxony (Niedersachsen, German state), many villages were and still are ceramic wares producers, that since the 13th century an improvement of the ceramic technology created the new form of pottery: stoneware [54]. Stoneware is the result of firing at high temperature special and rare clay from the Tertiary period found only in a few deposits near Coppengrave, Bengerode and Duingen. Plentiful deposits of various types of clay for tobacco pipes, stoneware as well as slips were at Duingen, where the stoneware clays is still mined today from pits in Hils Hollow, outside

²⁵ D. Gaimster in [53] affirmed that art-historical and scientific approaches to this material culture were performed by the British Museum in London, thanks to its stoneware collection and those present at the Victoria and Albert Museum and Museum of London.

Duingen Forest. Indeed, many of the old pits may still be recognized today as hollows in the woods [55].

According to archaeological excavation data in North Hesse and Lower Saxony, many of the stoneware production sites in this area were deserted between the middle of the 14th and the beginning of the 15th century, while at Coppengrave and Duingen the production persisted although typological developments are unclear due to the lack of stratigraphic evidences. From the 16th century, Duingen was the only site which was producing the fully fused stoneware in large quantity, suggesting export markets to the north for kitchen, storage and pharmaceutical usages. Duingen never developed an individual and characteristic style, shape and decoration were strongly influenced by Rhenish and Central German stoneware. Whereas, at the beginning of the 17th century, Coppengrave became a significant supplier of high-fired ceramics to Amsterdam.

In a close region, Hesse German state, stoneware production followed a parallel development between the 13th and 15th century and the manufactures became concentrated in few centres, as Dreihausen and Grossalmerode. Evidence of pottery production since the 12th century were found in Grossalmerode, firstly with proto-stoneware and later, around 1600, with real stoneware [55]. The centre was characterized by products as tankards, ovoid jugs with rich ornaments in the manner of German Renaissance stoneware influenced by Saxony production.

These distinctive and parallel new wares in Hesse and Lower Saxony constituted an expression of the general upswing and cultural flowering of the so called *Weserrenaissance* (or *Werraware*), which is visible also by elaborated architecture, art and craftsmanship and trade. In 1618, the 30-years war reduced the population and the pottery production decreased. Throughout the 17th century, squat tankards with rudimentary ornaments became more common in both Hesse and Lower Saxony centres, signing the end of the elaborated *Werraware*. Between the 18th and 19th century, some ceramic production persisted and extent to the modern period. Grossalmerode was characterized by increasing product specialization, individual workshops producing water bottles, pharmacy jars and industrial ceramics, as well as Duingen and Coppengrave [53], [54].

The Eastern German states of Saxony and Thuringia, as well as Hesse and Lower Saxony, have a tradition of stoneware manufacturing since the late Middle Ages. Several kinds of clays were located in these states explaining the variety of the ceramic products in this German area. Pottery, stoneware, earthenware, faience were produced, as well as porcelain called as *white gold* [55]. In this area the rare kind of clay deposits is unique and responsible of the Meissen porcelain production, first porcelain in Europe in 1708 in Dresden by Johann Friedrich Böttger under Augustus the Strong [56]. Furthermore, since wars in the 15th century affected the medieval glass

production in Bohemia, glass blowers were made also in Thuringia and Saxony following the Bohemian tradition.

In 1660, Duke Frederick William of Altenburg in Thuringia confirmed the rights of a one of the oldest potters' guild which organized both production and distribution of the ceramic products. The pottery trade was into the regions (except for Waldenburg and Altenburg which exported their products outside the boundaries), however, the Renaissance and Baroque wares had and nowadays have high relevance for both artistic and technical achievement [53]. Only recently there were chances for the excavations of the sites and the first selection of Saxon and Thuringian wares was exposed at the Hetjens-Museum in Düsseldorf in 1979.

In 1990, excavations in Dippoldiswalde (close to Dresden, Saxony) found out mould fragments and stoneware wasters dating the 17th century probably closely to a 30-years war. Documentary records affirm pottery production since 1620 and local production was identified as earthenware vessels and stove-tiles, as well as finer decorated output which are exposed into modern museum collections. Although it was attested a Dippoldiswalde local production, it still refers to these potteries as *Annaberg* and *Freiberg* types²⁶, because before the excavations the ceramic production was attributed to these two cities. The ornaments are characteristic of the 17th century including cartouches containing carved diaper applied armorial devices, rosettes, palmettes, fruit and figurative motifs as portrait busts, biblical and mythological personifications [53]. Painted overglaze enamel and gilded decoration were not found among the Dippoldiswalde findings but they are typical of Annaberg-type stoneware.

Upper Lausitz potteries of Muskau (the spa city called Bad Muskau) and Triebel and Lawer Silesian centre of Bunzlau (today Boleslawiec) were two main regional industries from the late 16th century to the early 20th century situated in the East of the Elbe, river in Saxony. Despite the wars and international conflicts, these centres supplied high-quality stoneware in Eastern Germany, Bohemia, Moravia and Poland. Archaeological finds in Görlitz and Zittau indicated regional ceramic industry but the loss of information and materials due to the World War II make difficult the interpretation of the events [53]. From excavated contexts in both Dresden and Görlitz, the local finds suggested that the production was limited to a narrow range of bellied or ovoid jugs, pitchers or bottles and cylindrical or biconic mugs with flat and turned bases. Decoration was restricted to geometric rouletting around the body, horizontal rilling and incised wavy lines. During the 17th century there was a parallel development in Saxony: ovoid jugs and

²⁶ Annaberg was an important city in Saxony located very close to Erzgebirge mountains and mines, where since 1600 cobalt and copper mining began replacing the silver industry [55]. Freiberg has a rich tradition of silver mining and the pottery production played an insignificant role but the attribution was made on the basis of the pewter mounts and only recently (1980s) there was evidenced by excavations that Freiberg was not a production location [55].

jars remained the mainstay of production but the decoration expanded including floral and geometric motifs. Furthermore, manganese-purple was introduced together with cobalt-blue to produce also bichrome effects.

As an alternative, wares were covered entirely in cobalt-blue using *Smaltebenurf* technique, originated during the 16th century and which uses cobalt with salt introduced during the firing in the kiln. The technique became common and it was introduced by the Thuringian stoneware industry of Zeitz and Bürgel, clouding the distinction between contemporary Saxon and Thuringian jugs and storage jars. Despite there is a lack of available information, probably their products travelled beyond the borders of the regional trade. Both Zeitz and Bürgel stoneware of the 18-19th century share a stoneware body from light and dark grey to grey-brown colours. One of the finest example found of *Smaltebenurf* technique dated 1836 with cobalt-blue is represented by the vessel where was decorated with the arms of the Duchy of Saxony-Weimar and the initials of the potter Carl Friedrich Wilhem Otto from Bürgel [53].

Bürgel was a city with a great prestige, more known than Zeitz, and pottery production gave to the city the name of *Pottery City*. The potters initially had and used their kilns inside the town limits but later, due to the danger of fire, they had to move outside (1675), producing earthenware and grey stoneware simultaneously in the same particular kiln called Kassel kiln. This kilns the flames extended horizontally to the long chamber where different temperature could be reached in depending on the distance of the object to the flames [55]. It was common cobalt-blue glaze and smalt and it was made using pure blue coloured glass mixed with lead oxide and salt casting it into the firing chamber, and when the smalt melted it formed the characteristic dark-blue apron. The information about Bürgel is derived primarily from written sources, which illustrate the conditions of the 18th until the 20th century.

Production techniques, number of workshops and distribution of the products all over Central Germany were described also by Rottländer [57]. On the other hand, there are only a few data about sites like Peine, Cottbus, Brandis, Bischofswerda and Bautzen.

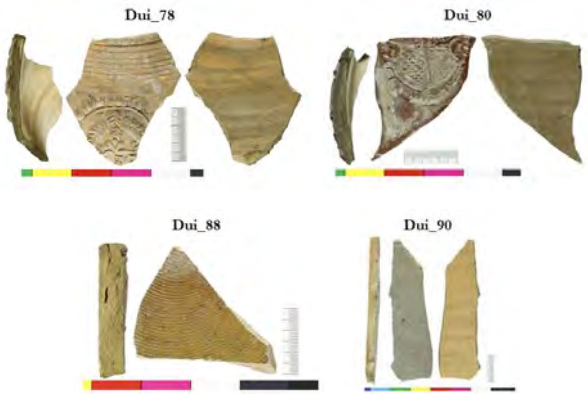
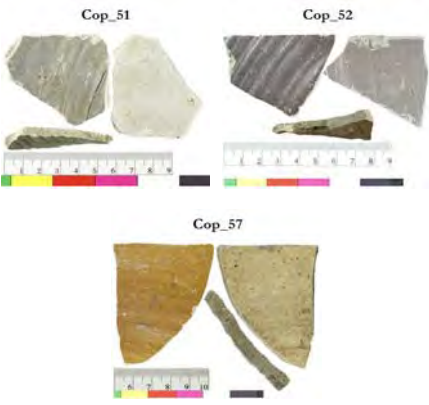
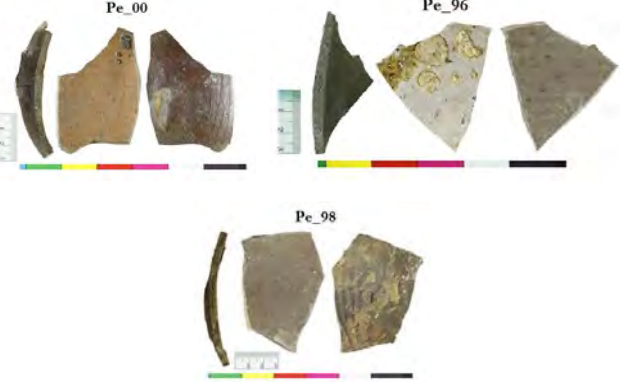
3.3.3.2. Central-Eastern German sherds

The excavated pottery wasters and kilns imply a local established workshop and gave a first impression on the produced types and style of ceramics. Furthermore, there are no other archaeological or historical sources available and archaeometric analyses offer a new possibility to find out more about the applied technology and the distribution of the ceramic products.

The studied materials are: stoneware, near-stoneware, unglazed earthenware and glazed earthenware and all the German sherds investigated in this research are reported in **Tabella.5**,

where few information are added for each sites thanks to the guidance of the archaeologist Nadine Holesch²⁷.

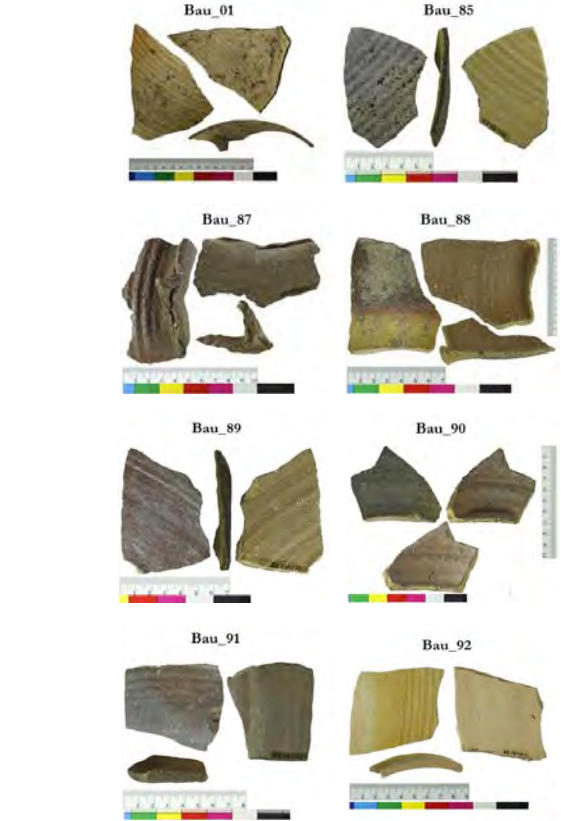

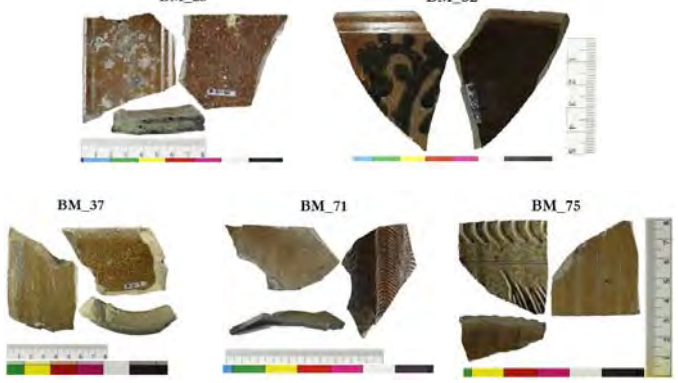
Table.5. German ceramic sherds analysed in this research are grouped on the basis of their provenance and a brief description of the sherds and the sites is given [52], [57]–[65].

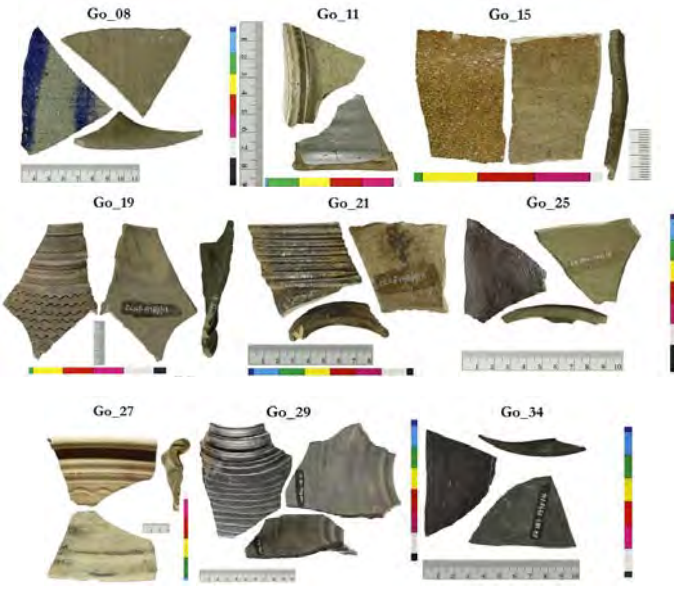

Lower Saxony	
 <p>Dui_78 Dui_80 Dui_88 Dui_90</p>	<p>Duingen</p> <p>The sherds are stoneware and earthenware with variety of body colours and decoration (dark brown and grey glazes; greyish, yellow and light reddish bodies). There are present sherds with the typical medallion bearing, armorial motif decoration.</p>
 <p>Cop_51 Cop_52 Cop_57</p>	<p>Coppengrave</p> <p>These sherds are earthenware with light greyish layered bodies.</p> <p>Coppengrave was a local and national important centre of ceramic production. Its development can be traced from the 13th to 19th century mainly based on archaeological sources, due to the lack of written sources. Great spectrum of vessels (pots, jugs, pans, paltres, etc.) and beginning of the production of Proto-stoneware during the mid or the second part of the 13th century.</p>
 <p>Pe_00 Pe_96 Pe_98</p>	<p>Peine</p> <p>The sherds are near-stoneware and earthenware. Grey and light yellow bodies; dark reddish and purple slips.</p> <p>Peine was first mentioned in 1130. Not further information are available.</p>

²⁷ Nadine Holesch of Max-Planck-Institut für ethnologische Forschung in Halle/Saale is kindly acknowledge.

Hesse	
	<p style="text-align: center;">Grossalmerode</p> <p>The sherds present grey and light tan colours of body with simple bands of notch-rouletting.</p> <p>During 16th century the economy was focus on production of alum stone, coal mining and pottery. In 19th century clay pipes and melting pots were also exported to Amerika.</p>
Thuringia	
	<p style="text-align: center;">Bürgel</p> <p>The sherds are earthenware and stoneware with light grey and yellowish bodies. Blue and dark brown salt-glazes, blue glaze and painted slip decorations are present.</p> <p>The town of Bürgel was founded by the monastery and mentioned first in 1234 as oppidum and 1307 as civitas. Famous for stoneware vessels with blue cobalt salt-glaze.</p>
Brandenburg	
	<p style="text-align: center;">Cottbus</p> <p>The sherds are earthenware with greenish-grey, light red and red layered bodies.</p>

Saxony	
	<p style="text-align: center;">Brandis</p> <p>The sherds are earthenware with light yellow bodies and with dark green glazes, yellow glaze, brown slip painting and dark purple slip decoration.</p> <p>Fireclay production was an important business emerged from local pottery workshops.</p> <p>Traces of pottery production are found thanks to a kiln dated around the 13th-4th century excavated by a local.</p>
	<p style="text-align: center;">Dippoldiswalde</p> <p>The sherds present light brown bodies with dark slip, grey glaze and low relief decoration.</p> <p>The site was mentioned the first time on 1218. The silver mining foundation is very important for the town, since the 15th and 16th century also lead and copper mining.</p> <p>Ceramic findings of Dippoldiswalde were firstly and wrongly attributed to Annaberg and Freiberg productions, Kiln and pottery stacking were known from the 18th-19th century, found at the Obertorplatz close to the city centre.</p>
	<p style="text-align: center;">Bischofswerda</p> <p>The sherds present grey and light grey ceramic bodies with concentric rilling around the bodies.</p> <p>Bischofswerda was a typical town called <i>Ostkolonisation</i> (<i>Colonisation of eastern parts of Germany</i>) since around 1200, reason of the plan (outline of the town) laid out in a grid pattern.</p> <p>Misfired pottery were found at the Töpfergasse (now called the Neumarkt) and Altmarkt, dated 15th-19th century, which evidences the production of renaissance stove tiles and the use of salt glazing technique.</p>

	<p style="text-align: center;">Bautzen</p> <p>The sherds present light tan, brown and yellowish colouration with concentric rilling around the bodies as decoration.</p> <p>Bautzen was at first mentioned as <i>Budusin</i>, a Slavic settlement in 1002 by Bishop Thietmar von Merseburg.</p> <p>It was importance in the middle ages due to the passage of the river Spree, crossroad of important national highways (<i>Via Regia</i>) and place of the religious and profane power of the whole Upper Lusatia.</p> <p>The potters produced near-stoneware and earthenware. <i>Falke-Gruppe</i>, as a special kind of high decorated near-stoneware, know from all over Europe, were also produced here.</p>
	<p style="text-align: center;">Kamenz</p> <p>The rim sherds present light grey and brown ceramic bodies with dark brown slips and glaze.</p> <p>Kamenz is situated on the passage of the <i>Via Regia</i> across the river Schwarze Elster, founded during the <i>Ostkolonisation</i> (<i>Colonisation of eastern parts of Germany</i>).</p> <p>Misfired pottery findings mainly yellow earthenware decorated with roller stamps are dated at 14th century.</p>
	<p style="text-align: center;">Bad Muskau</p> <p>Ceramic sherds with light tan and grey bodies decorated with yellow and brown glazes and low relief motifs.</p> <p>Excavation and finds in Bad Muskau, called Muzakow or Muskau, supplied evidence of early stoneware production since the 15th century. Individual pieces display a glaze similar to a salt-glaze. Stoneware was produced with a variety of glaze colours and decorations.</p>

	<p style="text-align: center;">Görlitz</p> <p>Ceramic sherds present grey and light grey bodies with grey and blue glaze, light tan glaze and dark slips. Rim sherds with concentric rilling around the bodies.</p> <p>The city is situated close to the river Neiße and the crossing of Via Regia from Rhineland and Leipzig to Breslau and eastward and the north-south route from the Baltic Sea to Bohemia. The town was founded at around 1210-1220 during the <i>Ostkolonisation</i> (<i>Colonisation of eastern parts of Germany</i>).</p> <p>Görlitz had trade monopoly of the <i>Waidhandel</i>, where <i>Waid</i> is a plant for colouring textiles in blue, very important in Middle Ages, for the whole eastern territories.</p> <p>Findings from of misfired pottery from Postplatz (today in Poland) provided evidence of pottery production in Görlitz.</p>
	<p style="text-align: center;">Zittau</p> <p>The ceramic sherds present light grey and yellowish body and rim sherds with concentric rilling around upper the body. Surfaces with brown slip paintings are also present.</p> <p>Zittau was part of the <i>Sechstädtebund</i> (<i>union of 6 towns of the Upper Lusatia</i>: Zittau, Kamenz, Görlitz, Bautzen, Löbau, Lauban) initiated from emperor (Kaiser) Karl IV, giving to the 6 towns better opportunities to protected themselves from attacks of the robber knights as well as consolidation of the trade and economy.</p> <p>Pottery kilns were found at the cemetery of the Kreuz (church), terminus post-quem is the construction of the church earlier than 1380. Near-stoneware and stoneware were found at the Töpferberg decorated by engobe painting. Moreover, during the 13th century in Zittau potters produced near-stoneware and earthenware and during the early 14th they produced sintered stoneware. Zittau and Waldenburg are the two places in Saxony where stoneware was produced so early.</p>

3.4. Bibliography

- [1] N. V. Chukanov, *Infrared spectra of mineral species*, vol. 1. Dordrecht: Springer Netherlands, 2014.
- [2] G. E. De Benedetto, R. Laviano, L. Sabbatini, and P. G. Zambonin, “Infrared spectroscopy in the mineralogical characterization of ancient pottery,” *J. Cult. Herit.*, vol. 3, no. 3, pp. 177–186, Jul. 2002.
- [3] R. Ravisankar, S. Kiruba, P. Eswaran, G. Senthilkumar, and a. Chandrasekaran, “Mineralogical Characterization Studies of Ancient Potteries of Tamilnadu, India by FT-IR Spectroscopic Technique,” *E-Journal Chem.*, vol. 7, no. s1, pp. S185–S190, 2010.
- [4] S. Shoval, “Using FT-IR spectroscopy for study of calcareous ancient ceramics,” *Opt. Mater. (Amst.)*, vol. 24, no. 1–2, pp. 117–122, Oct. 2003.
- [5] D. Anglos, M. Solomidou, I. Zergioti, V. Zafiropoulos, T. G. Papazoglou, and C. Fotakis, “Laser-induced fluorescence in artwork diagnostics: An application in pigment analysis,” *Appl. Spectrosc.*, vol. 50, no. 10, pp. 1331–1334, 1996.
- [6] A. Nevin, G. Spoto, and D. Anglos, “Laser spectroscopies for elemental and molecular analysis in art and archaeology,” *Appl. Phys. A*, vol. 106, no. 2, pp. 339–361, Dec. 2011.
- [7] L. Caneve, F. Colao, R. Fantoni, and L. Fiorani, “Scanning lidar fluorosensor for remote diagnostic of surfaces,” *Nucl. Instruments Methods Phys. Res. Sect. A Accel. Spectrometers, Detect. Assoc. Equip.*, vol. 720, pp. 164–167, 2013.
- [8] L. Caneve, F. Colao, C. Giancristofaro, F. Persia, G. Ricci, and A. Tati, “Laser Induced Fluorescence and ultrasound techniques to study thermal modification induced on white marbles .,” in *LACONA IX*, 2011.
- [9] V. Lazic, F. Colao, R. Fantoni, A. Palucci, V. Spizzichino, I. Borgia, B. G. Brunetti, and A. Sgamellotti, “Characterisation of lustre and pigment composition in ancient pottery by laser induced fluorescence and breakdown spectroscopy,” *J. Cult. Herit.*, vol. 4, pp. 303–308, Jan. 2003.
- [10] L. F. Vieira Ferreira, T. M. Casimiro, and P. Colomban, “Portuguese tin-glazed earthenware from the 17th century. Part 1: pigments and glazes characterization,” *Spectrochim. Acta. A. Mol. Biomol. Spectrosc.*, vol. 104, pp. 437–44, Mar. 2013.
- [11] M. Gaft, R. Reisfeld, G. Panczer, P. Blank, and G. Boulon, “Laser-induced time-resolved luminescence of minerals,” *Spectrochim. Acta Part A Mol. Biomol. Spectrosc.*, vol. 54, no. 13, pp. 2163–2175, Nov. 1998.
- [12] R. Salh, “Defect related luminescence in silicon dioxide network: a review,” *Cryst. Silicon Prop. Uses*, pp. 135–172, 2011.
- [13] B. J. Bozlee, A. K. Misra, S. K. Sharma, and M. Ingram, “Remote Raman and fluorescence studies of mineral samples,” *Spectrochim. Acta. A. Mol. Biomol. Spectrosc.*, vol. 61, no. 10, pp. 2342–8, Aug. 2005.
- [14] C. MacRae and N. Wilson, “Luminescence database I—minerals and materials,” *Microsc. Microanal.*, vol. 14, pp. 184–204, 2008.
- [15] V. Spizzichino and R. Fantoni, “Laser Induced Breakdown Spectroscopy in archeometry: A review of its application and future perspectives,” *Spectrochim. Acta - Part B At. Spectrosc.*, vol. 99, pp. 201–209, 2014.
- [16] M. Bacci, a. Casini, C. Cucci, M. Picollo, B. Radicati, and M. Vervat, “Non-invasive spectroscopic measurements on the Il ritratto della figliastra by Giovanni Fattori: Identification of pigments and colourimetric analysis,” *J. Cult. Herit.*, vol. 4, no. 4, pp. 329–336, 2003.
- [17] M. Bacci, D. Magrini, M. Picollo, and M. Vervat, “A study of the blue colors used by Telemaco Signorini (1835-1901),” *J. Cult. Herit.*, vol. 10, no. 2, pp. 275–280, 2009.
- [18] L. Boselli, S. Ciattini, M. Galeotti, M. R. Lanfranchi, C. Lofrumento, M. Picollo, and A. Zoppi, “An unusual white pigment in La Verna sanctuary frescoes: an analysis with micro-Raman, FTIR, XRD and UV-VIS-NIR FORS,” *e-Preservation Sci.*, vol. 6, pp. 38–42, 2009.
- [19] A. Ceglia, W. Meulebroeck, P. Cosyns, K. Nys, H. Terryn, and H. Thienpont, “Colour and Chemistry of the Glass Finds in the Roman Villa of Treignes, Belgium,” *Procedia Chem.*, vol. 8, pp. 55–64, 2013.
- [20] A. Ceglia, W. Meulebroeck, H. Wouters, K. Baert, K. Nys, H. Terryn, and H. Thienpont, “Using optical spectroscopy to characterize the material of a 16th c. stained glass window,” in *Proc. SPIE 8422*, 2012, vol. 8422, p. 84220A.
- [21] L. Caneve, A. Diamanti, F. Grimaldi, G. Palleschi, V. Spizzichino, and F. Valentini, “Analysis of fresco by laser induced breakdown spectroscopy,” *Spectrochim. Acta Part B At. Spectrosc.*, vol. 65, no. 8, pp. 702–706,

- Aug. 2010.
- [22] K. Melessanaki, M. Mateo, S. C. Ferrence, P. P. Betancourt, and D. Anglos, “The application of LIBS for the analysis of archaeological ceramic and metal artifacts,” *Appl. Surf. Sci.*, vol. 197–198, pp. 156–163, Sep. 2002.
- [23] S. Legnaioli, F. A. Garcia, a. Andreotti, E. Bramanti, D. D. Pace, S. Formola, G. Lorenzetti, M. Martini, L. Pardini, E. Ribechini, E. Sibilía, R. Spiniello, and V. Palleschi, “Multi-technique study of a ceramic archaeological artifact and its content,” *Spectrochim. Acta - Part A Mol. Biomol. Spectrosc.*, vol. 100, pp. 144–148, 2013.
- [24] a. J. López, G. Nicolás, M. P. Mateo, V. Piñón, M. J. Tobar, and a. Ramil, “Compositional analysis of Hispanic Terra Sigillata by laser-induced breakdown spectroscopy,” *Spectrochim. Acta Part B At. Spectrosc.*, vol. 60, no. 7–8, pp. 1149–1154, Aug. 2005.
- [25] a. Erdem, a. Çilingiroğlu, a. Giakoumaki, M. Castanys, E. Kartsonaki, C. Fotakis, and D. Anglos, “Characterization of Iron age pottery from eastern Turkey by laser- induced breakdown spectroscopy (LIBS),” *J. Archaeol. Sci.*, vol. 35, no. 9, pp. 2486–2494, Sep. 2008.
- [26] V. N. Rai, “Laser-Induced Breakdown Spectroscopy: a Versatile Technique of Elemental Analysis and Its Applications,” *arXiv:1407.0132 [physics.optics]*, pp. 1–35, 2014.
- [27] F. Anabitarte, A. Cobo, and J. M. Lopez-Higuera, “Laser-Induced Breakdown Spectroscopy: Fundamentals, Applications, and Challenges,” *ISRN Spectrosc.*, vol. 2012, pp. 1–12, 2012.
- [28] A. W. Miziolek, V. Palleschi, and I. Schechter, Eds., *Laser-Induced Breakdown Spectroscopy (LIBS): Fundamentals and Applications*. Cambridge, UK: Cambridge University Press, 2006.
- [29] E. W. Washburn, “The dynamics of capillary flow,” *Phys. Rev.*, vol. 17, no. 3, pp. 273–283, 1921.
- [30] J. Kastner, B. Harrer, G. Requena, and O. Brunke, “A comparative study of high resolution cone beam X-ray tomography and synchrotron tomography applied to Fe- and Al-alloys,” *NDT E Int.*, vol. 43, no. 7–3, pp. 599–605, Oct. 2010.
- [31] J.-Y. Buffière, H. Proudhon, E. Ferrie, W. Ludwig, E. Maire, and P. Cloetens, “Three dimensional imaging of damage in structural materials using high resolution micro-tomography,” *Nucl. Instruments Methods Phys. Res. Sect. B Beam Interact. with Mater. Atoms*, vol. 238, no. 1–4, pp. 75–82, Aug. 2005.
- [32] L. Salvo, P. Cloetens, E. Maire, S. Zabler, J. . Blandin, J. . Buffière, W. Ludwig, E. Boller, D. Bellet, and C. Josserson, “X-ray micro-tomography an attractive characterisation technique in materials science,” *Nucl. Instruments Methods Phys. Res. Sect. B Beam Interact. with Mater. Atoms*, vol. 200, pp. 273–286, Jan. 2003.
- [33] L. Salvo, M. Suéry, A. Marmottant, N. Limodin, and D. Bernard, “3D imaging in material science: Application of X-ray tomography,” *Comptes Rendus Phys.*, vol. 11, no. 9–10, pp. 641–649, Nov. 2010.
- [34] F. Casali, “X-Ray digital radiography and computed tomography for cultural heritage,” *Archeometriai Műhely*, vol. 1, pp. 24–28, 2006.
- [35] M. P. Morigi, F. Casali, M. Bettuzzi, D. Bianconi, R. Brancaccio, S. Cornacchia, a. Pasini, a. Rossi, a. Aldrovandi, and D. Cauzzi, “CT investigation of two paintings on wood tables by Gentile da Fabriano,” *Nucl. Instruments Methods Phys. Res. Sect. A Accel. Spectrometers, Detect. Assoc. Equip.*, vol. 580, no. 1, pp. 735–738, Sep. 2007.
- [36] G. Artioli, “Scientific methods and cultural heritage,” p. 520, 2010.
- [37] L. Jacobson, F. C. de Beer, and R. Nshimirimana, “Tomography imaging of South African archaeological and heritage stone and pottery objects,” *Nucl. Instruments Methods Phys. Res. Sect. A Accel. Spectrometers, Detect. Assoc. Equip.*, vol. 651, no. 1, pp. 240–243, Sep. 2011.
- [38] M. A. Kulkova and A. M. Kulkov, “Investigations of Early Neolithic ceramics from Eastern Europe by X-Ray microtomography and petrography,” in *Bruker Micro-CT User Meeting 2014*, 2014, pp. 30–37.
- [39] G. Cultrone, E. Sebastián, K. Elert, M. J. de la Torre, O. Cazalla, and C. Rodríguez-Navarro, “Influence of mineralogy and firing temperature on the porosity of bricks,” *J. Eur. Ceram. Soc.*, vol. 24, no. 3, pp. 547–564, Mar. 2004.
- [40] M. M. Jordan, M. A. Montero, S. Meseguer, and T. Sanfeliu, “Influence of firing temperature and mineralogical composition on bending strength and porosity of ceramic tile bodies,” *Appl. Clay Sci.*, vol. 42, no. 1–2, pp. 266–271, Dec. 2008.
- [41] S. M. Hassan, “Use of Mercury Intrusion Porosimetry (MIP) Technique to Measure the Porosity of Anodes in Solid Oxide Fuel Cell (SOFC),” vol. 3224, no. 6, pp. 14–20, 2015.

- [42] N. Cuomo di Caprio, *Ceramica in Archeologia 2. Antiche tecniche di lavorazione e moderni metodi di indagine*, L'Erma di. 2007.
- [43] D. Calaon, E. Zendri, and G. Biscontin, *Torcello scavata. Patrimonio condiviso. Gli scavi archeologici 2012-2014*. Venezia, Regione Veneto, 2014.
- [44] I. Caravale, Alessandra Toffoletti, *Anfore Antiche: Riconoscerle e identificarle*. IRECO, 1997.
- [45] A. Toniolo, "Anfore dell'area Lagonare," in *La circolazione delle ceramiche nell'Adriatico tra tarda antichità e altomedioevo: III incontro di studio CER.AM.IS*, S. Gelichi and C. Negrelli, Eds. Mantova, 2007, pp. 91–106.
- [46] S. Gelichi and C. Negrelli, "Anfore e commerci nell'alto Adriatico tra VIII e IX secolo," *MEFRM*, vol. 120, no. 2, pp. 307–326, 2008.
- [47] S. Yona Waksman, "ARCHAEOLOGICAL APPROACHES TO CERAMICS PRODUCTION AND IMPORTS IN MEDIEVAL CYPRUS," in *Cypriot Medieval Ceramics, Reconsiderations and New Perspectives*, D. Papanikolaou-bakirtzi and N. Coureas, Eds. NICOSIA 2014, 2014, pp. 257–277.
- [48] A. Pecci, "Amphorae and unglazed wares: the contents," in *L'Isola del Vesovo. Gli Scavi Archeologici intorno alla Cattedrale di Comacchio*, S. Gelichi, Ed. Firenze, 2009, p. 40.
- [49] D. Calaon, S. Gelichi, and C. Negrelli, "The Ceramic from an Early Medieval Emporium," in *L'Isola del Vesovo. Gli Scavi Archeologici intorno alla Cattedrale di Comacchio*, S. Gelichi, Ed. Firenze, 2009, pp. 38–39.
- [50] G. Pietro Brogiolo, N. Gauthier, and N. Christie, *Towns and Their Territories Between Late Antiquity and the Early Middle Ages*. BRILL, 2000.
- [51] S. Gelichi and M. Baldassarri, *Pensare/Classificare. Studi e ricerche sulla ceramica medievale per Graziella Berti*. All'Insegna del Giglio, 2010.
- [52] H. G. Stephan, "Steinzeug und Irdenware: Diskussionsbeitrag zur Abgrenzung und Definition mittelalterlicher deutscher Steinzeuggruppen," in *BAR International Series 440*, 1988, pp. 81–117.
- [53] D. R. M. Gaimster, *German Stoneware, 1200-1900: Archaeology and Cultural History: Containing a Guide to the Collections of the British Museum, Victoria & Albert Museum, and Museum of London*. British Museum Publ., 1997.
- [54] G. Hansen, *Everyday Products in the Middle Ages: Crafts, Consumption and the individual in Northern Europe c. AD 800-1600*. Oxbow Books, 2015.
- [55] B. Adler, *Early Stoneware Steins from the Les Paul Collection: A Survey of All German Stoneware Centers from 1500 to 1850*. Beatrix Adler, 2005.
- [56] K. Domoney, a. J. Shortland, and S. Kuhn, "Characterization of 18Th-Century Meissen Porcelain Using Sem-Eds*," *Archaeometry*, vol. 54, no. 3, pp. 454–474, Jun. 2012.
- [57] A. Rottländer, *Bürgeler Keramik, Eine Darstellung der Geschichte des Bürgeler Töpferhandwerks anhand der Sammlung des Keramik-Museum*. Apolda, 1995.
- [58] S. Krabath, "Die Entwicklung der Keramik im Freistaat Sachsen vom späten Mittelalter bis zum 19. Jahrhundert. Ein Überblick," in *Keramik in Mitteldeutschland Stand der Forschung und Perspektiven. Veröffentlichungen des Landesamtes für Archäologie, Band 57*, R. Smolnik, Ed. Dresden, 2012, pp. 35–172.
- [59] S. Krabath, "Europäische Steinzeugproduktion der Neuzeit im Überblick," in *Von den Anfängen der Bunzlauer Keramik. Funde des 15.-17. Jahrhunderts aus einem mitteleuropäischen Zentrum der Töpferei*, 2012, pp. 263–328.
- [60] H.-G. Stephan and J. Baart, *Coppengrave. Studien zur Töpferei des 13. bis 19. Jahrhunderts in Nordwestdeutschland, Materialhefte zur Ur- und Frühgeschichte Niedersachsens*. Coppengrave, 1981.
- [61] K. Brüning, *Handbuch der historischen Stätten Deutschlands, Niedersachsen und Bremen, Band 2, 3. Auflage*. Stuttgart, 1986.
- [62] G. W. Sante, *Handbuch der historischen Stätten Deutschlands, Hessen, Band 4, 3. Auflage*. 1993.
- [63] H. Patze, *Handbuch der historischen Stätten Deutschlands, Thüringen, Band 9, 2. Auflage*. 1989.
- [64] W. Schlesinger, *Handbuch der historischen Stätten Deutschlands, Sachsen, Band 8*. 1990.
- [65] H.-G. Stephan, *Das „Pottland“. Mittelalterliche und neuzeitliche Töpferei von landesgeschichtlicher Bedeutung und Keramik von europäischem Rang in Niedersachsen*. 2012.
- [66] R. Barbini, F. Colao, V. Lasic, R. Fantoni, A. Palucci, and M. Angelone, "On board LIBS analysis of marine sediments collected during the XVI Italian campaign in Antarctica," *Spectrochim. Acta - Part B At. Spectrosc.*, vol. 57, no. 7, pp. 1203–1218, 2002.

- [67] J. Rouquerolt, D. Avnir, C. W. Fairbridge, D. H. Everett, J. H. Haynes, N. Pernicone, J. D. F. Ramsay, K. S. W. Sing, and K. K. Unger, "Recommendations for the characterization of porous solids," 1994.
- [68] S. Gelichi, "Venezia tra archeologia e storia: la costruzione di una identità urbana," in *Le città italiane tra la tarda Antichità e l'Alto Medioevo*, 2004, pp. 151–183.
- [69] M. Bortoletto, "Murano, Mazzorbo e Torcello: tre siti a confronto. Indagini archeologiche nella Laguna nord di Venezia," in *Archeologia delle acque 1*, 1999, pp. 55–74.
- [70] M. Bassani, *Antichità Lagunari. Scavi Archeologici e Archivistici*. Roma: Hesperia, 29, 2012.

4. Results and Discussion

Summary

This chapter presents the results obtained from the analysis performed on ceramic samples both laboratory-made and historical. The chemical and morphological investigations were carried out through a multi-analytical approach which includes the use of tradition and non-tradition techniques. The investigation strategy provided insights on the features of the studied materials and their technological productions. Particular emphasis was given to the relationship between chemical-morphological features and the production techniques in terms of raw materials used and firing conditions.

4.1. Analysis and Characterization of Raw ceramic specimens made in Laboratory

Raw ceramic samples *ad hoc* made in laboratory following traditional methods and firing them at different temperatures, were firstly analysed in order to study the relationship between raw material composition, firing temperatures and the final chemical-physical features. This innovative approach allowed a systematic study starting by known conditions. Therefore, chemical and mineralogical composition as well as microstructure and morphology were studied by means of diagnostic techniques for each sample before and after firing at the selected temperatures. In particular, the pioneering application of X-ray μ -CT¹ performed in order to investigate the microstructure in terms of total porosity (open and closed porosity) of the raw ceramics was explored and the results are reported.

4.1.1. Raw Materials Characterization

The three clay materials (LS, G and S) and sand used to produce raw ceramic samples were chemically characterized by FT-IR, μ -Raman and XRD analyses.

The analytical techniques were able to identify the composition of the raw materials investigated and in **Fig.16-18** are shown the most significant results obtained. The observed FT-IR absorption bands (**Fig.16**) are given in the **Tab.6**, where their relative intensity and tentative

¹ Thanks to the collaboration with Engineer Alexander Kulkov of “Geomodel” Saint-Petersburg State University, Peterhof, and Dr. Arianna Kulkova of Herzen State University, in Saint-Petersburg, Russia.

vibrational assignments are reported. Attributions of mineralogical phases were made on the basis of data reported in literature [1]–[11].

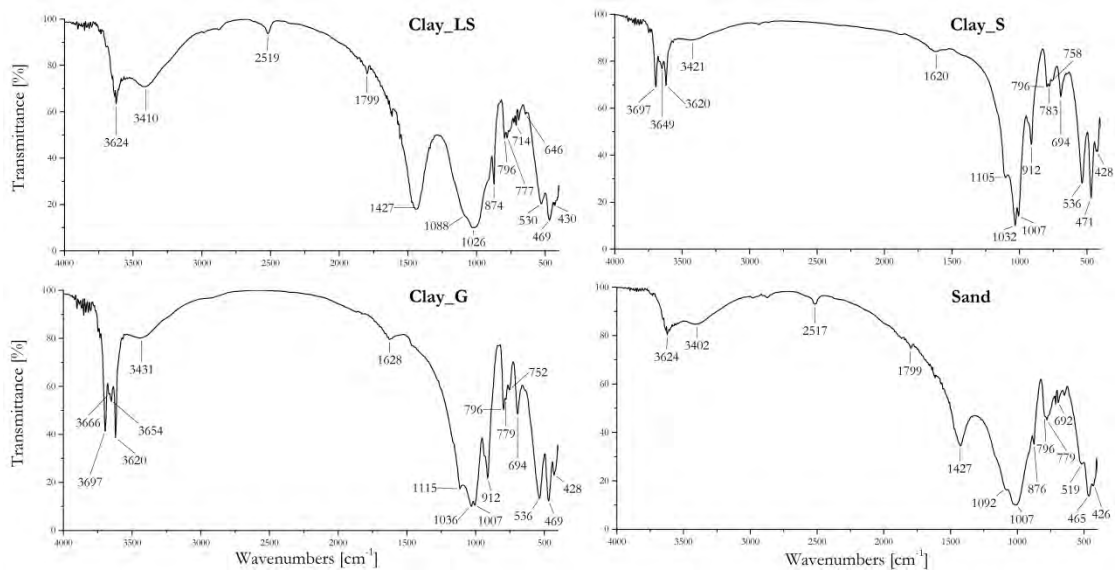


Figure.16. FT-IR spectra of the raw materials used for the laboratory-made samples.

IR absorption bands at 3624 cm^{-1} and the broad band at 3410 cm^{-1} in clay_LS spectrum are due to the inner O-H stretching modes and H-O-H stretching of interlayer water molecules, respectively. These bands are typically ascribed to the presence of smectite minerals, such as montmorillonite clay mineral [6], [10], [12]. Calcite is detected by the presence of the characteristic peaks at 2519 , 1799 , 1429 and 874 cm^{-1} [6]. Both of these minerals are detected, though in different relative intensity, in both LS clay and sand samples. Characteristic peaks at 3697 , 3666 , 3649 - 3654 and 3620 cm^{-1} present in the German clays S and G are due to the inner O-H stretching vibrations and are considered as diagnostic features of kaolinite [6], [13]. Furthermore, kaolinite is detected also by the peaks at 1105 - 1115 , 1007 and 912 cm^{-1} due to Si-O, Si-O-Al and Al-O-H stretching vibrations, respectively. Quartz is well detected in all the samples: 1088 - 1092 cm^{-1} due to Si-O stretching mode, the distinctive doublet at 796 and 777 - 783 cm^{-1} and the peak at 692 - 694 cm^{-1} due to Si-O symmetrical stretching and bending modes respectively [13], [14]. Muscovite (1026 - 1036 , 1007 and 530 cm^{-1}) as well as feldspars (752 - 758 , 646 and 465 - 471 cm^{-1}) were also detected [3], [5], [8].

Table.6. FT-IR vibrational frequency assignments of the analysed raw materials [1]–[11].

Raw Materials				Tentative vibrational assignment	
LS	S	G	Sand		
IR frequency (cm ⁻¹) with relative intensity					
	3697 s	3697 s		O-H str. (inner surface OHs)	Kaolinite
		3666 vw		O-H str.	Kaolinite
	3649 w	3654 w		O-H str.	Kaolinite
3624 s	3620 s	3620 s	3624 m	O-H str.	Smectite/Kaolinite
3410 bd	3421 bd	3431 bd	3402 bd	O-H str.	Water/Smectite
2519 w			2517 w	-CO ₃ ²⁻	Calcite
1799 w			1799 vw	-CO ₃ ²⁺	Calcite
	1620 w	1628 w		O-H-O bend.	Water
1427 vs			1427 s	-CO ₃ ²⁻	Calcite
	1105 s	1115 m		Si-O str.	Kaolinite
1088 sh			1092 sh	Si-O str.	Quartz
1026 vs	1032 vs	1036 vs		Si-O str.	Silicates/clays/ Muscovite
	1007 s	1007 s	1007 vs	Si-O/Si-O-Al str.	Kaolinite/ Muscovite
	912 s	912 s		Al-O-H	Kaolinite
874 s			876 w	-CO ₃ ²⁻	Calcite
796 m	796 m	796 m	796 w	Si-O str.	Quartz
777 m	783 m	779 w	779 w	Si-O str.	Quartz
	758 w	752 w		Al-O-Si bend.	Feldspar
714 w				-CO ₃ ²⁻	Calcite
	694 m	694 vw	692 w	Si-O bend.	Quartz
646 vw				Si-O-Si bend./Al-O-Si str.	Silicates/Feldspar
530 s	536 s	536 s	536 w	Si-O-Al ^{IV} /Fe-O bend.	Kaolinite/Muscovite/Hematite
			519 w		Pyroxenes
469 s	471 s	469 s	465 s	Si-O-Si deformation mode	Silicates/Feldspar/Clays
430 m	428 m	428 m	426 w	Si-O mixed deformation	Silicates

s: strong; vs: very strong; w: weak; vw: very weak; m: medium; sh: shoulder; bd: broad band.
str.: stretching mode; bend.: bending mode.

μ -Raman results are shown in **Fig.17** and in **Tab.7** are reported the assignments of the mineralogical phases detected for the raw materials by comparing the obtained data with those reported in literature [7], [10], [15]–[19].

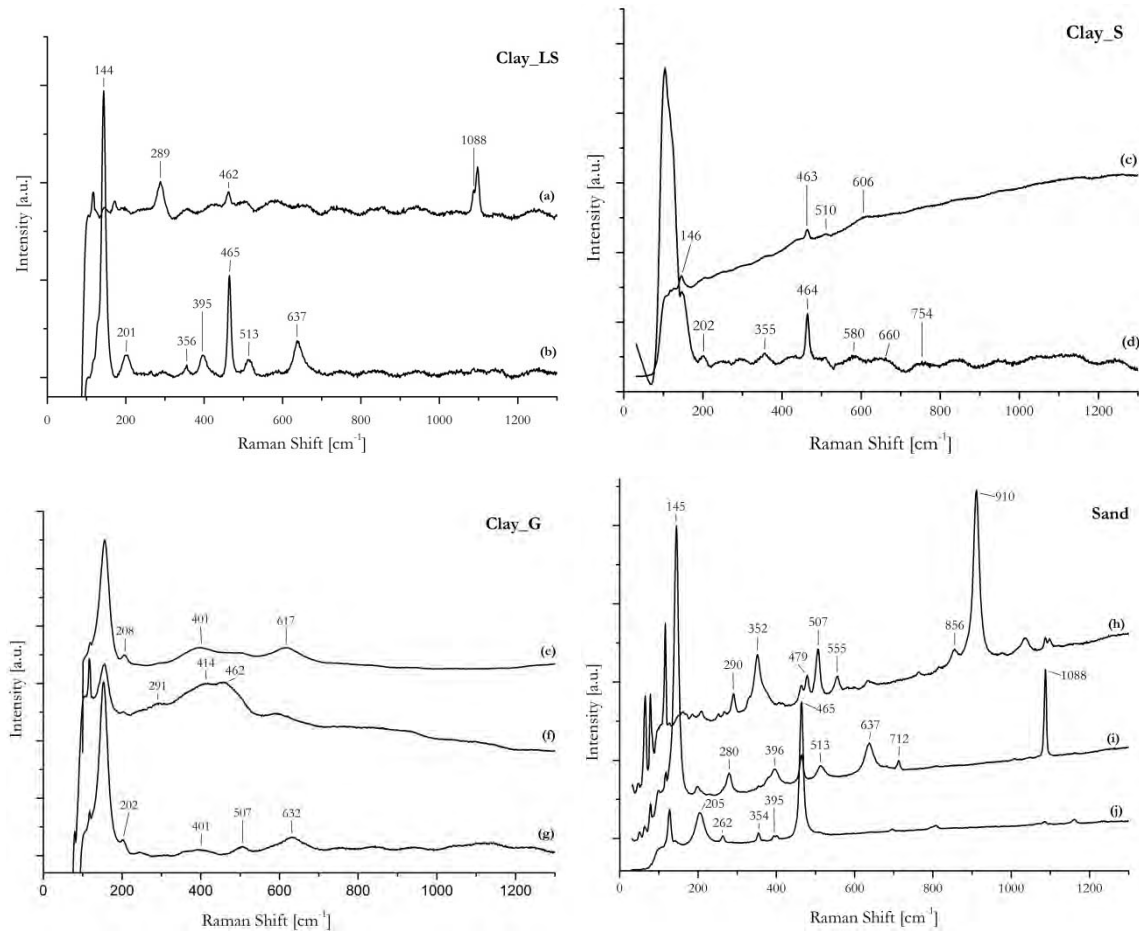


Figure.17. μ -Raman spectra obtained from different points of the raw materials.

As reported in the **Tab.7**, μ -Raman spectra show the presence of:

- quartz (144-145, 205-208, 355-356, 462-465 cm^{-1}),
- calcite (280-289, 712 and 1088 cm^{-1} , as reported in the spectra related to LS clay and sand samples in **Fig.17 (a)** and **(i)**),
- anatase (144-145, 395-396, 513 and 637 cm^{-1} , in **Fig.17 (b)** and **(i)**),
- hematite (291, 401 and 606 cm^{-1}),
- kaolinite (280-291, 632-637, 660 and 754 cm^{-1}),
- montmorillonite (910 cm^{-1})
- albite and feldspars (414, 479, 507-513, 555 cm^{-1}).

The attributions on the basis of FT-IR and μ -Raman spectra are supported by XRD results, as it seen in **Fig.18**.

Summarizing the chemical and mineralogical characterization of the raw materials:

- i) LS consists of a Ca-rich clay with quartz, montmorillonite, muscovite, calcite, feldspars and hematite;
- ii) G and S seem to have similar composition, both are kaolinite-rich clays composed of quartz, kaolinite, feldspars, hematite and titanium oxides (anatase and rutile);
- iii) sand is a silica-rich sand with quartz, feldspars, calcite (in low relative content) and muscovite.

Table.7. μ -Raman wavenumbers for the raw materials. A tentative vibrational assignments is given [7], [10], [15]–[19].

Raw Materials				Tentative vibrational assignment	
LS	S	G	Sand		
Raman frequency (cm ⁻¹)					
1088			1088	-CO ₃ ²⁻ /C-O str.	Calcite
			910	Al-O-H bend.	Montmorillonite
	754			O-H bend.	Kaolinite
			712	-CO ₃ ²⁻	Calcite
	660			Al-O-Si bend.	Kaolinite
637		632	637	Ti-O/Al-O str.	Anatase/Kaolinite
		617		Ti-O str.	Rutile
	606			Fe-O str.	Hematite
			555		Albite/Feldspars
513	510	507	479, 507-513	Al-O-Si bend.	Feldspars
462-465	463-464		465	Si-O-Si bend.	Quartz
		414			Albite/Feldspars
		401		Fe-O bend.	Hematite
395			395-396	Ti-O	Anatase
356	355		352-354	Si-O str.	Quartz
289		291	280-290	Fe-O/O-H-O bend.	Hematite/Kaolinite
201	202	202-208	205		Quartz
144	146		145		Anatase/Quartz

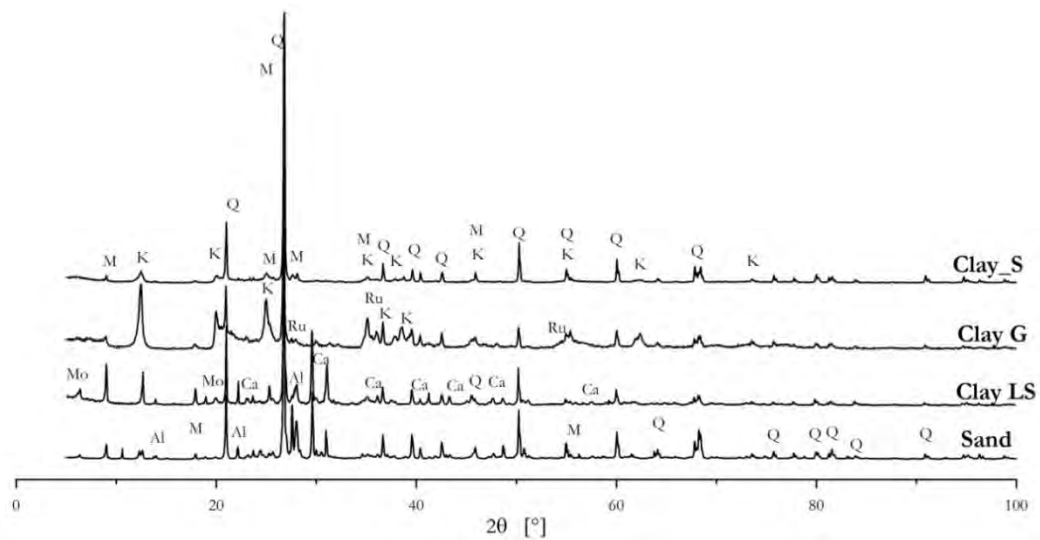


Figure.18. XRD patterns of the raw materials. Q for quartz, Ca for calcite, M for muscovite, Mo for montmorillonite, K for kaolinite, Ru for rutile and Al for albite.

4.1.2. Chemical, Mineralogical and Microstructural Changes of the Raw Ceramic samples after Firing.

In order to monitor the chemical, mineralogical and microstructural changes of the laboratory-made samples, FT-IR, XRD, SEM-EDX, MIP and μ -CT techniques were used. The raw ceramics of the three pastes (LS, S and G) at room-temperature (unfired, T0) and those fired at 400°C (T1), 700°C (T4), 900°C (T6) and 1000°C (T7) were analysed.

FT-IR spectra of LS paste at different temperatures were compared and are shown in **Fig.19**.

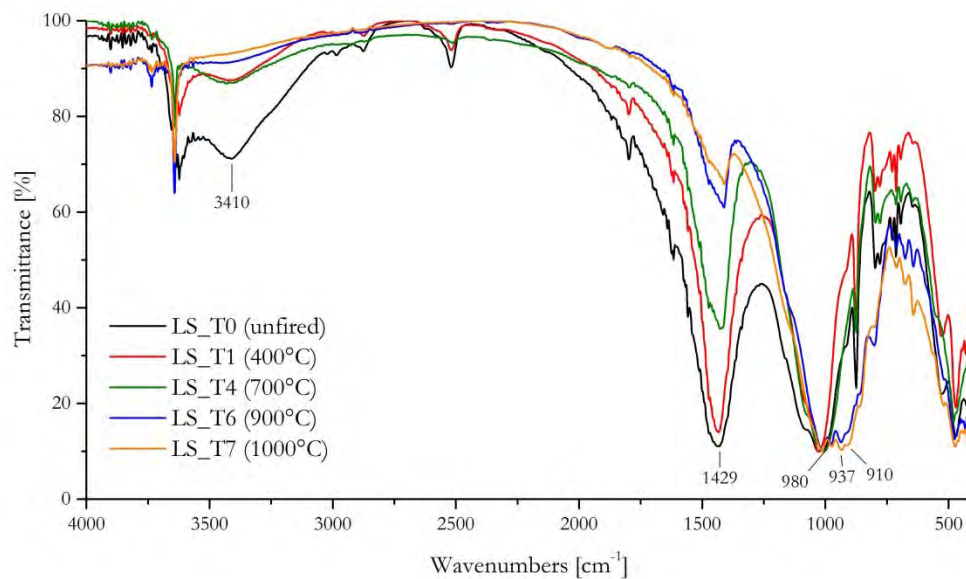


Figure.19. FT-IR spectra of the LS raw ceramics unfired (T0) and fired at 400°C (T1), 700°C (T4), 900°C (T6) and 1000°C (T7).

FT-IR bands related to mineralogical phases subjected to the main reactions occurring during firing were analysed. The intense broad band at 3410 cm^{-1} in the sample LS_T0 attributed to the presence of smectite (montmorillonite) decreases until it disappears after firing at 1000°C (**Fig.20 (a)**). Plots in **Fig.20** were realized using relative intensity ratios at selected FT-IR peaks standing out the transformation processes which occur throughout firing LS samples. Ratio of intensities related to the peaks at 1026 cm^{-1} and at 3410 cm^{-1} , attributed to Si-O stretching mode of silicates and -OH stretching mode of montmorillonite, respectively, is plotted in **Fig.20 (a)** and describes the dehydroxilation process of montmorillonite mineral. **Fig.20 (b)** plots the intensity ratio at 1429 cm^{-1} , of -CO_3^{2-} stretching mode of calcite, and 1026 cm^{-1} showing the decomposition process of calcite.

Montmorillonite dehydroxilates between 700° and 900°C and above this temperature can form other firing products such as spinel, anorthite and mullite [20]. The absence of the OH stretching band in the spectra of LS_T6 and LS_T7 samples fired at 900°C and 1000°C , respectively, corresponds to the collapse of the montmorillonite crystalline structure. The characteristic peak at 1429 cm^{-1} ascribable to calcite mineral, significantly starts decreasing in LS sample fired at 700°C (T4) when begins the decomposition of carbonates (**Fig.20 (b)**) [21], [22]. Decomposition of calcite forms reactive oxide, CaO, able to react at higher temperature with silicates present in the matrix forming new mineral phases as gehlenite ($\text{Ca}_2\text{Al}_2\text{SiO}_7$) and wollastonite (CaSiO_3) [23].

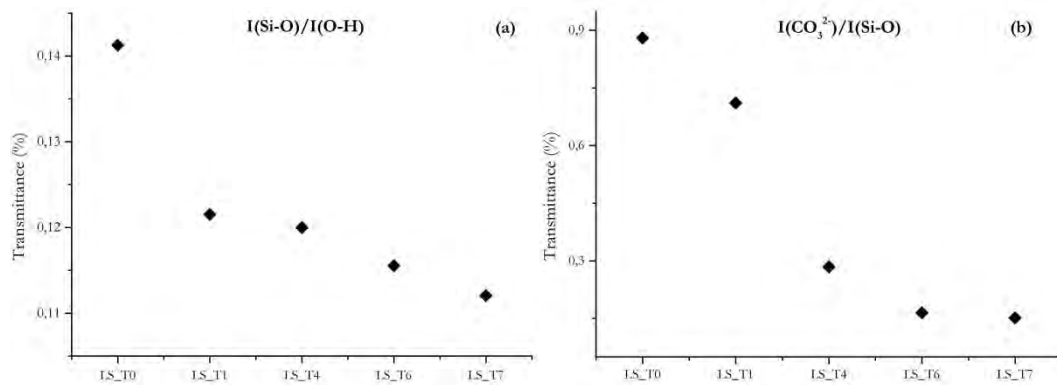


Figure.20. (a) FT-IR relative intensity ratios at 1026 cm^{-1} (Si-O stretching mode of silicates) and 3410 cm^{-1} (-OH stretching mode attributed to montmorillonite) and **(b)** FT-IR relative intensity ratios at 1429 cm^{-1} (-CO_3^{2-} stretching mode of calcite) and 1026 cm^{-1} for each LS samples.

LS_T7 spectrum, related to the raw ceramic paste fired at 1000°C , still shows the presence of calcite, due to the relative high content of the mineral in the raw materials and probably to the firing duration. Interesting results are shown in the LS_T6 and LS_T7 spectra, where new FT-IR bands appear at around $980\text{-}910\text{ cm}^{-1}$, suggesting the formation of new phases as products of

high temperature reactions. In particular, the three peaks at 980, 937 and 910 cm^{-1} were attributed to gehlenite ($\text{Ca}_2\text{Al}_2\text{SiO}_7$) and wollastonite (CaSiO_3) [6], [14]. These Ca-Al-silicates and Ca-silicates are formed by the reactions of free-lime from the de-carbonated calcite with fired clay and quartz, respectively, at temperature above 800-850°C. These new phases are considered as indicator minerals of the reached kiln temperature, and they remain stable at least to 1100°C [13], [14], [24]–[26]. Both phases were detected also in the XR diffractogram of the samples LS_T6 fired at 900°C, as shown in **Fig.21**, supporting the FT-IR attributions.

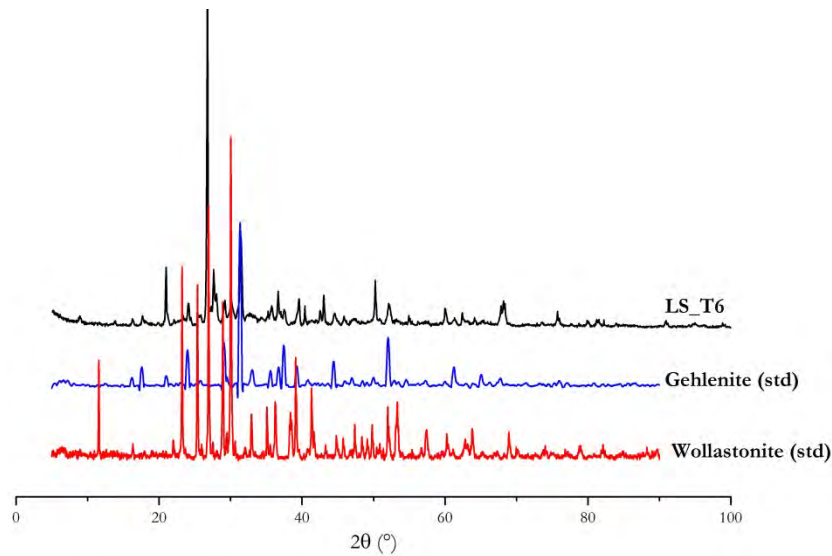


Figure.21. XRD patterns of LS_T6 (fired at 900°C) compared with standard diffractograms of gehlenite and wollastonite [27].

Morphological study of LS samples carried out by scanning electron microscope, shows the microstructure at different densification stages depending on firing temperature. Photomicrographs of each samples at magnifications 100x and 500x are presented in **Fig.22**.

The images of LS_T0 sample show a bulk composed of separated grains which start to be more and more aggregated in LS_T1 and LS_T4. At 700°C (LS_T4) the presence of some slightly deformed edges in the paste may identify a previous stage in the development of vitrification process. LS_T6 (fired at 900°C) images show a high degree of densification, whereas, LS_T7 show a molten “glassy” phase which cements and solidifies the microstructure.

Morphological and microstructural changes were quantified carrying on porosity studies by means of MIP and μ -CT. MIP provides information about open porosity in the pore size range between 0,003 – 20 μm (meso and macro pores). Instead, tomography technique was use to study the total porosity (closed and open porosity) in the range of around 1 to 100 μm . Open porosity refers to pores which communicate with the outside of the material, while closed porosity refers to isolated pores inside the materials; the sum of both gives the total porosity. As reported in

literature, the porosity in ceramic materials can be connected to chemical-mineralogical composition of the raw materials used, mechanical properties and manufacturing technologies [28]–[30].

Pore volume and volume distributions of open porosity investigated by MIP technique are shown in **Fig.23**. Moreover, all the parameters calculated, such as total cumulative volume (cm^3/g), total open porosity (%), average pore radius (μm), bulk density (g/cm^3) and apparent density (g/cm^3) obtained by the average of at least three measurements for each sample are reported in **Tab.8**.

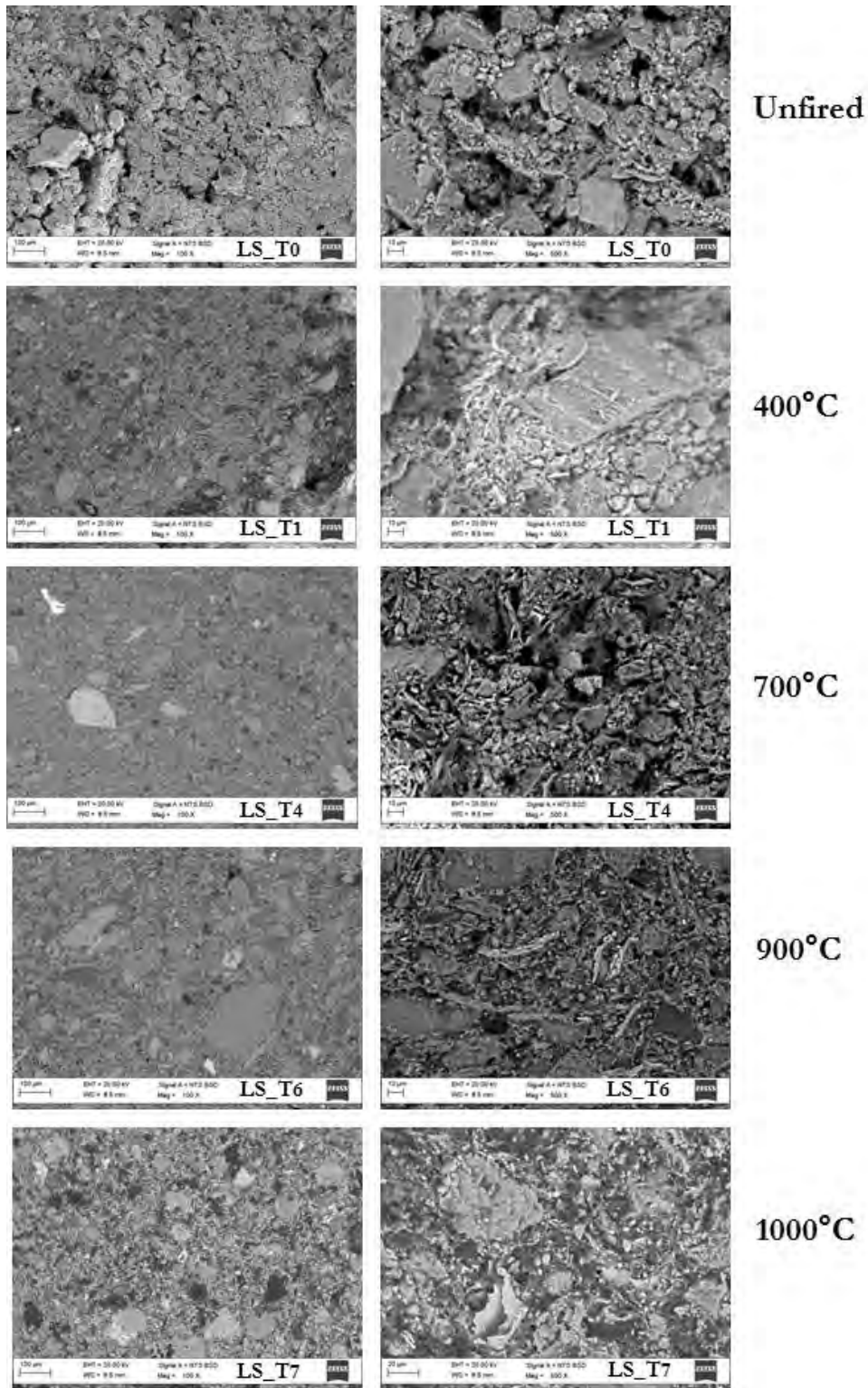


Figure.22. SEM micrographs of polished cross-sections of raw ceramic samples (LS) unfired and fired at different temperatures. Magnitudes of 100x and 500x are reported on the left and on the right, respectively.

Table.8. Porosity data obtained by MIP measurements. The average of the three measurements with standard deviation is given.

Sample code	Total Cumulative Volume (cm ³ /g)	Total open Porosity (%)	Average pore radius (μm)	Bulk Density (g/cm ³)	Apparent Density (g/cm ³)
LS_T0	0,16 ± 0,00	30,29±0,59	0,32± 0,00	1,90±0,07	2,72±0,13
LS_T1	0,17± 0,00	31,80±0,79	0,31± 0,03	1,91±0,01	2,80±0,02
LS_T4	0,21± 0,01	36,22±2,16	0,27± 0,05	1,72±0,04	2,69±0,15
LS_T6	0,31± 0,00	47,37±0,79	0,61± 0,01	1,54±0,03	2,93±0,10
LS_T7	0,31± 0,00	47,87±0,07	0,74± 0,01	1,56±0,01	2,99±0,02

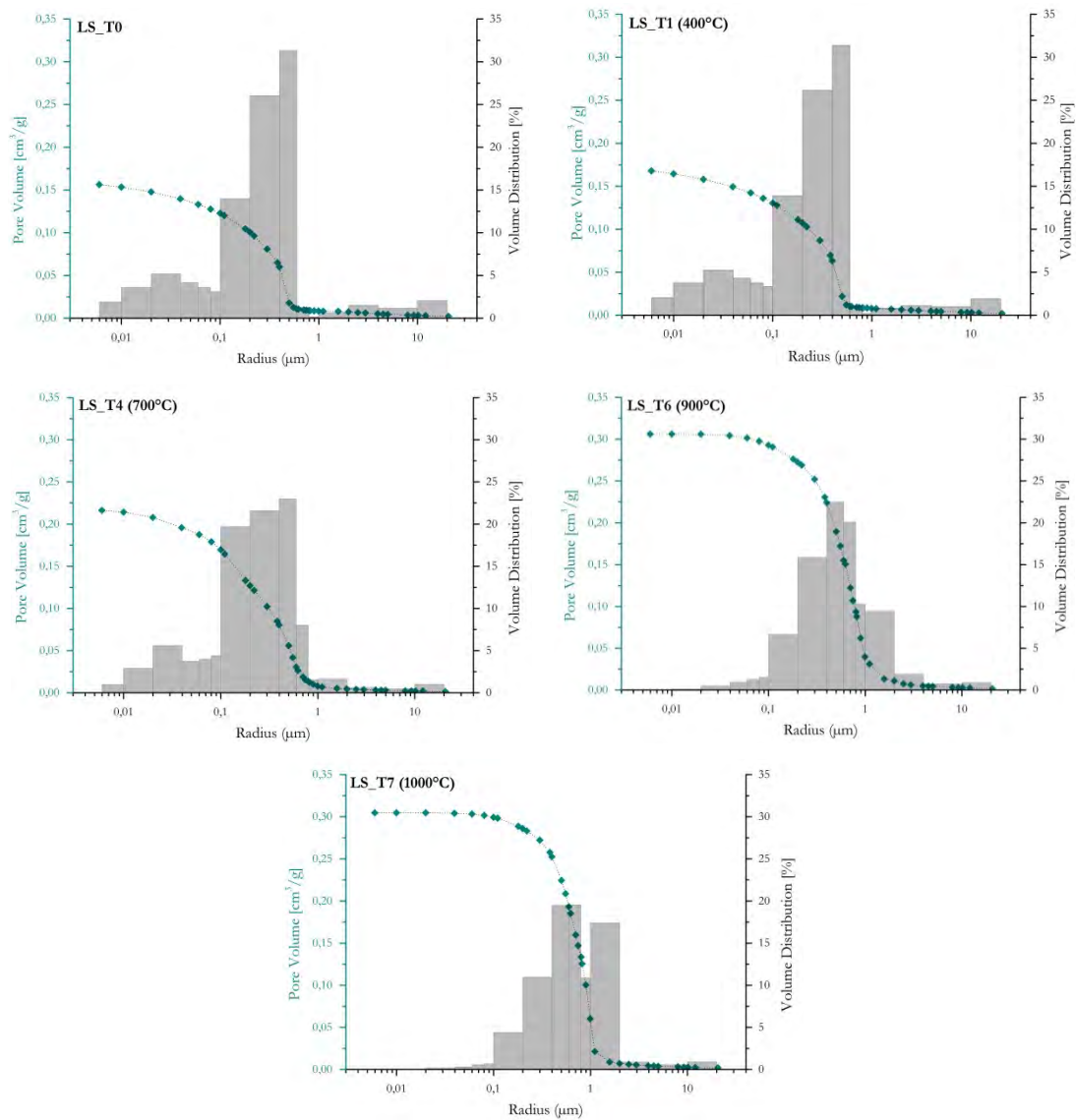


Figure.23. Porosity distribution and cumulative volume vs pore radius of the LS samples unfired and fired at different temperatures.

From a first observation on the data presented in the **Tab.8**, variations of the considered porosimetry parameters depending on firing temperature are noticed. Total cumulative volume, total open porosity as well as average pore radius increase for samples fired at higher temperatures. In order to underline these changes, in **Fig.24-25** are presented different diagrams which show clearly the trends of cumulative volume, pore size distribution and average pore radius of the LS samples.

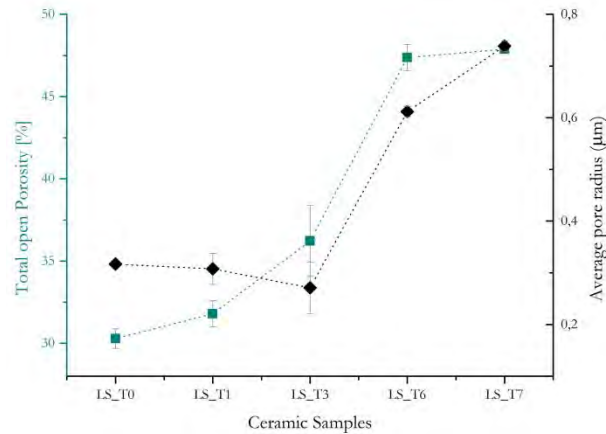


Figure.24. Total open porosity (in cyan) and average pore radius (in black) with standard deviation bars of LS samples unfired and fired at different temperatures.

The comparison of the results at different thermal treatments shows an increase of around 15% of the porosity, in terms of total open porosity (%) and cumulative volume (cm^3/g), up to 900°C due to the de-carbonation reaction that releases CO_2 and dehydroxylation of the clay minerals. Between $900\text{-}1000^\circ\text{C}$ vitrification process occurs and there is a slight decrease of the open porosity and an increase of the average pore size. In **Fig.25** (on the right) it can be seen a shift of the pore distribution curves to greater values of pore radius for LS_6 and LS_T7 samples fired at 900° and 1000°C , respectively. These data suggest that the glassy molten tends to fill the pores, as expected, and in particular smaller size pores. However, these results seem to be in contrast with the SEM observations which suggested an increasing of densification at higher firing temperatures.

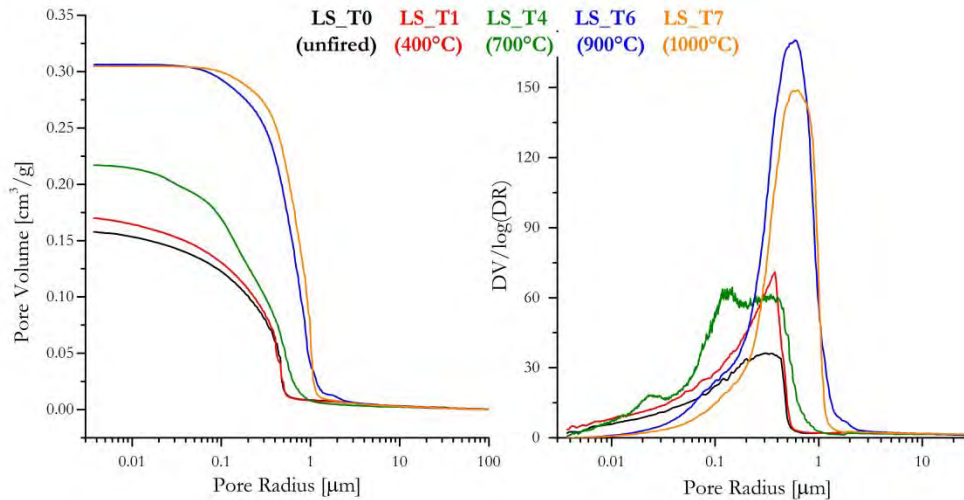


Figure.25. Cumulative pore volume (on the left) and pore size distribution curves (on the right) versus pore radius of LS samples fired at different temperatures.

Closed porosity is impossible to measure through MIP technique and data about it can only be gained with measurements of the apparent density [31]. The apparent density of the LS samples decreases at 700°C and increases at higher temperatures (**Tab.8**) indicating a greater total porosity (open and closed) at 700°C and its reduction at 900-1000°C. Therefore, closed porosity may change throughout firing process and these variations need to be investigated by other techniques.

The total porosity was analysed by x-ray μ -CT. The 3D tomographic data were elaborated by sophisticated image processing software in order to extract the voids (open and closed pores) and calculate the distributions of the total pore volume as a function of pore size in the range between 1 to 100 μm . Tomographic pictures of the voids present in LS samples are reported in **Fig.26**. Tomographic analyses carried out on LS samples fired at 400°C (T1), 700°C (T4), 900°C (T6) and 1000°C (T7) are graphically reported in **Fig.27**. It is necessary to underline that the obtained values cannot be compared with those obtained by MIP measurements because they refer to both different ranges and types of pores. Considering the trend of the total porosity in this range, it increases significantly in the sample LS_T4 (fired at 700°C) and then decreases at 900° and 1000°C. The reduction of total porosity at higher temperatures may be in accordance to the morphological observations made on the basis of SEM images, where the samples fired at high temperature (900° and 1000°C) have a more compact aspect than that one related to samples fired at lower temperature (400° and 700°C). Moreover, taking into account the considerations about total porosity made on the basis of apparent density calculated by MIP and the trends of total porosity by μ -CT, the results suggest comparable porosity behaviours in the two different pore radius range.

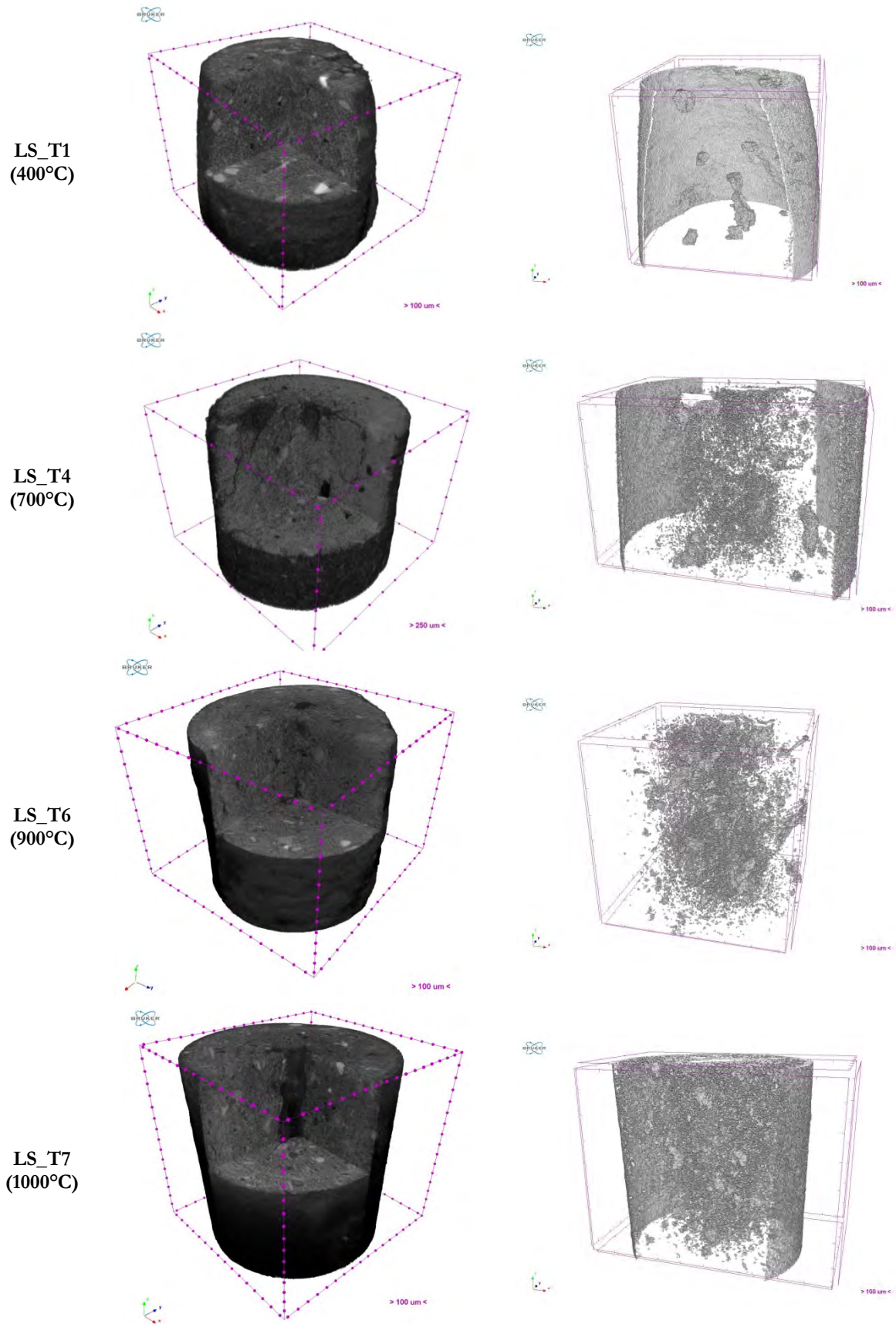


Figure.26. μ -CT results of LS samples fired at different temperatures. 3D sections (on the left) and void extractions (on the right).

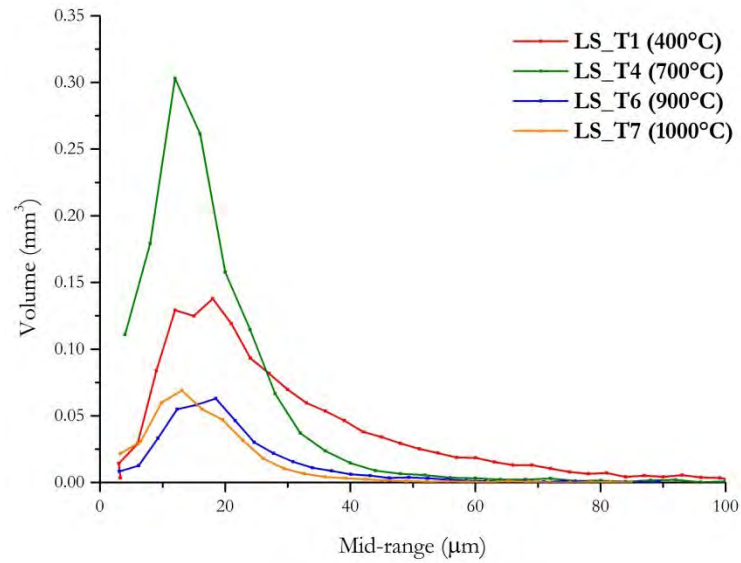


Figure.27. Pore volume vs pore radius calculated by μ CT results of LS samples fired at different temperatures.

Same investigation strategy was adopted for the study of G and S raw ceramic pastes fired at the different temperatures.

G and S pastes seem to have similar chemical and mineralogical composition due to similar raw materials used. All the FT-IR spectra of the both pastes fired at different temperature are reported in **Fig.28**. Absorption bands in the range of $3700\text{--}3620\text{ cm}^{-1}$, attributed to OHs stretching and bending modes characteristic of kaolinite clay minerals, disappear in the spectra related to both G and S samples fired at 900°C (T6). Furthermore, the main peak at around 1036 cm^{-1} ascribable to silicates and clay minerals shifts to greater wavenumbers and the peak at 912 cm^{-1} of kaolinite disappears in the spectra of both G and S samples fired at 700°C . These spectra variations may be due to the kaolinite dehydroxilation which begins at around 600°C and forms metakaolinite ($\text{Al}_4[\text{Si}_4\text{O}_{10}](\text{OH})_8 \rightarrow 2\text{Al}_2\text{Si}_2\text{O}_7 + 4\text{H}_2\text{O}\uparrow$) at higher temperatures [20].

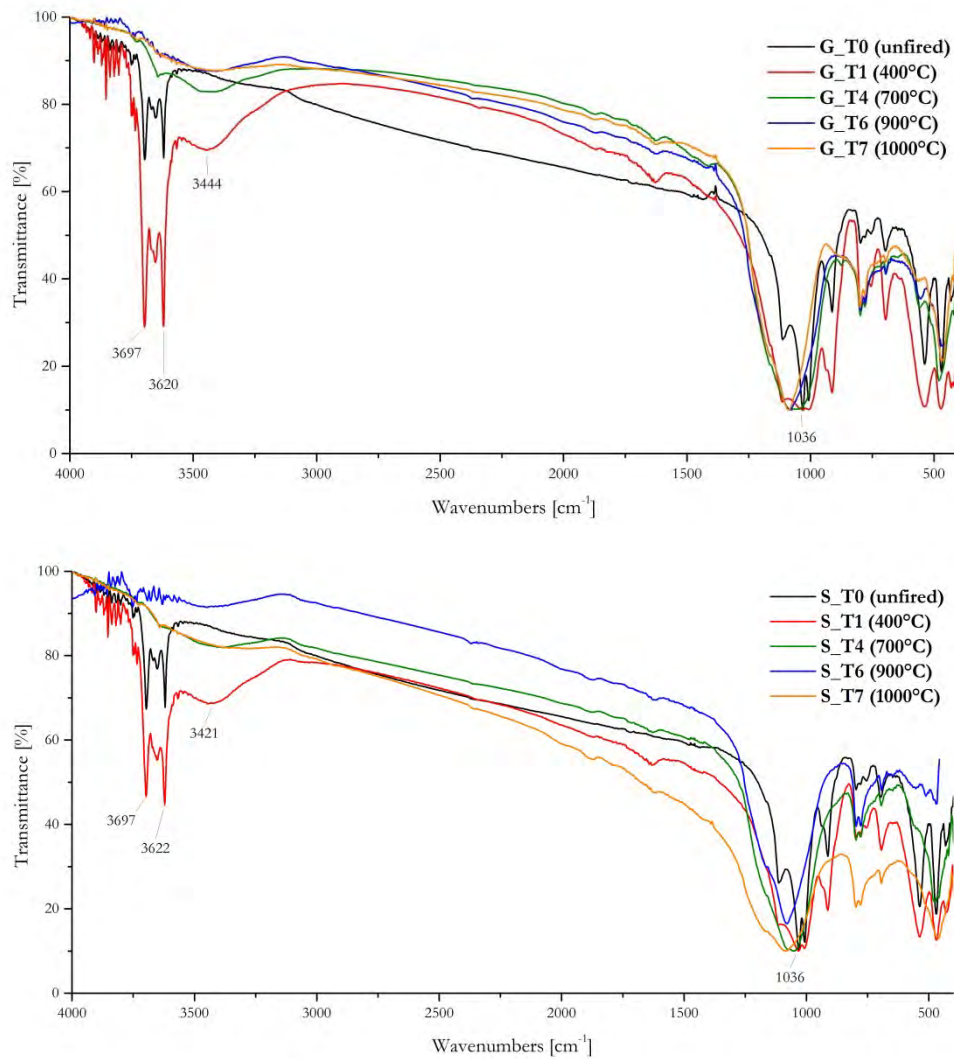


Figure.28. FT-IR spectra of the G (on the top) and S (on the bottom) raw ceramic pastes unfired (T0) and fired at 400°C (T1), 700°C (T4), 900°C (T6) and 1000°C (T7).

Morphological studies by SEM technique show (**Fig.29 (a) and (b)**) a morphology denser and more aggregated for samples fired at higher temperatures (900°-1000°C), as well as shown for the LS samples. Furthermore, sample fired at 1000°C of S paste presents crystal's rounded edges owing to the arising liquid phase.

Fig.30-33 plot the mercury intrusion curves, the trends of total open porosity (%) and average pore radius (μm) of both G and S pastes. In **Tab.9** porosimetry parameters are reported.

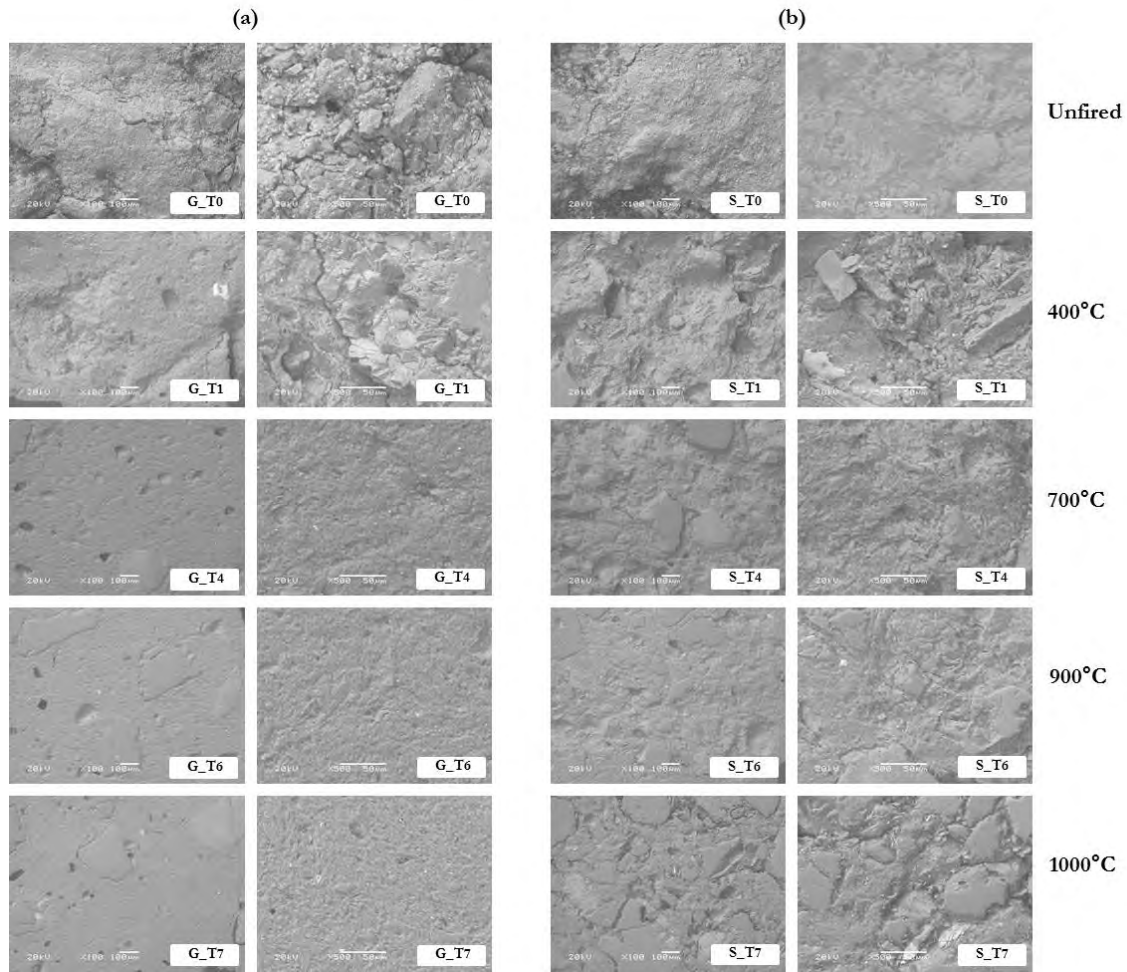


Figure.29. Photomicrographs obtained by SEM analyses at 100x and 500x of magnitudes. **(a)** G samples and **(b)** S samples fired at different temperatures.

Table.9. Porosity data obtained by MIP measurements of both G and S pastes. The average of the three measurements with standard deviation is given.

Sample code	Total Cumulative Volume (cm ³ /g)	Total open Porosity (%)	Average pore radius (µm)	Bulk Density (g/cm ³)	Apparent Density (g/cm ³)
G_T0	0,15±0,00	29,30±1,09	0,02±0,00	1,89±0,06	2,68±0,13
G_T1	0,18±0,00	32,16±0,38	0,03±0,00	1,82±0,02	2,69±0,04
G_T4	0,21±0,00	35,46±0,44	0,04±0,00	1,72±0,04	2,67±0,08
G_T6	0,21±0,00	36,71±0,47	0,04±0,00	1,76±0,01	2,78±0,04
G_T7	0,16±0,00	31,17±0,10	0,07±0,00	1,89±0,01	2,75±0,01
S_T0	0,11±0,00	23,08±0,49	0,03±0,00	2,07±0,06	2,70±0,10
S_T1	0,11±0,01	23,55±2,80	0,02±0,00	2,05±0,05	2,69±0,15
S_T4	0,15±0,01	29,36±0,61	0,03±0,00	1,91±0,03	2,70±0,01
S_T6	0,16±0,00	29,16±0,37	0,05±0,00	1,88±0,08	2,66±0,13
S_T7	0,15±0,01	30,58±1,40	0,51±0,04	2,00±0,02	2,88±0,08

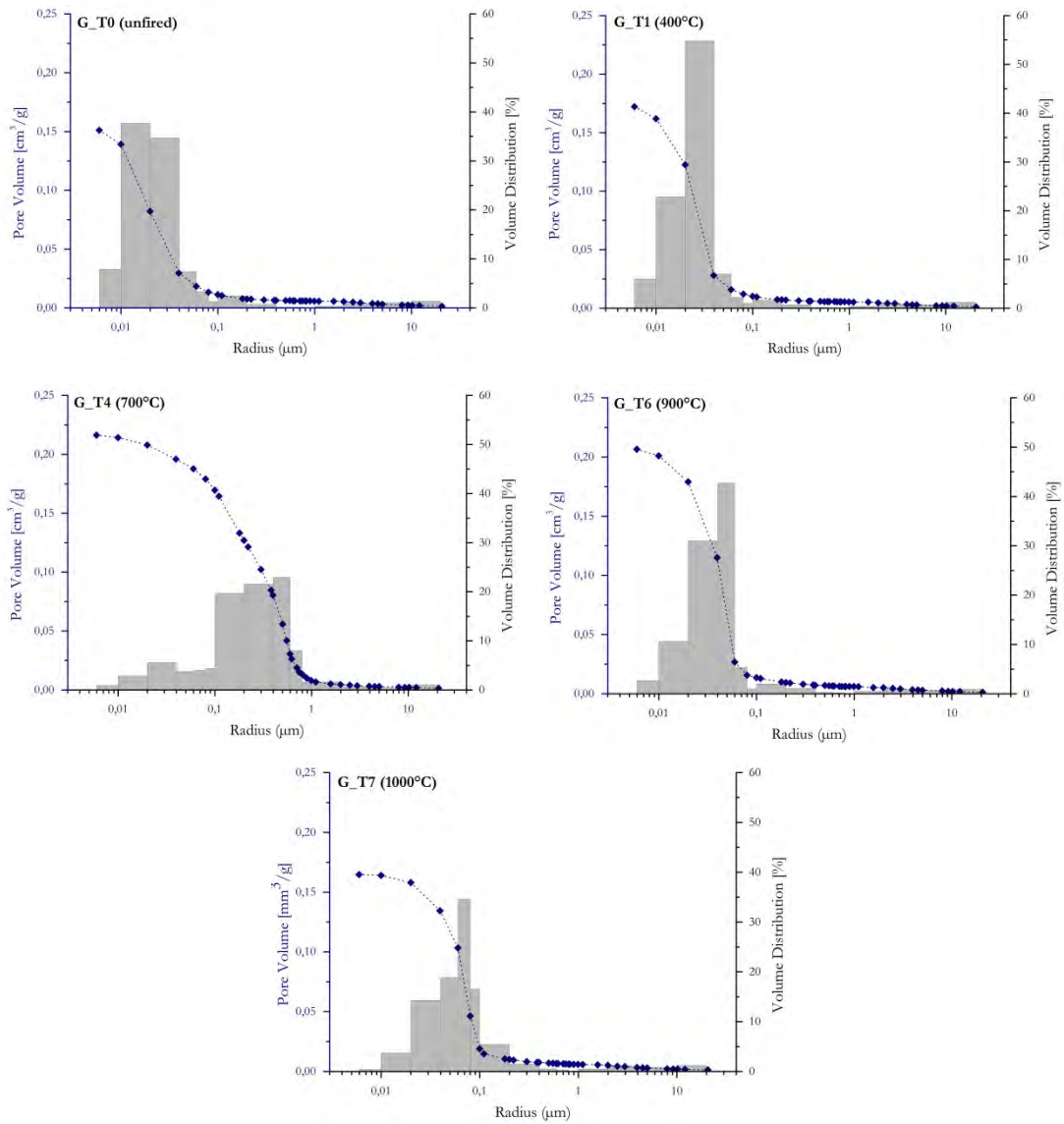


Figure.30. Porosity distribution and cumulative volume vs pore radius of the G samples unfired and fired at different temperatures.

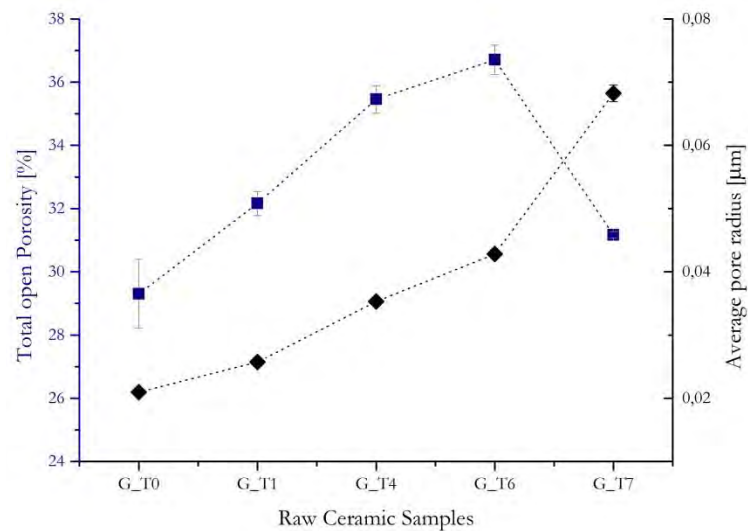


Figure.31. Total open porosity (in blue) and average pore radius (in black) with standard deviation bars of G samples unfired and fired at different temperatures.

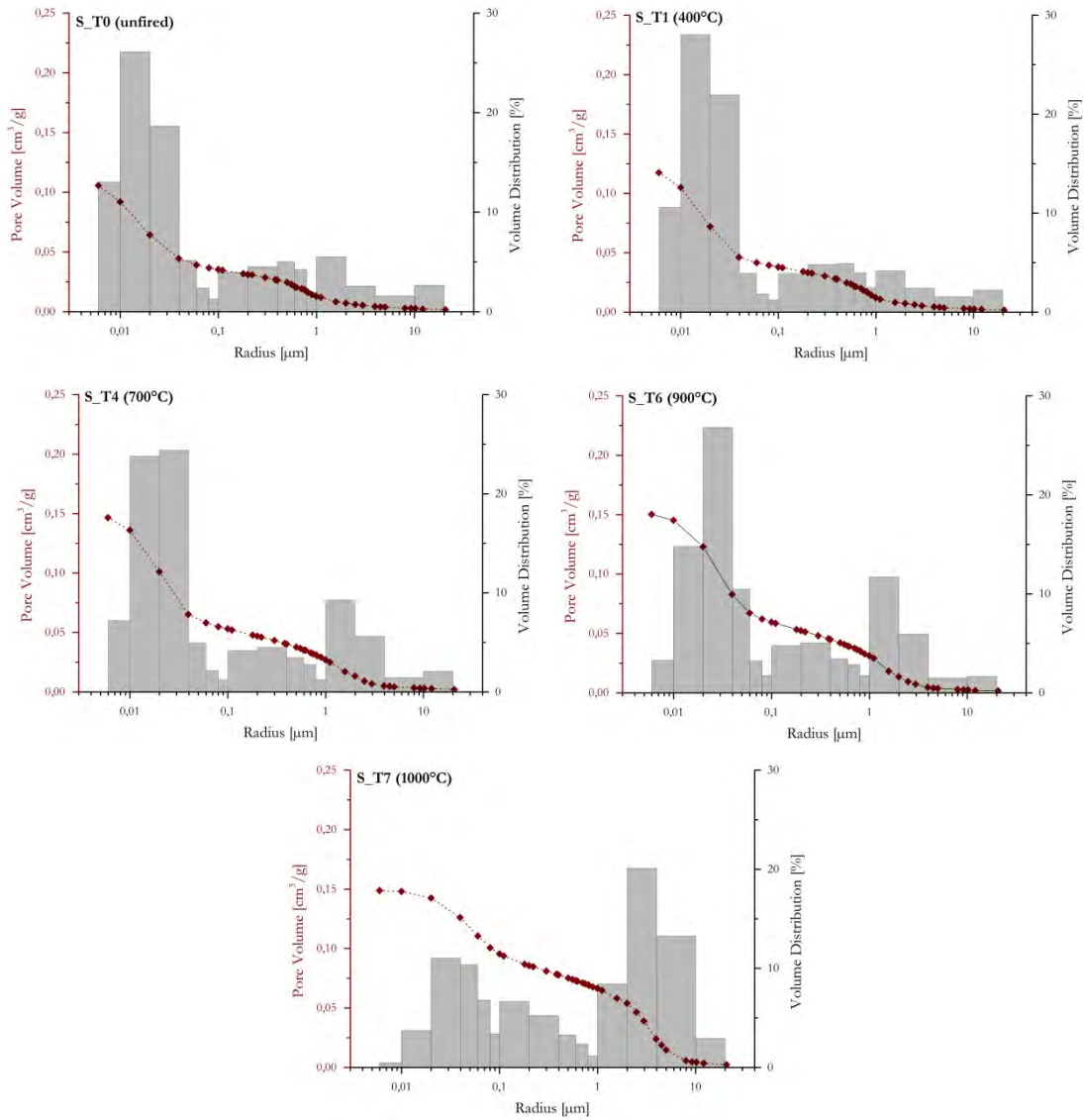


Figure.32. Porosity distribution and cumulative volume vs pore radius of the G samples unfired and fired at different temperatures.

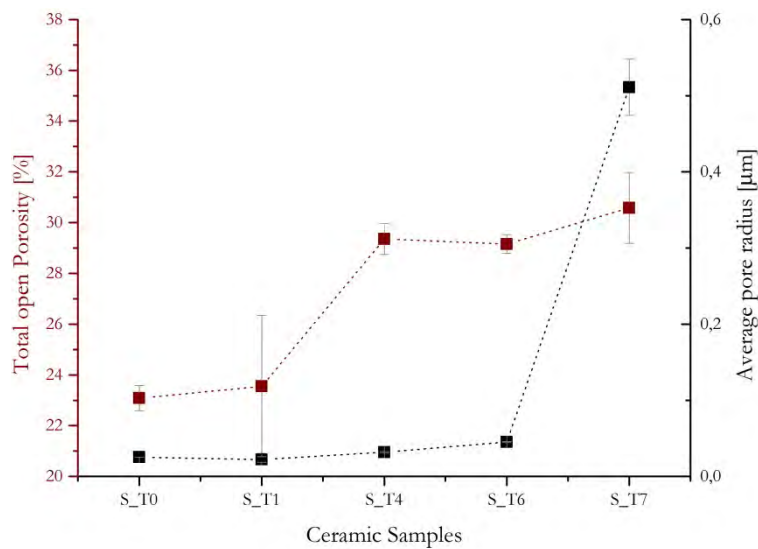


Figure.33. Total open porosity (in brown) and average pore radius (in black) with standard deviation bars of S samples unfired and fired at different temperatures.

The two pastes show notable changes as firing temperature increases, however they display different behaviours despite chemical analysis of the raw materials are similar. Total open porosity (**Fig.31**) and cumulative pore volume (**Fig.34** on the top-left) of G samples increase up to 900°C (G_T6) and drastically decrease (of around 15%) at 1000°C (G_T7). The average pore radius (μm) increases up to 1000°C and the pore distribution curves (**Fig.34** on the top-right) exhibit a shift until 0,08 μm for the sample G_T7 fired at 1000°C.

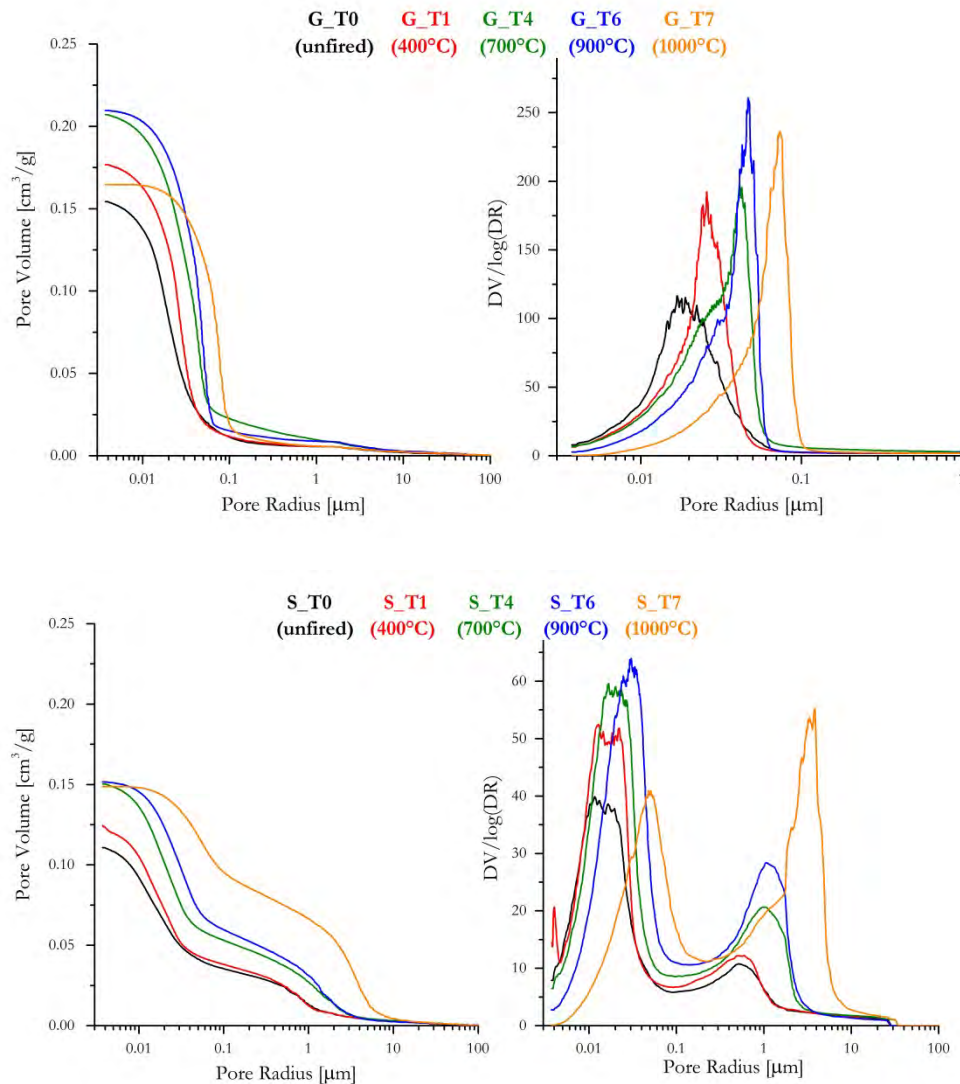


Figure.34. Cumulative pore volume (on the left) and pore size distribution curves (on the right) versus pore radius of G (on the top) and S (on the bottom) samples fired at different temperatures.

S samples display a significant increase of the total open porosity and cumulative pore volume (**Fig.34** on the bottom-left) up to 700°C (S_T4), whereas variations connected to samples fired at 900°C (S_T6) and 1000°C (S_T7) appear minimal (less than 5%). The average pore radius seems to be very similar up to 900°C, and increases from 0,05 to 0,051 μm for the samples fired at 1000°C. Comparing the pore distributions of both G and S samples (**Fig.34** on the right) they

have a uni-modal and bi-modal tendency, respectively, suggesting different grain size in the ceramic matrix. This indication may be supported by the lower total open porosity revealed of the S samples than that one of G samples and by SEM analysis which show different crystal size in particular at microphotographs of G and S samples fired at 1000°C (**Fig.29** on the bottom). As well as noticed in LS samples, both G and S pates promote a greater pore radius in samples fired at 900-1000°C, indicating that the smallest pores usually present among the clay mineral particles were first reduced by the liquid-phase formed at these temperature thus increasing the size of the large ones [32].

Total porosity vs pore radius of G and S samples calculated by μ -CT in the range between 1-100 μm are presented in **Fig.35 (a)** and **(b)**. Furthermore, μ -CT images results are reported for both G and S samples in **Fig.36-37**. Total porosity trends of G and S pastes exhibit a different behaviour as observed by MIP results. G paste seems to be similar to LS paste: the total porosity increases at 700°C and decreases at 900°-1000°C, according to SEM images which show a more densification stage at higher temperatures.

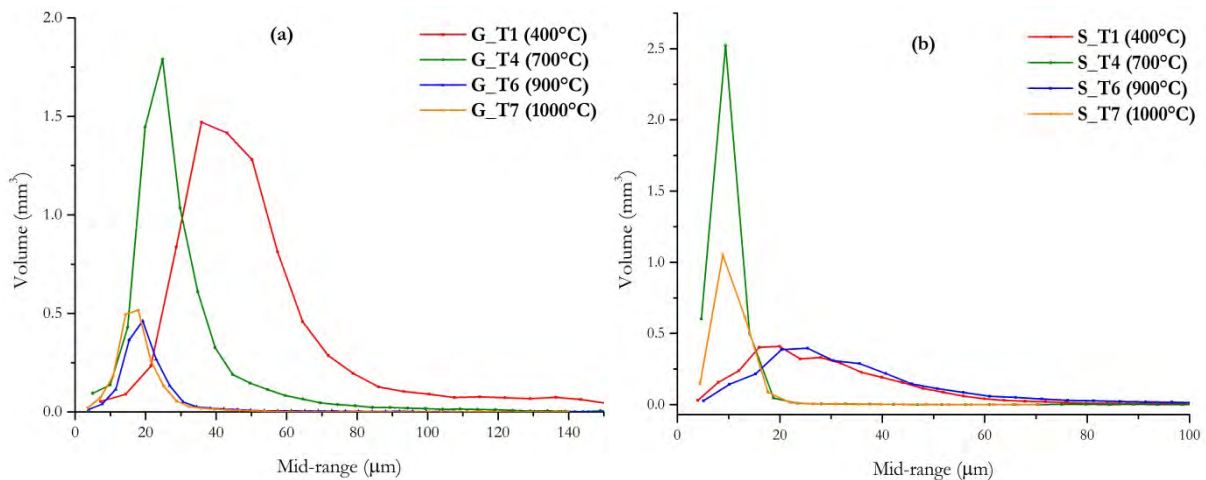


Figure.35. Pore volume vs pore radius calculated by μ -CT results of G samples **(a)** and S samples **(b)** fired at different temperatures.

In the case of S paste, the plot in **Fig.35 (b)** emphasizes the variations which occur in the matrix at 700°C (S_T4) and 1000°C (S_T6), suggesting that the reactions of dehydroxilation of clay minerals and the beginning of silicate melting strongly affect the microstructure of the raw ceramic samples.

Apparent density of S samples calculated by MIP provided insights regarding total porosity [31]. Its values, reported in **Tab.9**, indicate a similar total porosity² of S samples fired up to

² Considerations on total porosity (close and open pores) from MIP results were made on the basis of its opposite behaviour compared to that of apparent density [31].

700°C, a slight increase at 900°C and a more significant decrease at 1000°C. Examining the total porosity evaluated by μ -CT in the greater pore radius range, it seems to have a different behaviour with an almost opposite trend, due to the increase of the total porosity in particular at 700° and 1000°C. These data confirm and underline the influence of closed porosity on the behaviour of the raw ceramic pastes submitted to thermal treatments.

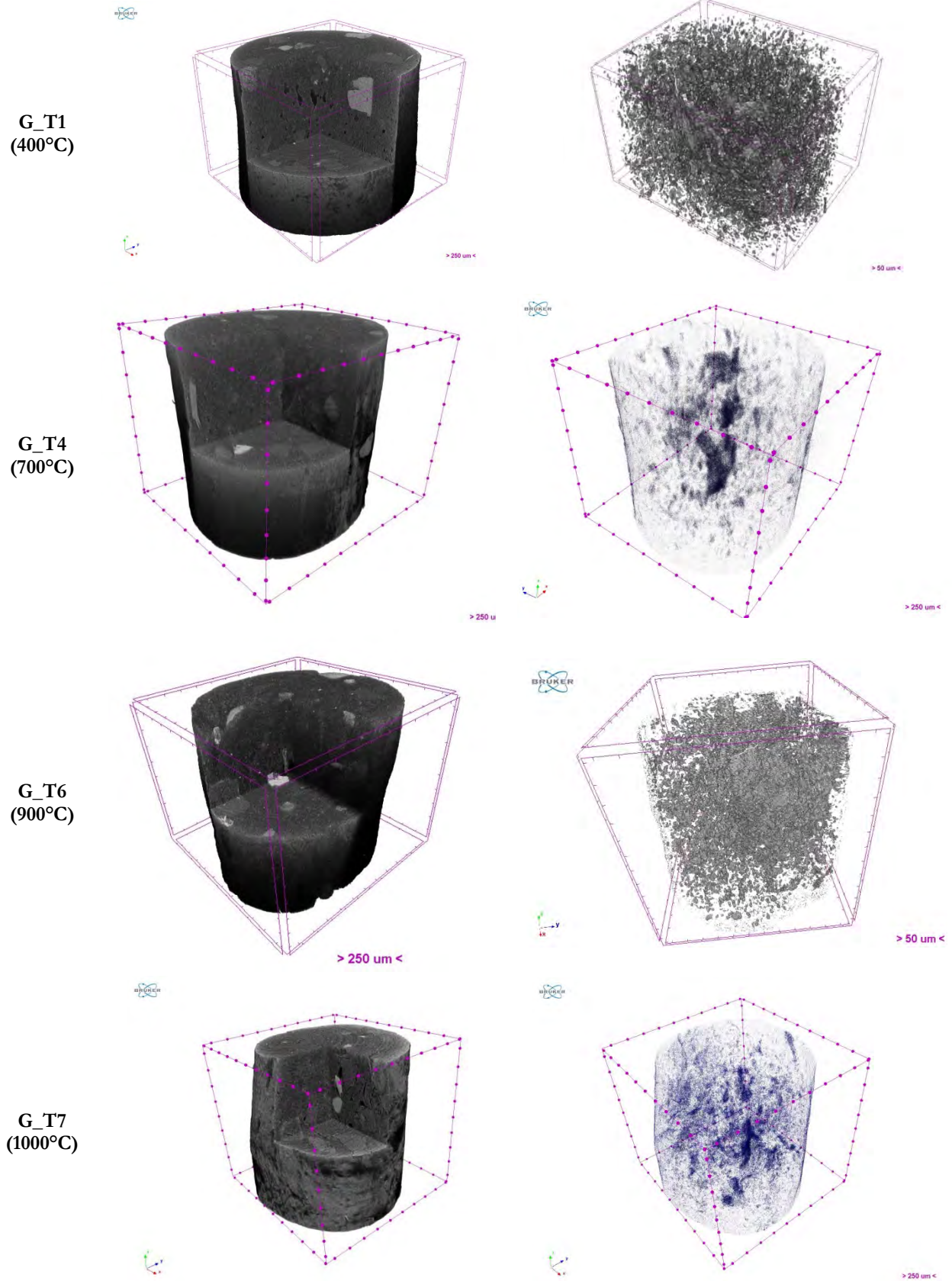


Figure.36. μ -CT results of G samples fired at different temperatures. 3D sections (on the left) and void extractions (on the right).

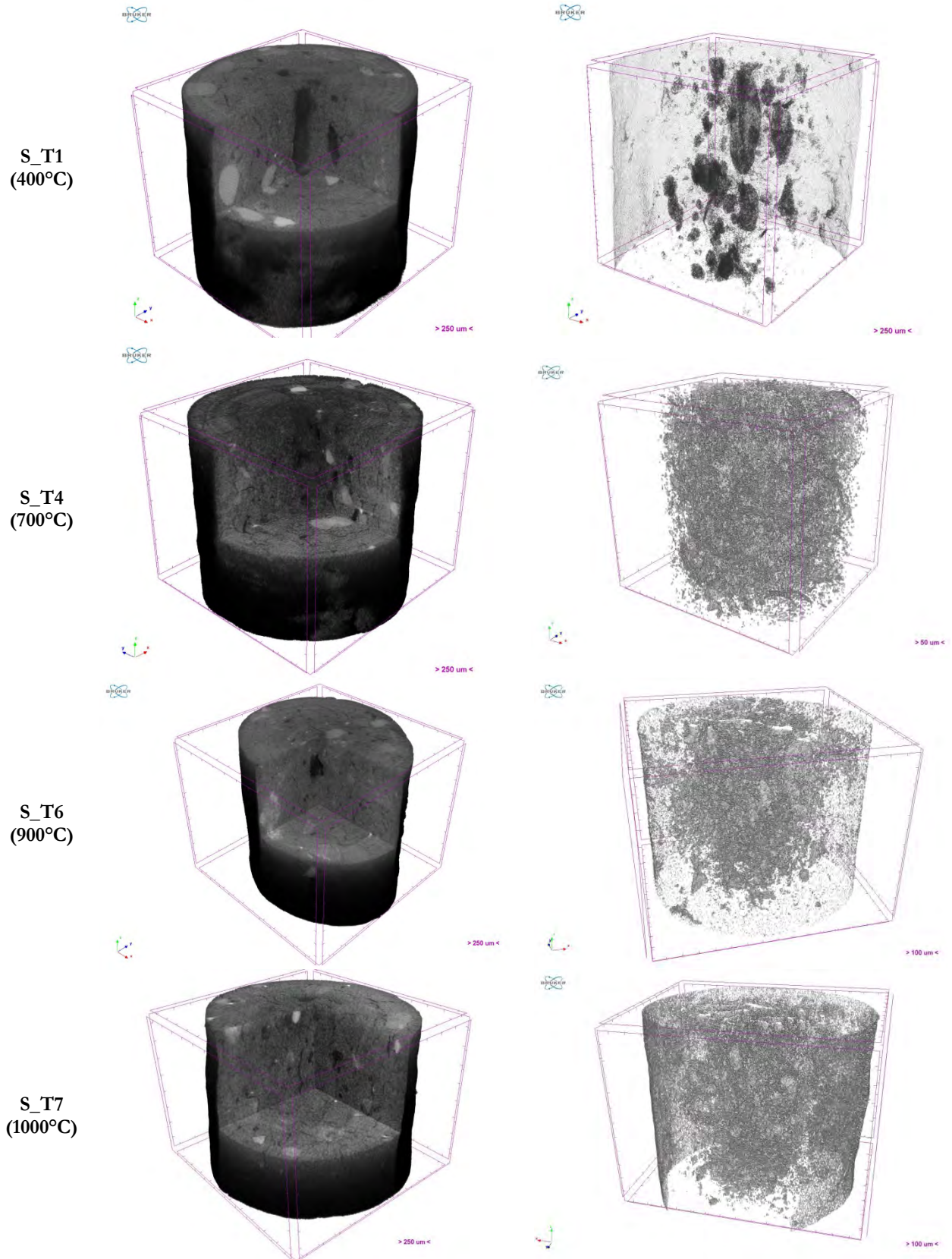


Figure.37. μ -CT results of S samples fired at different temperatures. 3D sections (on the left) and void extractions (on the right).

4.1.3. Brief Conclusions on the Chemical, Mineralogical and Microstructural Changes of the Raw Ceramic samples after Firing.

The investigation strategy adopted in order to study the chemical, morphological and microstructural modifications which occur during firing ceramic materials allowed to identify the main features affected by firing temperatures. The Ca-rich LS paste and the both G and S rich in kaolinite exhibit the main changes at 700° and 900°C, corresponding to the carbonate decomposition and dehydroxilation reactions which modify both chemical composition, well revealed by FT-IR spectroscopy, and microstructure in terms of porosity and morphology of the matrix. Moreover, there were identified some of the indicators linked to firing temperatures. Bounded water in clay crystal lattice, new mineral phases and carbonate minerals, revealed by FT-IR analysis, play an important role in firing temperature determination. SEM images allowed to both describe the morphology of the ceramic samples and identify particular features strictly connected to the maximum firing temperature, as the crystal aggregation, melting phase and continuity of the solid in terms of densification effects. Thus, SEM micrographs are able to give insights on the microstructural changes and densification stages which clearly provide technological information on the artefact. Porosity investigation cannot be directly connected to the aspect and consequently to firing temperature, because, as it is seen from the reported data, it provide information only regarding the open porosity [28], [33]. Total porosity is necessary in order to completely describe the morphological changes occurring during the firing process. A lack of studies on total porosity calculation has been found in literature. The obtained results by μ -CT are very promising and, although they seem to be difficult to interpret, may open new insights in considering other ranges and the trend of total porosity influenced by the closed porosity, parameter that needs to be studied for a complete awareness of the ceramic material features.

4.2. Characterization of Ceramics from Torcello

Archaeological ceramic fragments from the excavation site at Torcello, in the Venetian Lagoon, were investigated with the aim to verify the connection between chemical composition and physical-morphological features on archaeological samples, as well as evaluate the effectiveness of the applied analytical techniques. The selected sherds were initially divided in three groups from an archaeological point of view, thanks to the suggestions received by the archaeologists Dr. Diego Calaon and Prof. Cudio Negrelli of Ca' Foscari University of Venice. The archaeometric results obtained by chemical-mineralogical and morphological studies are presented and discussed in this paragraph. They outlined a similar but at the same time variable production techniques in Late Antique and Early-Medieval globular amphorae and an own production for the single-glaze potteries.

4.2.1. Chemical and Mineralogical Characterization. Results and Discussion

Chemical characterization of the archaeological sherds was carried out by means FT-IR and μ -Raman spectroscopies, where mineralogical attributions were performed on the basis of the data reported in literature.

FT-IR spectroscopy allowed to identify the chemical composition of the analysed sherds. The most significant spectra are reported in **Fig.38-39** and in **Tab.10** are summarised the FT-IR results along with the tentative vibrational assignments.

FT-IR results showed similar chemical-mineralogical composition of the ceramic fragments mainly composed of quartz, calcite, smectite (montmorillonite), kaolinite, feldspars and iron oxides.

Quartz is inferable by the shoulder at $1140-1172\text{ cm}^{-1}$, the peak at $1064-1089\text{ cm}^{-1}$ due to Si-O stretching, the characteristic doublet at $794-800$ and $770-780\text{ cm}^{-1}$ related to Si-O symmetric stretching, and the peak at $685-699\text{ cm}^{-1}$ assigned to Si-O bending mode [12], [17], [34]. The broad band centred at around $3400-3440\text{ cm}^{-1}$ is present in all the samples and is due to -OH stretching vibration mode in the interlayer region of montmorillonite clay mineral (smectite) [12]. The presence of this band may indicate firing temperature lower than 900°C , because above this temperature montmorillonite dehydroxylates and produces spinel and/or other firing products as anorthite and mullite not detected in the analysed samples [20].

The presence of montmorillonite is also shown by the peaks at 1040-1049 cm^{-1} and 471-479 cm^{-1} , due to Si-O stretching mode and Si-O-Si deformation, respectively [2], [35]. As clay mineral, kaolinite was also detected by the peaks at: 1030-1037 cm^{-1} ascribed to Si-O-Si stretching mode, 1008-1016 and 900-933 cm^{-1} attributed to Si-O and Al-O-H stretching modes, respectively [2], [12], [17], [36].

Table.10. FT-IR results of the analysed ceramic bodies coming from the Venetian Lagoon. Tentative vibrational assignments is given on the basis of data reported in literature [2], [6], [9], [12], [20], [26], [37].

Late Antique Amphorae				Single-glaze potteries			
1151_4	1151_5	1157	6001_1	1078_2	1151_1		
IR frequency with relative intensity (cm^{-1})						Tentative vibrational assignment	
	3540 bd			3551 bd		O-H str.	Water/Gypsum
3400 bd	3411 bd	3406 bd	3453 bd	3420 bd	3458 bd	O-H str.	Water/Smectite*/Gypsum
1795 vvw		1795 vw					Calcite
1616 vw	1617 w		1620 vw	1617 vw	1623 vw	O-H-O bend.	Water
	1466 vw		1473 sh			$-\text{CO}_3^{2-}$	Calcite
1432 s	1446 m	1421 vs	1442 s	1434 w	1431 vw	$-\text{CO}_3^{2-}$	Calcite
				1080 vs	1080 vs	Si-O str./Al-O-Si str.	Quartz/Amorph. Al-Si ^b
1049 vs	1043 vs	1047 vs	1040 vs	1040 sh	1049 vs	Si-O str.	Smectite*
		1008 sh				Si-O/Si-O-Al str.	Kaolinite/Muscovite
930 sh		921 sh				Al-O-H	Kaolinite
876 s	875 sh	875 s	868 m			$-\text{CO}_3^{2-}$	Calcite
795 m	796 m	795 m	799 w	797 w	796 s	Si-O str.	Quartz
779 m	779 m	771 m	768 m	781 w	779 s	Si-O str.	Quartz
					727 w	Al-O-Si bend.	Feldspar
714 w			713 w			Si-O bend./ $-\text{CO}_3^{2-}$	Calcite
692 w	694 w	685 vw	691 w	699 vw	694 m	Si-O bend.	Quartz
		638 vw	652 w	641 vw	639 w	Si-O-Si bend.	Silicates/Feldspar
		575 w		574 w			Magnetite
			551 m				Hematite
517 w		528 vw				Si-O-Al ^{IV} /Fe-O bend.	Kaolinite/Muscovite/Hematite
	471 s	473 m				Al-O/Si-O-Si deformation mode	Feldspar/Hematite/Smectite*
459 - 418 s	457 - 434 - 420 m	425 m	458 w	458-417 m	463 s	Si-O mixed deformation	Silicates

Early Medieval Globular Amphorae						
1154_8	1154_10	1159_2	1167_1	1210_1		
IR frequency with relative intensity (cm ⁻¹)					Tentative vibrational assignment	
3553 w			3546 w	3546 w	O-H str.	Water/Gypsum
3402 w	3434 bd	3427 bd	3407 w	3406 w	O-H str.	Water/Smectite*/Gypsum
	1797 vw					Calcite
1627 vw	1618 w	1635 m		1624 vw	O-H-O bend.	Water
			1460 vw	1452 w	-CO ₃ ²⁻	Calcite
1440 m-bd	1429 m	1428 w	1430 w	1433 w	-CO ₃ ²⁻	Calcite
1140 sh	1172 sh			1155 sh	Si-O str.	Quartz
			1089 vs	1079 vs	Si-O str./Al-O-Si str.	Quartz/Amorph. Al-Si ^b
1042 vs		1044 vs		1042 vs	Si-O str.	Smectite*
	1030 vs		1036 vs		Si-O-Si str.	Kaolinite
					Si-O/Si-O-Al str.	Kaolinite/Muscovite
928 sh		900 sh			Al-O-H	Kaolinite
	874 s			839 vw	-CO ₃ ²⁻	Calcite
798 m	796 m	799 m	794 w	798 vw	Si-O str.	Quartz
777 m	779 m	769 m	773 m	778 w	Si-O str.	Quartz
731 w				728 w	Al-O-Si bend.	Feldspar
714 w	711 m				Si-O bend./-CO ₃ ²⁻	Calcite
695 w	694 w	699 vw	688 w	697 w	Si-O bend.	Quartz
				648 w	Si-O-Si bend.	Silicates/Feldspar
575 w				602-592 w		Magnetite
				568 w		Hematite
517 w				516 w	Si-O-Al ^{IV} /Fe-O bend.	Kaolinite/Muscovite/Hematite
476 m	466 s	462 s	479 s	471-459 m	Al-O/Si-O-Si deformation mode	Feldspar/Hematite/Smectite*
451 - 414 s			458-425 w	445-417 m	Si-O mixed deformation	Silicates

Early Medieval Globular Amphorae					
5155_23	1155_1	1188_4	1224_2		
IR frequency with relative intensity (cm ⁻¹)				Tentative vibrational assignment	
		3545 w	3500 bd	O-H str.	Water/Gypsum
3421 bd	3440 bd	3396 w		O-H str.	Water/Smectite*/Gypsum
					Calcite
	1631 w	1621 w		O-H-O bend.	Water
1468 m				-CO ₃ ²⁻	Calcite
1441 m	1430 w	1427 m	1430 vw	-CO ₃ ²⁻	Calcite
	1161 sh		1146 sh	Si-O str.	Quartz
	1078 vs		1064 vs	Si-O str./Al-O-Si str.	Quartz/Amorph. Al-Si ^b
	1048 vs	1046 vs		Si-O str.	Smectite*
1037 vs			1036 vs	Si-O-Si str.	Kaolinite
			1016 vs	Si-O/Si-O-Al str.	Kaolinite/Muscovite
			933 sh	Al-O-H	Kaolinite
875 w		875 w		-CO ₃ ²⁻	Calcite
798 w	798 m	800 m		Si-O str.	Quartz
780 w	774 m	770 m	775 w	Si-O str.	Quartz
731 w		728 w	733 w	Al-O-Si bend.	Feldspar
717 w		712 w	720 vw	Si-O bend./-CO ₃ ²⁻	Calcite
685 w	685 w	694 vw	688 w	Si-O bend.	Quartz
634 w	646 w	647 w		Si-O-Si bend.	Silicates/Feldspar
573-602 w		602 w	575 w		Magnetite
		567 w			Hematite
525 w		515 w		Si-O-Al ^{IV} /Fe-O bend.	Kaolinite/Muscovite/Hematite
471 m		479-466 m	472 s	Al-O/Si-O-Si deformation mode	Feldspar/Hematite/Smectite*
458 - 419 s	457 s	455-419 m	456-433-417 m	Si-O mixed deformation	Silicates

s: strong; vs: very strong; w: weak; vw: very weak; m: medium; sh: shoulder; bd: broad band.
str.: stretching mode; bend.: bending mode.

*Smectite, probably montmorillonite.

Some samples show two different peaks at around 3540-3553 and 3396-3411 cm^{-1} may be due to the presence of gypsum rehydrated during burial period. Gypsum in ceramic body might be an impurity in the clay minerals or, more probably, an alteration product due to the reactions involving the released sulphate anions and Ca^{2+} either present in water or derived by dissolution of secondary calcite [6], [10], [38]. These archaeological fragments come from an excavation site in the Venetian Lagoon and the amount of sulphate anions in the seawater is generally low, therefore, other sources may be contamination of hydrocarbons or sulphate-reducing bacterial colonies, which are suitable with the lagoon-like environment [38]. The presence of gypsum as post-burial alteration and its bands attributed to $-\text{OH}$ stretching mode may interfere in estimating firing temperature due to its overlapping with the OHs related to clay minerals. The presence of feldspar (727-733 and 634-648 cm^{-1}), hematite (541-550 and 471-479 cm^{-1}) and magnetite (575-580 cm^{-1}) were also detected [12], [34]. Iron oxides in ceramic body, as hematite and magnetite, provide information about the atmospheric condition during firing: oxidizing and reducing atmosphere, respectively. The presence of both may indicate variable conditions during the firing process probably due to uneven fuel or ventilation.

Interesting is calcite detected in different amount in all the samples. The main detected $-\text{CO}_3^{2-}$ peaks are: 1795-1797 (calcite overtone/combination bands), 1452-1478, 1421-1442, 874-875 and 711-720 cm^{-1} [6], [26], [37]. The presence of calcite can provide information about raw materials, technological production, firing temperature and use of the artefact [39]. Particular regards it has to be given to the fact that calcite is often found in archaeological ceramics and its origin can be primary or secondary. The former may come from the raw material used for manufacturing the pottery or introduced as a temper by the potters. Carbonate tempers used by potters may cause high porosity, defects and fractures due to the mechanical damage that takes place during and after their thermal decomposition. For this reason, potters usually used limestone as a temper for pottery vessels but not for cooking pots [40]. The secondary calcite includes calcite crystals grown from alteration and/or precipitation after the firing process [26]. The presence of the peak at around 1452-1473 cm^{-1} may indicate reformed calcite. Though FT-IR measurements it is possible to distinguish primary and secondary calcite due to the main $-\text{CO}_3^{2-}$ band of the reformed calcite that has usually a broad and asymmetric shape with a rounded top at greater wavenumbers, as shown in some of the spectra of Torcello fragments (**Fig.38 (b)**) [26]. Ceramic sherds from Torcello were divided in sub-groups, further subdivision than that proposed by archaeologists, on the basis of the presence of primary or secondary calcite as it is reported in **Tab.11**.

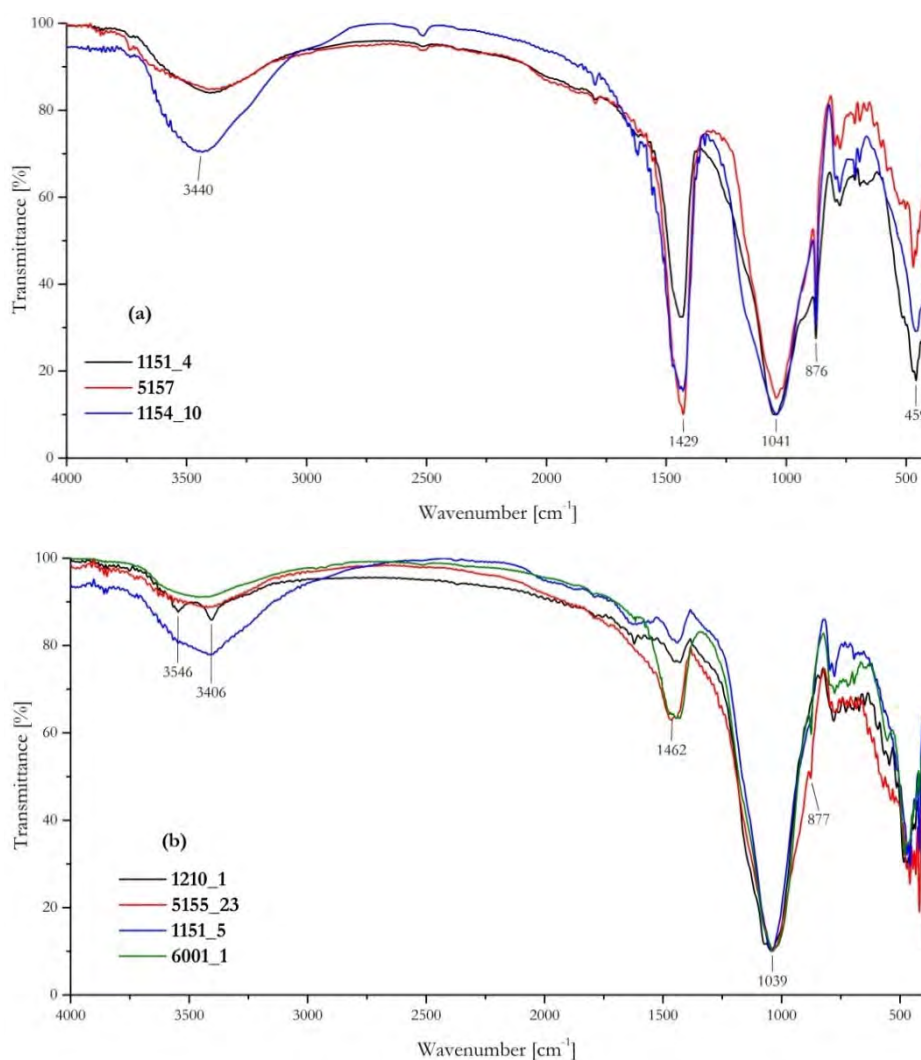


Figure.38. FT-IR spectra of representative ceramics from Torcello, which are mainly composed of fired clay, quartz and primary **(a)** and secondary **(b)** calcite.

Table.11. Summary of the discrimination in sub-groups on the basis of the presence of primary or secondary calcite ascribed by FT-IR results.

	Late Antique Amphorae	Early Medieval Globula Amphorae	Single-Glaze potteries
P	5157, 1151_4	1154_10, 1188_4, 1159_2, 1224_2, 1155_1	1078_2, 1151_1
S	6001_1, 1151_5	5155_23, 1210_1, 1167_1, 1154_8	

P=primary calcite; **S**= secondary calcite.

The presence of calcite, even if secondary, and the absence of IR bands related to Ca-silicates phases (such as gehlenite, wollastonite, diopside and anorthite) suggest firing temperature lower than 900°C, probably in the range of 700°-850°C [26].

FT-IR spectra of the glazes present in the two single-glaze potteries do not provide further information regarding the composition of the glaze and colouring agents in the siliceous matrix (**Fig.39 (a) and (b)**).

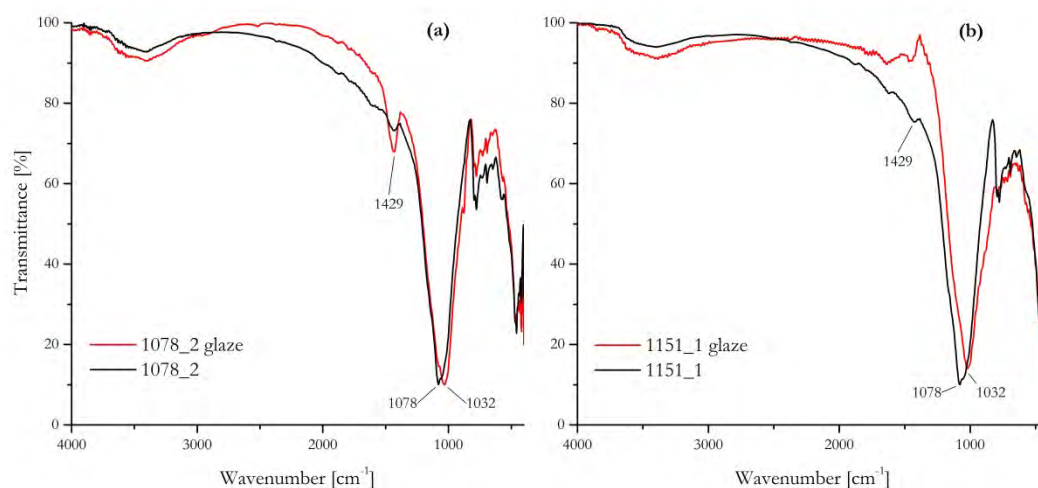


Figure.39. FT-IR results of the bodies and glazes of two single-glaze potteries 1078_2 and 1151_1, **(a)** and **(b)** respectively.

Analyses carried out by means of μ -Raman spectroscopy on the glaze of the single-glaze potteries allowed to provide indications on glaze composition and firing temperature. The analyses were carried out on fragments previously embedded in polyester resin and then polished in order to obtain a flat surface of the body-glaze cross-section. Colomban et.al. demonstrated the capability of Raman technique to discriminate crystalline and amorphous phases of silica, and in particular, the correlation between Raman bands and both composition and firing temperature of the glass/glaze [41]–[44]. The amorphous silica phase show two main Raman bands: the first one is located at around 500 cm^{-1} related to the bending vibration of isolated SiO_4 tetrahedras; the second one, at around 1000 cm^{-1} , is related to the Si-O stretching vibration modes. Both the shape and intensity of these bands depend on the nature of the glaze and/or the tetrahedral unit network. 1078_2 and 1151_1 fragments seem to be very similar and their Raman spectrum (**Fig.40**) exhibits a weak broad band at around 500 cm^{-1} and an intense broad band centred at around 940 cm^{-1} . The strong Raman intensity of the latter band may indicate a weakly connected tetrahedral units which allows a large-amplitude oxygen motion in the stretching mode [45]. Furthermore, Na, K, Ca and Pb, added in the glaze as oxides with the function of flux agents, change both the connectivity and partial ionic charge of terminal oxygen atoms modifying bond length and Raman bands. In according with the results of Colomban et.al., the predominance in the Raman spectra of the band at around 1000 cm^{-1} (at 940 cm^{-1} for both 1078_2 and 1151_1

Torcello sherds) corresponds to lead-rich glaze fired at low temperature (at around 700°-800°C) [44], [46], [47]. The estimated firing temperature of the glaze layers by Raman measurements is in agreement with the estimated firing temperature of the bodies inferred by FT-IR results, which may be between 700°-850°C.

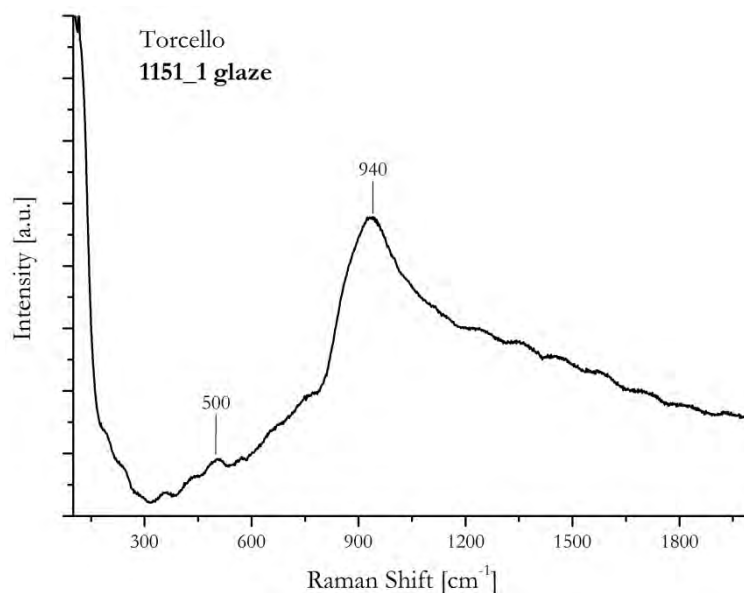


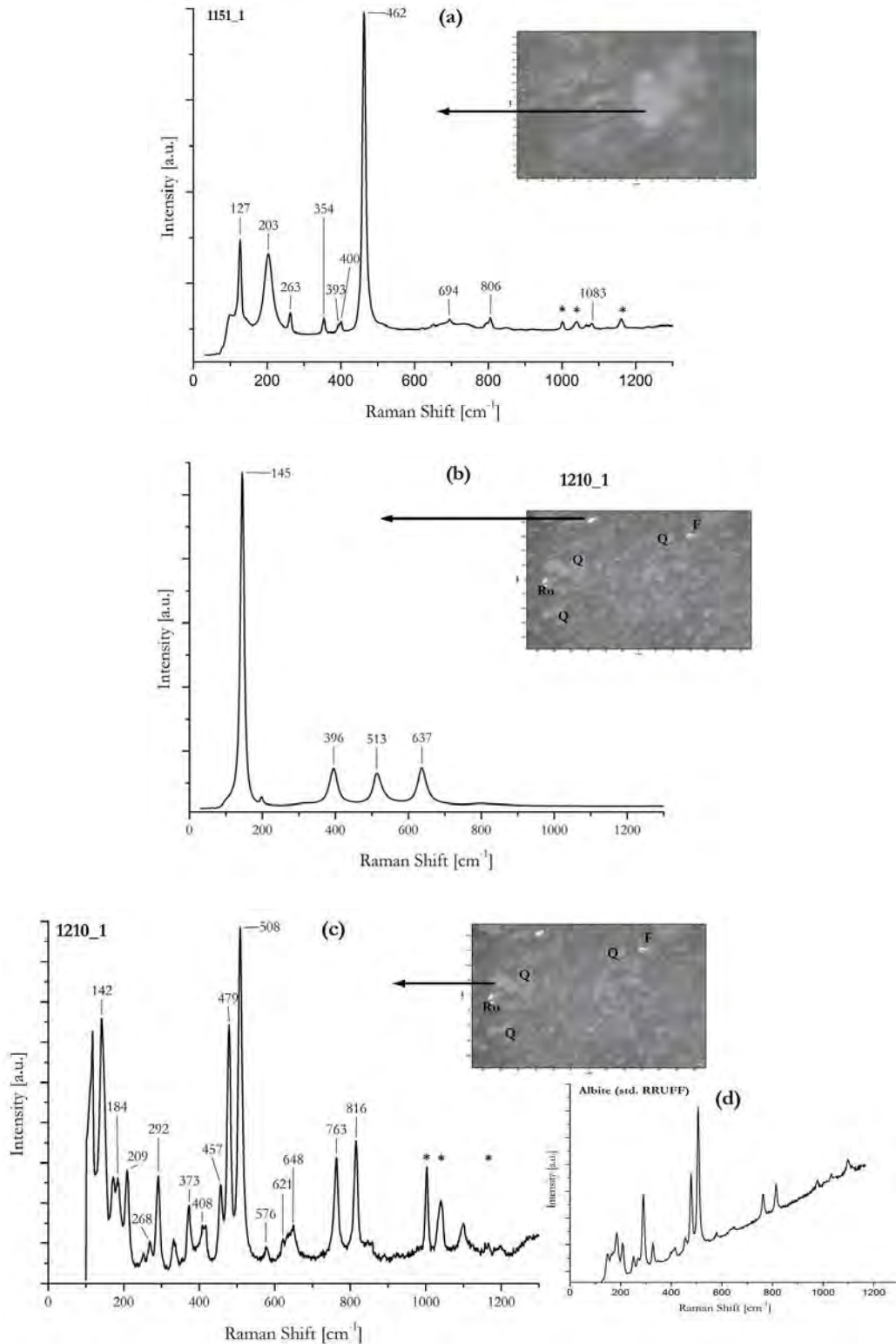
Figure.40. μ -Raman spectrum of the glaze coating of the sample 1151_1 from Torcello.

μ -Raman analyses were performed also on the ceramic body of the selected fragments from Torcello, showing a similar chemical composition. Representative μ -Raman spectra are reported in **Fig.41 (a)-(f)**. Attributions to mineral phases is given on the basis of data reported in literature [7], [10], [11], [15], [17], [27], [48]–[52]. The main phases detected are:

- quartz (by the Raman bands at 125-127, 202-3, 354, 392-393 cm^{-1} , the very intense peak at 462 cm^{-1} due to the Si-O-Si bending mode and 806 cm^{-1});
- anatase (145, 396, 513 and 637 cm^{-1}) and rutile (242, 441 and 609 cm^{-1});
- kaolinite (145-146, 201, 287, 349-357, 476 and 650-658 cm^{-1});
- montmorillonite (209, 268, 455, 817 and 918 cm^{-1});
- illite (457, 621-623, 633 and 794-797 cm^{-1});
- feldspars (172, 183-184, 209, 251-252, 268, 292-293, 330-332, 412-413, 455-457, 479-480, 508-510, 576, 648, 762-763 and 816-817 cm^{-1});
- hematite (206, 291-296, 373, 403-408 and 412 cm^{-1});
- gypsum (684 and 851-852 cm^{-1});
- calcite (151-158, 279 and 1088 cm^{-1}).

The presence of both montmorillonite and illite confirms the firing temperature inferred by FT-IR results. Montmorillonite dehydroxylates above 700°C and at higher temperature than

900°C may produce firing products as spinel, anorthite and mullite. Crystalline structure of illite begins to break down between 700° and 850°C [35]. Furthermore, the detected peaks at around 201 and 287 cm^{-1} ascribed to kaolinite may be due to bending modes of O-H-O, which can persist in the structure up to 750°-800°C [10], [35], [53]. These data suggest a reached kiln temperature of around 700°-800°C.



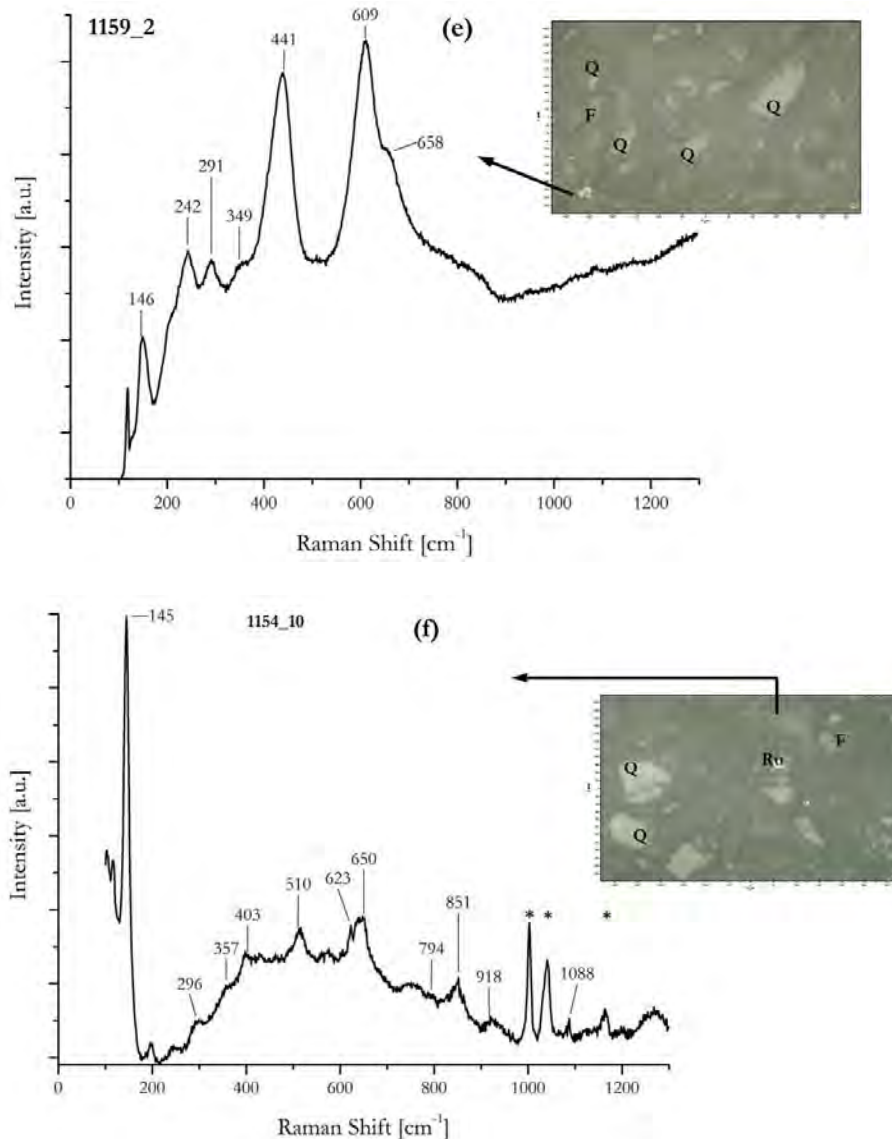


Figure.41. Representative μ -Raman spectra of the ceramic sherds coming from Torcello. **(a)** quartz; **(b)** anatase; **(c)** feldspar and hematite; **(d)** albite spectrum, as standard from RRUFF database; **(e)** rutile and kaolinite; **(f)** mixture of feldspar, gypsum, montmorillonite and illite. (* indicates peaks related to the polyester resin used to embed the ceramic fragments). The pictures beside the spectra show the surface of the samples and the measured points. Furthermore, letters on the pictures identify measured points: Q=quartz; Ru=rutile; F=feldspar.

Raman results confirmed the presence of calcite, gypsum and hematite. Furthermore, μ -Raman technique is able to identify titanium oxides and both rutile and anatase were detected, as often present in ceramic paste as they are impurities in clay and sand materials. The transition anatase–rutile occurs firing above 900°C but it can be influenced by other minerals in the ceramic matrix, thus an estimation of firing temperature on the basis of titanium oxides may be uncertain and, furthermore, it has to be considered that TiO_2 as rutile phase could be directly present in the paste [15], [54]. Concerning the presence of feldspars, μ -Raman spectroscopy was able to identify

albite recognized by the data reported in literature and comparison with standard spectrum reported in RRUFF database available online (**Fig.41 (d)**) [27].

4.2.2. Petrographic and Mineralogical Results and Discussion

Polished cross-sections as well as thin sections of ceramic fragments were made of selected samples in order to study the mineralogical composition and structure features of the ceramic body by means of stereomicroscope and petrographic analysis using polarising optical microscope. Groundmass, colour of the paste and presence of inclusions characterize the ceramic matrix and may allow to provide insights on the technological productions [55]–[58].

Colour of the ceramic paste depends on mineralogical composition and firing conditions. Iron oxides give colouration to the paste and have various colours depending on their oxidation and hydration states. Hematite (Fe_2O_3) gives red to pink colour, whereas magnetite (Fe_3O_4), which can be formed from iron oxides as hematite in reducing atmosphere, gives a grey-dark colour [39], [59]. The single-glaze potteries, 1078_2 and 1151_1 samples shown in **Fig.42**, have a dark-grey colourations suggesting reducing atmosphere and/or low firing temperature, in according with the spectroscopic results in which magnetite was detected by FT-IR measurements and the estimated low firing temperature at around $700^\circ\text{--}800^\circ\text{C}$.

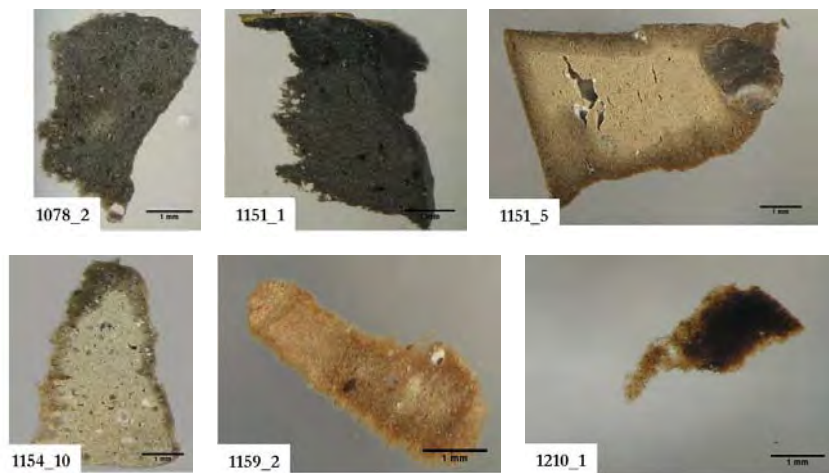


Figure.42. Photographs of ceramic fragments obtained by stereomicroscope on cross-sections embedded with polyester resin and polished.

The other fragments have variable colours, as it can be seen in **Fig.42**, between light tan and brownish, suggesting different firing condition probably due to low carbon content and/or oxidizing atmosphere, since the firing temperature was estimated as low temperature also in these sherds. The matrix show different fabrics with coarse and fine-grained inclusions of aplastic materials. Observation by polarizing optical microscope of ceramic thin sections allowed to

investigate on the nature of inclusions showing the presence of quartz, calcite, alkali-feldspars and muscovite. Representative thin section photos in both parallel and cross light are reported in Fig.43.

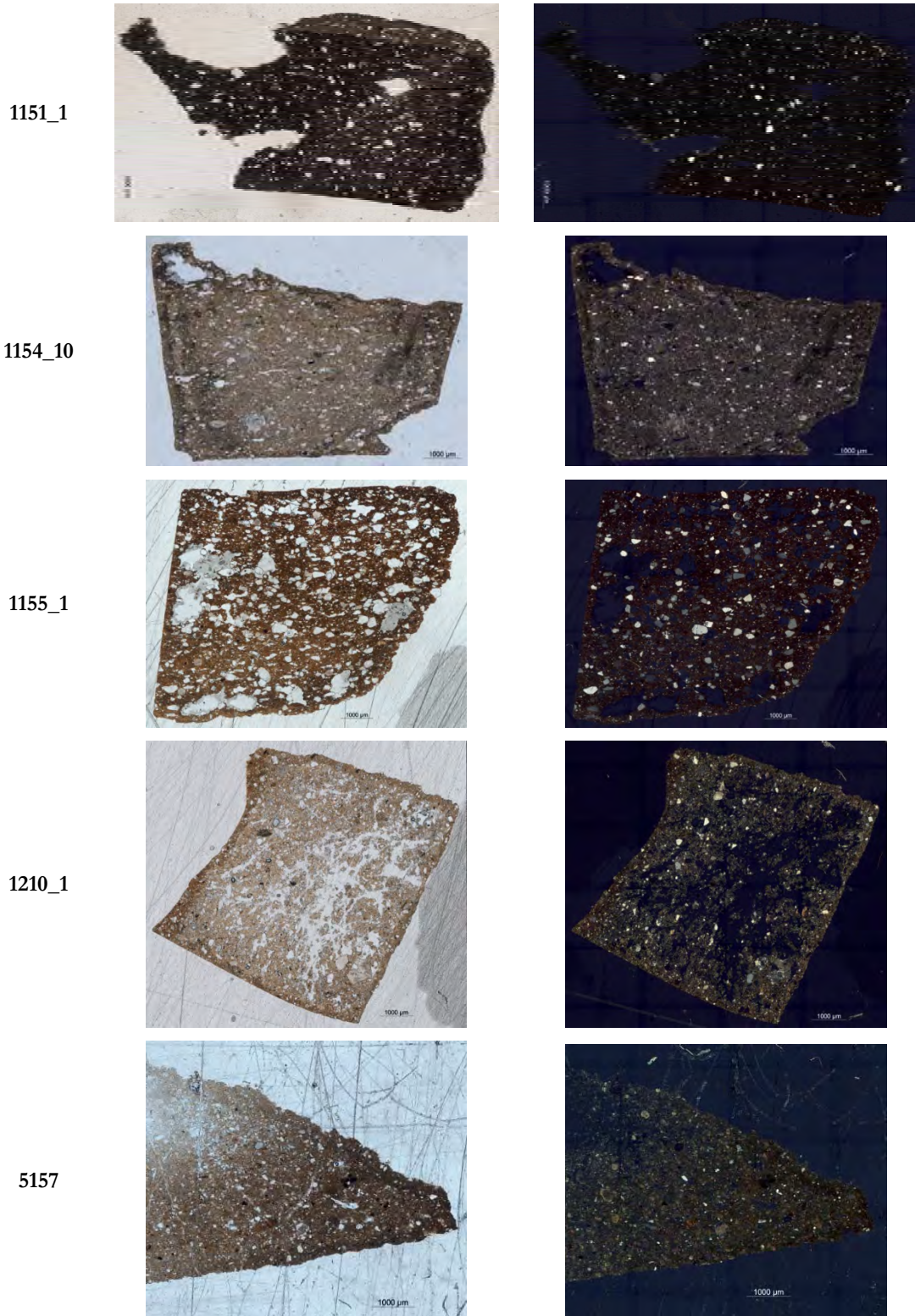


Figure.43. Representative ceramic thin sections photomicrographs of fragments coming from Torcello obtained by petrographic microscope. On the left in parallel light; on the right in cross light.

The non-pleochroic, colourless and untwinned minerals were identified mainly as quartz crystals and rarely muscovite, recognized by its high birefringence and its interference colours of second-third order. Non-pleochroic, colourless and twinned crystals were detected and attributed to plagioclase and probably calcite minerals. The former presents a polysynthetic twinning and inclined extinction that are distinctive features able to distinguish it from the other minerals. Identification of plagioclase supports μ -Raman results since albite is a plagioclase feldspar mineral.

In general, inclusions are abundant (20-25%), medium-sorted and characterized by both angular/sub-angular and sub-rounded grains of variable dimension between 0,15 and 0,45 mm, suggesting that the potteries were tempered by the potters.

Fabric features observed by microscope did not allow a clear distinction in sub-groups. It can be affirmed that:

- i) the glazed potteries seem to be very similar and belong to an own production;
- ii) Late antique amphorae (5157 sample) show a fine-grained inclusion of 0,15-0,2 mm;
- iii) globular amphorae cannot be distinguished very clearly, but it can be notice that 1155_1 sample exhibits a slight different fabric characterized by abundant inclusions of greater dimension (0,2-0,45 mm). This sample is supposed to be of Aegean production from the archaeological indications obtained, and the hypothesis of the same provenance for the sample 1154_10 is not supported by these analyses. 1154_10 and 1210_1 show similar fabrics with inclusion of 0,17-0,24 mm and the observation cannot allow to make consideration on their provenance.

4.2.3. SEM-EDX Analyses. Results and Discussion

Morphological and microstructural observation were performed by SEM-EDX techniques. As reported in the case of laboratory specimens, microphotographs obtained by electron microscope allowed the evaluation on firing conditions considering the textural features of the ceramic bulk related to firing temperature, as well as the chemical and mineralogical composition [21], [30], [60]–[62]. The selected samples were investigated and the most representative results are shown in **Fig.44**.

The bulk microstructures of the single-glaze potteries (1078_2 and 1151_1) seem to be similar, supporting the hypothesis they were produced with similar production technique. All the analysed samples show distinct and separated grains in the clay matrix, where the slightly deformed edges may indicate a beginning of vitrification process which starts at 700°C.

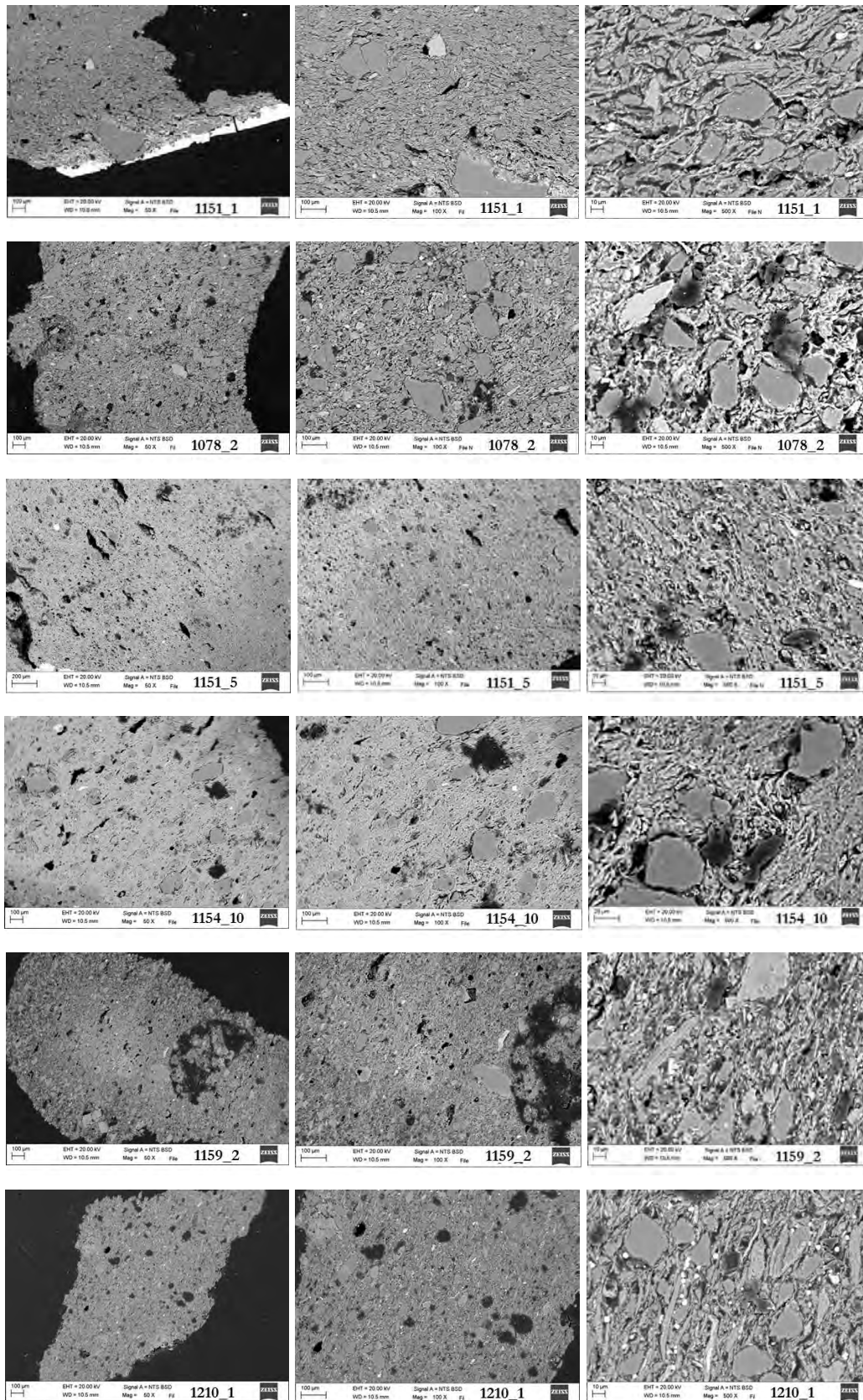


Figure.44. Scanning electron microphotos obtained at magnification of 50x, 100x and 500x (from the left to the right) of the representative sherds from Torcello.

1151_5, 1154_10 and 1159_2 samples show higher densification stage than the other samples and integrating these observation with chemical and mineralogical results, they may be fired at around 800°-850°C. The firing temperature has to be lower than 900°C because of the presence of calcite (primary calcite with a strong FT-IR signal in the case of 1154_10 for instance) and the absent of new-formed firing products as gehlenite and anorthite. 1210_1 sample exhibits a clay matrix not molten with a low densification stage and the absence of a glassy phase suggest low firing temperature, between 700° and 800°C.

1151_5, 1154_10 and 1159_2 samples seem to have a directional elongated-shape porosity which may be due to the forming technique adopted; whereas, 1210_1 and 1078_2 samples exhibit an arbitrary rounded-shape porosity.

Elemental maps and chemical analyses carried out by means of SEM-EDX techniques were performed in order to describe the chemical composition and minero-petrographic features.

In **Fig.45** are reported chemical maps and EDX results of the single-glaze sample 1151_1. Elemental analyses show that the glaze is composed mainly of PbO, SiO₂ and Al₂O₃, supporting μ -Raman results which suggested lead-glaze for the single-glazed potteries. The thickness of the coating layer is very thin and irregular, it ranges between 25 and 65 μ m. The presence of the small-scale glaze/body interactions in terms of extension of chemical elements mobilisation, and the absence of new-formed phases as K-Pb feldspars confirms single firing procedure and low firing temperature [63]. These results agree with those obtained by chemical and morphological analyses and archaeological information.

Elemental analyses for chemical elements of interest, such as Al, Ca, Fe, K, Mg, Na, Si, Ti, S, were performed in order to provide insights on the mineralogical composition of the ceramic body with the joint use of EDX punctual analyses. In **Fig.46-48** chemical maps, as multispectral images, and composition of some ceramic fragment are reported as examples. Imaging data elaboration by means of ImageJ software is also given in order to emphasise the nature of inclusions and the pores in the clay matrix. Ceramic sherds present a variety of inclusions: quartz, calcite, K and Na feldspars, titanium oxides, iron oxides, amphibole and probably augite. The mineralogical attribution is given by the results of EDX punctual analyses and the use of mineralogy database [64]. The presence of pyroxene as augite is detected in 1151_5 sample and may indicate firing temperature at around 800°-850°C because this phase may be formed by the reaction between quartz and dolomite at that temperature [65]–[67]. These results are in agreement with the morphological observation and the estimated temperature of this sherds by spectroscopic techniques.

Dolomite ($\text{CaMg}(\text{CO}_3)_2$) is often found in ceramic pastes and was not directly detected by FT-IR and μ -Raman spectra probably due to its bands overlapping those of calcite mineral and/or the sensitivity of the techniques [22], [25], [68].

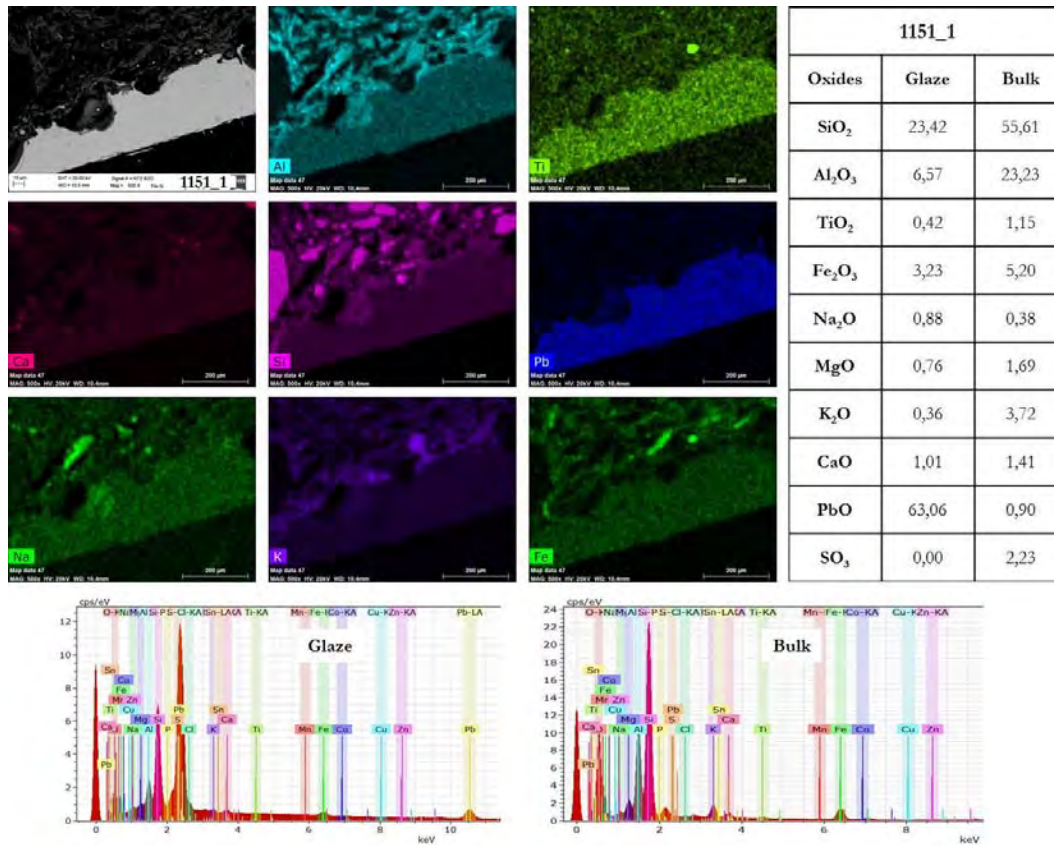


Figure.45. SEM microphotograph of polished cross sectional ceramic fragment (single-glazed pottery 1151_1) along with its elemental maps and relative SEM-EDX spectrum.

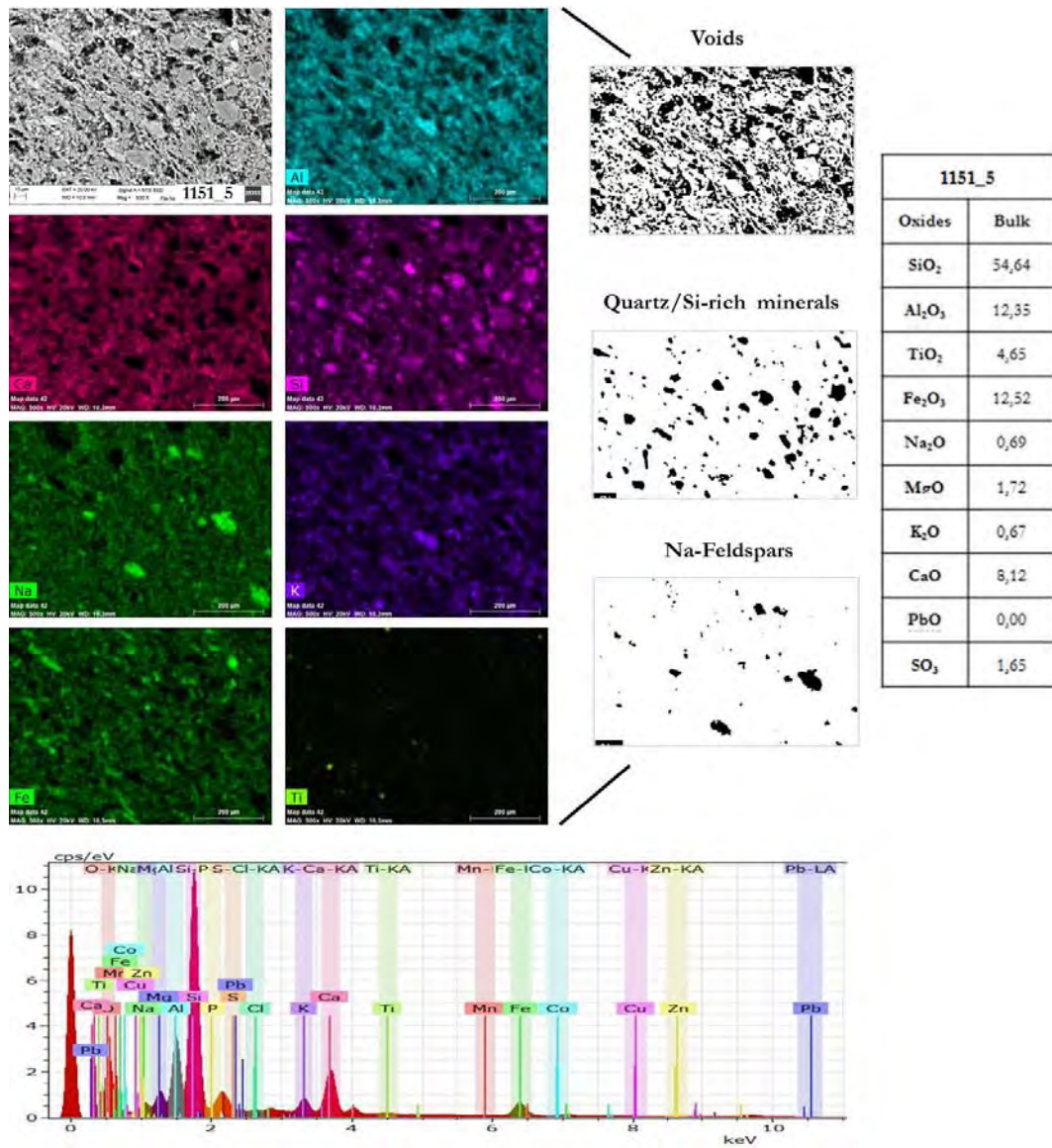


Figure.46. Chemical maps and composition of 1151_5 sherd from Torcello obtained by SEM-EDX analyses. Imaging data elaboration shows voids and inclusions present in the ceramic paste.

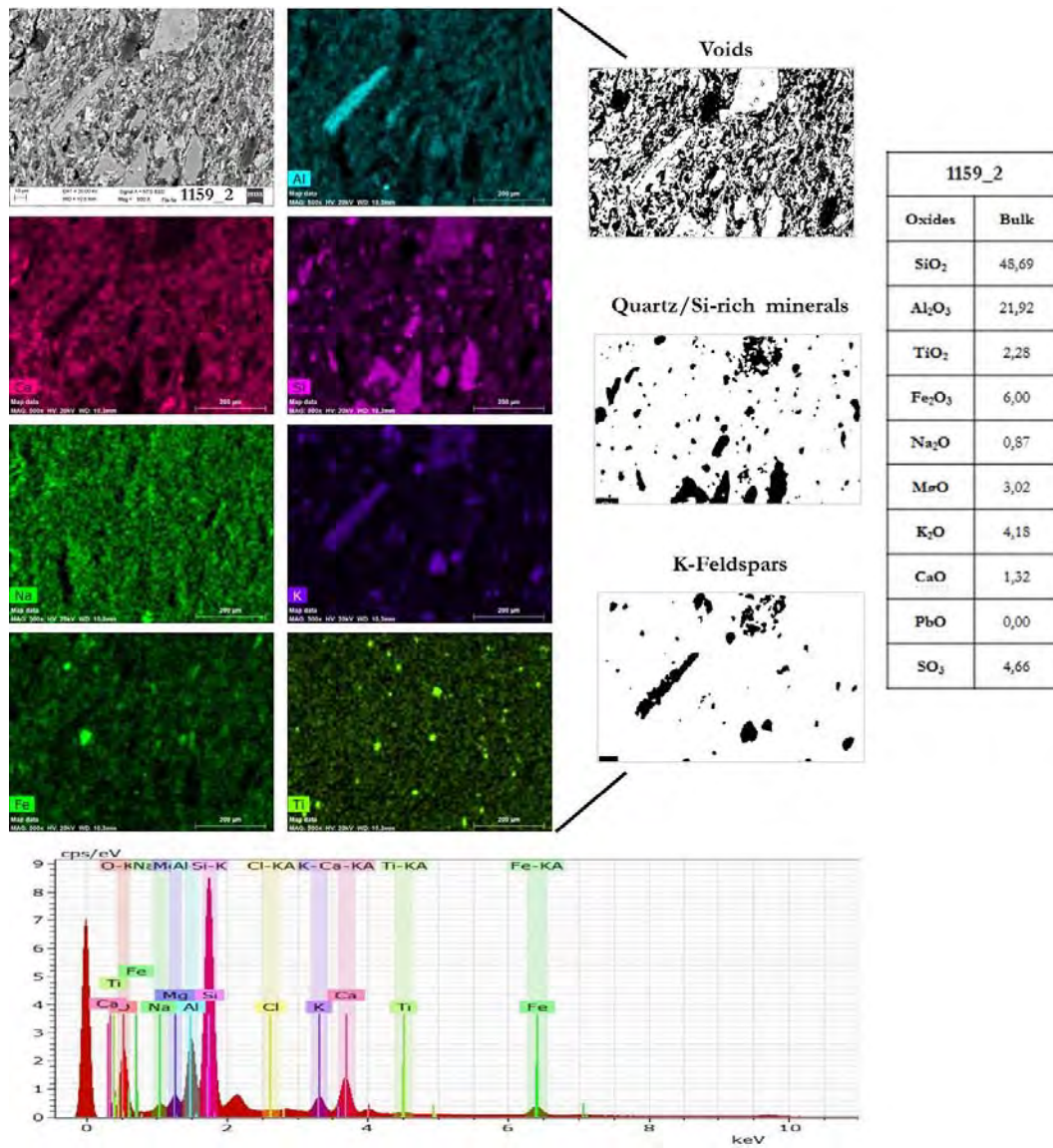


Figure.47. Chemical maps and composition of 1159_2 sherd from Torcello obtained by SEM-EDX analyses. Imaging data elaboration shows voids and inclusions present in the ceramic paste.

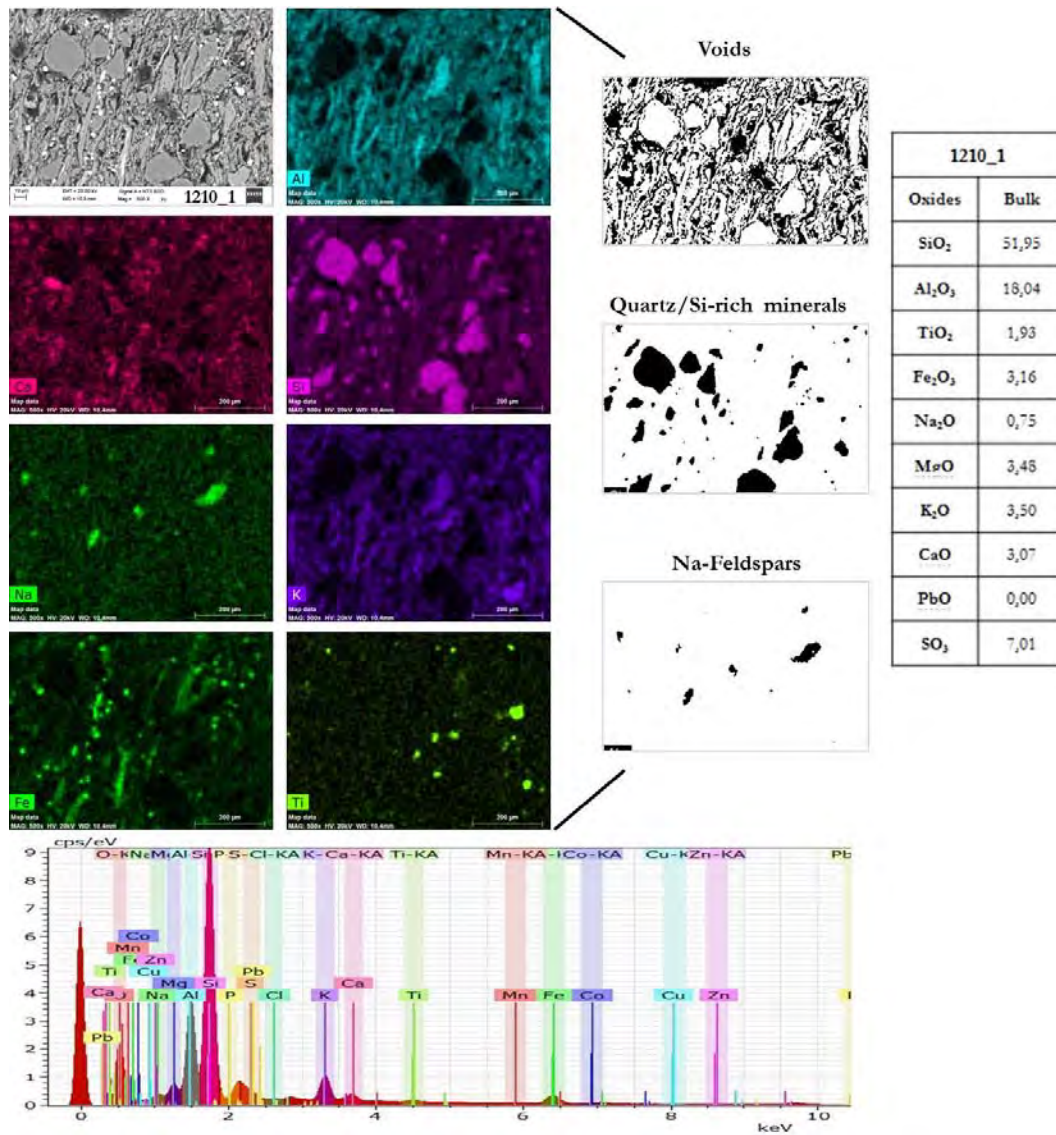


Figure.48. Chemical maps and composition of 1210_1 sherd from Torcello obtained by SEM-EDX analyses. Imaging data elaboration shows voids and inclusions present in the ceramic paste.

4.2.4. Microstructural and Porosimetry Results and Discussion

A microstructural feature that should be considered characterizing ceramic materials is the porosity, connected to both physical properties and production technique of the object [29], [69]. Porosimetry analyses were carried out using Mercury Intrusion Porosimetry (MIP) and X-ray Micro-Computed Tomography (μ -CT) techniques. The former provides information on open macro and meso porosity, the latter on total (open and closed) porosity between 1 to 100 μm and both allow quantitative investigation. These techniques were applied in this research in the study of raw laboratory-made ceramics underlining the importance in evaluating the total porosity in order to completely describe the microstructure of the materials. The promising results obtained suggest the application of these techniques on real case study as the archaeological potteries from Torcello.

Total cumulative volume, average pore radius, total porosity as well as bulk and apparent density of the open porosity were calculated by MIP techniques, as reported in **Tab.12**. MIP tests were carried on at least three samples, as suggested by the rule Normal 4/80, for each sherds and the reported results are given as average of those repetitions along with its standard deviation.

Total open porosity (%) of the analysed sherds ranges between 15 and 34% and the average pore radius between 0,15 and 0,27 μm . Diagrams in **Fig.49 (a)** and **(b)** show the variability of both total open porosity and average pore radius. Comparing the obtained results with those reported in literature, Torcello potteries seem to have medium to high open porosity [69], [70].

Table.12. Porosity data obtained by MIP measurements of the analysed German sherds. The average of three measurements with their standard deviation is reported.

Sample code	Total cumulative volume [cm ³ /g]	Average pore radius [μm]	Total porosity [%]	Bulk density [g/cm ³]	Apparent density [g/cm ³]
1210_1	0,16 \pm 0,03	0,21 \pm 0,11	18,25 \pm 2,39	1,16 \pm 0,06	1,42 \pm 0,03
1159_2	0,26 \pm 0,02	0,17 \pm 0,01	28,47 \pm 3,47	1,10 \pm 0,05	1,54 \pm 0,11
1154_10	0,21 \pm 0,01	0,25 \pm 0,00	24,66 \pm 2,31	1,16 \pm 0,07	1,54 \pm 0,12
1155_1	0,10 \pm 0,03	0,27 \pm 0,11	15,08 \pm 8,36	1,48 \pm 0,42	1,78 \pm 0,67
6001_1	0,16 \pm 0,00	0,27 \pm 0,00	22,49 \pm 5,04	1,40 \pm 0,33	1,82 \pm 0,54
1151_5	0,16 \pm 0,03	0,15 \pm 0,03	20,52 \pm 7,59	1,57 \pm 0,17	2,14 \pm 0,45
1151_4	0,18 \pm 0,01	0,32 \pm 0,10	15,50 \pm 1,61	0,88 \pm 0,41	1,05 \pm 0,65
5157	0,22 \pm 0,02	0,15 \pm 0,05	33,89 \pm 3,70	1,53 \pm 0,31	2,32 \pm 0,53
1151_1	0,16 \pm 0,02	0,26 \pm 0,01	26,04 \pm 1,65	1,65 \pm 0,08	2,23 \pm 0,31

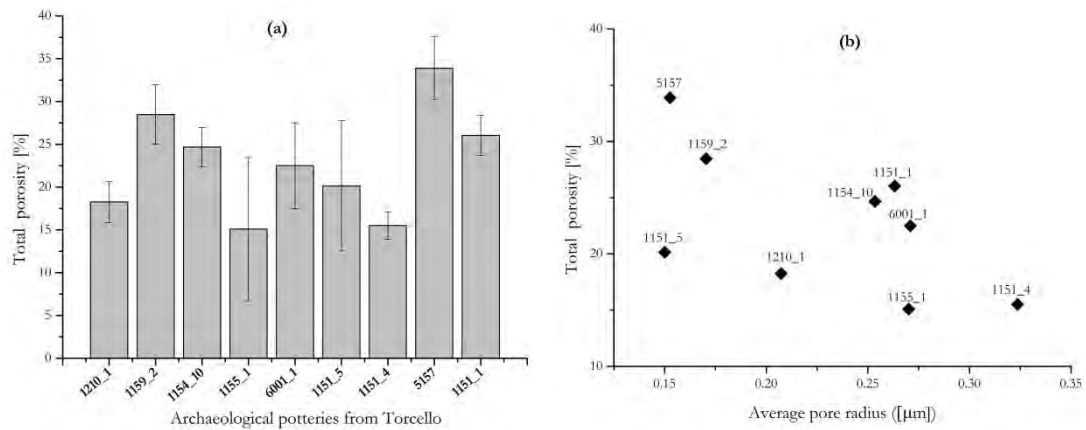


Figure.49. Histogram of the total open porosity **(a)** and diagram of total open porosity vs average pore radius **(b)** of selected ceramic sherds from Torcello.

In **Fig.50-51** are reported the pore volume and volume distributions of open porosity for each analysed sherd. The samples mostly exhibit an unimodal pore size distribution suggesting fine to intermediate texture. Sherds as 1151_1, 1151_4, and 1155_1 show a variable pore size distribution indicating a heterogeneous open porosity [71], [72]. From the obtained results it can be difficult a discrimination of the samples in base on the technological productions, however it can be notice that there are some correlation between the chemical-mineralogical composition and porosimetry results. On the basis of this correlation, three groups were differentiated:

1. The sherds which exhibit the highest values in the unimodal pore size distribution curves (**Fig.51**) are 1159_2, 1154_10 and 5157 which include primary calcite detected by FT-IR technique. Probably in these potteries calcite in the raw materials begins its decomposition due to the firing temperature at around 800°-850°C (SEM-EDX observation allowed to estimate that temperature for 1159_2 and 1154_10 samples) forming voids which were not replaced by newly formed minerals depending on both low firing temperature and maybe the duration of the firing [29].

2. 1210_1, 6001_1 and 1151_5 samples show lower values of the unimodal pore size distribution curves and include secondary calcite. It might be explained by the formation of calcite crystals into the ceramics after the firing which may occupy the voids in the matrix. As already mentioned, secondary calcite may be formed by: i) re-carbonation process in ceramics with initially carbonatic composition; ii) precipitation of carbonate solutions that filter into the ceramics; iii) alteration of Ca-bearing minerals into the matrix [26].

3. Particular results are shown from 1151_1, 1151_4, and 1155_1 sherds which present low values of heterogeneous pore size distribution curves and include primary calcite. It may be due to the composition of the raw materials (low calcite content) and/or low firing temperature,

estimated between 700°-800°C, which not allowed de-carbonation process of all the calcite crystals present in the matrix.

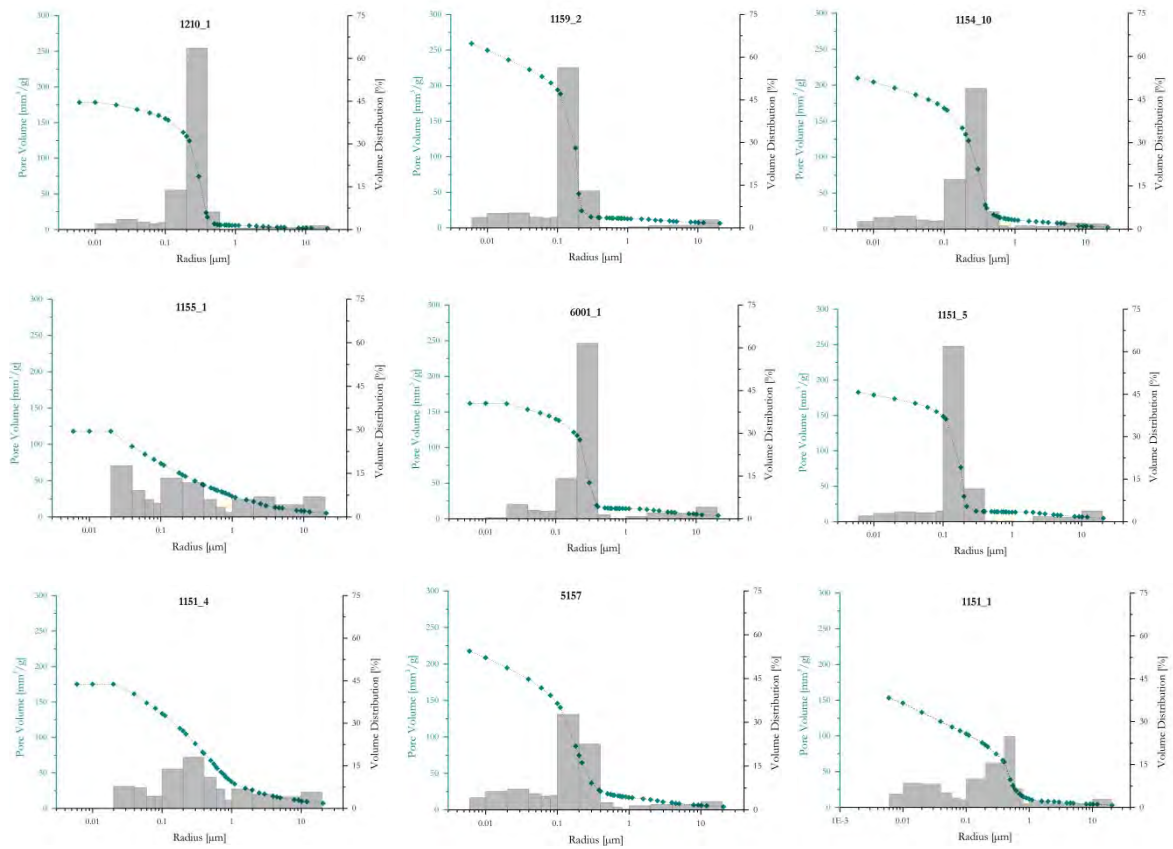


Figure.50. Cumulative pore volume and volume distribution versus pore radius of the analysed sgerds from Torcello. (The scale in the axes is the same in order to underline the differencies of the sherds)

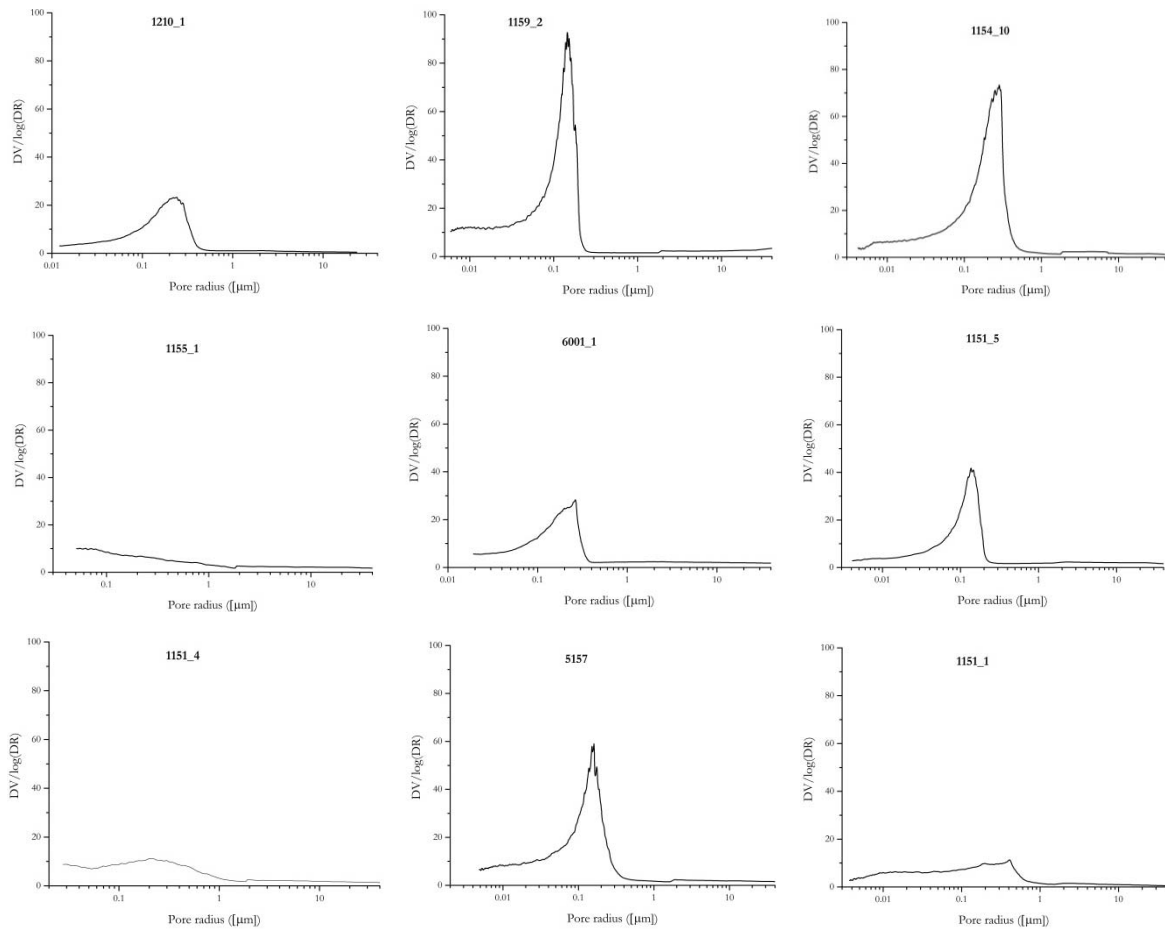


Figure.51. Pore size distribution curves of the analysed sgerds from Torcello. (The scale in the axes is the same in order to underline the differences of the sherds).

Basing on the obtained results, selected samples were analysed by means of μ -CT in order to investigate the total porosity in the range between 1 and 100 μm . Pore size distributions of the open and closed porosity versus pore radius are graphically reported in **Fig.52**. Furthermore, tomographic images of the analysed sherds are presented in **Fig.53**, where it is shown imaging elaboration in order to extract the voids present into the sample.

The analysed samples show unimodal pore distribution curves and the main peaks related to the pore radius are between 19 and 25 μm . 1154_10 and 1159_2 sherds exhibit lower total porosity than that of 1210_1 and 1151_5 samples. These last two sherds with higher total porosity are those including secondary calcite, while the first two with lower total porosity include primary calcite. The values obtained by μ -CT cannot be compared with those obtained by MIP measurements because they refer to both different ranges and types of pores. However, it can be noticed that MIP results on the open porosity showed the opposite trends for these samples.

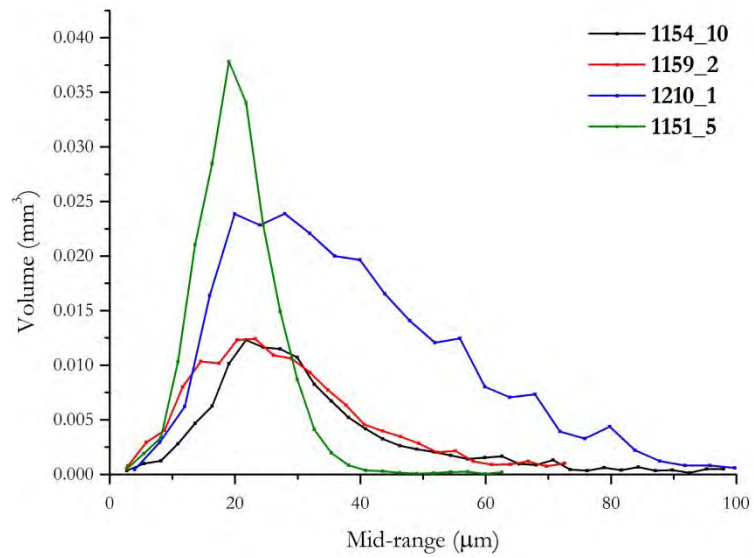


Figure.52. Pore volume vs pore radius calculated by μ -CT results of selected Torcello samples.

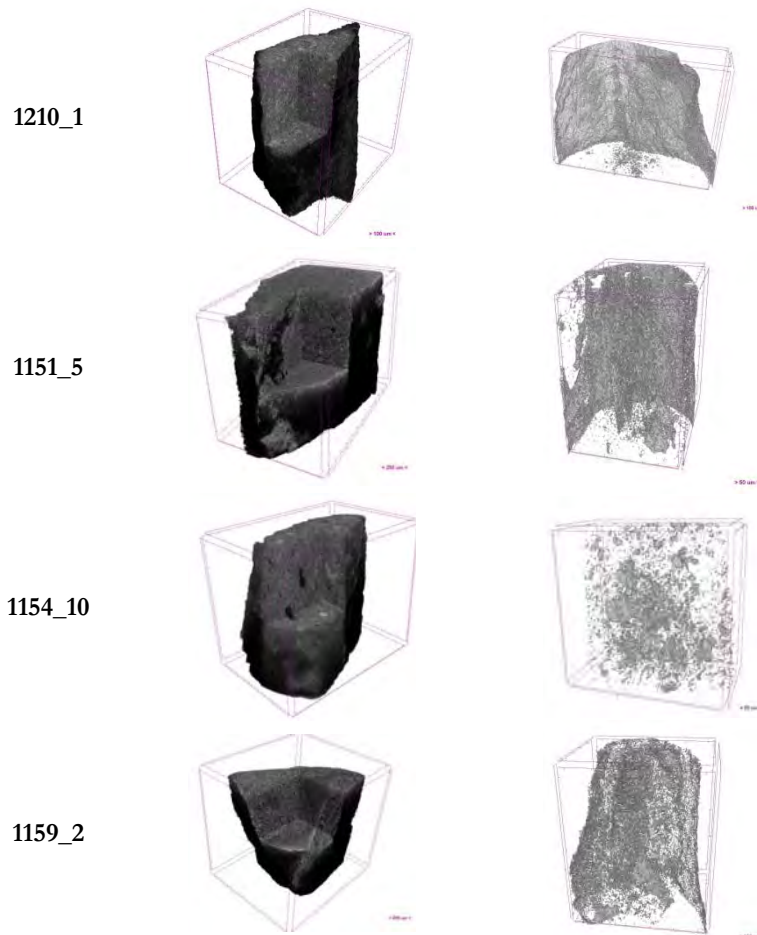


Figure.53. μ -CT results of Torcello samples. 3D sections (on the left) and void extractions (on the right).

Integrating and combining the tomographic data with the observations made on the basis of the results obtained by MIP, probably the secondary calcite in 1210_1 and 1151_5 sample has been formed by precipitation process after burial period where water can easily penetrate in open connections allowing precipitated calcite formation [26]. Furthermore, it may suggest that secondary calcite tends to reform in smaller pores. These consideration may explain the low open meso and macro porosity calculated by MIP and the high total porosity obtained by μ -CT.

The lower total porosity measured by tomographic analyses of 1154_10 and 1159_2 sherds may be in agreement with the morphological observations which suggested higher densification stage and firing temperature.

4.2.5. Brief Conclusions on the Archaeometric study on Archaeological Potteries from the Venetian Lagoon

The multi-analytical approach used in the archaeometric study of the ceramic sherds from Torcello, in the Venetian Lagoon, allowed to evaluate the composition of the raw materials used and estimate firing conditions. The results showed similar chemical and mineralogical composition and low firing temperature 700°-800°C and 800°-850°C. Late Antique and Early-Medieval globular amphorae did not exhibit particular features able to distinguish these two groups from a chemical and microstructural point of view. Instead, single-glaze potteries show distinguishable features allowing to affirm that these potteries have a different production technique in comparison with the other two groups.

Significant results are those regarding the presence of calcite mineral which is found in the ceramic paste as part of raw materials (primary calcite) and as crystals reformed after firing during the burial period (secondary calcite). FT-IR technique allowed the discrimination between primary and secondary calcite and the reported results showed their influence on microstructural features. These data underline the relevance in considering post-burial alteration and contamination throughout the study of archaeological ceramics.

Interesting are the porosimetry results which are connected to both firing temperature and mineralogical composition of the potteries. Furthermore, X-ray μ -CT tomography brought out the different behaviour of the porosity considering both open and closed pores and greater pore radius.

Concluding, the complementary methods used in this research were able to investigate both chemical-mineralogical and morphological features of the analysed samples, showing promising results concerning the use of tomography technique applied in archaeological potteries for microstructural characterization.

4.3. Characterization of German Ceramic Sherds

Historical ceramics from different German sites, macroscopically described in the chapter 3.3.3, were investigated in this research with the aim to test the investigation strategy on real case study as historical potteries and link morphological and physical features with chemical composition. Furthermore, the effectiveness of the proposed innovative techniques is evaluated with the aim to encourage the use of non-destructive and micro-destructive methods.

The investigation was performed by a multi-spectroscopic approach considering chemical-mineralogical composition and morphological features. The obtained results are presented following the analytical technique used in order to simplify the data discussion.

4.3.1. FT-IR Analyses. Results and Discussion

FT-IR analyses were carried out on both ceramic bulks and coating layers, when present. FT-IR spectra related to the ceramic matrix of all the samples are reported and summarized in **Tab.13**, where the tentative vibrational assignments made on the basis of FT-IR spectra of minerals are given, as reported in literature [6], [9], [14], [17].

On the basis of the FT-IR results, the ceramic sherds may be divided in three groups taking in to account their mineralogical composition and the considerations related to firing temperature. The three groups, summarised in **Tab.14**, include:

- potteries fired at around 750-850°C
- potteries fired at around 900-950°C
- potteries fired above 950°C.

In general all fragments contain quartz, as the main component, feldspar and hematite. Quartz was detected by the very strong peak at 1082-1090 cm^{-1} due to the Si-O stretching vibration, the shoulder at 1163-1178 cm^{-1} , the characteristic doublet at 795-800 and 773-781 cm^{-1} probably due to symmetrical stretching mode and the peak at 692-696 cm^{-1} attributable to symmetrical bending mode [13], [14], [73]. Feldspar minerals, such as albite, orthoclase and microcline, are common minerals in potteries and their IR absorption features partly overlap in the ranges of 1200-900 cm^{-1} and 800-700 cm^{-1} making difficult their identification because of the overlapping with other silicates, as quartz, present with strong absorption bands in those ranges. Nevertheless, the presence of feldspar minerals may be attributed to the peaks at 725-742 and 613-664 cm^{-1} [5], [13], [34]. FT-IR bands at 536-557 and 469-472 cm^{-1} were ascribed to hematite, suggesting oxidizing kiln condition. Indeed, the presence of hematite and magnetite, iron oxides usually found in ceramic body, provides information about firing conditions: oxidizing or reducing atmospheres respectively [1], [5], [11], [13], [14].

Table.13. FT-IR vibrational frequency assignments of the analysed ceramic bodies. The wavenumbers are a summary of all the ceramic bodies coming from each German site taken in to consideration in this work [6], [9], [14], [17].

Saxony							
Bad Muskau	Bautzen	Bischofswerda		Brandis	Görlitz		
		Bi_50, Bi_56, Bi_60	Bi_58				
IR frequency with relative intensity (cm ⁻¹)						Tentative vibrational assignments	
	3697w	3697 w	3697 w	3697 w		O-H str.	Kaolinite
	3622w	3620 w	3618 w	3622 w		O-H str.	Kaolinite/Illite/ Smectite. ^a
						O-H str.	Water/Smectite. ^a
	3405 bd	3411 bd	3429 bd	3433 bd		O-H str.	Water/Smectite. ^a
	1880 w	1876 w				Calcite str.	Calcite
	1620w	1618 w	1624 w	1624 w	1631 vw	O-H-O bend.	Water/ Smectite. ^a
		1427 w				-CO ₃ ²⁻	Calcite
1169 sh	1176 sh		1169 sh	1163 sh	1169 sh	Si-O str.	Quartz
1090 vs	1088 vs	1088 vs	1088 vs	1086 vs	1090 vs	Si-O str. / Al-O- Si str.	Quartz/Amorph. Al-Si ^b
1036 sh	1030 sh	1034 sh	1029 sh	1032 sh	1043 sh	Si-O-Si str.	Kaolinite
		1011 sh		1007 sh		Si-O/Si-O-Al str.	Kaolinite/Muscovite
955 vw						OH deformation	Inner hydroxyl groups of Kaolinite
910 w	912 m	912 w	912 w	912 w	904 w	Al-O-H	Kaolinite
		877 vw				-CO ₃ ²⁻	Calcite
796 m	796 s	796 m	798 m	796 s	796 m	Si-O str.	Quartz
777 m	777 s	777 m	779 m	779 s	775 m	Si-O str.	Quartz
742 w					725 w	Al-O-Si bend.	Feldspar
						Si-O bend. /- CO ₃ ²⁻	Calcite
694 w	694 m	694 w	692 w	692 m	696 w	Si-O bend.	Quartz
615 w				649 vw	613 w		Feldspar
548 m				536 m	558 m		Hematite
532 m	519 w	536 w				Si-O-Al ^{IV} / Fe-O bend.	Kaolinite/Muscovite/ Hematite
	482 m					Si-O-Si Bend	Illite
471 s	469 s	471 s	471 s	471 s	471 s	Al-O/Si-O deformation mode	Feldspar/Hematite/ Smectite. ^a
459 – 418 m					459-418 s	Si-O mixed deformation	Silicates

Saxony							
Dippoldiswalde			Zittau				
Di_80	Di_82, Di_05	Di_89, Di_00, Di_96	Zi_30, Zi_33, Zi_42, Zi_46	Zi_37	Zi_49		
IR frequency with relative intensity (cm ⁻¹)						Tentative vibrational assignments	
3697w			3691 vw	3691 vw	3693 vw	O-H str.	Kaolinite
3629w			3627 vw	3627 vw	3626 vw	O-H str.	Kaolinite/Illite/ Smectite. ^a
					3552 w	O-H str.	Water/ Smectite. ^a
					3408 w	O-H str.	Water/Smectite. ^a
						Calcite str.	Calcite
1622 vw			1622 w	1622 w	1622 w	O-H-O bend.	Water/ Smectite. ^a
			1423 vw	1423 vw		-CO ₃ ²⁻	Calcite
1167 sh	1165 sh	1176 sh	1176 sh		1176 sh	Si-O str.	Quartz
1086 vs	1090 vs	1088 vs	1086 vs	1086 vs	1086 vs	Si-O str. /Al- O-Si str.	Quartz/Amorph. Al-Si ^b
1043 sh			1032 sh	1039 vs		Si-O-Si str.	Kaolinite
						Si-O/Si-O-Al str.	Kaolinite/ Muscovite
						OH deform.	Inner hydroxyl groups of Kaolinite
910 sh	906 vw	901 w	912 w	912 w	912 vw	Al-O-H	Kaolinite
			897 vw			-CO ₃ ²⁻	Calcite
796 s	796 s	800 w	796 m	796 m	796 m	Si-O str.	Quartz
779 s	779 s	773 vw	779 m	779 m	779 m	Si-O str.	Quartz
		733 w				Al-O-Si bend.	Feldspar
						Si-O bend. /-CO ₃ ²⁻	Calcite
694 m	694 m		694 w	694 w	694 w	Si-O bend.	Quartz
					674 w		Feldspar (Microcline)
540 sh	546 w	546 m	555 w	555 w	555 w		Hematite
	513 m					Si-O-Al ^{IV} / Fe-O bend.	Kaolinite/Muscovite /Hematite
						Si-O-Si Bend	Illite
465 s	469 m	461 s				Al-O/Si-O deformation mode	Feldspar/Hematite/ Smectite. ^a
			449 m	449 m	466 m	Si-O mixed deformation	Silicates

Saxony		Turingia	Hesse	Brandenburg		
Kamenz		Bürgel	Grossalmerode	Cottbus		
Ka_12, Ka_22, Ka_28	Ka_18 Ka_20					
IR frequency with relative intensity (cm ⁻¹)					Tentative vibrational assignments	
3699 vw				3660 vw	O-H str.	Kaolinite
3622 vw					O-H str.	Kaolinite/Illite/ Smectite. ^a
					O-H str.	Water/Smectite. ^a
				3390 bd	O-H str.	Water/Smectite. ^a
1873 vw	1873 vw		1878 vw		Calcite str.	Calcite
1618 vw		1624 vw	1618 vw	1622 vw	O-H-O bend.	Water/ Smectite. ^a
				1432 s	-CO ₃ ²⁻	Calcite
1174 sh	1171 sh	1178 sh	1171 sh		Si-O str.	Quartz
1092 vs	1090 vs	1084 vs	1092 vs	1086 vs	Si-O str./ Al-O-Si str.	Quartz/Amorph. Al-Si ^b
1049 sh		1034 bd		1036 vs	Si-O-Si str.	Kaolinite
				1012 sh	Si-O/Si-O-Al str.	Kaolinite/Muscovite
955 vw	950 w		955 sh		OH deformation	Inner hydroxyl groups of Kaolinite
910 vw	900 vw	910 w	912 w	928 sh	Al-O-H	Kaolinite
871 w				874 w	-CO ₃ ²⁻	Calcite
796 m	796 m	796 s	798 m	796 m	Si-O str.	Quartz
779 m	779 m	777 s	781 m	777 m	Si-O str.	Quartz
		731 m			Al-O-Si bend.	Feldspar
				714 w	Si-O bend. /- CO ₃ ²⁻	Calcite
696 w	696 w	694 m	692 m		Si-O bend.	Quartz
615 w	615 w		628 w	647 w		Feldspar
555 w	538 w	548 m	540 m			Hematite
				517 w	Si-O-Al ^{IV} /Fe- O bend.	Kaolinite/Muscovite/H ematite
					Si-O-Si Bend	Illite
478 s	464 s	459 s	469 s	472 m	Al-O/Si-O deformation mode	Feldspar/Hematite/ Smectite. ^a
428 m			420 m	457-418 w	Si-O mixed deformation	Silicates

Lower Saxony							
Duingen		Coppengrave		Peine			
Dui_88, Dui_90	Dui_78 Dui_80	Cop_51, Cop_57	Cop_52	Pe_96 Pe_00	Pe_98		
IR frequency with relative intensity (cm ⁻¹)						Tentative vibrational assignments	
	3695w	3697 vw	3697 w		3699 w	O-H str.	Kaolinite
	3622w	3622 vw	3622 w		3622 w	O-H str.	Kaolinite/Illite/ Smectite. ^a
						O-H str.	Water/Smectite. ^a
	3384 bd	3415 bd	3415 bd		3404 bd	O-H str.	Water/Smectite. ^a
		1886 vw	1886 vw			Calcite str.	Calcite
	1631 w	1628 w	1628 w	1626 w	1608 w	O-H-O bend.	Water/ Smectite. ^a
	1431 vw				1429 vs	-CO ₃ ²⁻	Calcite
1173 sh		1165 sh	1165 sh	1173 sh	1101 sh	Si-O str.	Quartz
1092 vs	1086 s	1090 vs	1090 vs	1088 vs		Si-O str./ Al- O-Si str.	Quartz/Amorph. Al-Si ^b
	1034 vs		1032 vs		1036 vs	Si-O-Si str.	Kaolinite
	1005 sh		1011 sh			Si-O/Si-O- Al str.	Kaolinite/Muscovite
						OH deformation	Inner hydroxyl groups of Kaolinite
	912 w	914 sh	914 vw		914 w	Al-O-H	Kaolinite
					874 m	-CO ₃ ²⁻	Calcite
795 s	798 m	798 m	796 m	796 s	795 m	Si-O str.	Quartz
777 s	781 m	779 m	777 m	779 s	777 m	Si-O str.	Quartz
						Al-O-Si bend.	Feldspar
					714 w	Si-O bend. /- CO ₃ ²⁻	Calcite
694 w	692 m	694 m	692 w	692 m	692 w	Si-O bend.	Quartz
	628 w		615 w		664 w		Feldspar
542 w	540 m		555 sh		532 m		Hematite
				557 m		Si-O- Al ^{IV} /Fe-O bend.	Kaolinite/Muscovite /Hematite
						Si-O-Si Bend	Illite
471 s	469 s	472 s	474 s	463 s	471 s	Al-O/Si-O deformation mode	Feldspar/Hematite/ Smectite. ^a
422 m	420 m		420 sh			Si-O mixed deformation	Silicates

s: strong; vs: very strong; w: weak; vw: very weak; m: medium; sh: shoulder; bd: broad band.

str.: stretching mode; bend.: bending mode.

^aSmectite, probably montmorillonite.

The first group discriminated by FT-IR results, is formed by samples from Bautzen, Bischofswerda, Brandis, Dippoldiswalde (Di_80), Coppingrave, Kamenz (Ka_12, Ka_22, Ka_28), Zittau, Cottbus, Duingen (Dui_78 and Dui_80) and Peine (Pe_98). The estimated firing temperature, on the basis of pottery composition, is between 750°-850°C. **Fig.54 (a)** and **(b)** show the characteristic spectra of this group. These sherds are characterized by the presence of kaolinite as clay mineral, identified in FT-IR spectra by absorption bands at 3699-3620, 1029-1049, 1005-1012 and 910-914 cm^{-1} [1], [14], [34]. In the range 3690-3620 cm^{-1} are present only two peaks instead of the characteristic four peaks of kaolinite, due to the stretching vibration of inner -OHs, suggesting that the mineral is in disordered state [13], [74]. Furthermore, the relatively low intensity of these bands suggests that the dehydroxylation of kaolinite is not completed, and the decrease in intensity may be attributed to both dehydroxylation process and collapse of crystal frame work. The transformation from kaolinite ($\text{Al}_2\text{Si}_2\text{O}_5(\text{OH})_4$) to metakaolinite ($\text{Al}_2\text{Si}_2\text{O}_7+2\text{H}_2\text{O}$) takes place at around 600°C but small amount of -OH can persist up to 750-800°C [13], [75]. Smectite, probably montmorillonite with typical absorption band centred at 3400 cm^{-1} and peak at 469-474 cm^{-1} , was inferred by FT-IR results confirming relative low firing temperature [13]. Montmorillonite was identified in all the spectra except for sherds from Dippoldiswalde (Di_80) and Zittau (Zi_30, Zi_33, Zi_37, Zi_42, Zi_46). Calcite in different relative amounts (**Fig.54 (b)**) was also detected in particular sherds of this group: potteries from Cottbus, Duingen (Dui_78, Dui_80), Peine (Pe_98), Zittau (Zi_30, Zi_33, Zi_37, Zi_42, Zi_46) and Bischofswerda (Bi_50, Bi_56, Bi_60), which form a sub-group into the first one. FT-IR spectra show absorption bands due to $-\text{CO}_3^{2-}$ stretching mode at 1873-1886 (very weak), 1423-1444 and 874-897 cm^{-1} [8]–[10], [13], [14], [17]. The presence of calcite in pottery may indicate: the use of carbonatic clay raw materials, calcite as the impurity of clay and/or secondary calcite due to precipitation or alteration during burial of the ceramic sherds [26]. Furthermore, the detection of calcite may allow to estimate the firing temperature. The high intensity of calcite peaks in Cottbus and Pe_98 fragments and the non-presence of Ca-silicate secondary minerals (as gehlenite and wollastonite) suggest firing temperature below 800°-850°C.

The second group includes sherds from Bad Muskau, Görlitz, Bürgel and Dippoldiswalde (Di_89, Di_96 and Di_00) probably fired at temperature of around 900-950°C. In addition to quartz and hematite, FT-IR spectra (**Fig.54 (c)**) show characteristic peaks of kaolinite at around 901-912 cm^{-1} and the absence of FT-IR bands in the range between 3690 and 3620 cm^{-1} related to -OH stretching modes, which may be due to firing temperature at around 900°-950°C.

The third group consists on ceramic fragments coming from Grossalmerode, Duingen (Dui_88 and Dui_90) and Peine (Pe_96 and Pe_00), probably fired at high temperature above 950°C. Characteristic spectra of this group are shown in **Fig.54 (d)**. As result of FT-IR analyses,

they are characterized by a simple composition of quartz and hematite. Peak at around 912 cm^{-1} ascribable to kaolinite is very weak, probably due to its dehydroxylation and transformation in metakaolinite followed by amorphization, which can be caused by the destruction of the aluminosilicate sheets [76]. In Lower Saxony, German state where Duingen and Peine are located, there are available quite rare and good quality of tertiary clays, as well as close to Grossalmerode, in Hesse state. If these clays are composed of small amount of CaCO_3 , as shown in Dui_78 and Dui_80 for instance, but fired at a temperature above 950°C , they give a simple mineralogical composition of quartz and hematite, as seen in the case of this third group discriminated by FT-IR spectra [64], [77]–[80].

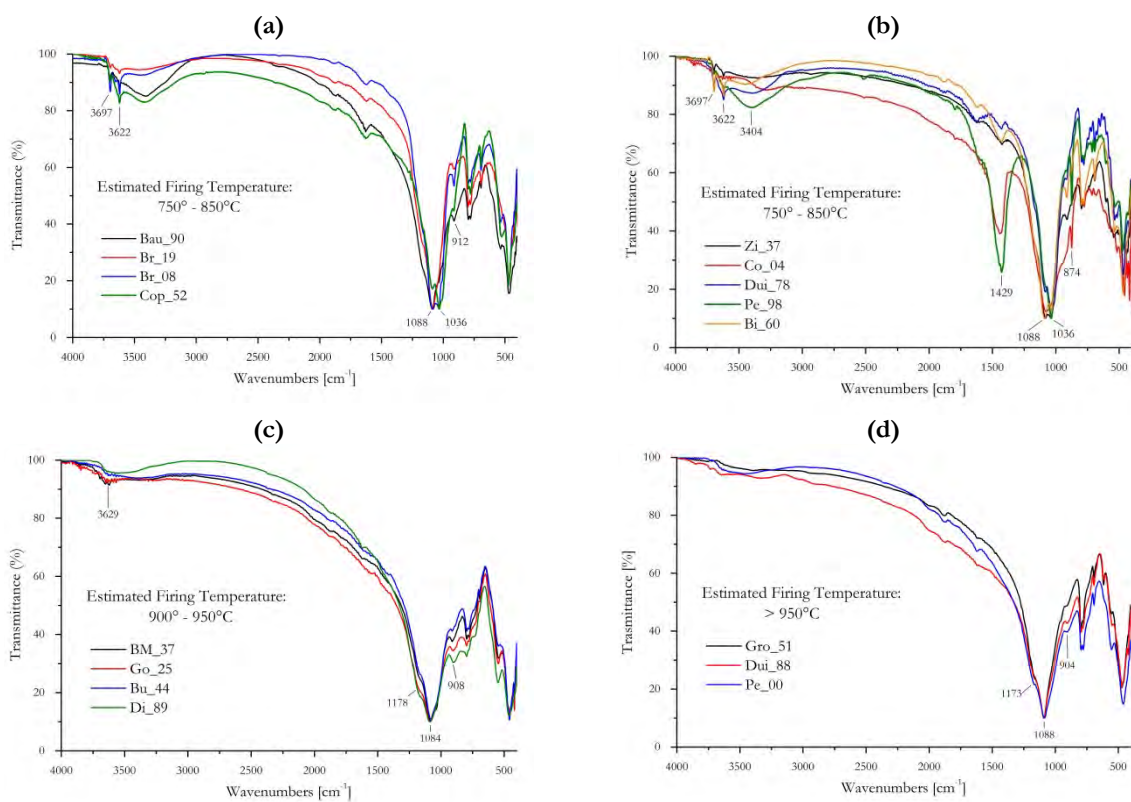


Figure.54. FT-IR spectra of representative German potteries. **(a)** ceramic sherds fired at $750\text{-}850^\circ\text{C}$ belonging to the first discriminated group; **(b)** ceramic sherds fired at $750\text{-}850^\circ\text{C}$ belonging to the first discriminated group where it is evident the presence of characteristic peaks attributed to calcite mineral; **(c)** and **(d)** ceramic sherds fired at $900\text{-}950^\circ\text{C}$ and $>950^\circ\text{C}$ belonging to the second and third group respectively.

Table.14. Estimated firing temperature discrimination of German sherds and their mineralogical composition inferred by FT-IR results.

Estimated Firing Temperature	Ceramic sherds	Chemical-mineralogical composition
750-850°C	Dippoldiswalde (Di_80)	Quartz, feldspar, hematite, kaolinite
	Zittau (Zi_30, Zi_33, Zi_37, Zi_42, Zi_46) Cottbus (Co_04, Co_05, Co_06, Co_07) Duingen (Dui_78, Dui_80) Peine (Pe_98) Bischofswerda (Bi_50, Bi_56, Bi_60)	Quartz, feldspar, hematite, kaolinite, calcite*
750-850°C	Brandis (Br_08, Br_09, Br_11, Br_14, Br_19) Bautzen (Bau_85, Bau_87, Bau_88, Bau_89, Bau_90, Bau_91, Bau_92, Bau_01) Bischofswerda (Bi_58) Coppengrave (Cop_51, Cop_52, Cop_57) Zittau (Zi_49) Kamenz (Ka_12, Ka_22, Ka_28)	Quartz, feldspar, hematite, kaolinite, smectite**
	Bad Muskau (BM_23, BM_32, BM_35, BM_37, BM_71, BM_75) Görlitz (Go_08, Go_11, Go_15, Go_19, Go_21, Go_25, Go_27, Go_29, Go_34) Bürgel (Bu_36, Bu_43, Bu_44, Bu_48, Bu_49, Bu_50) Dippoldiswalde (Di_89, Di_96, Di_00) Kamenz (Ka_18, Ka_20)	Quartz, feldspar, hematite, kaolinite
900-950°C	Grossalmerode (Gro_51, Gro_57, Gro_58, Gro_60) Duingen (Dui_88, Dui_90) Peine (Pe_96, Pe_00) Dippoldiswalde (Di_82, Di_05)	Quartz, hematite, kaolinite***

* in different relative amounts; ** probably montmorillonite; *** only a weak peak at around 912 cm⁻¹ is present.

As already observed, FT-IR absorption peaks of other minerals, such as illite, may be interfered by quartz and feldspar bands, making difficult their identification. However, the presence of illite is confirmed by Raman spectroscopy, as it is shown in the followed paragraph.

Obtained results on **coating layers** and/or **glazes** present in some of the ceramic sherds did not give further information about pigments/colorants and composition of the layer in comparison to those obtained by other techniques. For instance, in **Fig.55** the FT-IR spectra of the glazes of Bu_36, Br_08 and decorated layer of Zi_30 and Ka_22 are reported. Actually, the spectra show only the characteristic peaks of quartz ($1088\text{--}1032\text{ cm}^{-1}$ due to Si–O and Si–O–Si asymmetric stretching; $785\text{--}775\text{ cm}^{-1}$ and $465\text{--}457\text{ cm}^{-1}$ related to Si–O symmetric stretching and Si–O bending respectively) and a weak peak at 914 cm^{-1} ascribable to kaolinite presents as clay mineral in the ceramic body [6], [14].

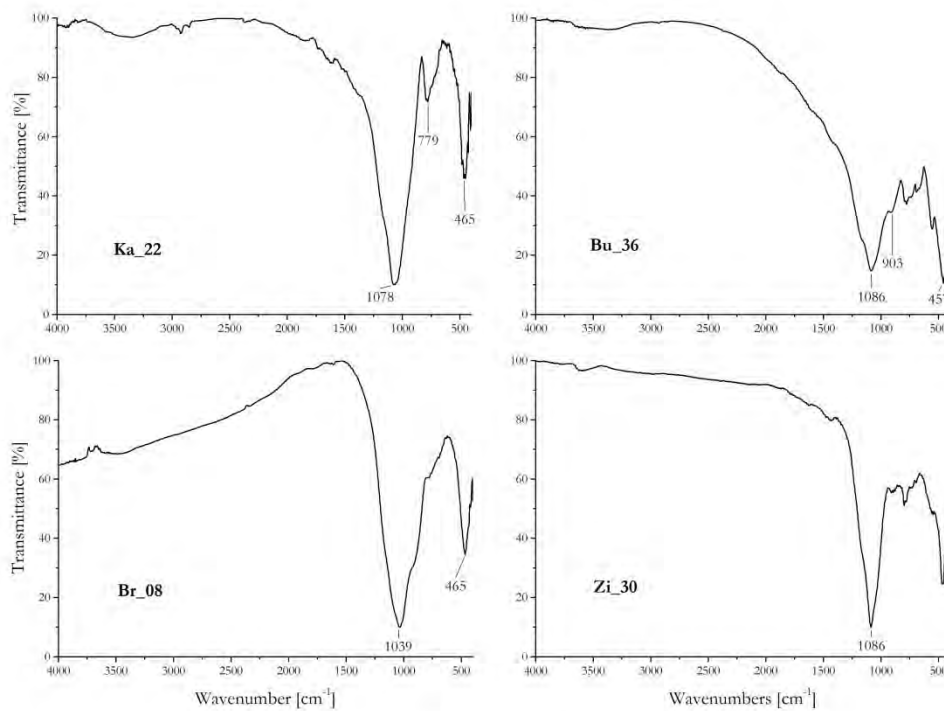


Figure.55. Representative FT-IR spectra of coating layers present in ceramic sherds as Ka_22 glaze; Bu36, blue glaze; Br_08, green glaze; Zi_30 decorated layer, reddish-brownish.

4.3.2. μ -Raman Analyses. Results and Discussion

μ -Raman system provides punctual analyses and more than 10 points for each ceramic sample were considered. The analyses were carried out on selected fragments previously embedded in polyester resin and polished in order to obtain a flat surface of body-glaze cross-section, and then analysed by Raman spectroscopy³.

Representative micro-Raman spectra are given in **Fig.56-60**, and in **Tab.15** are summarize the Raman bands of the detected mineral phases.

All samples show the presence of bands at around 144, 204, 356 and 395 cm^{-1} , ascribable to quartz in free and isolated form, and at a very intense and narrow signal at around 465 cm^{-1} due to Si-O-Si bending vibration (**Fig.56**) [10], [17], [27]. Other mineralogical phases detected by Raman spectroscopy are: anatase, rutile, hematite, magnetite, kaolinite, illite and montmorillonite. Rutile (237, 442, 609 cm^{-1}), anatase (143, 393, 513, 637 cm^{-1}) and the coexistence of anatase–rutile phase (**Fig.57**) were detected in the ceramic bodies [15], [54], [81]. Raman technique is able to discriminate the titanium oxides and then provide information about firing condition. The pure phase of rutile can be obtained only at firing temperature above 900°C. It has to be considered that the transition anatase–rutile can be also influenced by other minerals in the ceramic matrix. Furthermore, TiO_2 as rutile phase could be directly used in the paste in order to provide a lighter shade and/or present as impurity in quartz and feldspars, giving then an uncertain estimation of thermal treatment [15], [54]. Both hematite (bands at around 227, 296, 412 and 612 cm^{-1}) and magnetite (671-679 cm^{-1}) were detected in the ceramic body (**Fig.58**). The presence of hematite in the Raman spectra confirms the FT-IR results; while bands ascribable to magnetite indicate an incomplete phase transformation [10], [17], [82]. In some samples, amorphous carbon/carbon black materials were detected by Raman spectroscopy in the range between 1350-1600 cm^{-1} . Carbon may be originated by adding wood or bone ash in ceramic paste acting as fluxing agent, and associated with magnetite may suggest reducing atmosphere [42], [83]. Since the simultaneous presence of hematite, magnetite and black carbon, double firing process may be suggested. Bands at around 143, 207, 232, 344-351 cm^{-1} are due to the symmetric bending modes of the O-Si-O and O-Al-O groups attributed to kaolinite clay mineral [10], [53], [84]. Peaks at around 807, 958-966 and the very weak peak at 1123 cm^{-1} , as it is shown in **Fig.59**, may be related to the presence of metakaolinite, formed from the dehydroxylation reaction of kaolinite. Furthermore, the lack of intense peaks at 408 and 965 cm^{-1} due to the transformation of kaolinite into mullite mineral at high temperature (1100-1300°C), confirms the estimated firing temperatures between 700 and 1000°C [85]. Illite (460-463, 703-713 and 771-778 cm^{-1}) is

³ μ -Raman analyses were performed at the Department of Chemical Sciences of University of Padua in collaboration with Prof. Danilo Pedron, who is kindly acknowledged.

identified in ceramic sherds from Bautzen, Duingen (Dui_80) (shown in **Fig.60**), Bishofswerda and Coppingrave [10]. The presence of this clay mineral indicates a firing temperature below 800-850 °C, temperature at which the skeleton of illite crystal collapses [10]. Moreover, in some pottery samples such as Bau_88, Bi_60, Cop_57, Dui_80 and Zi_47, are present peaks in the range between 810-840 cm^{-1} usually attributed to Al-OH bending mode of smectite minerals, such as montmorillonite [10]. Raman bands at around 411-416 and 504-522 cm^{-1} were also detected and attributed to the presence of feldspar, probably Na-feldspar (albite) [7].

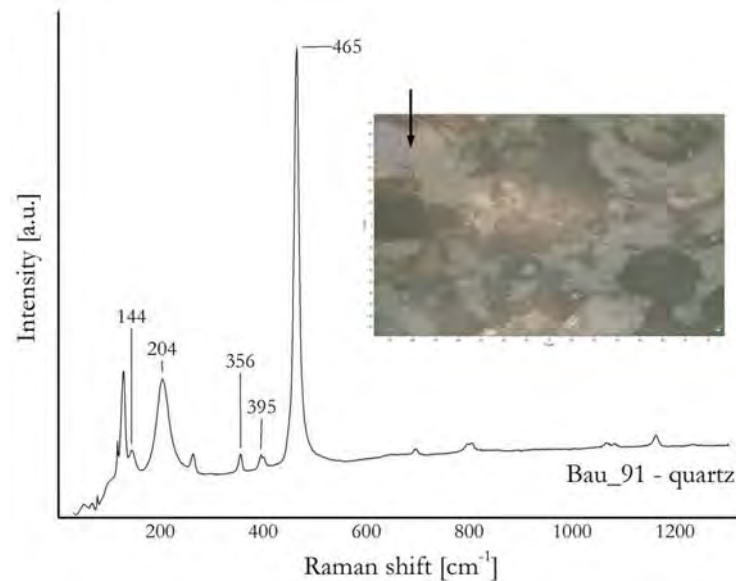


Figure.56. μ -Raman spectrum of the ceramic fragment Bau_91 showing the characteristic peaks of quartz and the photo (20x) of the measured point.

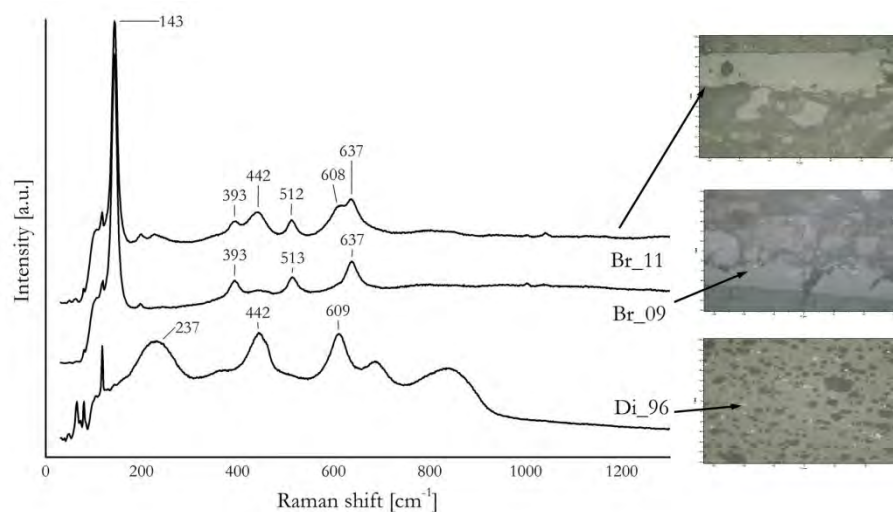


Figure.57. μ -Raman spectra of rutile (Di_96), anatase (Br_09) and rutile-anatase phase (Br_11), and photos (20x) of the analysed samples.

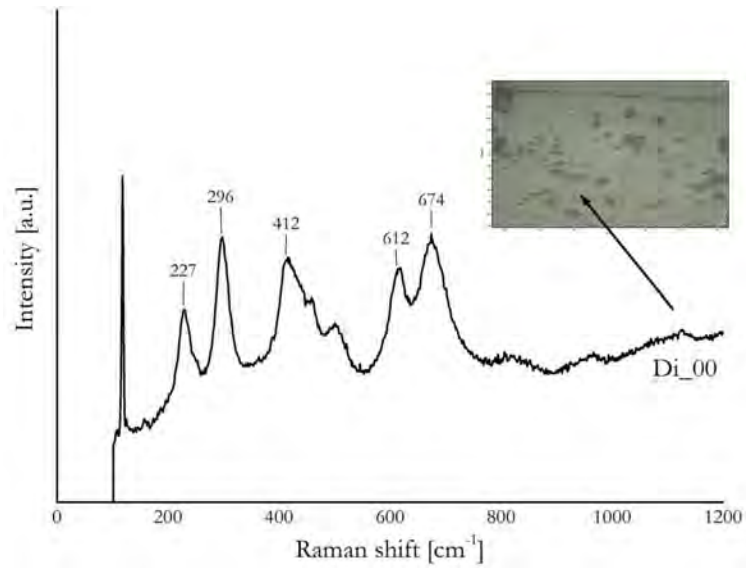


Figure.58. μ -Raman spectrum of hematite and magnetite identified in the sample Di_00 and photo (20x) of the analysed sherd.

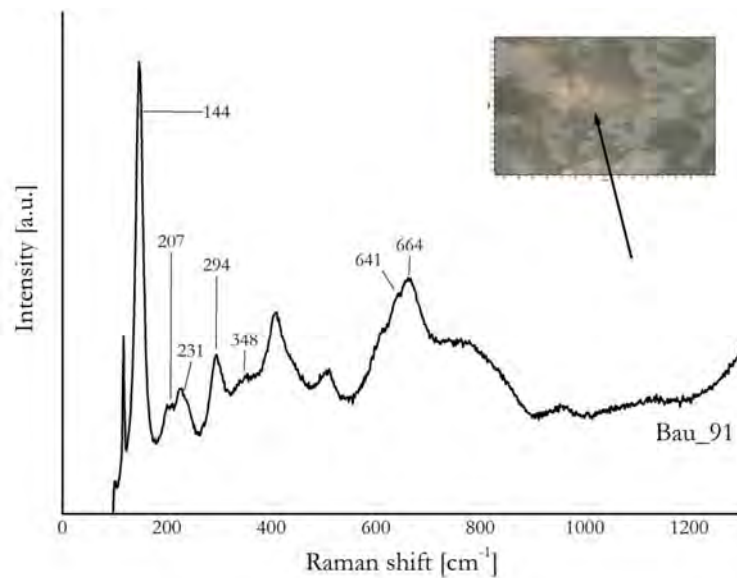


Figure.59. μ -Raman spectrum of the characteristic peaks attributed to kaolinite clay mineral and photo (20x) of the sample analysed, Bau_91.

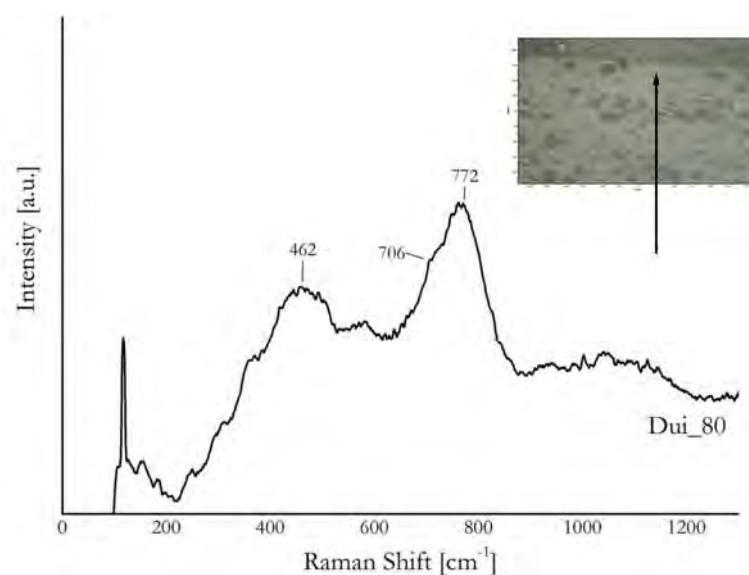


Figure.60. μ -Raman spectrum of illite mineral identified in the ceramic sherd Dui_80 and photo (20x) of the analysed point.

μ -Raman spectroscopy played an important role in both the identification and discrimination of some minerals in the ceramic body, as it is discussed above, and in the study of glaze coatings such as those present in sherds from Bürgel and Brandis [86].

Raman spectra of the coating layers of Br_09 (green glaze), Bau_90 (dark brownish slip), Cop_57 (light yellow-brownish glaze) and Zi_47 (brownish slip) reported in **Fig.61**, show two bands considered as the two main features of silicate glasses observable in Raman spectra. The first one appears between 300 and 600 cm^{-1} corresponding to Si–O–Si bending vibrations within intertetrahedron linkages. The second one, which typically is in the range between 900 and 1300 cm^{-1} , is due to Si–O stretching modes of silica-rich glassy phase and in these samples it is present as a broad band at around 940–950 cm^{-1} [87]. Bu_36 and Bu_44, decorated by blue glaze (see **Fig.62**), present Raman bands associated with lead glassy phases in the spectral range between 970 and 1070 cm^{-1} , as well as BM_32 and Di_96. Interesting is that these data are connected with the firing temperature of the glaze. As reported in the literature [47], the broad band around 940 cm^{-1} is related to glaze fired between 600 and 900°C and the second range (970–1000 cm^{-1}) is related to higher temperatures presumably above 950°C. These data are in accordance with the results obtained by FT-IR analyses and the inferred firing temperatures.

Raman spectra of the blue glaze covering Bu_36 and Bu_44 samples are reported in **Fig.62**. Both show two peaks at 194–201 and 509–512 cm^{-1} attributed to cobalt blue⁴ or cobalt(II)

⁴ Cobalt blue is a very stable pigment and has been used since ancient Egypt and re-evaluated during the Ming Dynasty (1271–1425) as colouring in Chinese porcelain [152]. For the first time at the beginning of XIX century, cobalt blue as a pure alumina-based pigment was synthesized by Louis-Jacques Thenard. Afterward the pigment was produced in France, Norway, Bohemia and Germany, where Saxony mining industries had a revival and had the finest specimens of cobalt produce [153]–[155].

aluminate (CoAl_2O_4). Bu_36 glaze shows a weak peak at 438 cm^{-1} attributed to zinc oxide (ZnO) present in the blue decoration as glaze flux in the middle- and higher-temperature ranges [88], [89]. The weak Raman signal of ZnO may be due to a low concentration of the compound and/or to the fact that the ZnO is a weak scatterer [90]. Peaks at 626 , 708 and 774 cm^{-1} are attributed to cassiterite (SnO_2) as pigment in the white dots, which decorate the Bu_36 glaze. Bu_44, in addition to Raman bands ascribable to cobalt blue, exhibits a broad Raman band at 825 cm^{-1} , attributable to cobalt silicate, due to the reaction of cobalt oxides and silica matrix at high temperature [54], [81], [82].

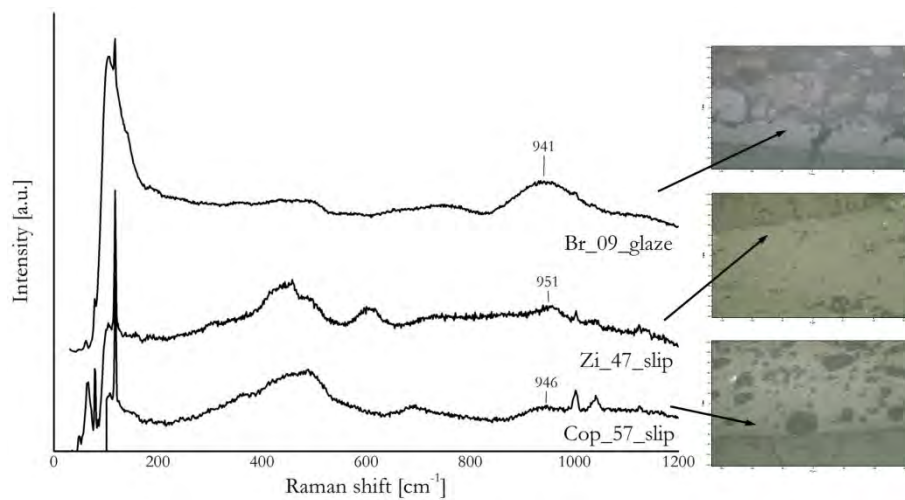


Figure.61. Raman spectra of coating layers of Br_09, Zi_47 and Cop_57 with their relative photos (20x). (Peaks at around 103 and 1039 cm^{-1} are the most intense bands due to the resin used to embed the ceramic fragments).

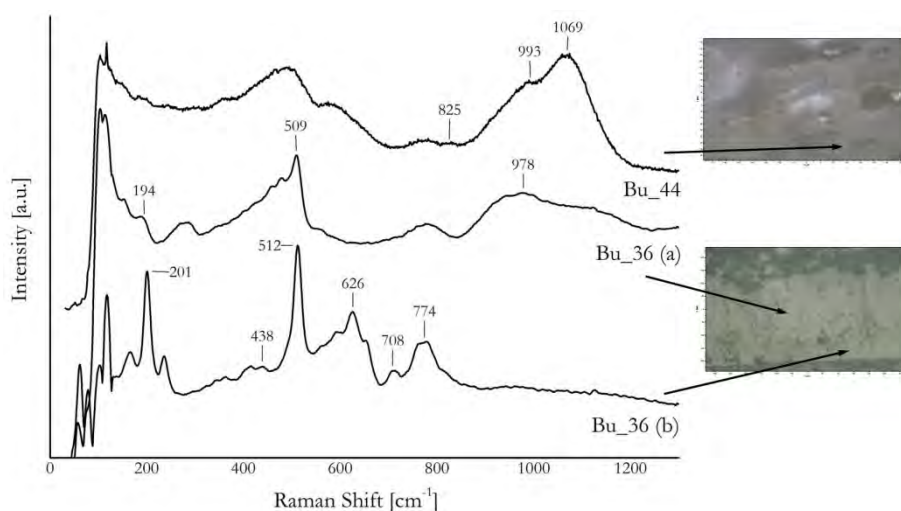


Figure.62. Raman spectra of glaze layers of ceramic sherds from Bürgel (Bu_36 and Bu_44) with their relative photos (20x). Bu_36 (b) shows in addition to the characteristic peaks attributed to cobalt blue, peaks ascribable to white zinc and cassiterite.

Table.15. Table of the characteristic Raman frequencies of the phases detected in the German sherds.

Chemical phase - Mineral	Characteristic frequencies (cm ⁻¹)
Quartz	144, 204, 356, 395, 465
Rutile	237, 442, 609
Anatase	143, 393, 513, 637
Hematite	227, 296, 412, 612
Magnetite	671-679
Kaolinite	143, 207, 232, 344-351
Metakaolinite	807, 958-966, 1123
Illite	460-463, 703-713, 771-778
Montmorillonite	810-840
Cobalt blue	194-201, 509-512
Cobalt silicate	825
White zinc	438
Cassiterite	626, 708, 774

4.3.3. LIF Analyses. Results and Discussion

LIF spectroscopy was used in this research with the aim to investigate the production technology of ceramic materials by means of a non-destructive approach. Therefore, the potentiality of this technique to investigate ceramic materials was explored. LIF technique was already used as a diagnostic tool in the field of cultural heritage but a few application on pottery studies were found in literature [81], [91], [92]. The analyses were performed at the ENEA research centre laboratory in Frascati (Rome)⁵, where it has been developed and patented a LIF scanning system [92], capable to collect hyperspectral fluorescence images scanning large areas for applications on cultural heritage surfaces.

Ceramic fragments were analysed exploiting the mineral luminescence and carrying on fast analyses in a non-destructive and non-invasive way. Luminescence in minerals and glaze ceramic depends on activator elements, such as impurity ions and lattice defects, on composition and structure of the glass [93], [94]. Interpretation of LIF spectra of ceramics, as well as other heterogeneous materials often present in cultural heritage, can be difficult and complicated due to the characteristic fluorescence broad bands and their overlapping in the spectrum. Furthermore, there is a lack of studies regarding its application on archaeological and historical ceramic and

⁵ Thanks to the collaboration with Dr. Luisa Caneve, who is kindly acknowledged.

glass materials, and only a few publication were found in literature [81], [95].

LIF spectroscopy was carried out on both glaze and body of all the ceramic fragments selected in this research, but only few of them gave fluorescence signals, in particular those decorated with glaze. LIF results discussed in this paragraph regards those obtained from the pottery sherds coming from Bürgel, Brandis, Cottbus, Duingen and Peine. In **Fig.63-64** the main spectra acquired on glazes and ceramic bodies are shown.

The LIF spectra of blue glaze in both Bu_36 and Bu_44 sherds (**Fig.63**) show bands in UV, blue and green regions probably due to Pb^{++} doped silicas [81]. In the UV region the fluorescence may be also due to Al^{3+} , Li^+ , K^+ and Na^+ doped SiO_2 [94]. LIF band at ~ 450 nm can be attributed to cobalt blue pigments, which shows a characteristic fluorescence signal at 442 nm [96]. The spectrum of Bu_36 blue glaze shows in addition two more bands in UV and red regions ascribed to ZnO, also detected by Raman spectroscopy [97], [98]. Fluorescence spectrum of white glaze (white decorating spots) in Bu_36 can be attributed to SnO_2 , that shows luminescence at ~ 450 and ~ 510 nm when cassiterite is activated by W and Ti [99], [100]. Tin oxide (SnO_2) can be used as opacifier agent in glass production, as in the ancient Egyptian glasses, and at around the IX century it was discovered that small amount of cassiterite could act as opacifier also in ceramic glaze, as it was already found in blue and white ceramics coming from Turkey [101], [102].

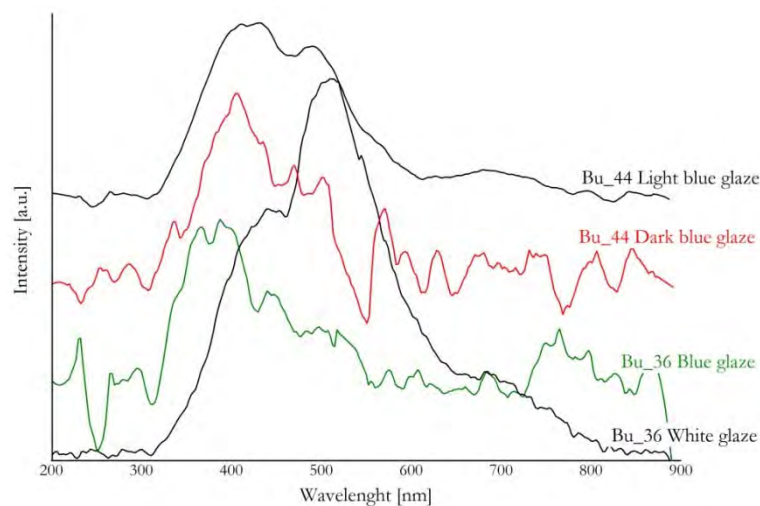


Figure.63. LIF spectra of ceramic glaze of two sherds coming from Bürgel (Bu_36 and Bu_44).

LIF spectra of Cottbus, Dui_88, Dui_90 and Pe_98 ceramic bodies (**Fig.64.**) show different signals in the blue, green and red regions. Dui_88 and Dui_90 present blue (~ 350 nm) and red (~ 700 nm) fluorescence bands probably connected to plagioclase (Na-feldspar) with Mn^{2+} activator element, Ti^{3+} and/or Fe^{3+} in the Al^{3+} tetrahedral sites of feldspar lattice [98], [103]. Pe_98 and all Cottbus samples have bands at ~ 430 , 500 and 680 nm. These fluorescence bands

suggest the attribution to the intrinsic fluorescence of calcite mineral caused by crystal defects, Fe^{2+} and Mn^{+2} in the Ca^{2+} sites [104]–[108]. The presence of calcite detected by LIF in these ceramic fragments is confirmed by FT-IR analyses. LIF spectra of these samples do not show silicate's fluorescence emission bands probably because the quenching of Fe^{2+} , which can be an activator element in calcite mineral. If present enough Fe^{2+} , it can be noticed the quenching effect: an intensity damping due to the absorption of energy by the element, generally a metallic element, adjacent to the emitting substance [108].

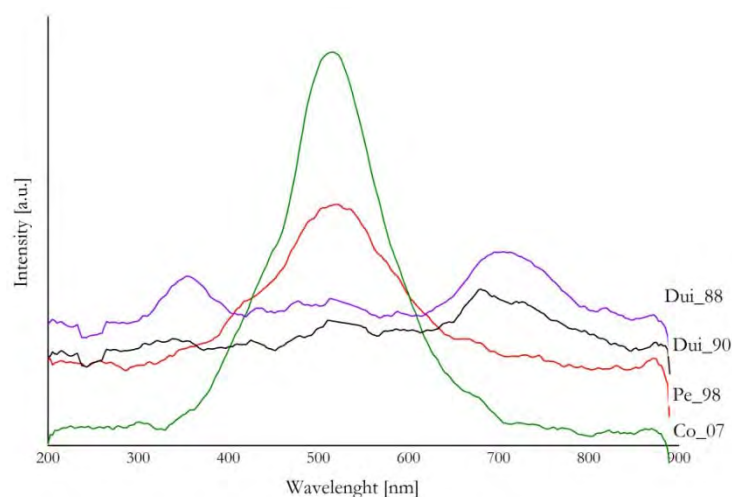


Figure.64. LIF spectra of ceramic body of sherds from Cottbus, Duingen and Peine.

Since the obtained results were able to identify particular elements and phases present in ceramic bodies and glazes, LIF spectroscopy can be considered a promising technique useful to investigate potteries by a non-destructive way. LIF technique is considered as a molecular spectroscopy and at the same time it can provide information regarding elemental composition due to activator elements in the crystal lattice which produce luminescence signals. This double capability distinguishes LIF technique among other molecular spectroscopies and elemental analyses.

Ceramic sherds from Bürgel, Brandis, Duingen, Cottbus and Peine were investigated more in detail by other methods in order to integrate the obtained data. The selection of these samples was made on the basis of the interesting LIF results which exhibited luminescence signals.

These samples were then analysed by UV-Vis Spectrophotometry, XRF and LIBS techniques, and their results are reported and discussed in the followed paragraphs.

4.3.4. UV-Vis Spectrophotometry Analyses. Results and Discussion

This analysis was performed at TU Bergakademie Freiberg, in Germany, at the Department of Mineralogy⁶. The obtained reflectance spectra were compared with those reported in literature related to pigments and glass materials [109]–[111]. The use of this technique has the aim to investigate the chemical composition of the glaze in order to provide information regarding the technologies adopted. A few works were found in literature about UV-Vis spectrophotometry applied in potteries and glazes [48], [112], however, this techniques seems to be a powerful tool to investigate by a non-destructive way pigments and colouring agents in glass and glaze. Moreover, its use offers advantage to be portable allowing low-cost in situ measurements [110].

Significant results obtained by UV-Vis spectrophotometry on glazed study are discussed in this section. In **Fig.65** are reported UV-Vis spectra of blue glaze covering Bu_36 and Bu_44 potsherds. Cobalt blue, named also Thénard blue, develops blue colour when the metal element is tetrahedral coordinated by four oxygen ions. This configuration allows three transitions and, as it is reported in literature, only two of them are detectable by spectrophotometry analysis: one in the visible (550-650 nm) and the other in the near-infrared ranges (1200-1500 nm) [110], [111]. The blue glaze spectra of Bu_44 and Bu_36 samples (**Fig.65**), show absorption bands in the range 500-650 nm, compatible with cobalt blue and smalt spectra available in literature. Actually, in the spectrum of Bu_44 (dark blue) are clearly present the three characteristic sub-bands of cobalt blue located at 535, 594 and 647 nm. The three sub-peaks are due to the Jahn–Teller (JT) effect responsible for the split transitions ${}^4A_2 \rightarrow {}^4T_1$ (P) in a tetrahedral coordination of Co^{2+} [113], [114]. The same three sub-bands are also detected in the spectrum of Bu_44 light blue glaze but less intense, as expected. Furthermore, as it was studied by A. Ceglia et.al. [110], the position of the absorption bands of cobalt can provides reliable information able to distinguish the glass matrix. The peak located at 535 nm indicates sodic glass instead calco-potassic glass, which presents the first peak in the visible range located in shorter wavelength (520 ± 5 nm) [110], [115]. Na-rich glaze composition of this sherd suggests that Bu_44 sample may be the typical Bürgel stoneware with cobalt-blue salt-glaze (*Smaltebenwurf*). Salt-glaze procedure provides a glossy and shiny covering, waterproof and resistant to chemicals, by throwing salt into the kiln during the firing process [77], [116]. These results are supported by SEM-EDX analyses (see in the next paragraphs), where high content of sodium chloride (NaCl) was detected in the glaze layer. The identification of this glaze production technique, allowed to estimate the firing temperature greater than 900°C. At high temperatures the sodium salts vaporize and react with the clay body forming a sodium aluminium silicate or salt-glaze. As reported in literature, most of the salt

⁶ Thanks to the collaboration and cooperation of Prof. Gerhard Heide and Margitta Hengst, which are kindly acknowledged.

glazers begin the salting process at temperatures higher than 1000°C, in depending on the kind of salt chosen and firing conditions (reducing atmosphere is beneficial). Sodium chloride, as well as sodium carbonate and sodium bicarbonate are only some of the sodium sources mostly used for this procedure. Bu_44 pottery probably was fired at temperature lower than 1000°C, but it has to be considered that sodium chloride is more potentially volatile and the use of dump salt, as often used by salt-glaze potters, promotes the chemical reactions due to the presence of steam in the kiln [117]. Thus, the salt-glaze procedure was performed at low temperature, in this way the salt reacts with other oxides present in the glaze providing particular chromatic effects, as Bu_44 glaze exhibits. Furthermore, elemental analyses carried out by XRF, LIBS and SEM-EDX techniques showed PbO into the glaze of this particular sample. Usually salt-glaze potteries are lead-free but its detection may allow to assume the use of Pb as flux agent promoting lower melting point [89], [118]. The firing temperature estimated by spectroscopic techniques of the Bu_44 ceramic body may be between 900°-950°C, thus, the glaze may not be fired at higher temperature, for this reason the presence of PbO as flux agent.

Bu_36 blue glaze presents UV-Vis spectrum characterized by a broad band centred at around 600 nm, typical of the cobalt blue colour present in mixture with other compounds, as zinc white, which contribute in the visible range spectrum by an overlapping of bands [111], [114].

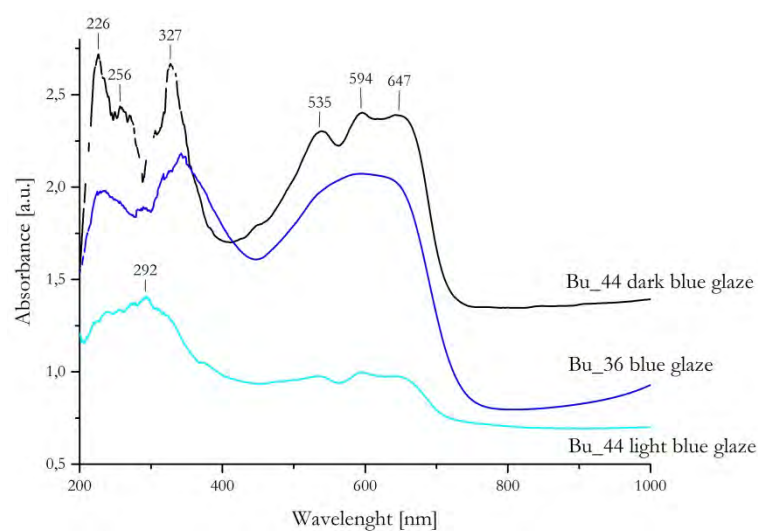


Figure.65. UV-Vis spectra of blue glaze present on Bu_36 and Bu_44 potsherds.

Absorption bands at around 226 and 256 nm may be due to Pb^{2+} ion, which has its characteristic peaks in the UV range between 230 and 250 nm [111]. Moreover, as reported by Vieira Ferreira et.al. [49], white glazes absorb in the UV region at around 300 nm as well as pottery pastes, as it is shown in **Fig.66**. Actually, white pigments, like white titanium (TiO_2), usually absorb in the UV range at around 200-400 nm [109], [119].

Potsherds from Brandis have green glazes (Br_08 and Br_09) and yellowish glaze (Br_11). UV-Vis spectra are shown in **Fig.67**. Green glass and glaze can be usually obtained using chrome (Cr^{3+}) or copper (Cu^{2+}) compounds [120]. Both spectra of glaze coatings of Br_08 and Br_09 (even if the latter is less intense due to the dark and opaque colouration) present a lack of absorption band at around 550 nm, typical of green pigments, and an absorption band centred at around 800 nm, characteristic of Cu^{2+} (whereas Cr^{3+} compounds exhibit absorption bands centred at 450 and 650 nm) [112], [121], [122]. Furthermore, bands in the range between 300-400 nm may be due to the contribution of ferric ions, probably Fe^{3+} , which may be responsible of the yellow colouration particularly in the case of Br_11 glaze [112], [122], [123].

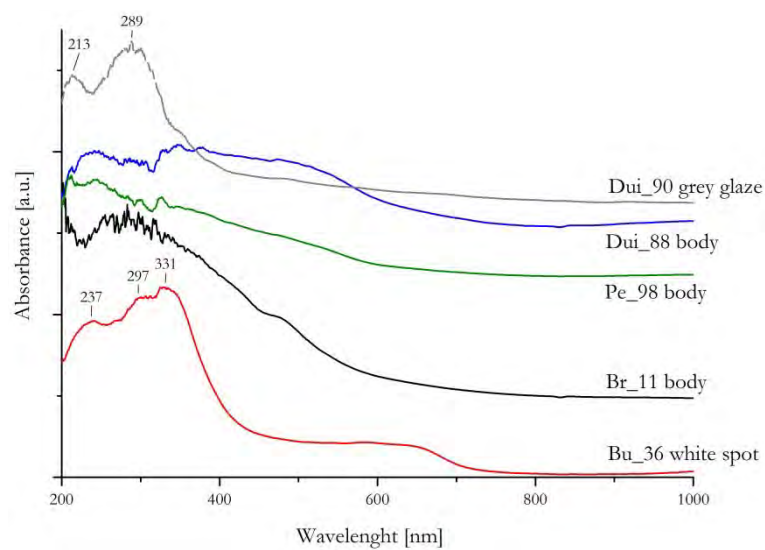


Figure.66. UV-Vis spectra of white spot present in the blue glaze of Bu_36, grey glaze of Dui_90, and ceramic bodies spectra of Dui_88, Pe_98 and Br_11.

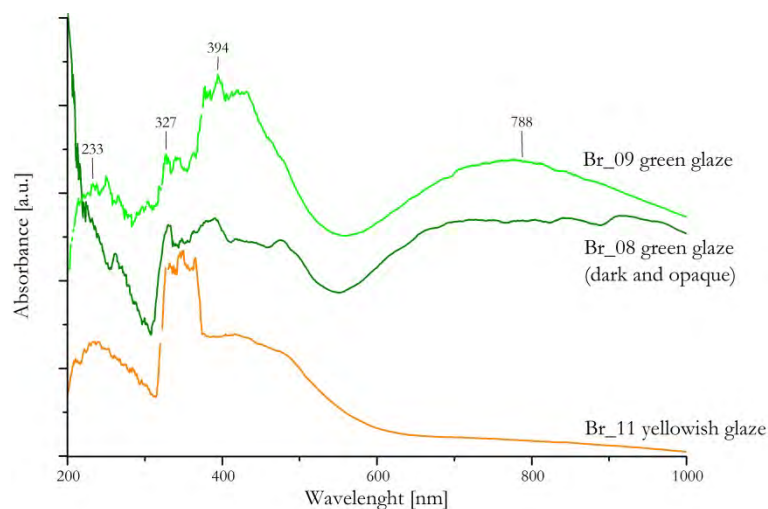


Figure.67. UV-Vis spectra of green and yellow glazes present in the potsherds from Brandis.

4.3.5. XRF and LIBS Analyses. Results and Discussion

In order to examine in depth the chemical composition and integrate the LIF and UV-Vis spectrophotometry results, elemental analyses of the same ceramics from Brandis, Bürgel, Cottbus, Duingen and Peine were carried out by means of XRF and LIBS techniques. The former is the most used technique in archaeometric studies applied in ceramic investigation and many papers are available in literature [48], [124]–[127]. The latter instead, only recently has become a powerful tool in archaeological material investigation and it has been applied for characterization of several kind of cultural heritage materials, such as pottery, glasses and paintings [128]–[131]. Both of them do not require sample preparation, and offer significant advantages as to be fast, portable and multi-elemental methods [132].

XRF results were able to confirm some consideration discussed in the previous paragraphs about the chemical composition of ceramic matrix and glaze of the selected potsherds. Semi-quantitative XRF analyses of major and minor elements detected in these German sherds are summarized in the followed **Tab.16**.

All the ceramic bodies are composed by Si, Al, K, Ca, Ti and Fe, typical elemental composition in ceramic materials. The same elements were also detected in all coating layers of the samples from Bürgel and Brandis, with the addition of PbO. The presence of PbO (18–66 wt.%) indicates the use of lead-glaze, then firing temperature between 800°–950°C. Furthermore, aluminium oxide and calcium oxide were used as stabilizing oxide for silica and fluxe, respectively. Co was found in the blue glazes of Bu_36 and Bu_44, confirming the use of cobalt blue as the colouring agent. Moreover, trace of Zn, found in Bu_36 and not in Bu_44 glaze, confirms the data obtained by Raman and LIF analyses. In samples from Brandis decorated by green glaze (Br_08 and Br_09), Cu was detected. UV-Vis spectra showed absorption bands related to the presence of Cu²⁺, and XRF analysis supports this data. Copper in the decorated layer may be attributed to so-called ramina, copper oxide (CuO) which produces an intense green coloration, as these two samples from Brandis show [133]. Ti in XRF results of all the samples is due to the minerals rutile and anatase (TiO₂), also detected in Raman spectra, used in both glaze, to nucleate the crystal in a low-viscosity glaze, and ceramic body [54]. Anatase/rutile are often present as accessory minerals in clays and they may contain Fe, which is present in all the analysed ceramic bodies with around 10 ± 4 wt.% in average, as shown in the XRF semi-quantitative results [134].

Table.16. Semi-quantitative XRF analyses on the bulk and glaze of the selected German sherds coming from Bürgel, Brandis, Cottbus, Duingen and Peine, given as normalised % concentration (wt%).

Sample		Al ₂ O ₃	SiO ₂	K ₂ O	CaO	TiO ₂	Fe ₂ O ₃	ZnO	PbO	CoO	CuO	tot
Bu36	bulk	30.73	61.13	2.57	0.37	2.14	1.31	0.23	0.67	--	--	99.15
	glaze	6.32	28.46	--	18.18	1.58	2.45	3.95	38.14	0.88	--	99.97
Bu43	bulk	22.64	44.64	11.95	7.92	4.15	7.83	--	0.87	--	--	100.00
	slip	18.63	37.97	4.70	6.03	3.90	7.71	--	18.99	--	--	97.93
Bu44	bulk	28.23	51.84	9.26	1.36	4.79	4.53	--	--	--	--	100.00
	glaze	17.67	43.85	3.85	6.59	4.18	5.30	--	17.67	0.74	--	99.84
Bu48	bulk	28.41	52.91	7.10	0.89	4.97	5.52	--	--	--	--	99.80
Bu49	bulk	18.46	46.86	17.75	5.11	5.11	4.87	--	1.85	--	--	100.00
Br08	bulk	23.92	53.54	4.44	1.14	6.72	9.20	--	--	--	--	98.97
	glaze	20.12	39.67	1.98	6.52	10.48	12.92	--	7.37	--	0.94	100.00
Br09	bulk	24.85	49.56	3.88	1.55	8.91	9.55	--	0.80	--	--	100.00
	glaze	9.74	19.47	0.13	1.09	1.69	1.95	--	61.40	--	4.54	100.00
Br11	bulk	26.07	46.23	8.22	2.23	7.45	7.80	--	0.79	--	--	98.78
	glaze	2.20	18.56	0.00	2.20	1.93	7.91	--	66.20	0.11	--	99.10
Br14	bulk	25.48	45.38	5.95	3.40	7.44	9.32	--	--	--	--	96.97
	slip	8.21	39.80	9.70	6.47	2.74	30.85	--	--	--	--	97.76
Br19	bulk	25.62	52.41	4.08	0.93	7.42	8.60	--	--	--	--	99.06
Pe96	bulk	18.61	59.81	3.99	2.47	4.18	10.96	--	--	--	--	100.00
Pe98	bulk	23.18	55.36	4.77	2.59	3.27	9.09	--	--	--	--	98.27
Pe00	bulk	22.66	57.72	3.46	1.55	3.46	9.24	--	--	--	--	98.09
Co04	bulk	5.52	19.64	3.31	51.92	0.95	16.08	--	--	--	--	97.42
Co05	bulk	11.10	33.58	8.32	26.57	1.46	18.83	--	0.13	--	--	100.00
Co06	bulk	9.11	26.72	6.31	40.32	1.03	14.09	--	0.24	--	--	97.81
Co07	bulk	13.14	37.37	5.11	24.09	1.46	18.83	--	--	--	--	100.00
Dui78	bulk	24.87	52.51	4.01	2.35	3.45	10.05	--	--	--	--	97.24
Dui80	bulk	25.67	55.49	4.40	1.34	3.18	9.79	--	0.12	--	--	100.00
Dui88	bulk	14.71	54.34	5.15	3.93	3.43	12.77	--	--	--	--	94.33
Dui90	bulk	16.07	57.25	3.79	3.43	5.24	9.70	--	--	--	--	95.48

In order to evaluate the variability of chemical composition of the analysed samples, binary diagrams, using chemical concentration of the elements present in the ceramic bulks, were generated and reported in **Fig.68**. XRF results show similar relative amount of Ti in the samples from Duingen and Peine (in average 3.83 ± 0.95 wt.% and 3.64 ± 0.48 wt.% respectively) and in the binary diagrams, which take in to consideration the concentration of TiO_2 vs. SiO_2 and TiO_2 vs. Fe_2O_3 (**Fig.68 (a)** and **(b)**), Duingen and Peine potteries seem almost to overlap. In fact, FT-IR results also propose a similar mineralogical composition of the raw materials used in Duingen and Peine ceramics suggesting the provenance of the clays from Lower Saxony. Moreover, the distinction among the potteries coming from the different sites is observed. In these binary plots, it is possible to clearly isolate Cottbus and Brandis samples, characterized by a low and high content of Ti. High relative content of Ca (24–52 wt.%) is present in all the Cottbus samples, suggesting the use of naturally Ca-rich clays or clay tempered with calcite. Cottbus group is also well discriminated by binary plots reported in **Fig.68 (c)** and **(d)**, where the samples are disposed with about the same trend.

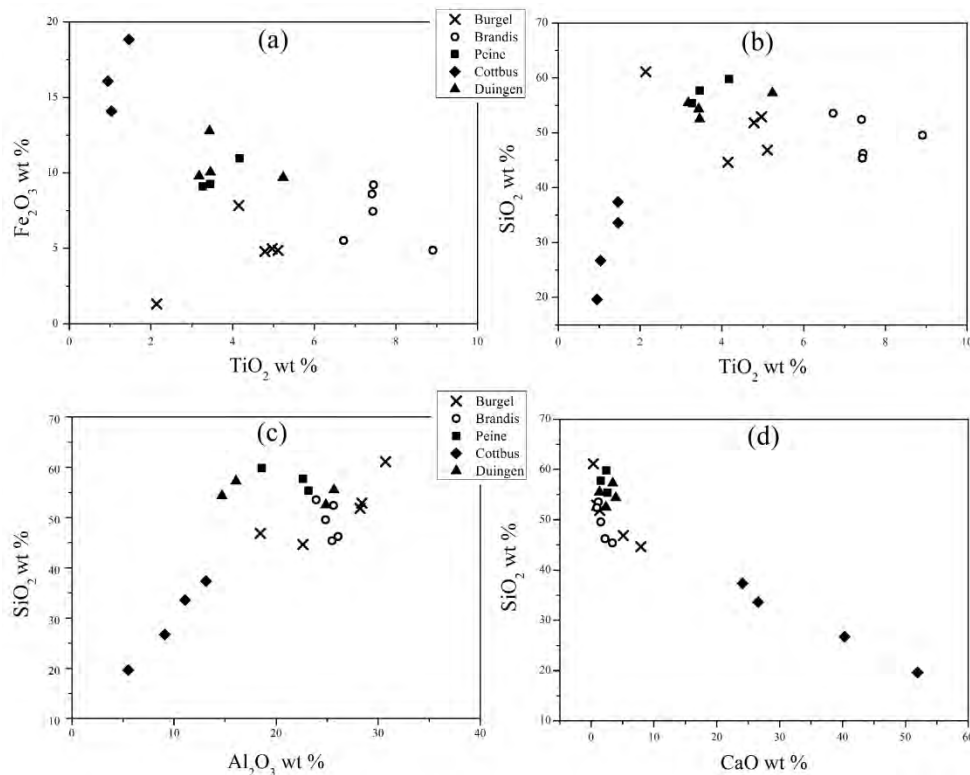


Figure.68. Binary diagrams of selected major and minor oxides obtained by XRF semi-quantitative analyses in weight percent (wt.%) of the ceramic sherds coming from Bürgel, Brandis, Peine, Cottbus and Duingen. **(a)** Fe_2O_3 vs. TiO_2 ; **(b)** SiO_2 vs. TiO_2 ; **(c)** SiO_2 vs. Al_2O_3 ; **(d)** SiO_2 vs. CaO .

Multivariate statistical method (PCA) was used in order to examine graphically the grouping pattern of the samples in terms of chemical composition, with the advantage to use a statistical method able to consider more than two parameters, as in the case of the binary plots. Furthermore, multivariate analysis provides information without any hypothesis. In **Tab.17** are shown the eigenvalues of the correlation matrix of the five principal components extracted. Zn, Pb, Co and Cu were not included in the statistical analysis because not present in all the ceramic bodies.

Table.17. Extracted eigenvectors and eigenvalues related to the five principle components (PC) extracted.

	PC1	PC2	PC3	PC4	PC5
Al	0,48	-0,07	-0,04	-0,32	0,76
Si	0,45	-0,27	-0,28	0,47	-0,33
K	0,02	0,91	-0,18	0,29	0,12
Ca	-0,49	0,05	0,02	-0,45	-0,13
Ti	0,35	0,18	0,88	-0,04	-0,23
Fe	-0,43	-0,21	0,34	0,62	0,48
Eigenvalue	3,80	1,12	0,62	0,34	1,10
Variance (%)	63,39	18,73	10,38	5,74	1,70
Cumulative Variance (%)	63,39	82,12	92,50	98,24	99,94

The generated matrix in **Tab.17** starting by XRF data shows that the first two PCs explain 82,12 % of the total spatial variance, where PC1 and PC2 represent 63,39 and 18,73 % respectively. The cumulative variance provides sufficient information to reveal relationship among the selected samples. Actually, the higher this variance (%) is the better, and 82,12 % of variance explained on the first two components would usually be regarded as good [135]. The score plot of PC1 versus PC2 and the biplot, which reports also the loading plot, are shown in **Fig.69 (a)** and **(b)**, respectively. Cottbus samples are well isolated along the negative PC1 axis, Brandis and Bürgel are distributed in the positive quadrant of PC1 axis, while, as expected, Duingen and Peine potsherds overlap. Discrimination of clusters in quadrants depends on the

effect of elemental variables inferred from the loading plot. Negative PC1 axis is dominated by Ca and Fe; positive PC2 is strongly affected by K and negative PC2 values are related to a high content of Si and Al. Furthermore, angles between vectors (in blue) provide information about the correlations: i) small angle indicates high positive correlations between elemental compositions; ii) right angle indicates no correlation; iii) angle close to 180° indicates inverse correlations [124].

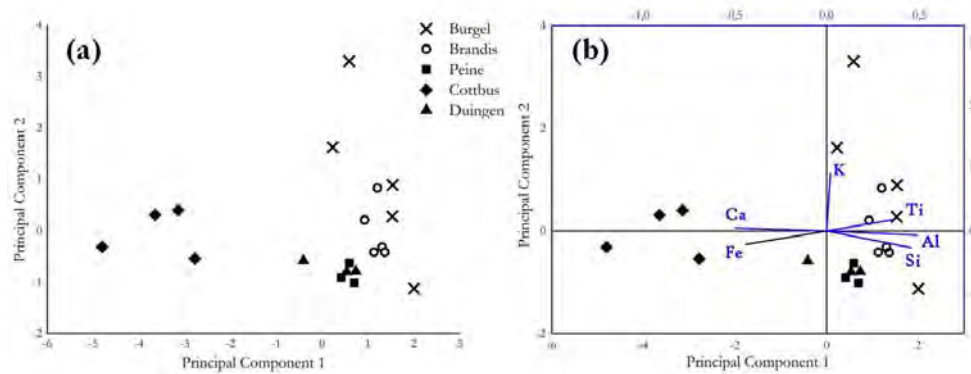


Figure.69. Score plot (a) and biplot (b) based on the first two PCs of the ceramic body compositional data obtained by means of XRF analysis.

LIBS technique, as elemental method, was applied to study the chemical composition of the German ceramic sherds. It is a very sensitive spectroscopic tool, and in this research it was used to investigate the elemental composition of the selected potteries analysing the superficial layers. It is considered a complementary technique to other laser based techniques such as Raman and LIF [136], and its application in ceramic study was explored with the aim to evaluate its capabilities and its joint use with other spectroscopic methods.

In the followed figure (**Fig.70**) are presented some of the spectra obtained by LIBS analyses. The attributions to the elements were made on the basis of literature data and database available online [129], [132], [137]. The results of the LIBS experiments are summarized in **Tab.18**, where the elements detected along with the corresponding spectral lines are presented. The analysed glazes contain Si, high content of Al and Ca, Fe and Ti. Elements such as K, Na and Mn were detected by LIBS and not by XRF measurements, indicating higher sensitivity of LIBS technique for light elements. Furthermore, Cu, Co, Zn and Pb were observed suggesting lead-base glazes and the pigments used responsible for their colourings.

Table.18. Elements and emission lines detected in the LIBS spectra of the investigated glazes [129], [132], [137].

Elements	Spectral lines (nm)
Al	394,34 (I); 396,19 (I)
Ca	393,34 (II); 396,92 (II)
Co	365,28 (I); 399,64 (I); 401,50 (II); 402,57 (I); 404,10 (II); 412,12 (I)
Cu	402,56 (I); 406,39 (I)
Fe	347,26 (I); 348,70 (I); 356,45 (I); 356,86 (I); 358,00 (I); 360,89 (I); 361,87 (I); 363,18 (I); 364,79 (I); 367,95 (I); 404,57 (I); 404,93 (I); 408,02 (I); 415,68 (I); 418,83 (I); 417,33 (II); 417,76 (I)
K	404,67 (I)
Mn	403,20 (I); 403,55 (I); 404,33 (I); 407,91 (I)
Na	411,31 (II); 412,52 (II)
Pb	357,07 (I); 363,90 (I); 367,16 (I); 368,41 (I); 401,92 (I); 406,01 (I); 405,71 (I); 416,60 (I);
Si	410,31 (I); 412,82 (II)
Ti	345,62 (II); 346,70 (II); 350,06 (II); 350,63 (II); 363,28 (I); 364,08 (I); 365,17 (I); 394,91 (I); 395,77 (I); 398,35 (I); 398,22-398,92 (I); 399,05-399,92 (I)
Zn	388,35 (I); 396,54 (I)

(I) and (II) refer to neutral atoms and charged ions emissions, respectively.

The presence of elements such as Co (in Bu_36 and Bu_43) and Cu (in Br_08 and Br_09) are ascribable to the use of cobalt blue and ramina, respectively, as colouring agents in glaze composition already discussed. LIBS provided further information on cover layer composition due to its high sensitivity in elemental detection. Intense emission lines of Fe and Mn were detected in Br_14 sherd (**Fig.70 (d)**), characterized by a dark coloured slip. Mn and Fe association was also found in literature and manganese as oxide or carbonate can be used to obtain a dark-purple glaze [48], [138]. Furthermore, both LIBS and XRF analyses did not detect Pb in this sample, suggesting that the coating layer is a slip, typically made by suspension clay in water that can have colour added [76], [89].

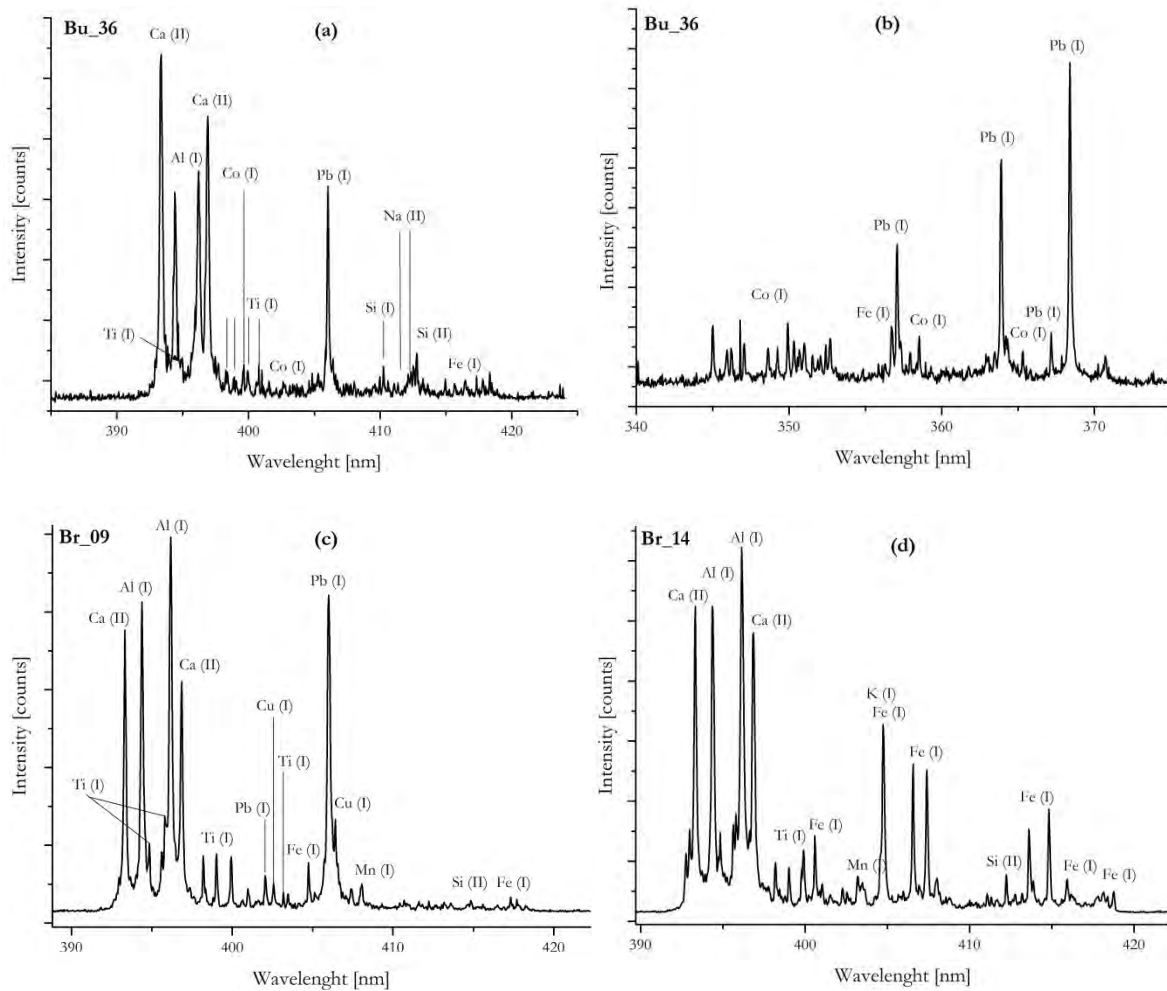


Figure.70. LIBS spectra of glaze ceramic sherds. **(a)** and **(b)** blue glaze of Bu_36 at different ranges; **(c)** green glaze of Br_09; **(d)** dark-purple slip of Br_14.

LIBS spectra exhibit different intensities of Al, Ca, Fe and Ti emission lines. With the aim to determine variations in terms of concentration, the intensity ratios of selected elements were calculated and multivariate statistical analyses (PCA) was performed. In **Tab.19** are shown the eigenvalues of the correlation matrix of the five principal components extracted. The first two PCs (PCA1 and PCA2) explain 86,82 % of the total spatial variance, therefore, those were chosen and biplot of PC1 versus PC2 is shown in **Fig.71**. Most of the samples are located along the negative PCA1 axis suggesting high content of Ti, whereas other samples have higher concentration of Ca and Pb.

Table.19. Extracted eigenvectors and eigenvalues related to the five principle components (PC) extracted for each intensity ratio of selected elements.

	PC1	PC2	PC3	PC4	PC5
Ca/Al	0,31	0,43	0,51	-0,57	0,31
Ca/Ti	0,47	0,15	-5,13 E-4	0,16	-0,59
Ca/Fe (1)	0,45	0,23	-0,14	0,10	0,06
Ca/Pb	0,38	-0,35	0,44	0,11	-0,32
Ca/Fe (2)	0,45	0,06	-0,27	0,45	0,56
Ti/Al	-0,31	0,39	0,56	0,63	0,05
Al/Pb	0,11	-0,67	0,34	0,05	0,34
Eigenvalue	4,20	1,87	0,61	0,20	0,07
Variance (%)	60,02%	26,80%	8,86%	2,95%	1,11%
Cumulative Variance (%)	60,02%	86,82%	95,68%	98,63%	99,74%

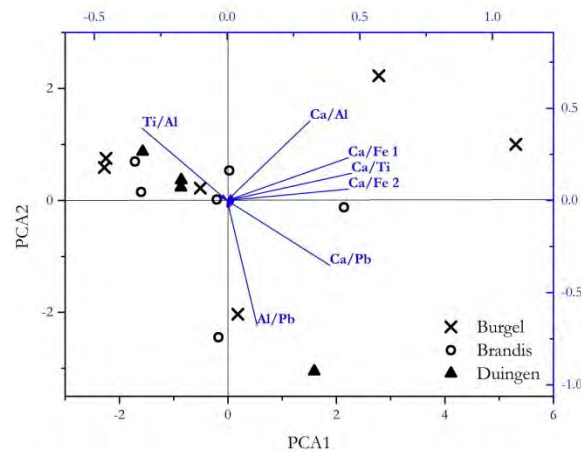


Figure.71. Biplot based on PAC1 and PCA2 of the intensity ratios of selected emission lines detected by LIBS analysis.

Cross-sectional elemental distribution in the glazes was investigated with the aim to evaluate the homogeneity and/or inhomogeneity of glaze production. It was exploited the LIBS ability to perform stratigraphic measurements in a micro-destructive way: the laser beam was shot several times (10 to 20 times) on the same point of the surface's sample going through the thickness of

the glaze layer. As an example, a set of spectra obtained by a LIBS stratigraphic analysis for 10 shots is reported in **Fig.72**. Glazes of Bürgel and Brandis samples were stratigraphically analysed in order to monitor the trend of elemental concentration into the glaze thickness. The aim is to investigate the chemical profiles from the external part of the glaze across its thickness and evaluate the diffusion of the elements into the glaze. Ca, Al and Pb emission lines were considered and their intensities were plotted in function of the depth (number of shots) to better evaluate the chemical trends across the glaze. It has to be noticed that the stratigraphic analysis allowed to investigate the glaze profiles and did not reach the ceramic body, as the Pb emission lines are well detected even after 20 shots. The diagrams of chemical diffusion profiles into the glaze thickness of representative samples are given in **Fig.73**.

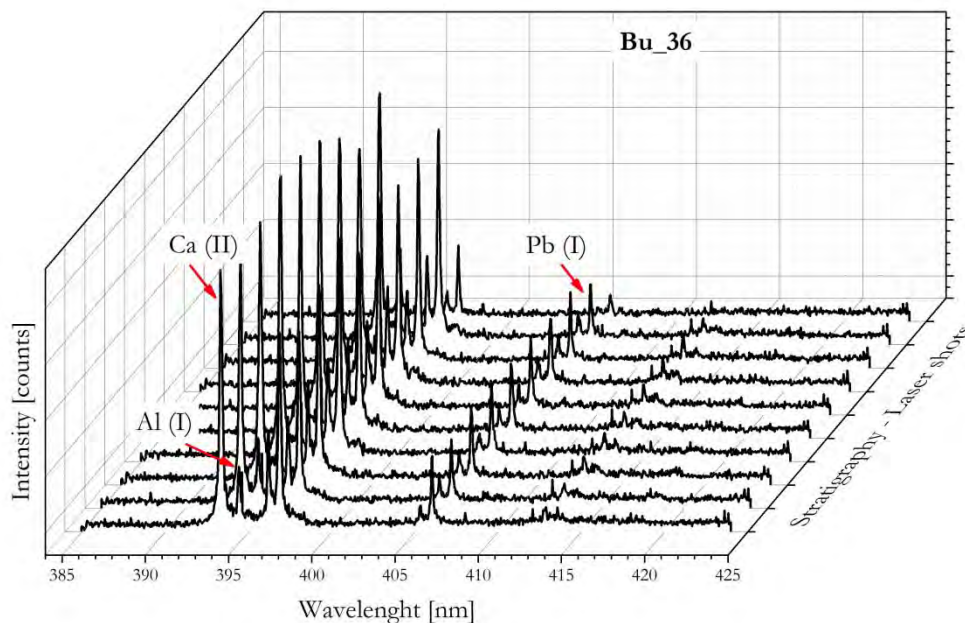


Figure.72. LIBS spectra of the Bu_36 sample obtained shooting the laser beam on the same point of the sample for 10 times.

The chemical elements profiles across the glaze thickness may provide insights on technological productions in terms of both firing temperature and time as well as cooling rate. The compositional profile is connected to the diffusion process of elements from the body to the glaze and vice versa occurring firing clay body covered with glaze [139]. The Pb content measured by LIBS in the glaze thickness (**Fig.73** black dots) seems to increase for the first 4-5 shots and then remain more or less constant across the layer in particular in Br_08 and Br_09 samples. The increase of Pb content might be referred to the Pb migration from the glaze to the body connected to the newly formed crystallites developed into the interface glaze/clay body and detected in the SEM micrographs discussed in the next paragraph. These crystallites are composed of K-Pb feldspers and may provide insights about firing condition and cooling rate as

their thickness increases as increasing temperature [87], [139]–[141]. Al content (**Fig.73** blue dots) is almost constant across the glazes with a slight decrease very after few shots for the Br_08 and Bu_44 samples. Bu_44 glaze shows an inhomogeneous distribution of Ca into the layer, probably due to the salt-glaze production technique adopted for this sherd, as discussed in the other paragraphs, which may form a non-uniform layer in terms of chemical diffusion.

The trends of Pb and Al may indicate that the diffusion process taken place at temperature above 750°C occurred in the analysed samples. The more stable trend of Pb content measured in Bu_43 and Bu_44 might suggest different firing conditions: higher temperatures and/or slower cooling rate, which promote a better diffusion of chemicals into the glaze [139].

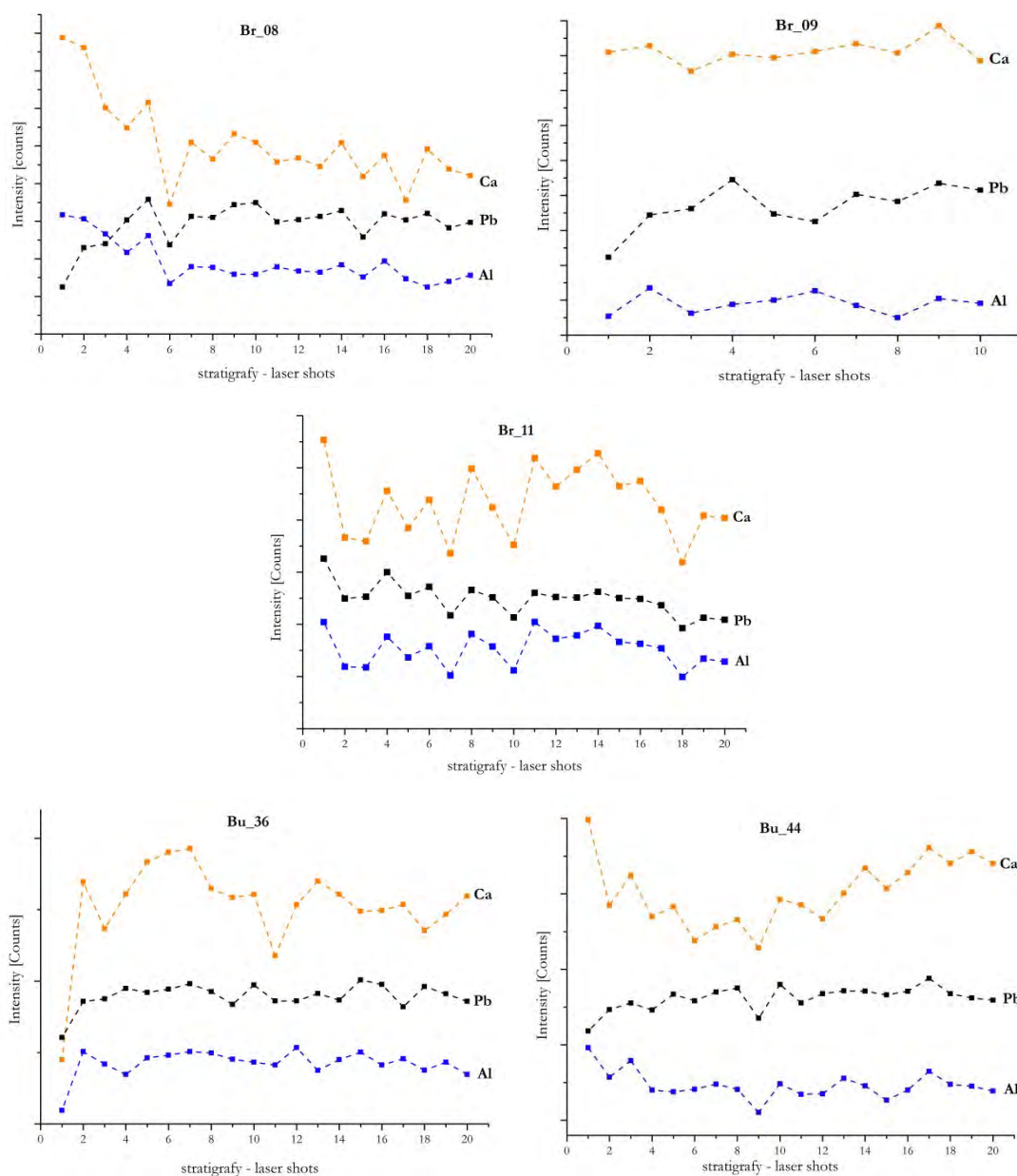


Figure.73. Intensity of Ca, Al and Pb elements detected by LIBS measurements as the results of stratigraphic analyses of glaze samples from Brandis and Bürgel.

Carrying on stratigraphic measurements, it must be considered that LIBS measurements on glaze/coating layer can be affected by interference caused by the ablation of the underlying layer, therefore, the main difficult is to distinguish the chemical composition of both ceramic body and glaze [95]. Relative intensity of particular elements, such as Pb typically present in the glaze layer, may help in distinguish the two different layers, as in the case of this research.

Furthermore, factors such as inhomogeneity, interferences among layers and matrix effect must be taken in to consideration for quantitative LIBS analyses, which are often carried out by using proper reference samples and/or effective approaches, as it is referred in literature [95], [136], [142]–[144].

4.3.6. Petrographic and Morphological Results and Discussion

Selected⁷ samples were submitted to petrographic and morphological investigation with the aim to obtain information on the production technology [55], [56], [58], [145]. The selected sherds were studied by means of an integrated analytical approach including petrographic, mineralogical, morphological and chemical investigations. **Tab.20** summaries the selected samples and the techniques applied for their investigation.

Polished cross-sections were observed through the stereomicroscope allowing to collect information about the ceramic body, especially on the mass background and colour, presence of inclusions and cover layers. Although the optical microscope is not considered as a sophisticated analytical technique, it is widely used as a primary method by conservation scientists and is able to provide information regarding macroscopic features of the objects [146], [147]. Petrographic thin-section observations were carried out under a polarising optical microscope in both cross and parallel light. This method is able to provide insights about mineralogical composition and texture of the ceramic body. Furthermore, SEM-EDX analyses allowed to analyse the micro-structure and chemical composition of the samples in terms of major and minor elements mapped on the surface of the polished cross-sections and single points in order to help in the mineral identification.

In this paragraph are reported and discussed the most significant results obtained by this analytical approach.

⁷ The methods used in this section are destructive and need small fragments of the potsherds. Therefore, considering sample preparation, time machine and elaboration data, a selection of the German sherds was made and only some samples were submitted under this kind of investigation.

Table.20. Samples selected for the morphological and mineralogical investigation.

Sample code	Stereomicroscope observation	Petrographic observation	SEM analysis	Chemical map
Bau_85	X	X		
Bau_88	X			
Bau_89	X			
Bau_91	X	X		
Bi_56	X			
Bi_60	X	X		
BM_32	X	X		
BM_35	X			
BM_75	X	X		
Br_09		X	X	X
Br_11			X	X
Br_14	X		X	X
Br_19	X	X	X	X
Bu_36	X		X	X
Bu_43	X		X	X
Bu_44	X	X	X	X
Bu_49		X		
Co_04		X		
Cop_51		X	X	X
Cop_52	X		X	X
Cop_57	X	X	X	X
Di_82		X		
Di_89		X		
Di_00		X		
Dui_78		X		
Dui_80	X		X	X
Dui_88		X		
Go_08		X		
Go_11		X		
Go_29		X		
Gro_51	X	X		
Ka_18	X			
Ka_20	X			
Ka_22	X			
Pe_00	X		X	X
Pe_98		X		

From a first observation of the photographs acquired by the stereomicroscope, the colour of the potsherds may provide insights on firing conditions in terms of temperature and/or atmosphere. Actually, as reported by M. Smith [55], light colour may indicate high firing temperature, oxidizing conditions and/or low carbon content; at the contrary, dark colour may indicate low firing temperature, reduced atmosphere and/or high carbon content.

The analysed potsherds can be divided in three main groups in base on the paste colour (see **Tab.21**).

The first group, represented by BM_75, BM_35, Bu_36, Bu_43, Bu_44, Bi_60 and Br_19, is characterized by light grey/light tan colour paste, which may suggest high temperature and/or high oxygen content during the firing process. Chemical and mineralogical characterization carried out by spectroscopic techniques, previously discussed, provided hypothesis about firing conditions under which the potteries were submitted. The samples from Bürgel and Bad Muskau were probably fired at high temperature (900-950°C) and both their colour and morphology may confirm this datum.

The second group includes Bi_56, Copo_52, Cop_57, Ka_22, BM_32, Gro_51 and Pe_00 samples, characterized by a dark grey paste.

The third group presents speckled paste and/or differences in bulk and surface colour: black/dark grey and yellowish/brownish colours.

The colour of these two groups suggests low firing temperature and/or reduced atmosphere. Furthermore, the so-called “*fire clouding*”, as shown in **Fig.74**, is caused by variations in temperature and atmosphere conditions due to a not well controlled fire and not consistent fuel and ventilation [55]. These considerations may support Raman results and the estimated firing temperatures. In fact, magnetite and magnetite/hematite combination were actually detected by Raman spectroscopy in these samples suggesting reducing firing condition and an incomplete phase transformation, and most of the samples included in second and third group are supposed to be fired at low temperature (750-800°C), as the groups inferred by FT-IR analysis suggest.

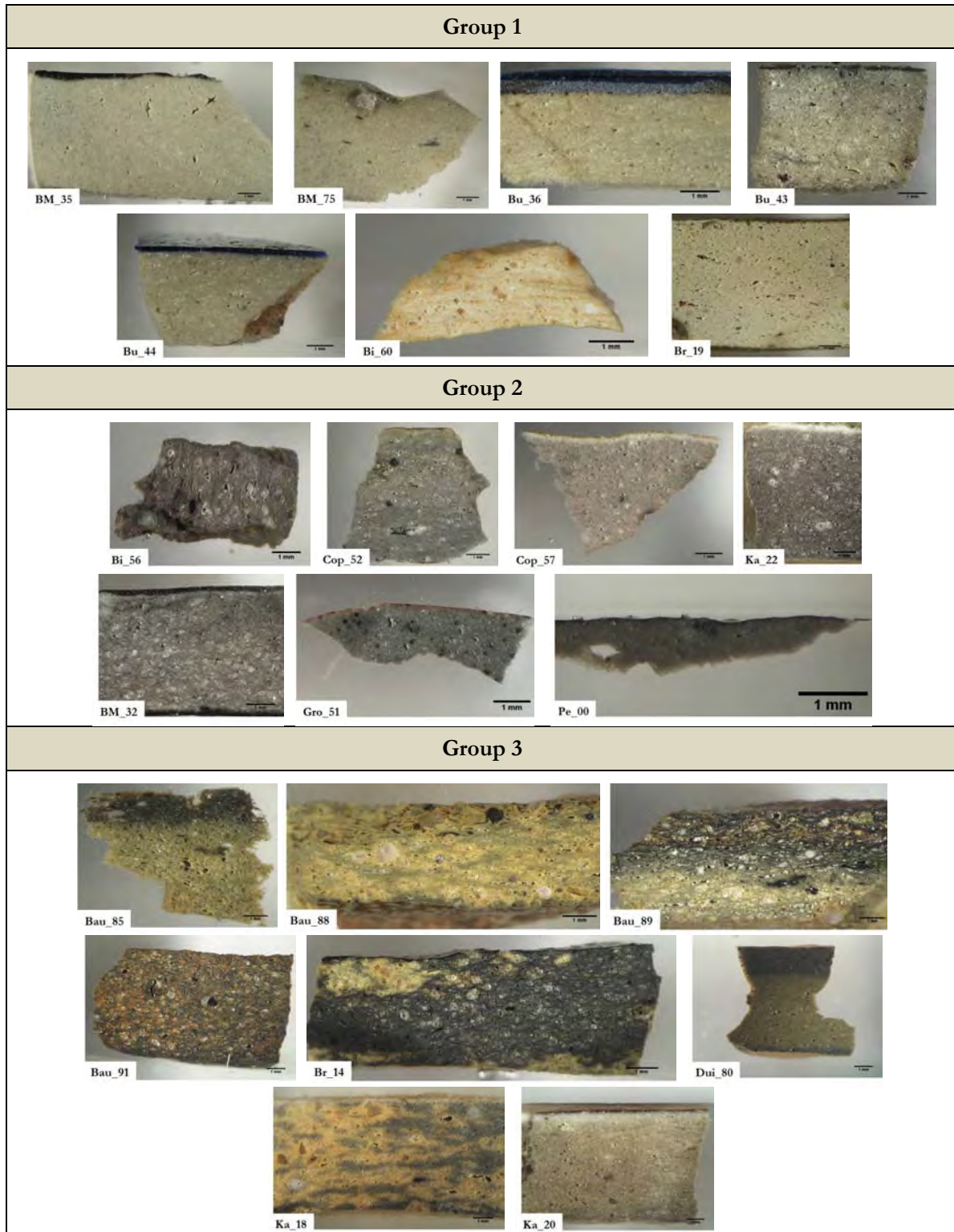
In general, the morphology of the paste seems to be solid and with great variability of inclusions in terms of shape and dimensions: grain size greater than 0,2 mm (up to 0,8 mm)⁸ and smaller than 0,1 mm, sub-rounded and coarse grains.

The grain size of the aplastic materials may provide useful information about the production techniques. Inclusion size greater than 0,1 mm is often considered as a temper, therefore deliberately added by the potter in order to modify the paste features in terms of workability and/or firing characteristics [55], [148]. Furthermore, coarse tempers may indicate other forming techniques than that of the wheel-thrown, preferred for fine fabrics because these kind of

⁸ Grain sizes of aplastic inclusions were measured by the software ImageJ.

inclusions would damage the potter's hands, or the use of it but with slow speed [149]. In order to better evaluate and describe the features of the present inclusions, petrographic analysis on the ceramic thin sections was performed.

Table.21. Stereomicroscope photographs of three groups of the German sherds divided in base on the colour of ceramic paste.



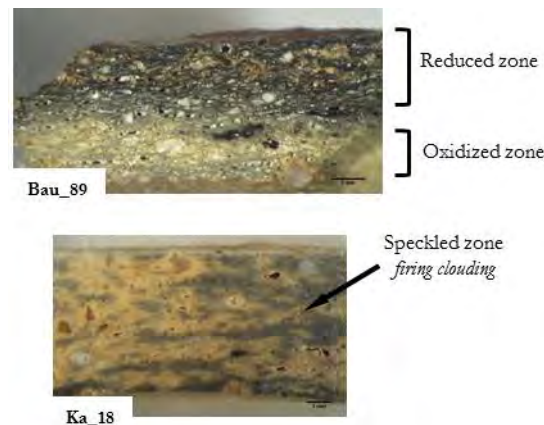


Figure.74. Stereomicroscope cross-section photos of two ceramic samples showing the presence of both oxidation and reduction zones in the ceramic pastes.

The observations of the ceramic thin sections by optical microscope show a variable fabric with both coarse and fine-grained non-plastic inclusions, angular/sub-angular and sub-rounded. The clay matrix exhibits variable colours from grey to light and dark brown. The non-plastic inclusions (20-30%) are mainly composed of quartz and rarely muscovite, both non-pleochroic and untwinned. Crystals with polysynthetic twinning were observed in Co_04 thin-section, attributed to the calcite inclusions, detected in the samples also by spectroscopic techniques. The grain size of the inclusions and their distribution is also variable in the analysed samples. Other mineral phases as biotite, pyroxene and opaque minerals are rarely recognisable and thus a discrimination of different groups on the basis of inclusion composition is uncertain. However, it may be possible to distinguish three groups according to similarities in shape and arrangement of the aplastic inclusions and groundmass. Representative examples for each group are reported in **Fig.75**.

- The first petrographic group is composed by Bi_60, Bau_85, Bau_91, Co_04, Cop_51 and Go_08 samples. It is characterized by abundant inclusions (25-30%) poorly sorted and with grain size up to 0,64 mm of diameter.
- The second group exhibits abundant inclusions (20-25%) quite uniformly distributed and maximum size of 0,23 mm. The components of this group are: BM_32, Br_09, Br_19, Cop_57, Dui_88 and Bu_44.
- The last group consists of Bu_49, Di_00, Di_82, Di_89, Dui_78, Go_11, Go_29, Gro_51 and Pe_98 samples characterized by a finely sorted sand (20%) with a homogeneous distribution and size less than 0,20 mm.

The presence of abundant non-plastic inclusions may suggest that the samples were tempered. Furthermore, differences in shape and size may indicate a different origin of raw materials and/or a different manufacturing process.

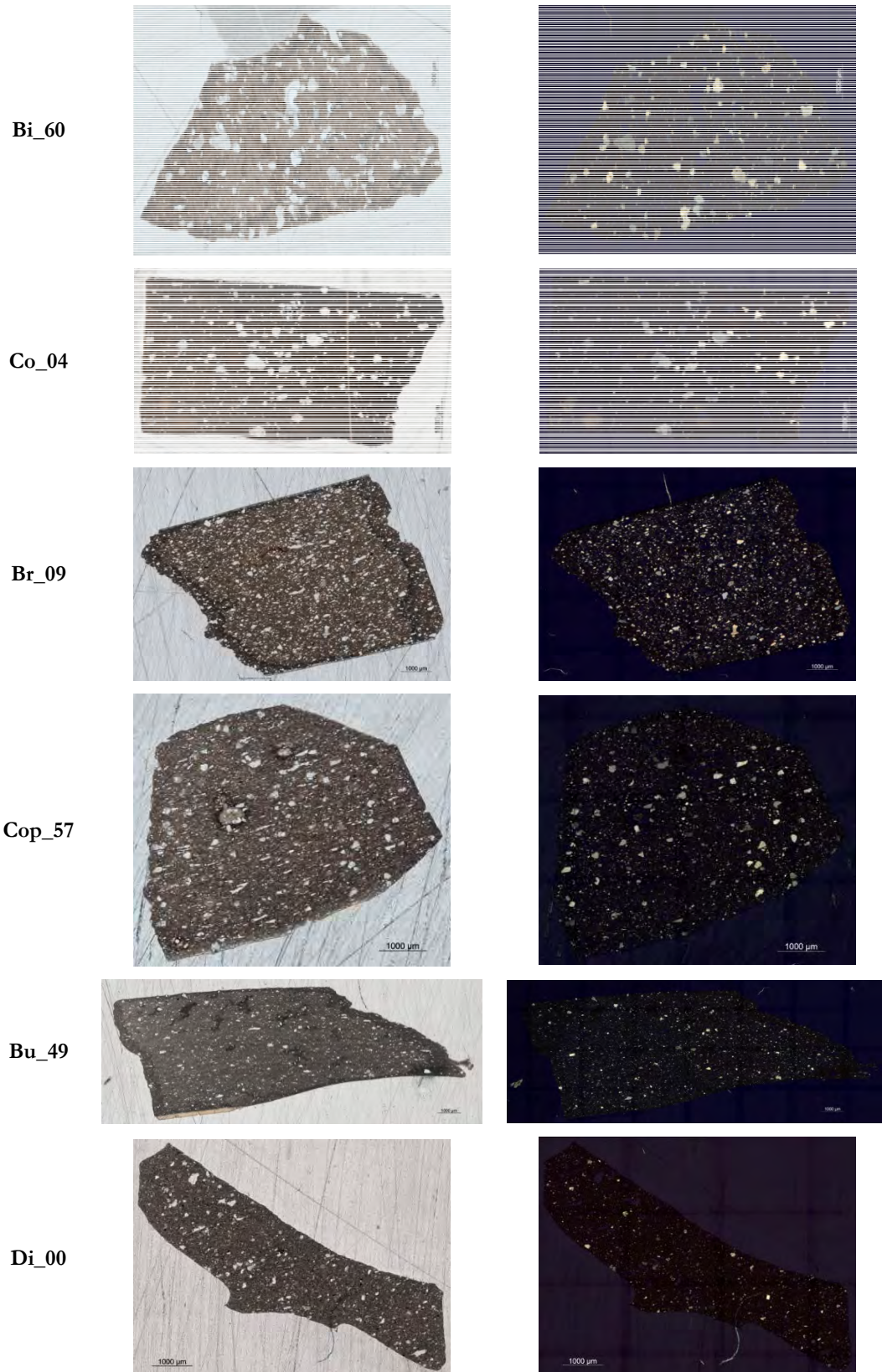
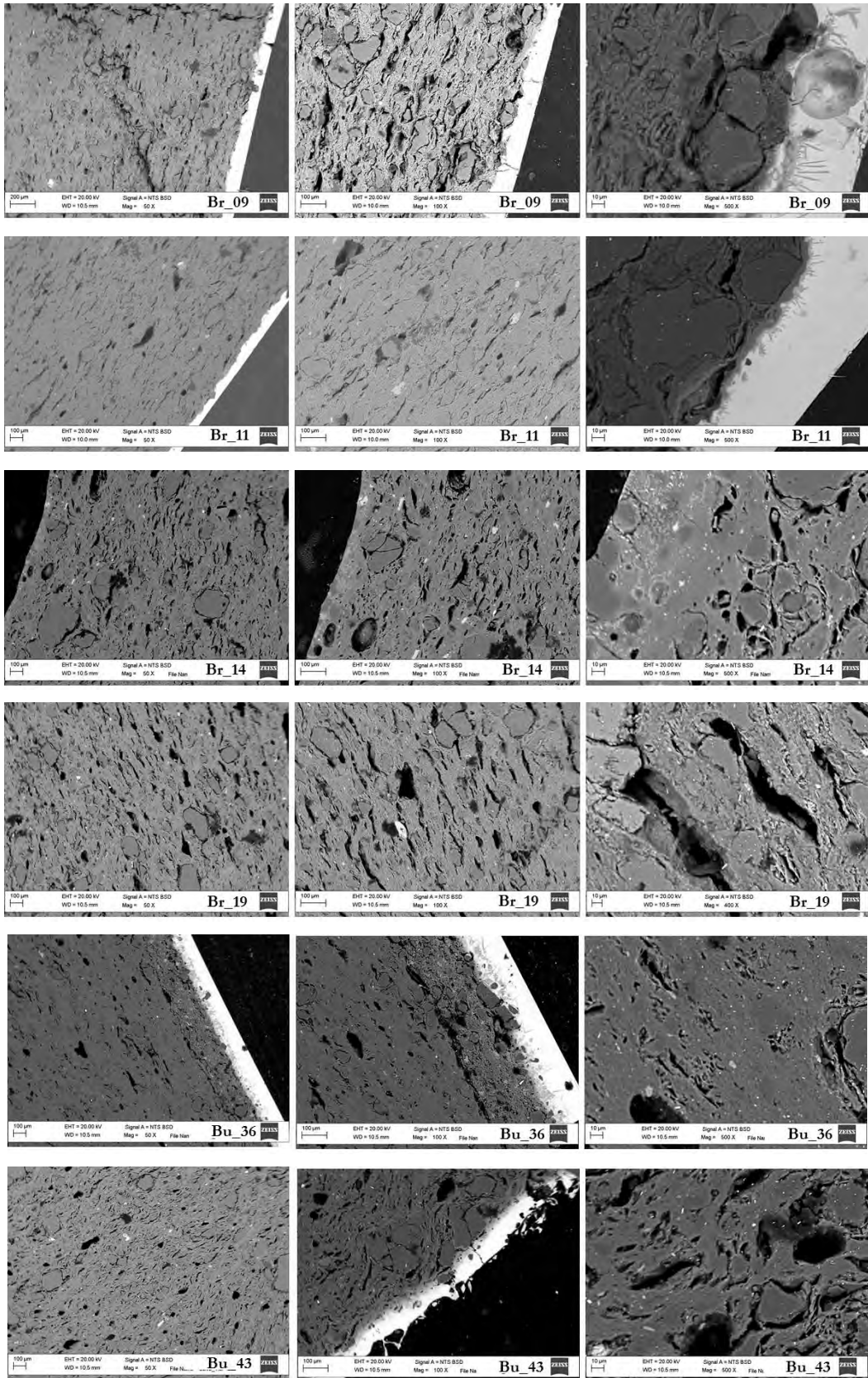


Figure.75. Representative thin section photomicrographs of German ceramic sherds observed by optical microscope with parallel and cross light, on the left and right respectively. Bi_60 and Co_04 are representative of the first group; Br_09 and Cop_57 for the second and Bu_49 and Di_00 for the third.

Microstructure, morphology, chemical and mineralogical composition, information connected to the technological production and firing process, were studied using SEM-EDX analysis [61]. German potsherds were selected taking in to account the proposed groups of the estimated firing temperature, with particular regard to those which present glaze layer. SEM microphotographs of the ceramic bodies and glazes (when present) are shown in **Fig.76**.

As can be seen, the bulk morphology of the analysed samples is quite different. Brandis samples show distinctive volumetric grains with irregular shape into the matrix, which appears not molten and characterized by sliver layers and plates. Therefore, this pottery production might have been fired at relatively low temperature. Furthermore, the surfaces present directional elongated-shape porosity, probably due to the forming technique adopted. Cop_51 sherd is similar to those from Brandis, characterized by distinctive irregular grains and in the microphotograph at 500x it is clear that the matrix is composed of single grains not completely fused with an inhomogeneous shape and dimension. Cop_52 and Cop_57 show different and arbitrary porosity, however the grains present are not of regular shape and not completely fused in the clay matrix, suggesting not very high firing temperature [60], [83]. Interesting are the results showed by sample from Duingen, Dui_80. From a morphological point of view, it seems to be composed of fine grain particles, almost of homogenous distribution and with a random and low porosity. These features may suggest high firing temperature, but the presence of calcite detected by FT-IR results suggested firing temperature at around 750°-850°C. Probably, the fine grain particles can be molten easier and/or the micro grains cannot be well distinguished in the microstructure. Bürgel samples and Pe_00 seem to be similar to Cop_52 and Cop_57 but the borders of the grains are less pronounced suggesting probably higher firing temperature.



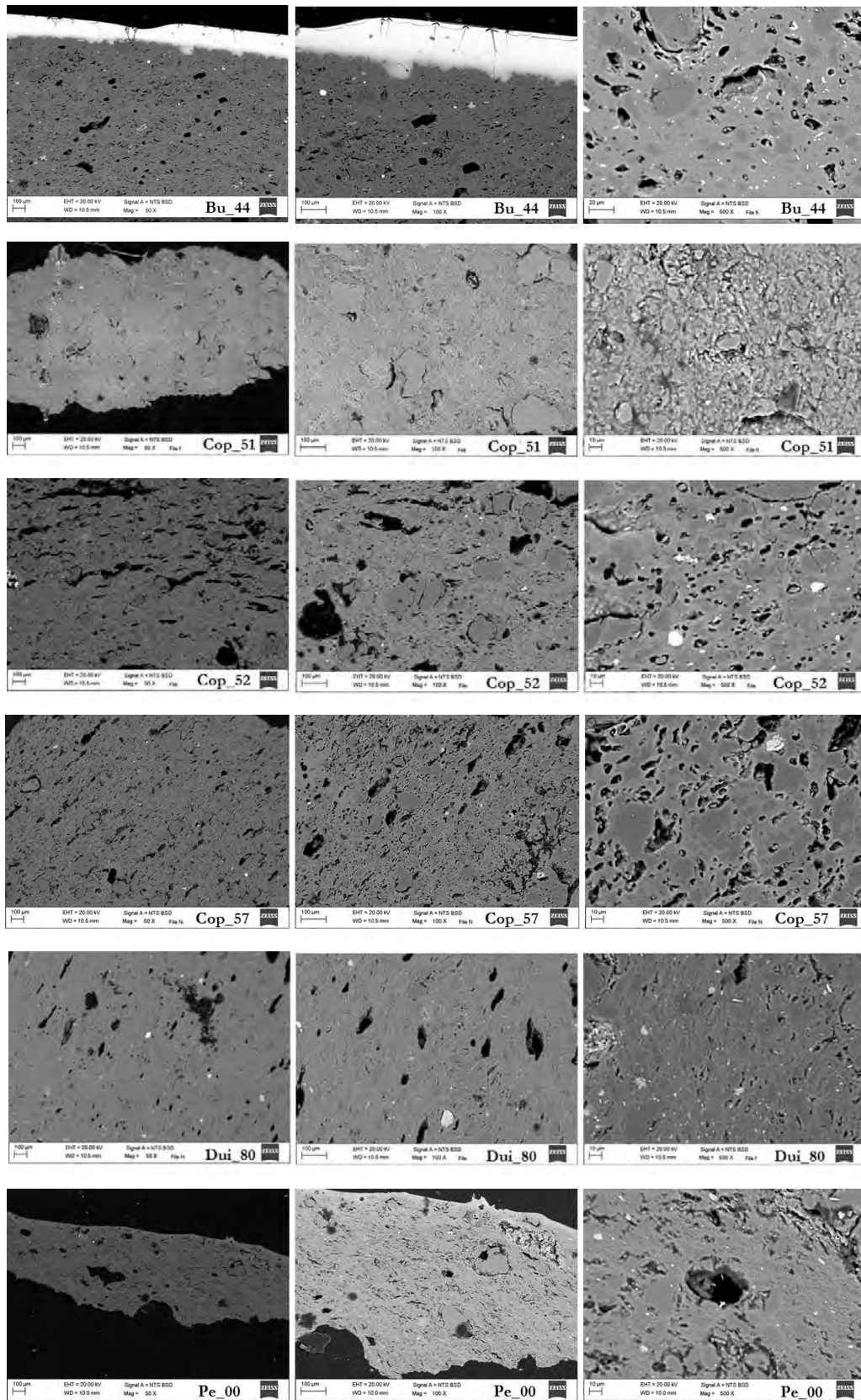


Figure.76. Scanning electron microphotographs obtained at magnification of 50x, 100x and 500x (from the left to the right) of significant ceramic samples from Brandis, Bürgel, Coppengrave, Duingen and Peine (from the top to the bottom).

Morphological and chemical analyses by means of SEM-EDX on the glazes present in samples Br_09, Br_11, Bu_36, Bu_43, Bu_44 are given in **Fig.77-79**. All the analysed glazes are lead-based glaze; gas bubbles and needle/rod-shaped crystals were detected in some of these samples. Br_09 green glaze, of around 70 μm thickness, is characterized by the presence of CuO, responsible of the green colouration, and high content of SiO₂, PbO and Al₂O₃. The needle/rod-shaped crystals detected in this sample are crystallites composed by potassium lead aluminium silicate ((Pb,K)AlSi₃O₈). They are newly formed lead potassium feldspars developed into the interaction layer between body and glaze forming an interface as a consequence of the diffusion process and migration of elements during firing [87]. Lead oxide reacts with quartz forming lead silicate melt at around 700°C and afterward begins the incorporation of atoms from the glaze into the clay body and vice versa [139], [141]. As reported by Molera et.al. [139], the diffusion process stops when a chemical gradient acting as a driving force no longer exists. The thickness of this crystal layer may increase with increasing firing temperature and the quantity and size of crystallites are related to the time and temperature parameters of firing process including the cooling rate, as well as original composition of glaze and body. Furthermore, due to the many factors involved in this process, the thickness of the interface may provide uncertain evaluation regarding the coating applied on unfired or biscuit fired bodies [140].

The K-Pb feldspars were detected in both Brandis and Bürgel samples, except in Bu_44 blue glaze. Crystallite interface in Brandis samples is thin (5-15 μm) and the needle-shape K-Pb feldspars are thin and of small dimensions (**Fig.80 (a)**). Bu_36 and Bu_43 instead present thicker interface (>50 μm) and crystallites more developed (**Fig.80 (b)**). Bu_44 glaze layer does not exhibit this kind of interface ascribable to the salt-glaze production technique which used common salt to produce glaze and PbO as flux confirmed also by the lower amount of PbO detected by EDX.

Experiments with lead-glaze applied on kaolinite-rich clay body fired at different firing temperatures and cooling rates were performed by Molera et.al. [139] and comparing the obtained results with data reported in literature, it might be possible to assume that the analysed samples were fired at temperatures which did not exceeds 850°C and 950°C for Brandis and Bürgel samples respectively, and with a slow cooling rate [139]. LIBS chemical profiles across the glaze layers showed as a result a quite uniform distribution of the elements into the glaze from Bürgel and a slight increase of Pb content for glaze from Brandis suggesting different firing conditions.

Br_11 sample is characterized by a lead-based glaze (70 μm thickness), very thin interface composed of K-Pb feldspars (5-7 μm) and yellow colouration ascribable to iron oxide detected in the glaze composition. Iron oxides can give different colourations in depending on the oxidizing

state of the element. Yellow colour is given by Fe^{3+} ions of ferric oxide (Fe_2O_3) formed in oxidizing atmosphere [150]. Bu_36 cross-section SEM image (at the top of **Fig.78**) shows a silica-rich layer probably due to an engobe as an interlayer between the body and lead-based glaze. The thickness of the glaze is around 148 μm . Furthermore, SEM-EDX spectra of the blue glaze exhibit SiO_2 , Al_2O_3 , PbO , K_2O and CaO . In this sample, the crystallites present in the interface glaze/clay body are composed by sodium lead aluminium silicates (Na-Pb feldspars), instead potassium as in Brandis samples. Moreover, SEM-EDX results show higher content of CoO and ZnO laying down into the layer closer to the engobe. CoO is responsible for the intense blue colouration, while ZnO may be added to produce opacity. The latter one is a network modifier and it works as opacifier when low calcium content is present, as in this case [54]. These SEM-EDX results are completely in agreement with those obtained by means spectroscopic techniques discussed in the previous paragraphs.

The sample Bu_43, shown at the top of the **Fig.79**, presents an irregular and coarse silica and lead-rich layer with a changeable thickness between 60-150 μm . In fact, from a macroscopic point of view, the potsherd is characterized by a black-dark greyish colour and rough surface. The dark colouration may be due to the combination of iron and manganese fired in reducing atmosphere [150]. Bu_44 exhibits a body-glaze interface not very sharp suggesting one-step firing technology and a glaze thickness of around 170 μm . As already described in details in UV-Vis results paragraph, this sample may be the typical Bürgel stoneware with cobalt-blue salt-glaze (*Smaltebenwurf*). SEM-EDX observations and elemental maps, shown at the bottom of the **Fig.79**, confirmed this glaze production technique suggesting the use of common salt (NaCl), in fact Na_2O and Cl are clearly detected. Furthermore, PbO detected by means of EDX ($\sim 20\%$) was used as flux agent in glaze procedure in order to decrease melting temperature.

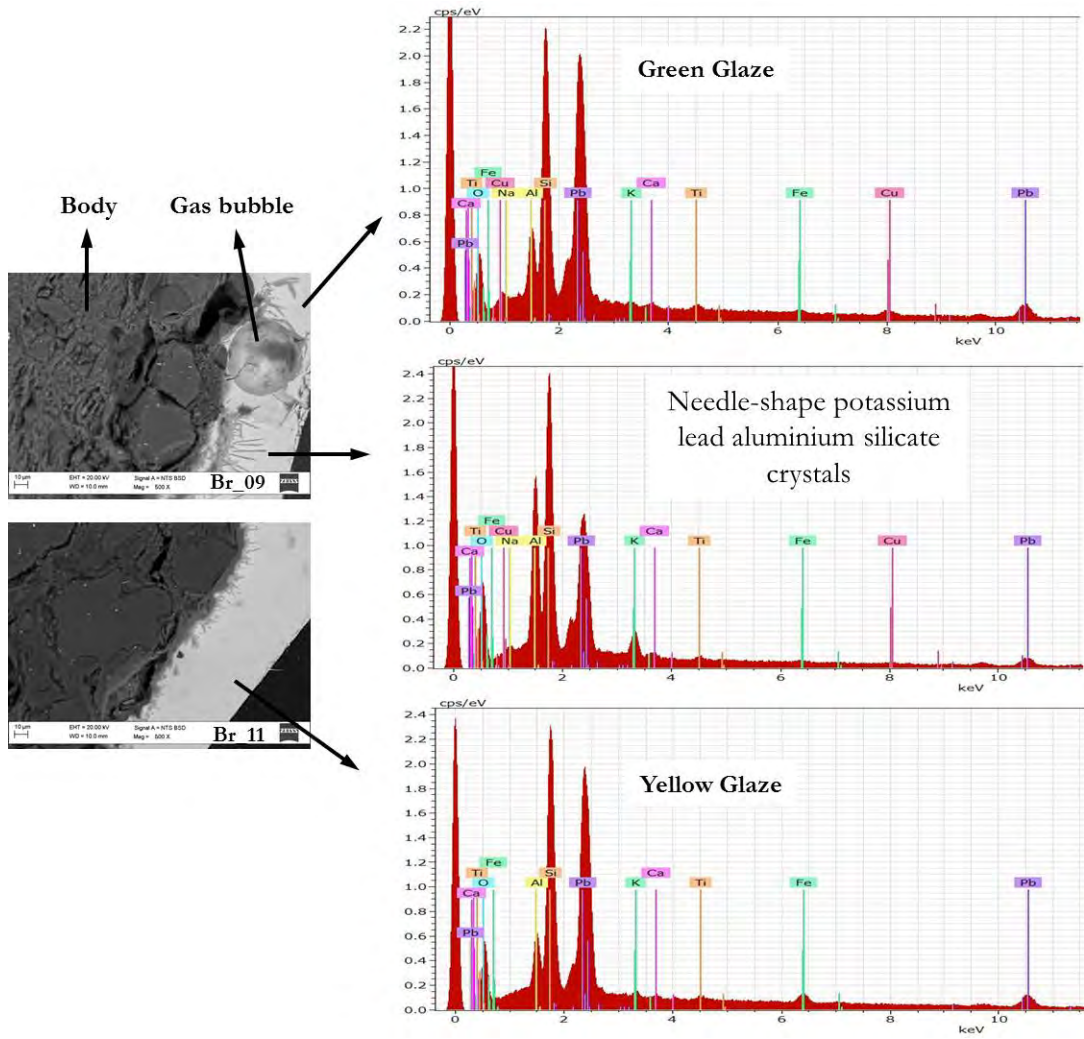


Figure.77. Cross-sectional SEM images at magnitude of 500x of the glaze-body interaction layer of Br_09 and Br_11 samples and relative EDX spectra of the glaze layers.

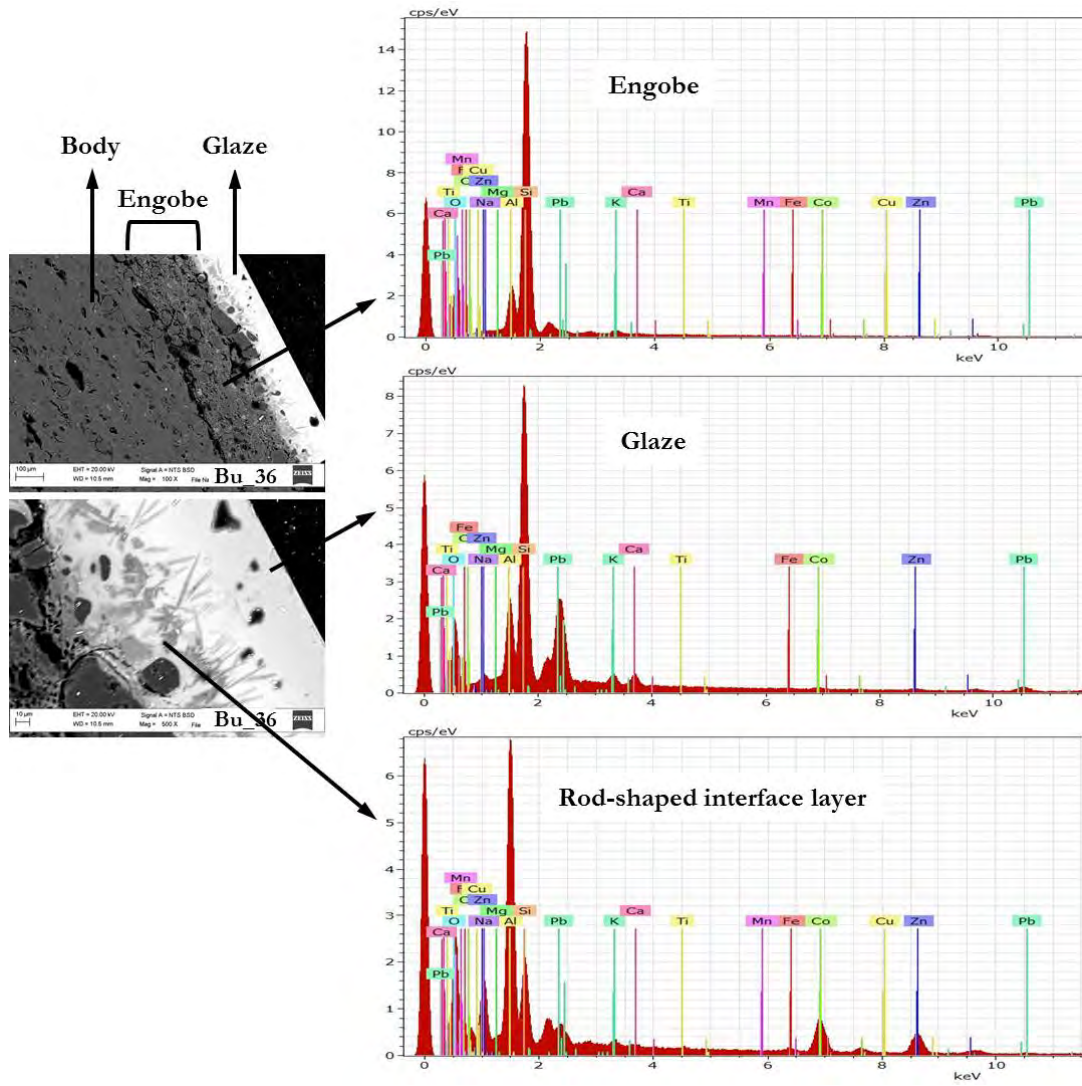


Figure.78. Cross-sectional SEM images of the glaze-body interaction layer of the sample Bu_36 at 100x and 500x and relative EDX spectra of the engobe and glaze.

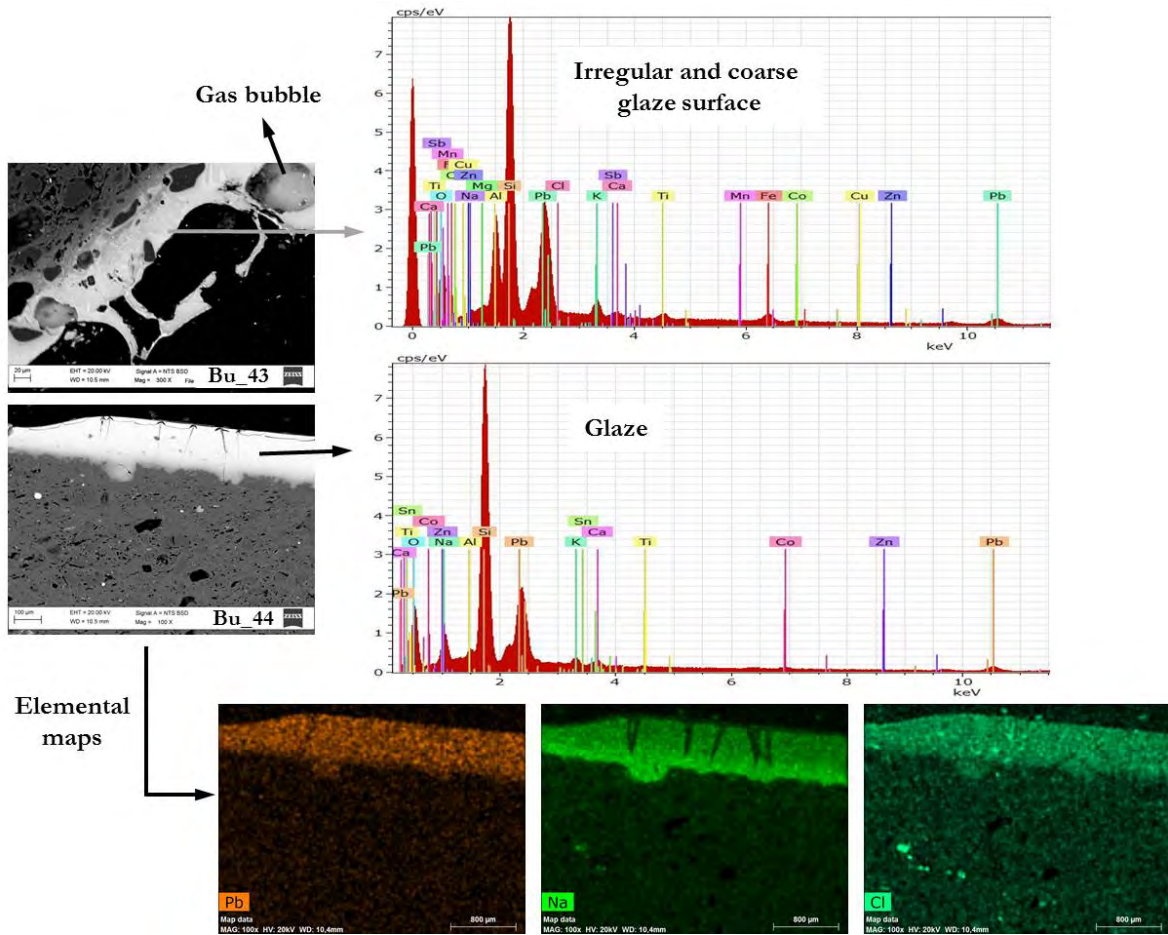


Figure.79. Cross-sectional SEM images of the interface glaze-body layer of Bu_43 and Bu_44 samples at 300x and 100x of magnitude respectively, and relative EDX spectra of the glazes. At the bottom, elemental maps of Pb, Na and Cl elements of the sample Bu_44 is given.

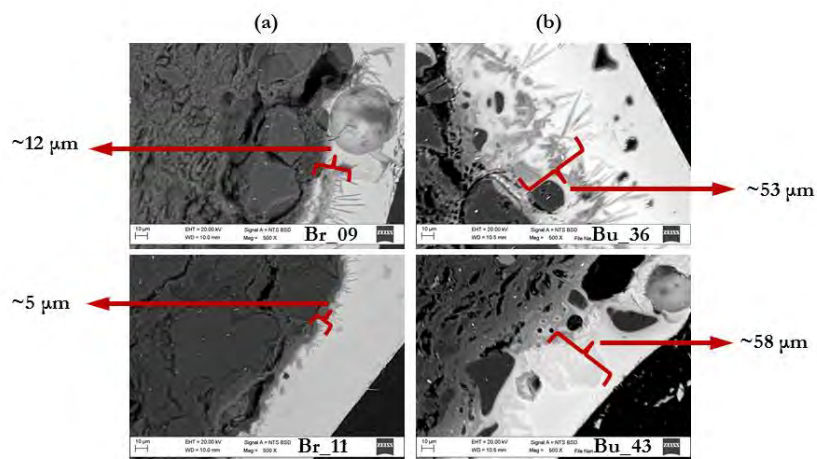


Figure.80. Glaze/clay bulk interface composed of newly formed crystallite in Brandis (a) and Bürgel (b) samples which exhibit different thickness as reported beside the SEM microphotos

Elemental maps of the ceramic bodies were acquired for chemical elements of interest, such as: Al, Ca, Fe, K, Mg, Mn, Na, O, P, Si and Ti, and the images were analysed as multispectral images, able to help in mineralogical identification by their chemical composition.

In **Fig.81** is shown some examples of the most significant elemental maps obtained, and the semi-quantitative data provided by means of EDX analysis are presented in **Tab.23**. Through these analyses was possible to detected and recognized inclusions present in the clay matrix. Quartz grains, as suggested by petrographic measurements on thin sections, represent the main kind of inclusion and are present with different distribution size into all the analysed samples. Rutile and/or anatase, as well as alkali feldspat and iron oxides are also detected but with less spread.

In order to extract quantitative data related to quartz inclusions and trying to perform a discrimination of the ceramic bodies in base on the inclusions detected, imaging data elaboration through ImageJ software was carried out considering the SiO₂ elemental maps, which identify quartz inclusions present in the ceramic matrix. Area, average size, perimeter and Feret diameter were calculated and reported in **Tab.22**. Feret diameter was selected as parameter for the particle size distribution, and in order to compare the results of all the samples, distribution curves were calculated and curve parameters compared (**Fig.82-83**) using OriginPro9 software.

Table.22. Quartz particle analysis calculated by ImageJ software from SEM-EDX SiO₂ elemental maps of the potsherds. Perimeter, Feret diameter and area values are given as mean values.

Sample code	Count	Total Area [mm ²]	Avarage size [µm]	Perim. [mm]	Feret* [µm]	Area [mm ²]
Br_09	286	1,64	5,73	0,25	89,53	18,35
Br_11	347	1,44	4,14	0,21	76,11	16,09
Br_14	875	1,73	1,98	0,14	49,73	19,42
Br_19	322	1,39	4,33	0,20	75,44	15,32
Bu_36	978	1,43	1,46	0,11	41,79	15,69
Bu_43	818	1,72	2,10	0,15	55,65	18,90
Bu_44	965	1,74	1,80	0,14	53,03	19,12
Cop_51	604	1,46	2,42	0,12	45,26	16,11
Cop_52	1082	3,94	3,64	0,25	66,28	43,42
Dui_80	2091	2,99	1,43	0,18	54,29	32,52

*Feret diameter has defined by ImageJ User Guide as the longest distance between any two points along the selection boundary, also known as maximum caliper.

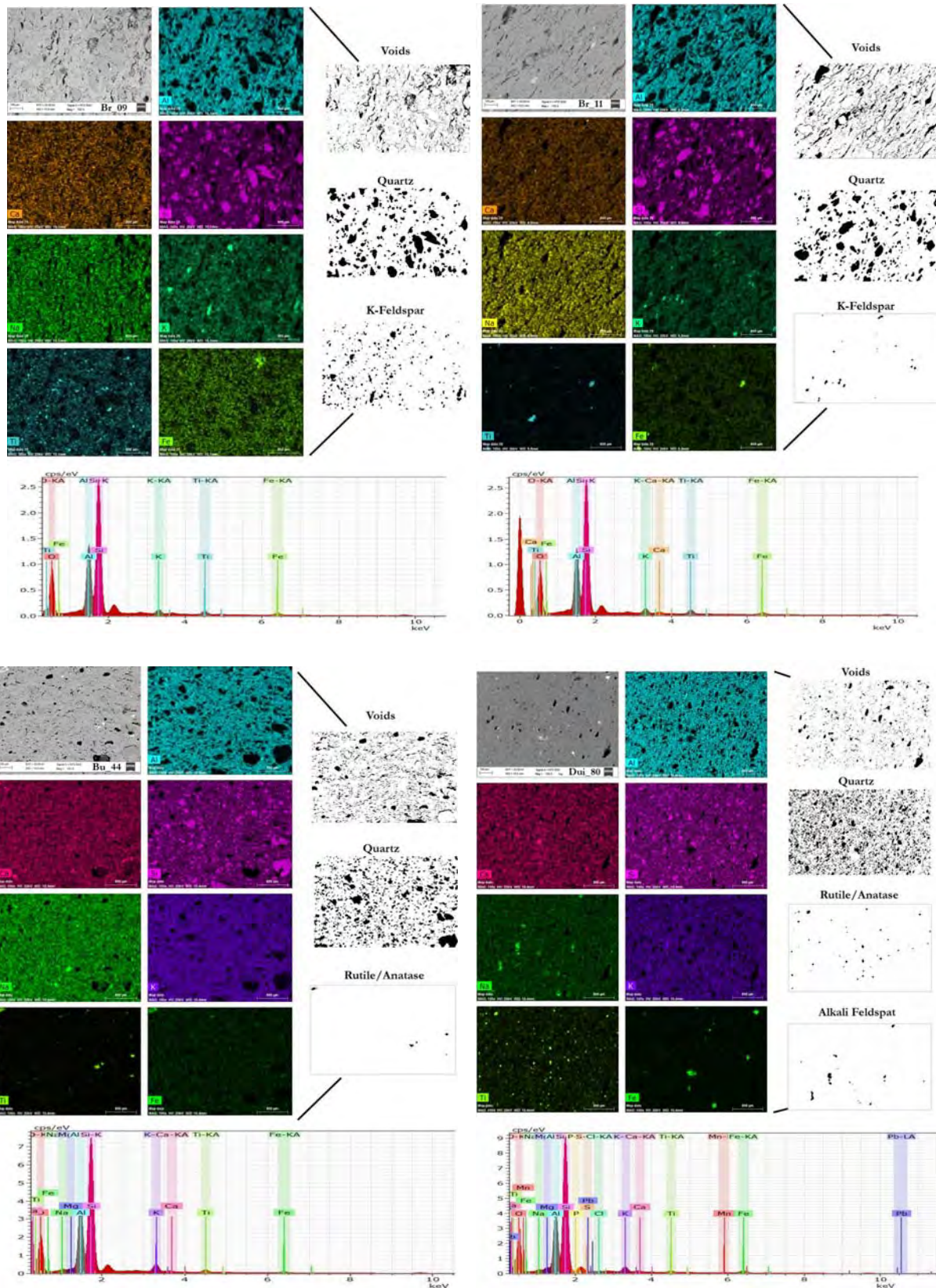


Fig.81. Examples of image segmentations, elemental maps and their SEM-EDX spectra of Br_09, Br_11, Bu_44 and Dui_80 potsherds.

4. Results and Discussion

Table.23. SEM-EDX semi-quantitative analyses (%) of bulks and glazes of the ceramic sherds.

Sample code		Na ₂ O	MgO	Al ₂ O ₃	SiO ₂	P ₂ O ₅	SO ₃	Cl	K ₂ O	CaO	TiO ₂	MnO	Fe ₂ O ₃	CoO	CuO	ZnO	SnO ₂	PbO
Br_09	bulk	0,39	0,70	27,47	63,30	0,56	1,50	0,07	0,42	0,53	2,11	n.d.	2,18	n.d.	n.d.	n.d.	0,06	0,02
	glaze_1	0,07	n.d.	4,22	24,09	n.d.	n.d.	n.d.	n.d.	0,76	2,38	0,42	1,50	n.d.	2,85	0,55	0,20	63,23
Br_11	bulk	0,24	0,65	38,41	45,63	1,35	0,65	n.d.	2,26	0,93	2,04	0,22	6,88	0,13	0,23	0,23	0,17	0,46
	glaze	0,01	n.d.	6,42	35,05	n.d.	n.d.	0,04	0,35	0,61	0,66	0,50	2,94	0,93	0,41	0,51	n.d.	52,49
Br_14	bulk	n.d.	0,30	36,68	49,56	0,57	0,38	n.d.	4,48	1,20	1,09	1,28	2,49	1,13	n.d.	0,09	0,74	n.d.
Br_19	bulk	0,16	1,08	40,49	46,59	1,21	0,46	0,05	1,80	1,34	1,65	0,85	3,10	n.d.	0,10	0,17	0,69	0,17
Bu_36	bulk	n.d.	0,09	29,33	63,27	0,13	0,22	n.d.	2,48	0,39	2,14	0,10	0,57	0,27	0,10	0,23	n.d.	0,67
	glaze_1	0,83	0,19	15,56	43,04	0,86	n.d.	n.d.	1,87	2,37	2,13	0,49	0,94	0,88	0,16	1,44	n.d.	29,24
Bu_43	bulk	0,24	0,22	41,54	47,92	0,50	0,52	n.d.	4,21	0,54	0,86	0,14	1,77	0,41	0,13	0,10	0,43	0,47
	glaze	n.d.	0,48	15,59	48,58	0,62	n.d.	n.d.	2,49	2,13	1,30	0,67	0,96	0,71	0,02	n.d.	n.d.	26,46
Bu_44	bulk	0,16	0,30	35,14	53,08	0,26	0,93	0,01	4,12	0,50	3,02	0,27	1,82	n.d.	n.d.	0,19	0,20	n.d.
	glaze	11,17	0,80	1,12	59,93	1,31	n.d.	n.d.	1,43	1,82	0,61	0,23	0,43	0,60	0,01	0,03	n.d.	20,51
Cop_51	bulk	0,14	0,40	34,79	52,35	3,29	3,06	n.d.	1,18	0,30	0,95	0,51	1,58	nd	0,17	0,01	n.d.	n.d.
Cop_52	bulk	0,27	0,71	20,68	68,74	0,73	1,05	n.d.	3,46	0,30	1,41	0,49	1,24	0,59	0,08	0,19	n.d.	0,05
Cop_57	bulk	0,09	1,25	8,92	73,93	3,32	6,32	0,10	1,21	0,38	1,62	0,44	1,66	0,09	0,36	0,30	n.d.	n.d.
Pe_00	bulk	0,59	1,28	36,57	54,94	0,91	0,49	0,04	1,26	0,35	0,92	0,19	2,42	0,08	0,05	0,12	0,03	n.d.

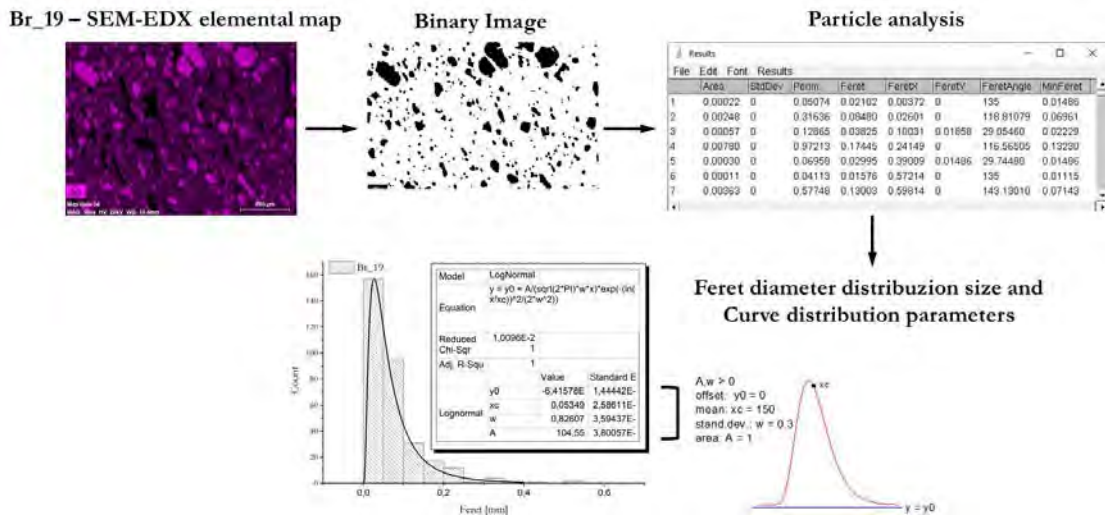


Figure.82. Imaging elaboration data carried out using ImageJ and OriginPro9 software in order to quantify and compare quartz grain size distribution of the ceramic samples.

Imaging data elaboration allowed to quantify quartz inclusions and discriminate the different fabrics. Brandis samples (Br_09, Br_11 and Br_19) show quartz particles with the greater size, while the thin particle size is observed in Dui_80 and Burgel samples. Differences in particle size or angularity of quartz may provide insights able to help in distinguish quartz deliberately added by the potter and naturally present in clay materials [55]. Therefore, the obtained results may suggest also different production techniques in terms of raw material selection. In general, as the quartz particles were detected in all the analysed samples, the firing temperature did not exceed 1000°C [83].

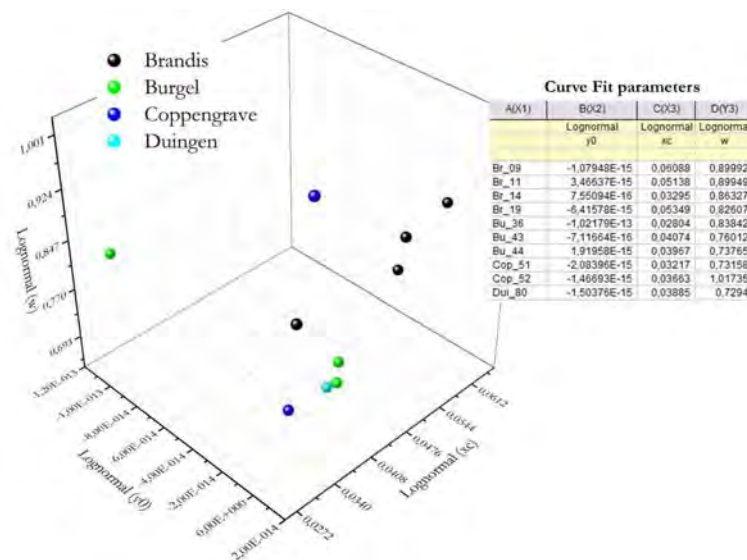


Figure.83. 3D plot obtained by curve fit parameters extracted from grain size distribution of quartz particles.

4.3.7. Porosimetry analyses (MIP) Results and Discussion

Porosity is a relevant microstructural feature of the ceramic material. It is related to several properties such mechanical resistance (strength, hardness), electrical and thermal conductivity, permeability, adsorption, etc. [69]. Various authors correlate the porosity of archaeological and historical potteries with firing temperatures, and more in general, with the manufacturing processes [29], [30], [69], [72]. However, is necessary to consider that there is not a direct correlation between porosity and firing temperature [151]. As G. Velraj reports, porosity can be considered the *prime factor* to differentiate clay bodies after firing, and high firing temperature leads to low porosity, especially if the bodies are glazed [30].

In this paragraph, porosimetry studies my means Mercury Intrusion Porosimetry (MIP) were carried out on selected German sherds. The aim was to obtain microstructural information of the ceramic bodies correlating these information with the technological production.

MIP is a destructive technique, therefore, significant samples were selected and analysed. The selection was made taking into account the representativeness of the samples and the chemical and mineralogical information collected by other techniques.

Cumulative volume, total porosity and pore size distribution were calculated and evaluated for Brandis, Burgel, Coppengrave and Duigen samples, as it is shown in the followed table (**Tab.24**). Total porosity of all the analysed potsherds ranges from around 2 to 27% (**Fig.84 (a)**) and the average pore radius is between 0,04 and 0,3 μm . Comparing these data with those reported in literature, the porosity of these samples seems to be not very high [69], [151]. In general, in these sherds the open porosity values are quite heterogeneous, suggesting that the porosity is not affected by the different pottery typology. Total porosity versus average pore radius in **Fig.84 (b)**. shows similar microstructural features for Brandis samples, which appear to be a homogeneous group. Most of the samples, show a unimodal distribution of pore sizes, while in some cases it can be noticed a second group of pores, which can be identify by a bimodal pore size distribution curve (**Fig.85-86**).

Table.24. Porosity data obtained by MIP measurements of the analysed German sherds. The average of three measurements with their standard deviation is reported.

Sample code	Total cumulative volume [cm ³ /g]	Average pore radius [μm]	Total porosity [%]	Bulk density [g/cm ³]	Apparent density [g/cm ³]
Bu_43	0,09±0,00	0,21±0,01	11,50±1,00	1,31±0,15	1,48±0,18
Bu_44	0,03±0,01	0,06±0,00	6,59±3,07	1,83±0,38	1,97±0,47
Br_09	0,17±0,01	0,05±0,00	18,20±2,03	1,05±0,21	1,29±0,33
Br_11	0,17±0,01	0,08±0,00	21,09±1,13	1,28±0,15	1,62±0,25
Br_14	0,07±0,01	0,19±0,02	12,37±5,87	1,67±0,51	1,92±0,71
Br_19	0,15±0,00	0,07±0,01	20,86±1,51	1,38±0,23	1,74±0,35
Cop_51	0,15±0,00	0,08±0,01	27,22±3,75	1,85±0,43	2,54±0,47
Cop_52	0,06±0,01	0,06±0,03	9,53±7,44	1,58±0,32	1,76±0,50
Cop_57	0,05±0,00	0,08±0,00	8,27±3,20	1,51±0,53	1,66±0,63
Dui_78	0,07±0,01	0,06±0,00	9,31±2,71	1,27±0,55	1,40±0,71
Dui_80	0,03±0,01	0,04±0,00	2,51±1,13	0,97±0,05	0,99±0,07
Dui_88	0,09±0,00	0,29±0,01	14,99±4,21	1,63±0,45	1,93±0,63

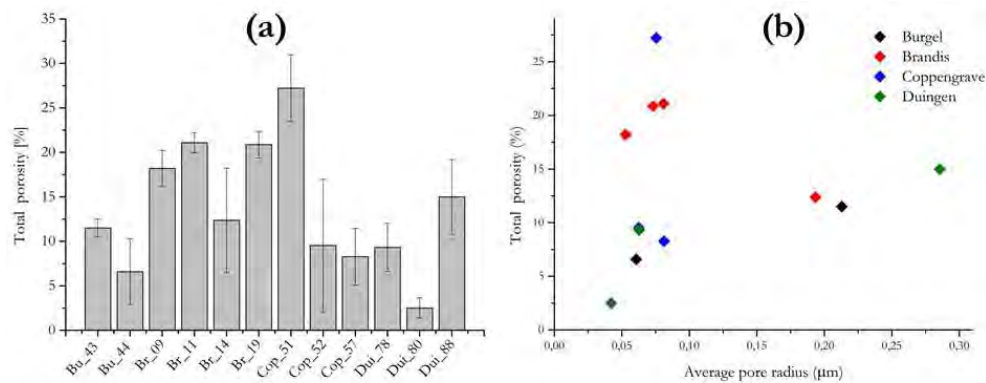


Figure.84. (a) Histogram representing the total porosity (%) and (b) total porosity vs. average pore radius (μm) diagram of all the analysed German sherds.

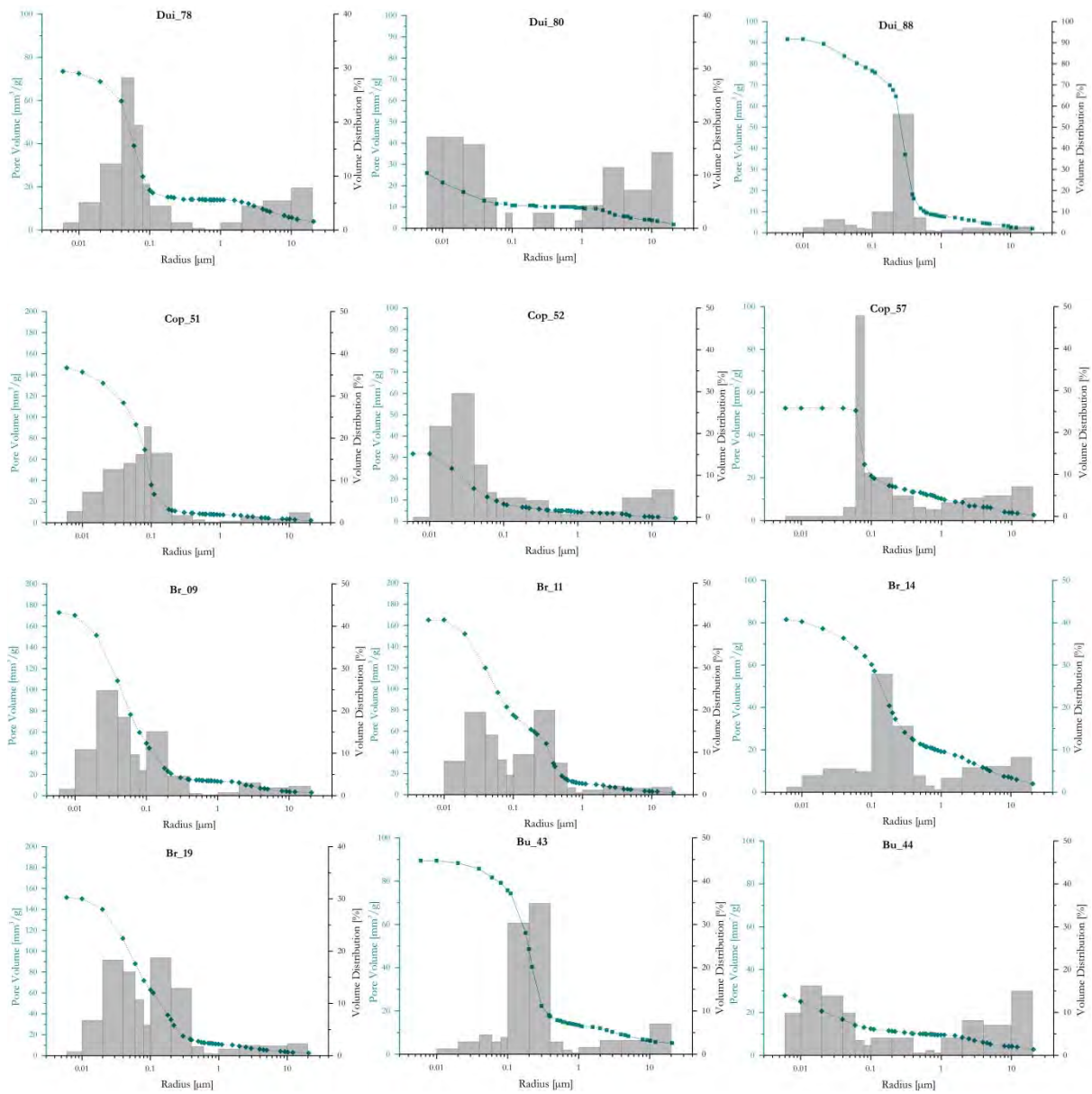


Figure.85. Cumulative pore volume and volume distribution versus pore radius of the analysed ceramic sherds. (When possible, it was used the same scale for each plot to better compare the diagrams). The diagrams are given as the most significant distributions among three measurements of each samples.

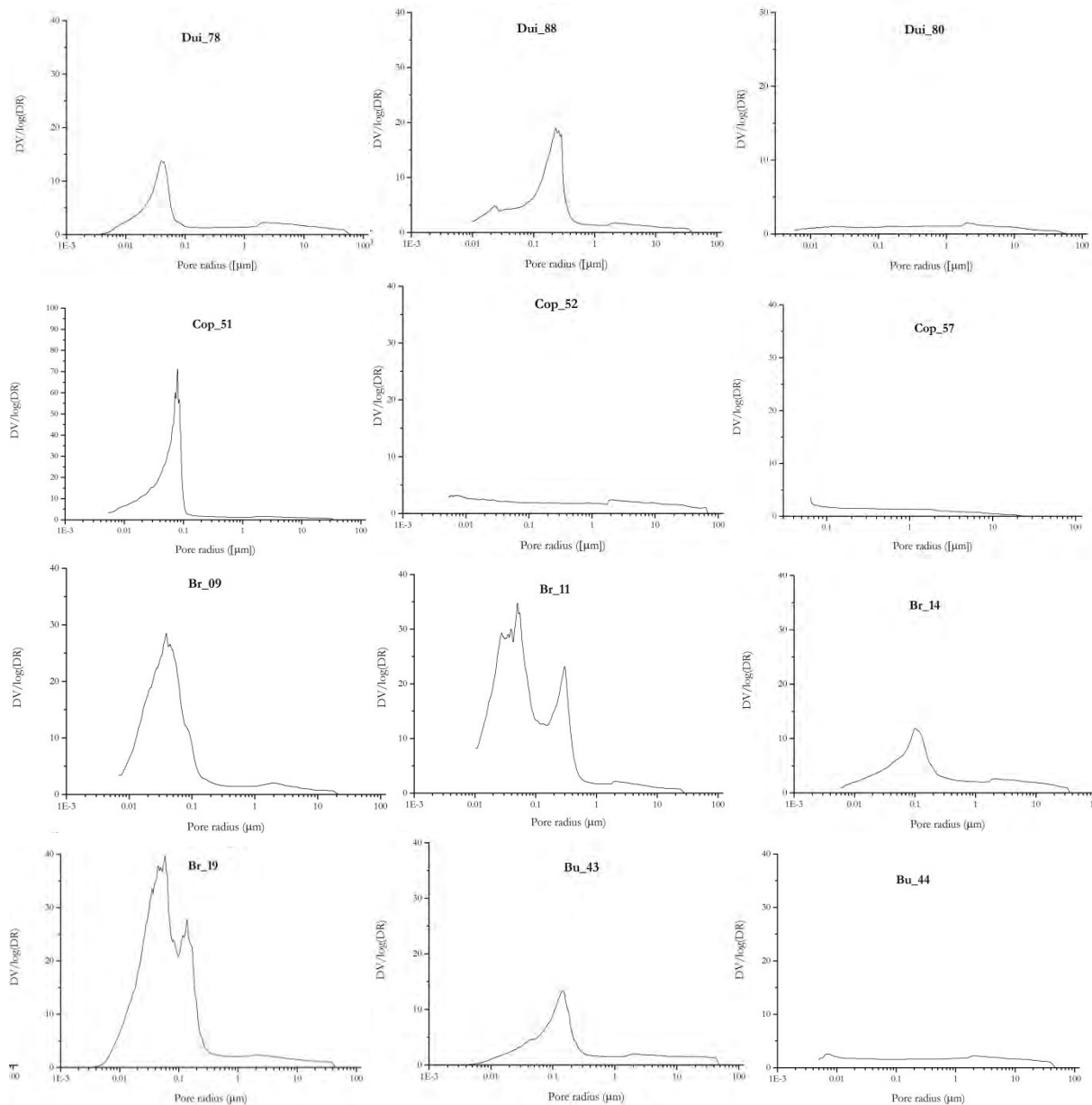


Figure.86. Pore size distribution curves. (When possible, it was used the same scale for each plot to better compare the curves).

Unimodal and polymodal curves may provide insights on the ceramic texture [69], [72]. Bimodal and polymodal curves are observed in Brandis samples suggesting coarse texture; while, unimodal curves may indicate fine and/or homogeneous texture, shown in **Fig.86**.

Porosimetry results of Dui_80 sample are in agreement with those obtained by SEM observations: the sherd seems to be composed by fine grain particles which may produce a ceramic with low porosity even if the estimated firing temperature on the basis of chemical analyses does not exceed 850°C. Ceramic sherds from Coppengrave (Cop_51, Cop_52 and Cop_57) exhibit very different pore distribution curves as well as total open porosity calculated by MIP. Cop_51 has greater open porosity than Cop_52 and Cop_57 potteries, that appear to be

similar, as the SEM observations showed. Furthermore, although the chemical and mineralogical results affirmed similar composition for these ceramics from Coppengrave, differences in morphology and microstructure suggest a different production techniques probably referred to the raw material manufacturing processes. Raw ceramic materials made in laboratory and their results and discussion showed how the differences in terms of grain size of the raw materials used can affect the microstructure although the composition and firing temperature are similar. Brandis sherds show a high open porosity in comparison with the other sherds, and in relation to their estimated firing temperature of about 750-850°C, porosimetry results allowed to confirm the low firing temperature together with their morphological features previously discussed. Bu_43 and Bu_44 also showed a similar chemical composition but different morphology and MIP results allowed to quantify the diversity of these samples. Bu_44 sherd exhibits a low total open porosity of around 6% and Bu_43 around 11%. The former is the salt-glaze pottery that, as expected, diverges from those ceramic sherds coming from the same site for both the glaze and body production technique adopted assuming different workshops.

It is interesting to notice as both chemical and microstructural investigations play fundamental roles in ceramic life cycle assessment.

4.3.8. Brief Conclusions on the Archaeometric study on German ceramic sherds

The multi-analytical approach adopted in the archaeometric study of historical German sherds allowed to estimate firing conditions used and provide significant insights regarding the production techniques applied. By using complementary methods, the investigation strategy provided the ability to obtain information about composition, firing condition and production techniques used in ceramic materials. Chemical and mineralogical analyses carried out by means spectroscopic techniques such as FT-IR and μ -Raman techniques provided the composition of the ceramic sherds discriminating three groups on the bases of the estimated firing conditions and raw materials used. FT-IR results on coating layers did not provide information about pigments/colorants into the glaze, however, the used of complementary techniques, such μ -Raman spectroscopy, was useful to investigate both composition and production technique.

Of particular interest is the application of innovative techniques applied to study the glaze covering the historical potteries. Through non-destructive way LIF spectroscopy and UV-Vis spectrophotometry revealed which colouring agents were used in the glazes adding fundamental information able to reconstruct the production techniques used. The successful results obtained encourage their application in other archaeological and historical glaze ceramics. Furthermore, potentially LIF spectroscopy could be capable to analyse artefacts of large dimension such as

glass windows and mosaics with glass tessera, thanks to its characteristics such as portability and the possibility to collect hyperspectral fluorescence images by the scanning setup. UV-Vis spectrophotometry have been recently used for ancient glass characterization, and its results being used in glaze study may open wider applications for pottery archaeometric investigations. Moreover, LIBS techniques used for chemical profiles across the glaze layer, applied exploiting its ability to perform stratigraphic analysis in a micro-destructive way, allowed to correlate the element diffusion to the firing temperature and cooling rate. These results integrated the SEM-EDX observations which brought to light a particular interface (glaze/clay body) composed of K-Pb and Na-Pb feldspars, related to glaze production techniques.

Another point of interest is the combination of chemical-mineralogical studies with those about morphology and microstructure. It is a complementary approach able to underline that similar both chemical and mineralogical compositions and estimated firing temperatures may produce ceramic materials with different morphological and microstructural features probably connected to the manufacturing processes of the used raw materials.

Concluding, the archaeometric investigation on these German sherds, on which no other archaeological or historical sources are available, offered a new possibility to find out more about the applied technology and the distribution of the ceramic products enlarging the awareness of these unique manufactures outstanding in medieval Central Europe and comparable only to China production.

Preliminary results of this study were published in *Microchemical Journal* [86].

4.4. Bibliography

- [1] R. Palanivel and G. Velraj, "FTIR and FT-Raman spectroscopic studies of fired clay artifacts recently excavated in Tamilnadu, India," *Indian J. pure Appl. Phys.*, vol. 45, no. June, pp. 501–508, 2007.
- [2] J. Madejová and P. Komadel, "Baseline Studies of the Clay minerals Society Source Clays: Infrared Methods," *Clay clays Miner.*, vol. 49, no. 5, pp. 410–432, 2001.
- [3] P. Sathya and G. Velraj, "FTIR spectroscopic and X-ray diffraction analysis of archaeological grey potteries excavated in Alagankulam, Tamil nadu, India," *Sci. York*, vol. 2, no. 5, pp. 4–6, 2011.
- [4] R. Ravisankar, G. Raja Annamalai, a Naseerutheen, a Chandrasekaran, M. V. R. Prasad, K. K. Satpathy, and C. Maheswaran, "Analytical characterization of recently excavated megalithic sarcophagi potsherds in Veeranam village, Tiruvannamalai dist., Tamilnadu, India," *Spectrochim. Acta. A. Mol. Biomol. Spectrosc.*, vol. 115, pp. 845–53, Nov. 2013.
- [5] G. Raja Annamalai, R. Ravisankar, A. Naseerutheen, A. Chandrasekaran, and K. Rajan, "Application of various spectroscopic techniques to characterize the archaeological pottery excavated from Manaveli, Puducherry, India," *Opt. - Int. J. Light Electron Opt.*, vol. 125, no. 21, pp. 6375–6378, Nov. 2014.
- [6] N. V. Chukanov, *Infrared spectra of mineral species*, vol. 1. Dordrecht: Springer Netherlands, 2014.
- [7] S. Bahçeli, G. Güleç, H. Erdogan, and B. Sogüt, "Micro-Raman and FT-IR spectroscopic studies of ceramic shards excavated from ancient Stratonikeia city at Eskihisar village in West-South Turkey," *J. Mol. Struct.*, vol. 1106, pp. 316–321, 2016.
- [8] G. Barone, V. Crupi, F. Longo, D. Majolino, P. Mazzoleni, D. Tanasi, and V. Venuti, "FT-IR spectroscopic analysis to study the firing processes of prehistoric ceramics," *J. Mol. Struct.*, vol. 993, no. 1–3, pp. 147–150, May 2011.
- [9] S. Shoval, "Using FT-IR spectroscopy for study of calcareous ancient ceramics," *Opt. Mater. (Amst.)*, vol. 24, no. 1–2, pp. 117–122, Oct. 2003.
- [10] M. A. Legodi and D. de Waal, "Raman spectroscopic study of ancient South African domestic clay pottery," *Spectrochim. Acta. A. Mol. Biomol. Spectrosc.*, vol. 66, no. 1, pp. 135–42, Jan. 2007.
- [11] M. Bayazit, I. Isik, and A. Issi, "Investigating the firing technologies of Part-Roman potsherds excavated from Kuriki (Turkey) using thermal and vibrational spectroscopic techniques," *Vib. Spectrosc.*, vol. 78, pp. 1–11, 2015.
- [12] R. Ravisankar and G. Senthilkumar, "Mineral analysis of coastal sediment samples of Tuna, Gujarat, India," *Indian J. Sci. Technol.*, vol. 3, no. 7, pp. 774–780, 2010.
- [13] R. Ravisankar, S. Kiruba, P. Eswaran, G. Senthilkumar, and a. Chandrasekaran, "Mineralogical Characterization Studies of Ancient Potteries of Tamilnadu, India by FT-IR Spectroscopic Technique," *E-Journal Chem.*, vol. 7, no. s1, pp. S185–S190, 2010.
- [14] G. E. De Benedetto, R. Laviano, L. Sabbatini, and P. G. Zambonin, "Infrared spectroscopy in the mineralogical characterization of ancient pottery," *J. Cult. Herit.*, vol. 3, no. 3, pp. 177–186, Jul. 2002.
- [15] D. de Waal, "Raman investigation of ceramics from 16th and 17th century Portuguese shipwrecks," *J. Raman Spectrosc.*, vol. 35, no. 89, pp. 646–649, Aug. 2004.
- [16] R. L. Frost and L. Rintoul, "Lattice vibrations of montmorillonite: an FT Raman and X-ray diffraction study," *Appl. Clay Sci.*, vol. 11, no. 2–4, pp. 171–183, 1996.
- [17] S. Akyuz, T. Akyuz, S. Basaran, C. Bolcal, and A. Gulec, "Analysis of ancient potteries using FT-IR, micro-Raman and EDXRF spectrometry," *Vib. Spectrosc.*, vol. 48, no. 2, pp. 276–280, Nov. 2008.
- [18] G. Velraj, K. Prabakaran, A. Mohamed Musthafa, and R. Hemamalini, "FT-IR and Micro-Raman Spectroscopic Studies of Archaeological Potteries recently excavated in Tamilnadu, India," *Recent Res. Sci. Technol.*, vol. 2, no. 10, pp. 94–99, 2010.
- [19] L. Damjanović, V. Bikić, K. Šarić, S. Erić, and I. Holclajtner-Antunović, "Characterization of the Early Byzantine Pottery from Caričin Grad (South Serbia) in Terms of Composition and Firing Temperature," *J. Archaeol. Sci.*, vol. 46, pp. 156–172, Mar. 2014.
- [20] C. M. Stevenson and M. Gurnick, "Structural collapse in kaolinite, montmorillonite and illite clay and its role in the ceramic rehydroxylation dating of low-fired earthenware," *J. Archaeol. Sci.*, vol. 69, pp. 54–63, 2016.
- [21] A. İssi, A. Kara, and A. O. Alp, "An investigation of Hellenistic period pottery production technology from Harabebezikan/Turkey," *Ceram. Int.*, vol. 37, no. 7, pp. 2575–2582, Sep. 2011.

- [22] R. García Giménez, R. Vigil de la Villa, M. D. Petit Domínguez, and M. I. Rucandio, “Application of chemical, physical and chemometric analytical techniques to the study of ancient ceramic oil lamps,” *Talanta*, vol. 68, no. 4, pp. 1236–46, Feb. 2006.
- [23] M. Trindade, M. Dias, J. Coroado, and F. Rocha, “Mineralogical transformations of calcareous rich clays with firing: A comparative study between calcite and dolomite rich clays from Algarve, Portugal,” *Appl. Clay Sci.*, vol. 42, no. 3–4, pp. 345–355, Jan. 2009.
- [24] A. Pecci, F. Grassi, L. Salvini, and G. Giorgi, “Cooking activities in a building yard during the Middle Age. Organic residues in potsherds recovered from the Carmine Convent in Siena,” in *34th Symposium on Archaeometry. 3-4 May 2004, Zaragoza, Spain*, 2006, no. May 2004, pp. 583–588.
- [25] M. J. Trindade, M. I. Dias, J. Coroado, and F. Rocha, “Mineralogical transformations of calcareous rich clays with firing: A comparative study between calcite and dolomite rich clays from Algarve, Portugal,” *Appl. Clay Sci.*, vol. 42, no. 3–4, pp. 345–355, 2009.
- [26] B. Fabbri, S. Gualtieri, and S. Shoal, “The presence of calcite in archeological ceramics,” *J. Eur. Ceram. Soc.*, vol. 34, no. 7, pp. 1899–1911, Jul. 2014.
- [27] “RRUFF Project website, an integrated database of Raman spectra, X-ray diffraction and chemistry data for minerals.” [Online]. Available: <http://rruff.info/>.
- [28] K. G. Harry and A. Johnson, “A non-destructive technique for measuring ceramic porosity using liquid nitrogen,” *J. Archaeol. Sci.*, vol. 31, no. 11, pp. 1567–1575, 2004.
- [29] G. Cultrone, E. Sebastián, K. Elert, M. J. de la Torre, O. Cazalla, and C. Rodríguez-Navarro, “Influence of mineralogy and firing temperature on the porosity of bricks,” *J. Eur. Ceram. Soc.*, vol. 24, no. 3, pp. 547–564, Mar. 2004.
- [30] G. Velraj, K. Janaki, a. M. Musthafa, and R. Palanivel, “Spectroscopic and porosimetry studies to estimate the firing temperature of some archaeological pottery shreds from India,” *Appl. Clay Sci.*, vol. 43, no. 3–4, pp. 303–307, Mar. 2009.
- [31] D. Donchev, “Controlling porosity and pore size distribution in green ceramics bodies via Freeze-casting method,” 2005.
- [32] J. García-Ten, M. J. Orts, a. Saburit, and G. Silva, “Thermal conductivity of traditional ceramics,” *Ceram. Int.*, vol. 36, no. 7, pp. 2017–2024, Sep. 2010.
- [33] U. Werr, “Porous Ceramics Manufacture – Properties – Applications,” *Ceram. Appl.*, vol. 2, no. 2, pp. 49–51, 2014.
- [34] G. Raja Annamalai, R. Ravisankar, a Rajalakshmi, a Chandrasekaran, and K. Rajan, “Spectroscopic characterization of recently excavated archaeological potsherds from Tamilnadu, India with multi-analytical approach,” *Spectrochim. Acta. A. Mol. Biomol. Spectrosc.*, vol. 133, pp. 112–8, Dec. 2014.
- [35] C. M. Stevenson and M. Gurnick, “Structural collapse in kaolinite, montmorillonite and illite clay and its role in the ceramic rehydroxylation dating of low-fired earthenware,” *J. Archaeol. Sci.*, vol. 69, pp. 54–63, May 2016.
- [36] B. J. Saikia and G. Parthasarathy, “Fourier Transform Infrared Spectroscopic Characterization of Kaolinite from Assam and Meghalaya, Northeastern India,” *J. Mod. Phys.*, vol. 1, no. 4, pp. 206–210, 2010.
- [37] G. Kurap, S. Akyuz, T. Akyuz, S. Basaran, and B. Cakan, “FT-IR spectroscopic study of terra-cotta sarcophagi recently excavated in Ainos (Enez) Turkey,” *J. Mol. Struct.*, vol. 976, no. 1–3, pp. 161–167, 2010.
- [38] M. Secco, L. Maritan, C. Mazzoli, G. I. Lampronti, F. Zorzi, L. Nodari, U. Russo, and S. P. Mattioli, “Alteration Processes of Pottery in Lagoon-Like Environments,” *Archaeometry*, vol. 53, no. 4, pp. 809–829, Aug. 2011.
- [39] N. Cuomo di Caprio, *Ceramica in Archeologia 2. Antiche tecniche di lavorazione e moderni metodi di indagine*, L’Erma di. 2007.
- [40] S. Shoal, M. Gaft, P. Beck, and Y. Kirsh, “Thermal behaviour of limestone and monocrystalline calcite tempers during firing and their use in ancient vessels,” *J. Therm. Anal.*, vol. 40, no. 1, pp. 263–273, 1993.
- [41] P. Colomban, “Raman spectrometry, a unique tool to analyze and classify ancient ceramics and glasses,” *Appl. Phys. A Mater. Sci. Process.*, vol. 79, no. 2, pp. 167–170, 2004.
- [42] P. Colomban and A. Tournié, “On-site Raman identification and dating of ancient/modern stained glasses at the Sainte-Chapelle, Paris,” *J. Cult. Herit.*, vol. 8, no. 3, pp. 242–256, Jul. 2007.

- [43] P. Colomban and V. Milande, "On-site Raman analysis of the earliest known Meissen porcelain and stoneware," *J. Raman Spectrosc.*, vol. 37, no. 5, pp. 606–613, May 2006.
- [44] P. Colomban, A. Tournie, and L. Bellot-Gurlet, "Raman identification of glassy silicates used in ceramics, glass and jewellery: a tentative differentiation guide," *J. Raman Spectrosc.*, vol. 37, no. 8, pp. 841–852, Aug. 2006.
- [45] P. Colomban and C. Truong, "Non-destructive Raman study of the glazing technique in lustre potteries and faience(9–14th centuries): silver ions, nanoclusters, microstructure and processing," *J. Raman Spectrosc.*, vol. 35, no. 3, pp. 195–207, 2004.
- [46] P. Colomban, "Polymerization degree and Raman identification of ancient glasses used for jewelry, ceramic enamels and mosaics," *J. Non. Cryst. Solids*, vol. 323, no. 1–3, pp. 180–187, 2003.
- [47] C. Ricci, C. Miliani, F. Rosi, B. G. Brunetti, and A. Sgamellotti, "Structural characterization of the glassy phase in majolica glazes by Raman spectroscopy: A comparison between Renaissance samples and replica processed at different temperatures," *J. Non. Cryst. Solids*, vol. 353, no. 11–12, pp. 1054–1059, May 2007.
- [48] L. F. Vieira Ferreira, D. P. Ferreira, D. S. Conceição, L. F. Santos, M. F. C. Pereira, T. M. Casimiro, and I. Ferreira Machado, "Portuguese tin-glazed earthenware from the 17th century. Part 2: A spectroscopic characterization of pigments, glazes and pastes of the three main production centers," *Spectrochim. Acta - Part A Mol. Biomol. Spectrosc.*, vol. 149, pp. 285–294, 2015.
- [49] L. F. Vieira Ferreira, I. Ferreira Machado, a. M. Ferraria, T. M. Casimiro, and P. Colomban, "Portuguese tin-glazed earthenware from the 16th century: A spectroscopic characterization of pigments, glazes and pastes," *Appl. Surf. Sci.*, vol. 285, pp. 144–152, Nov. 2013.
- [50] J. J. Freeman, A. Wang, K. E. Kuebler, B. L. Jolliff, and L. A. Haskin, "Characterization of Natural Feldspars By Raman Spectroscopy for Future Planetary Exploration," *Can. Mineral.*, vol. 46, no. 6, pp. 1477–1500, 2008.
- [51] A. Iordanidis and J. Garcia-Guinea, "A preliminary investigation of black, brown and red coloured potsherds from ancient upper macedonia, Northern Greece," *Mediterr. Archaeol. Archaeom.*, vol. 11, no. 1, pp. 85–97, 2011.
- [52] Š. Pešková, V. Machovič, and P. Procházka, "Raman spectroscopy structural study of fired concrete," *Ceram. - Silikaty*, vol. 55, no. 4, pp. 410–417, 2011.
- [53] R. L. Frost, "The Structure of the Kaolinite Minerals — A FT-Raman Study," *Clay Miner.*, vol. 32, no. 1, pp. 65–77, 1997.
- [54] C. B. Carter and M. G. Norton, *Ceramic Materials. Science and Engineering*, Second edi. Springer New York Heidelberg Dordrecht London, 2013.
- [55] M. S. Smith, "Chapter 6. Petrography," in *Woodland Pottery Sourcing in the Carolina Sandhills. Research Laboratories of Archaeology, University of North Carolina at Chapel Hill, Research Report No. 29*, J. M. Herbert and T. E. McReynolds, Eds. 2008, pp. 73–107.
- [56] G. Dal Sasso, L. Maritan, S. Salvatori, C. Mazzoli, and G. Artioli, "Discriminating pottery production by image analysis: a case study of Mesolithic and Neolithic pottery from Al Khiday (Khartoum, Sudan)," *J. Archaeol. Sci.*, vol. 46, pp. 125–143, Jun. 2014.
- [57] C. M. Belfiore, P. M. Day, a. Hein, V. Kilikoglou, V. La Rosa, P. Mazzoleni, and a. Pezzino, "Petrographic and chemical characterization of pottery production of the Late Minoan I kiln at Haghia Triada, Crete," *Archaeometry*, vol. 49, no. 4, pp. 621–653, 2007.
- [58] A. Mangone, L. C. Giannossa, G. Colafemmina, R. Laviano, and A. Traini, "Use of various spectroscopy techniques to investigate raw materials and define processes in the overpainting of Apulian red figured pottery (4th century BC) from southern Italy," *Microchem. J.*, vol. 92, no. 1, pp. 97–102, May 2009.
- [59] B. Velde and I. C. Druc, *Archaeological Ceramic Materials: Origin and Utilization*. Springer Science & Business Media, 2012.
- [60] A. Krapukaityt, I. Pakutinskien, S. Tautkus, and A. Kareiva, "SEM AND EDX CHARACTERIZATION OF ANCIENT POTTERY," *Lith. J. Phys.*, vol. 46, no. 3, pp. 383–388, 2006.
- [61] a. M. Musthafa, K. Janaki, and G. Velraj, "Microscopy, porosimetry and chemical analysis to estimate the firing temperature of some archaeological pottery shreds from India," *Microchem. J.*, vol. 95, no. 2, pp. 311–314, Jul. 2010.
- [62] A. Issi, A. Kara, F. Okyar, T. Sivas, and H. Sivas, "Characterization of hellenistic period megarian bowls from dorylaion," *Ceram. - Silikaty*, vol. 55, no. 2, pp. 140–146, 2011.

- [63] C. Capelli and R. Cabella, "Archaeometric analyses of Mediterranean glazed cooking wares," *ArcheoSciences*, vol. 34, pp. 45–57, 2010.
- [64] "Mindat.org." [Online]. Available: <http://www.mindat.org/loc-31685.html>.
- [65] M. Jordán, T. Sanfeliu, and C. D. la Fuente, "Firing transformations of Tertiary clays used in the manufacturing of ceramic tile bodies," *Appl. Clay Sci.*, pp. 87–95, 2001.
- [66] L. F. Vieira Ferreira, A. Gonzalez, M. F. C. Pereira, L. F. Santos, T. M. Casimiro, D. P. Ferreira, D. S. Conceição, and I. F. Machado, "Spectroscopy of 16th century Portuguese tin-glazed earthenware produced in the region of Lisbon," *Ceram. Int.*, vol. 41, no. 10, pp. 13433–13446, 2015.
- [67] M. Bayazit, I. Isik, S. Cerci, A. Issi, and E. Genc, "Ft-IR Spectroscopic Analysis of Potsherds Excavated From the First Settlement Layer of Kuriki Mound, Turkey," *Int. J. Mod. Phys. Conf. Ser.*, vol. 22, pp. 103–111, 2013.
- [68] J. Cui, N. Wood, D. Qin, L. Zhou, M. Ko, and X. Li, "Chemical analysis of white porcelains from the Ding Kiln site, Hebei Province, China," *J. Archaeol. Sci.*, vol. 39, no. 4, pp. 818–827, Apr. 2012.
- [69] C. Volzone and N. Zagorodny, "Mercury intrusion porosimetry (MIP) study of archaeological pottery from Hualfin Valley, Catamarca, Argentina," *Appl. Clay Sci.*, vol. 91–92, pp. 12–15, Apr. 2014.
- [70] S. Kramar and J. Lux, "Spectroscopic and porosimetric analyses of Roman pottery from an archaeological site near Mošnje, Slovenia," *Mater. Tehnol.*, vol. 49, no. 4, pp. 503–508, 2015.
- [71] R. Viola, a. Tucci, G. Timellini, and P. Fantazzini, "NMR techniques: A non-destructive analysis to follow microstructural changes induced in ceramics," *J. Eur. Ceram. Soc.*, vol. 26, no. 15, pp. 3343–3349, Jan. 2006.
- [72] G. Cultrone, E. Molina, and A. Arizzi, "The combined use of petrographic, chemical and physical techniques to define the technological features of Iberian ceramics from the Canto Tortoso area (Granada, Spain)," *Ceram. Int.*, vol. 40, no. 7, pp. 10803–10816, Aug. 2014.
- [73] R. Palanivel and U. Kumar, "Thermal and Spectroscopic analysis of ancient potteries," *Rom. J. Physiol.*, vol. 56, pp. 195–208, 2011.
- [74] V. C. Farmer and J. D. Russell, "Infrared Absorption Spectrometry in Clay Studies," *Clays Clay Miner.*, vol. 15, no. 1, pp. 121–142, 1967.
- [75] G. Cassani, S. Cipriano, P. Donat, R. Merlatti, D. Biasio, F. Cjastiei, V. Oderzo, M. Daszkiewicz, E. Bobryk, and V. Giulia, "Il Ruolo della Ceramica Grigia nella Romanizzazione dell'Italia Nord-Orientale: Produzione e Circolazione," 2002.
- [76] A. E. Lavat, M. C. Grasselli, and J. E. Tasca, "Phase changes of ceramic whiteware slip-casting bodies studied by XRD and FTIR," *Ceram. Int.*, vol. 33, no. 6, pp. 1111–1117, Aug. 2007.
- [77] D. R. M. Gaimster and R. J. C. Hildyard, *German Stoneware, 1200-1900: Archaeology and Cultural History: Containing a Guide to the Collections of the British Museum, Victoria & Albert Museum, and Museum of London*. British Museum Publ., 1997.
- [78] A. Moreras, "Analysis and Mapping of Potential Landslides in the Region of Hesse (Germany)," 2014.
- [79] M. M. Jordán, T. Sanfeliu, and C. de la Fuente, "Firing transformations of Tertiary clays used in the manufacturing of ceramic tile bodies," *Appl. Clay Sci.*, vol. 20, pp. 87–95, 2001.
- [80] G. Hansen, *Everyday Products in the Middle Ages: Crafts, Consumption and the individual in Northern Europe c. AD 800-1600*. Oxbow Books, 2015.
- [81] L. F. Vieira Ferreira, T. M. Casimiro, and P. Colombari, "Portuguese tin-glazed earthenware from the 17th century. Part 1: pigments and glazes characterization," *Spectrochim. Acta. A. Mol. Biomol. Spectrosc.*, vol. 104, pp. 437–444, Mar. 2013.
- [82] L. Kock and D. De Waal, "Raman studies of the underglaze blue pigment on ceramic artefacts of the Ming dynasty and of unknown origins," *J. Raman Spectrosc.*, vol. 38, no. August, pp. 1480–1487, 2007.
- [83] M. Özçatal, M. Yaygingöl, a. İssi, a. Kara, S. Turan, F. Okyar, Ş. Pfeiffer Taş, I. Nastova, O. Grupče, and B. Minčeva-Šukarova, "Characterization of lead glazed potteries from Smyrna (İzmir/Turkey) using multiple analytical techniques; Part II: Body," *Ceram. Int.*, vol. 40, no. 1, pp. 2153–2160, Jan. 2014.
- [84] K. H. Michaelian, "The Raman spectrum of kaolinite #9 at 21°C," *Can. J. Chem.*, vol. 64, no. 2, pp. 285–294, Feb. 1986.
- [85] S. Shoval, M. Boudeulle, and G. Panczer, "Identification of the thermal phases in firing of kaolinite to mullite by using micro-Raman spectroscopy and curve-fitting," *Opt. Mater. (Amst.)*, vol. 34, no. 2, pp. 404–

- 409, Dec. 2011.
- [86] G. Ricci, L. Caneve, D. Pedron, N. Holesch, and E. Zendri, “A multi-spectroscopic study for the characterization and definition of production techniques of German ceramic sherds ☆,” *Microchem. J.*, vol. 126, pp. 104–112, 2016.
- [87] M. Özçatal, M. Yaygingöl, a. İssi, a. Kara, S. Turan, F. Okyar, Ş. Pfeiffer Taş, I. Nastova, O. Grupče, and B. Minčeva-Šukarova, “Characterization of lead glazed potteries from Smyrna (Izmir/Turkey) using multiple analytical techniques; Part I: Glaze and engobe,” *Ceram. Int.*, vol. 40, no. 1, pp. 2143–2151, Jan. 2014.
- [88] L. Burgio and R. J. Clark, *Library of FT-Raman spectra of pigments, minerals, pigment media and varnishes, and supplement to existing library of Raman spectra of pigments with visible excitation.*, vol. 57, no. 7. 2001.
- [89] M. Burleson, *The Ceramic Glaze Handbook: Materials, Techniques, Formulas*. Lark Books, Crafts & Hobbies, 2003.
- [90] L. Boselli, S. Ciattini, M. Galeotti, M. R. Lanfranchi, C. Lofrumento, M. Picollo, and A. Zoppi, “An unusual white pigment in La Verna sanctuary frescoes: an analysis with micro-Raman, FTIR, XRD and UV-VIS-NIR FORS,” *e-Preservation Sci.*, vol. 6, pp. 38–42, 2009.
- [91] D. Anglos, M. Solomidou, I. Zergioti, V. Zafirooulos, T. G. Papazoglou, and C. Fotakis, “Laser-induced fluorescence in artwork diagnostics: An application in pigment analysis,” *Appl. Spectrosc.*, vol. 50, no. 10, pp. 1331–1334, 1996.
- [92] R. Fantoni, L. Caneve, F. Colao, L. Fiorani, A. Palucci, R. Dell’Erba, and V. Fassina, “Laser-induced fluorescence study of medieval frescoes by Giusto de’ Menabuoi,” *J. Cult. Herit.*, vol. 14, no. 3, pp. S59–S65, Jun. 2013.
- [93] D. Ehrh, “Photoluminescence in glasses and glass ceramics,” *IOP Conf. Ser. Mater. Sci. Eng.*, vol. 2, p. 12001, Jul. 2009.
- [94] R. Sahl, “Silicon Nanocluster in Silicon Dioxide: Cathodoluminescence, Energy Dispersive X-Ray Analysis,” *Cryst. Silicon - Prop. Uses*, pp. 135–172, 2011.
- [95] V. Lazic, F. Colao, R. Fantoni, A. Palucci, V. Spizzichino, I. Borgia, B. G. Brunetti, and A. Sgamellotti, “Characterisation of lustre and pigment composition in ancient pottery by laser induced fluorescence and breakdown spectroscopy,” *J. Cult. Herit.*, vol. 4, pp. 303–308, Jan. 2003.
- [96] A. Pelagotti, L. Pezzati, and N. Bevilacqua, “A study of UV fluorescence emission of painting materials,” *Art ’05–8th Int. ...*, 2005.
- [97] M. Castillejo, “Chapter 4.3. LaserInduced Fluorescence,” in *Handbook on the Use of Lasers in Conservation and Conservation Science*, Brussels: COST Action G7. Scott, A., 2008.
- [98] C. MacRae and N. Wilson, “Luminescence database I—minerals and materials,” *Microsc. Microanal.*, vol. 14, pp. 184–204, 2008.
- [99] M. R. Hall and P. H. Ribbe, “An Electron microprobe study of luminescence centers in cassiterite,” *Am. Mineral.*, vol. 56, pp. 31–45, 1971.
- [100] C. Farmer, A. Searl, and C. Halls, “Cathodoluminescence and growth of cassiterite in the composite lodes at South Crofty Mine, Cornwall, England,” *Mineral. Mag.*, vol. 55, no. September, 1991.
- [101] G. Rapp, *Archaeomineralogy*, vol. 8, no. Mitchell 1985. 2009.
- [102] P. Colomban, V. Milande, and L. Le Bihan, “On-site Raman analysis of Iznik pottery glazes and pigments,” *J. Raman Spectrosc.*, vol. 35, no. 7, pp. 527–535, 2004.
- [103] J. Götze, D. Habermann, U. Kempe, R. D. Neuser, and D. K. Richter, “Cathodoluminescence microscopy and spectroscopy of plagioclases from lunar soil,” *Am. Mineral.*, vol. 84, no. 7–8, pp. 1027–1032, 1999.
- [104] L. Caneve, F. Colao, C. Giancristofaro, F. Persia, G. Ricci, and A. Tati, “Laser Induced Fluorescence and ultrasound techniques to study thermal modification induced on white marbles .,” in *LACONA IX*, 2011.
- [105] A. Nevin, G. Spoto, and D. Anglos, “Laser spectroscopies for elemental and molecular analysis in art and archaeology,” *Appl. Phys. A*, vol. 106, no. 2, pp. 339–361, Dec. 2011.
- [106] B. J. Bozlee, A. K. Misra, S. K. Sharma, and M. Ingram, “Remote Raman and fluorescence studies of mineral samples,” *Spectrochim. Acta. A. Mol. Biomol. Spectrosc.*, vol. 61, no. 10, pp. 2342–8, Aug. 2005.
- [107] K. Polikreti and C. Christofides, “Laser induced micro-photoluminescence of marble and application to authenticity testing of ancient objects,” *Appl. Phys. A Mater. Sci. Process.*, vol. 90, no. 2, pp. 285–291, 2008.
- [108] D. Habermann, R. D. Neuser, and D. K. Richter, “Low limit of Mn²⁺-activated cathodoluminescence of

- calcite: state of the art,” *Sedimentary Geology*, vol. 116, no. 1–2, pp. 13–24, 1998.
- [109] M. Bacci, a. Casini, C. Cucci, M. Picollo, B. Radicati, and M. Vervat, “Non-invasive spectroscopic measurements on the Il ritratto della figliastra by Giovanni Fattori: Identification of pigments and colourimetric analysis,” *J. Cult. Herit.*, vol. 4, no. 4, pp. 329–336, 2003.
- [110] a. Ceglia, W. Meulebroeck, K. Baert, H. Wouters, K. Nys, H. Thienpont, and H. Terry, “Cobalt absorption bands for the differentiation of historical na and ca/k rich glass,” *Surf. Interface Anal.*, vol. 44, no. 2, pp. 219–226, 2012.
- [111] M. Bacci, D. Magrini, M. Picollo, and M. Vervat, “A study of the blue colors used by Telemaco Signorini (1835-1901),” *J. Cult. Herit.*, vol. 10, no. 2, pp. 275–280, 2009.
- [112] A. Ceglia, W. Meulebroeck, H. Wouters, K. Baert, K. Nys, H. Terry, and H. Thienpont, “Using optical spectroscopy to characterize the material of a 16th c. stained glass window,” in *Proc. SPIE 8422*, 2012, vol. 8422, p. 84220A.
- [113] M. Bacci and M. Picollo, “Non-Destructive Spectroscopic Detection of Cobalt (II) in Paintings and Glass,” *Stud. Conserv.*, vol. 41, no. 3, pp. 136–144, 1996.
- [114] I. Borgia, B. Brunetti, I. Mariani, A. Sgamellotti, F. Cariati, P. Fermo, M. Mellini, C. Viti, and G. Padeletti, “Heterogeneous distribution of metal nanocrystals in glazes of historical pottery,” *Appl. Surf. Sci.*, vol. 185, no. 3–4, pp. 206–216, 2002.
- [115] L. R. Green and F. Alan Hart, “Colour and chemical composition in ancient glass: An examination of some roman and wealden glass by means of ultraviolet-visible-infra-red spectrometry and electron microprobe analysis,” *J. Archaeol. Sci.*, vol. 14, no. 3, pp. 271–282, May 1987.
- [116] B. Adler, *Early Stoneware Steins from the Les Paul Collection: A Survey of All German Stoneware Centers from 1500 to 1850*. Beatrix Adler, 2005.
- [117] R. Dewar, *Stoneware*. University of Pennsylvania Press, 2002.
- [118] R. Hopper, *Making Marks: Discovering the Ceramic Surface*. Krause Publications Craft, 2004.
- [119] L. Boselli, S. Ciattini, M. Galeotti, M. R. Lanfranchi, C. Lofrumento, M. Picollo, and A. Zoppi, “An unusual white pigment in La Verna sanctuary frescoes: an analysis with micro-Raman, FTIR, XRD and UV-VIS-NIR FORS,” *e-Preservation Sci.*, vol. 6, pp. 38–42, 2009.
- [120] A. Bartecki, J. Burgess, and K. Kurzak, *Colour of Metal Compounds*. CRC Press, Science, 2000.
- [121] T. Cavaleri, A. Giovagnoli, and M. Nervo, “Pigments and Mixtures Identification by Visible Reflectance Spectroscopy,” *Procedia Chem.*, vol. 8, pp. 45–54, 2013.
- [122] M. Mohammadi, M. Nezamabadi, L. a. Taplin, and R. S. Berns, “Pigment Selection Using Kubelka – Munk Turbid Media Theory and Non-Negative Least Square Technique,” 2004.
- [123] A. Ceglia, W. Meulebroeck, P. Cosyns, K. Nys, H. Terry, and H. Thienpont, “Colour and Chemistry of the Glass Finds in the Roman Villa of Treignes, Belgium,” *Procedia Chem.*, vol. 8, pp. 55–64, 2013.
- [124] C. Papachristodoulou, A. Oikonomou, K. Ioannides, and K. Gravani, “A study of ancient pottery by means of X-ray fluorescence spectroscopy, multivariate statistics and mineralogical analysis,” *Anal. Chim. Acta*, vol. 573–574, pp. 347–53, Jul. 2006.
- [125] C. Papachristodoulou, K. Gravani, A. Oikonomou, and K. Ioannides, “On the provenance and manufacture of red-slipped fine ware from ancient Cassope (NW Greece): evidence by X-ray analytical methods,” *J. Archaeol. Sci.*, vol. 37, no. 9, pp. 2146–2154, Sep. 2010.
- [126] R. Scarpelli, R. J. H. Clark, and A. M. De Francesco, “Archaeometric study of black-coated pottery from Pompeii by different analytical techniques,” *Spectrochim. Acta. A. Mol. Biomol. Spectrosc.*, vol. 120, pp. 60–6, Feb. 2014.
- [127] H. Ida and J. Kawai, “Identification of glass and ceramics by X-ray fluorescence analysis with a pyroelectric X-ray generator,” *Anal. Sci.*, vol. 20, no. 8, pp. 1211–5, 2004.
- [128] a. Erdem, a. Çilingiroğlu, a. Giakoumaki, M. Castanys, E. Kartsonaki, C. Fotakis, and D. Anglos, “Characterization of Iron age pottery from eastern Turkey by laser- induced breakdown spectroscopy (LIBS),” *J. Archaeol. Sci.*, vol. 35, no. 9, pp. 2486–2494, Sep. 2008.
- [129] K. Melessanaki, M. Mateo, S. C. Ferrence, P. P. Betancourt, and D. Anglos, “The application of LIBS for the analysis of archaeological ceramic and metal artifacts,” *Appl. Surf. Sci.*, vol. 197–198, pp. 156–163, Sep. 2002.
- [130] F. Anabitarte, A. Cobo, and J. M. Lopez-Higuera, “Laser-Induced Breakdown Spectroscopy: Fundamentals,

- Applications, and Challenges,” *ISRN Spectrosc.*, vol. 2012, pp. 1–12, 2012.
- [131] L. Caneve, A. Diamanti, F. Grimaldi, G. Palleschi, V. Spizzichino, and F. Valentini, “Analysis of fresco by laser induced breakdown spectroscopy,” *Spectrochim. Acta Part B At. Spectrosc.*, vol. 65, no. 8, pp. 702–706, Aug. 2010.
- [132] K. Blagoev, M. Grozeva, G. Malcheva, and S. Neykova, “Investigation by laser induced breakdown spectroscopy, X-ray fluorescence and X-ray powder diffraction of the chemical composition of white clay ceramic tiles from Veliki Preslav,” *Spectrochim. Acta Part B At. Spectrosc.*, vol. 79–80, pp. 39–43, Jan. 2013.
- [133] L. Zamboni, “Fade to Grey 1 La ceramica grigia in area padana tra VI e I secolo a . C ., un aggiornamento,” vol. 15, pp. 74–110, 2013.
- [134] E. Murad, “Identification of minor amounts of anatase in kaolins by Raman spectroscopy,” *Am. Mineral.*, vol. 82, pp. 203–206, 1997.
- [135] M. Baxter, “Multivariate Analysis of Archaeometric Data An Introduction,” 2016.
- [136] V. Spizzichino and R. Fantoni, “Laser Induced Breakdown Spectroscopy in archeometry: A review of its application and future perspectives,” *Spectrochim. Acta - Part B At. Spectrosc.*, vol. 99, pp. 201–209, 2014.
- [137] “NIST Atomic Spectra Database Lines, <https://www.nist.gov/pml/atomic-spectra-database>.”
- [138] E. Rowe, *A Potter’s Geology*, Lulu Press. 2013.
- [139] J. Molera, T. Pradell, N. Salvado, and M. Vendrell-Saz, “Interactions between Clay Bodies and Lead Glazes,” *J. Am. Ceram. Soc.*, vol. 84, no. 5, pp. 1120–1128, 2001.
- [140] C. Fortina, I. M. Turbanti, and F. Grassi, “Glazed ceramic manufacturing in Southern Tuscany (Italy): Evidence of technological continuity throughout the medieval period (10th-14th centuries),” *Archaeometry*, vol. 50, no. 1, pp. 30–47, 2008.
- [141] M. s. Walton and M. S. Tite, “Production technology of Roman lead-glazed pottery and its continuance into late Antiquity,” *Archaeometry*, vol. 52, no. 5, pp. 733–759, 2010.
- [142] F. Colao, R. Fantoni, V. Lazic, and V. Spizzichino, “Laser-induced breakdown spectroscopy for semi-quantitative and quantitative analyses of artworks—application on multi-layered ceramics and copper based alloys,” ... *Part B At. Spectrosc.*, vol. 57, pp. 1219–1234, 2002.
- [143] K. Kuhn, J. a. Meima, D. Rammlmair, and C. Ohlendorf, “Chemical mapping of mine waste drill cores with laser-induced breakdown spectroscopy (LIBS) and energy dispersive X-ray fluorescence (EDXRF) for mineral resource exploration,” *J. Geochemical Explor.*, vol. 161, pp. 72–84, 2015.
- [144] A. Ciucci, M. Corsi, V. Palleschi, S. Rastelli, A. Salvetti, and E. Tognoni, “New Procedure for Quantitative Elemental Analysis by Laser-Induced Plasma Spectroscopy,” *Appl. Spectrosc.*, vol. 53, no. 8, pp. 960–964, 1999.
- [145] C. M. Belfiore, M. Di Bella, M. Triscari, and M. Viccaro, “Production technology and provenance study of archaeological ceramics from relevant sites in the Alcantara River Valley (North-eastern Sicily, Italy),” *Mater. Charact.*, vol. 61, no. 4, pp. 440–451, Apr. 2010.
- [146] I. Whitbread, “Pottery analysis: Petrology and thin-section analysis,” in *Encyclopedia of Archaeology*, 2010, pp. 1879–1881.
- [147] G. Artioli, “Scientific methods and cultural heritage,” p. 520, 2010.
- [148] W. R. Dickinson, “Temper sands in prehistoric Oceanian pottery: Geotectonics, sedimentology, petrography, provenance,” *Spec. Pap. Geol. Soc. Am.*, vol. 406, pp. 1–160, 2006.
- [149] P. T. Nicholson and I. Shaw, *Ancient Egyptian Materials and Technology*. Cambridge University Press, 2000.
- [150] S. Davison, *Conservation and Restoration of Glass*. 2003.
- [151] G. Cultrone, E. Molina, C. Grifa, and E. Sebastián, “Iberian Ceramic Production From Basti (Baza, Spain): First Geochemical, Mineralogical and Textural Characterization,” *Archaeometry*, vol. 53, no. 2, pp. 340–363, Apr. 2011.
- [152] F. Du and B. Su, “Further study of sources of the imported cobalt-blue pigment used on Jingdezhen porcelain from late 13 to early 15 centuries,” *Sci. China Ser. E Technol. Sci.*, vol. 51, no. 3, pp. 249–259, Mar. 2008.
- [153] J. Wisniak, “Louis-Jacques Thenard,” *Rev. CENIC. Ciencias Químicas*, vol. 33, no. 3, pp. 141–149, 2002.
- [154] L. J. Thenard, “Considérations générales,” vol. 15.

- [155] J. Jennings, *The Family Cyclopaedia: a manual of useful and necessary knowledge in domestic economy, agriculture, and chemistry and art*. London: printed for Sherwood, Gilbert and Piper, 1822.

5. Conclusions & Future Perspectives

The archaeometric study carried out in this research work aimed to define a scientific methodology able to correlate the production techniques and the chemical-physical characteristics of traditional ceramic materials.

The study began with the innovative and systematic procedure by considering known samples, as the raw ceramics laboratory-made, allowing to evaluate the relationship between chemical and microstructural changes and the influences of the firing conditions on the final products. The contribution of the applied analytical techniques was tested and the capability of the innovative techniques proposed, as non-destructive and micro-destructive, was assessed.

This multi-analytical approach was assessed in order to apply it in studying the real case studies and evaluating the peculiarities in both archaeological and historical ceramics.

The archaeometric study on archaeological and historical ceramics was able to collect innovative results in order to estimate the firing temperature and investigate the chemical and mineralogical composition of the artefacts. In general, it allowed to provide insights on their technology and expand the knowledge upon archaeological pottery excavated in Torcello and pottery production in Central-Eastern Germany. Furthermore, the analysed case studies raised interesting issues regarding for instance post-burial alterations in archaeological potteries and glaze production techniques in the historical ones.

Finely, the diagnostic techniques, both traditional and in innovative, were evaluated emphasizing their advantages and disadvantages, providing useful information for future investigation in this topic.

Consideration made on the basis of the obtained results regarding the analytical techniques used are reported and summarised in the following table (**Tab.20**). However, it was proved that the complementary and combined use of chemical and physical methods are necessary to investigate the technological-productive aspects of the ceramic materials.

The promising results obtained by the use of non-destructive and micro-destructive techniques encourage their use in archaeometric studies on ceramics.

- LIF spectroscopy and UV-Vis spectrophotometry enable to investigate on the glaze composition and its colouring agents in a completely non-invasive way offering an overview of the composition prior to sampling or submitting the object to further chemical analysis. LIF technique is not widely used in glass/glaze and ceramic investigations and further applications in this field would be needed to enlarge the awareness of its capability. Thanks to its characteristics such as portability, the possibility

to work remotely and to collect hyperspectral fluorescence images by the scanning setup, LIF system could be capable to analyse artefacts of large dimension such as glass windows and mosaics which present glass tessera.

- LIBS spectroscopy was used in this research for elemental analyses and in particular exploiting its capability to carry out stratigraphy analysis in a micro-destructive way. The results showed that the information regarding the chemical distribution into the glaze may be complementary to morphological information and connected to the technological production. LIBS technique showed advantages as high sensitiveness in determining heavy and light elements, its ability to analyse samples remotely and to be portable, but on the other hand, quantitative analysis may be difficult and complex, and in studying ceramics with glaze coatings it may be affected by interferences among the layers.
- Very interesting are the results obtained by the X-ray μ -CT. It is a new tool in cultural heritage material investigation and in this research was showed its application in microstructural studies which allowed porosimetry analyses of both closed and open pores with the respect of the integrity of the art object due to its non-destructiveness. Although the porosimetry results cannot be compare with those obtained by MIP due to the different measured pore size and typology (only open and meso-macro pores by MIP), the obtained results may be considered complementary to those obtained my MIP techniques and they underlined the relevance in considering both open and closed pores and the pore radius between around 1 to 100 μm . Indeed, it was showed that the tomography results are in agreement with SEM observations in showing the densification stage of ceramics fired at high temperatures. Due to the lack of closed porosity data in literature, the elaboration of the results were quite difficult and its application in further studies is encouraged. μ -CT is at moment an expensive and time-consuming tool (for both acquisition and elaboration data) but it can open new research topics in considering and measuring the total porosity of ceramic materials, and connecting the results with morphological features and technological production.

Table.20. Synthetic summary on the advantages and disadvantages of the adopted analytical techniques in ceramic investigation.

Diagnostic Technique	Advantages	Disadvantages
<p style="text-align: center;">FT-IR Spectroscopy</p> <p style="text-align: center;">[1]–[4]</p>	<ul style="list-style-type: none"> - Low amount of sample is requested (if used in transmission way); - Allows identification of several mineralogical phases and their hydration stage; - Is able to discriminate primary and secondary calcite; - Is able to detect simultaneously and quickly all the compounds present in the sample; - Elaboration data is supported by widespread literature; - Widely present in research laboratories; - Middle cost. 	<ul style="list-style-type: none"> - Is a destructive technique if it is used in transmission mode (few mg); - Shows some limitation in detecting particular phases which overlap with other compounds in the spectrum; - Provides chemical information and the attribution of mineral phases could be difficult in complex matrixes; - Does not allow identification of colouring agents in glaze composition.
<p style="text-align: center;">μ-Raman Spectroscopy</p> <p style="text-align: center;">[1], [5]–[7]</p>	<ul style="list-style-type: none"> - Non-destructive techniques; - Allows punctual analysis; - Allows the discrimination of different metal oxides (as iron and titanium oxides); - Allows the identification of colouring agents and glaze composition; - Allows estimation of temperature in base on Raman glassy phase signals; - Is able to analyse simultaneously and quickly all the spectral components present in the sample; - Portable systems are available. - Elaboration data is supported by literature and online database; - Middle cost. 	<ul style="list-style-type: none"> - Is not able to provide quantitative analyses; - Limitation in identifying some mineral phases; - In many cases pastes from clay minerals exhibit weak or complex Raman signals. - Not often present in laboratory tools
<p style="text-align: center;">LIF Spectroscopy</p> <p style="text-align: center;">[8]–[11]</p>	<ul style="list-style-type: none"> - Non-destructive and non-invasive technique; - Allows punctual analysis and scanning system (with both punctual and line brush) are available; - Provides molecular information and elemental clues; - Allows identification of colourant agents and glaze composition; - Is fast, allows remote, is portable allowing in situ analyses without sampling. 	<ul style="list-style-type: none"> - Does not allow quantitative analyses; - Complicated elaboration data due to the lack of database and data in literature; - Broad and overlapping bands; - The analysis regards the surface of the object which has to be clean without crusts and dirt - Not common in research laboratories.

<p style="text-align: center;">UV-Vis Spectrophotometry</p> <p style="text-align: center;">[12]–[14]</p>	<ul style="list-style-type: none"> - Non-destructive and non-invasive technique; - Allows identification of colourant agents and glaze composition; - Allows fast and in situ application without the necessity to sample the artefact; - Allows insights on colour chemistry and redox properties; - Not expensive and quite common in analytical laboratories 	<ul style="list-style-type: none"> - The analysis regards the surface of the object which has to be clean without crusts and dirt; - Does not provide information regarding mineralogical composition of the ceramic paste.
<p style="text-align: center;">XRF Spectroscopy</p> <p style="text-align: center;">[15]–[17]</p>	<ul style="list-style-type: none"> - Non-destructive technique; - Little or no pre-treatment of the sample; - Allows qualitative and semi-quantitative analyses on elemental composition; - Easy and fast to use; - Common tool and often present in research laboratories; - Portable tools are available; - Not expensive. 	<ul style="list-style-type: none"> - Does not allow identification of light elements (generally covers all elements from sodium to uranium); - Limits of detection depend upon the specific element and the sample matrix (generally are only modest and heavier elements have better detection limits than higher elements); - X-ray penetration is limited to the top layer; - Spectral positions are independent of the chemical state of the element.
<p style="text-align: center;">LIBS Spectroscopy</p> <p style="text-align: center;">[16], [18]–[20]</p>	<ul style="list-style-type: none"> - Allows qualitative and quantitative elemental analyses; - Portable, fast and remote; - Allows analyses of solids, gases or liquids; - Little or no sample preparation is necessary; - Allows rapid analysis (ablation and excitation processes are carried out in a single step); - Allows stratigraphic analyses; - Sensitive to the chemical state of the elements; - More sensitive and can detect a wider range of elements (particularly the light elements) than competing techniques such as XRF. 	<ul style="list-style-type: none"> - Micro-destructive technique (~0.1µg to 1mg); - Matrix effect in quantitative analyses; - Quantitative analyses may be complicated and affected by interferences among layers; - Not common in research laboratories; - Expensive.
<p style="text-align: center;">XRD</p> <p style="text-align: center;">[21]–[23]</p>	<ul style="list-style-type: none"> - Allows a detailed identification of crystalline mineral phases; - Complementary to spectroscopic techniques; - Provides both qualitative and quantitative analyses; - The most widely used method to determine crystal structures. 	<ul style="list-style-type: none"> - Destructive technique; - Elaboration data complicated due to the complexity of the silicate structures; - May require long time in identifying mineral compositions; - Expensive.

<p>Petrographic analyses on ceramic thin sections</p> <p>[24]–[26]</p>	<ul style="list-style-type: none"> - Allows mineralogical identification of inclusions present in the clay matrix; - Allows to evaluate the shape and grain-size of inclusions; - Allows evaluation of the clay matrix texture. 	<ul style="list-style-type: none"> - Destructive; - Thin section preparation needs time, equipment and specialized operators and laboratories; - Thin section preparation not very common in research laboratories; - Expensive.
<p>SEM-EDX</p> <p>[27]–[29]</p>	<ul style="list-style-type: none"> - Allows to investigate the morphology and microstructure of the samples; - EDX measurements provide elemental analyses and their distribution; - High resolution of images (~3-4 nm) and high magnification (up to ~30000x). 	<ul style="list-style-type: none"> - Destructive technique; - Preparation samples is requested; - Expensive.
<p>MIP</p> <p>[30]–[32]</p>	<ul style="list-style-type: none"> - Allows to measure open porosity (pore volume and distribution of meso and macro pores); - Determination of the pore-size distribution curves of a wide variety of porous materials. 	<ul style="list-style-type: none"> - Destructive technique; - Partial information regarding porosity (it cannot measure closed pores); - Not very common in research laboratories; - Uses toxic compound, as mercury; - Expensive.
<p>X-ray μ-CT</p> <p>[33]–[37]</p>	<ul style="list-style-type: none"> - Non-destructive technique; - Covers a wide range of microstructural feature observation; - Allows investigation on total porosity (both closed and open pores), pore size distribution, shape and tortuosity; - Resolution can be up to nm; - May be used to investigate volume and distribution of inclusions in the clay matrix; - Portable systems are available for in situ analyses; - Systems have been developed able to analyse objects of different sizes (from micro to macro). 	<ul style="list-style-type: none"> - Not common; - Difficult data elaboration; - Imaging acquisition and elaboration data are time consuming; - Expensive.

Aiming at deeply investigating the microstructural features of ceramic materials, this year two proposals in two calls for proposals at different international research centres were submitted¹. The first one, “The effect of production techniques on historical ceramic morphology”, was submitted at ILL Institute (Grenoble, France); and the second one, “The effect of production techniques on historical ceramic morphology: a study by neutron grating interferometry”, was submitted at MLZ (Garching-Munich, Germany). Both of the proposals had the aim to compare and expand the morphological and microstructural results previously obtained on ceramic samples by MIP, SEM and X-ray μ -CT with those obtained by SANS (Small Angle Neutron Scattering) and neutron grating interferometry (nGI) measurements, at ILL and MLZ respectively. SANS measurements will be carried out by D11 instrument, at ILL Institute, which has a very large Q-range ranging from 5×10^{-4} up to $0,7 \text{ 1/\AA}$, giving the possibility to characterise the complex materials over many orders of magnitude, which is important as many length scales need to be probed [38]. nGI will be used at MLZ Institute, as it is a novel imaging technique which allows to obtain dark-field images (DFI) of an object [39]–[41].

The use of neutrons will be profitable due to their high penetration power in the matter and the opportunity to use contrast method applying heavy water to study the ratio of open/closed pores which will help to identify the role of closed porosity on the material microstructure, its behaviour/evolution during the firing processes and its effect on the mechanical properties of ceramic materials. With these experiments, it will be explored this non-destructive approach for the study of peculiar features of pottery matrix that could open a new investigation route to identify the pottery in terms of preparation parameters and production-site technology.

Both of the proposed proposals were judged as research with high level of interest, and the measurements will be placed in December 2016 and in March 2017.

Currently, this research work provided a publication in *Microchemical Journal* [42] and some results were presented in national and international conferences, as TechnArt2015, LIMS2015, ISA2016, etc. Part of the archaeometric research was also presented on the occasion of the European Researchers' Night (VenetoNight) in 2014 at Ca' Foscary University where it aroused interest and curiosity. The research activity supplied collaborations with national and international institutions as ENEA Research Centre in Frascati (Rome), University of Padova, St-Petersburg University, TU-Bergakademie Freiberg, Senckenberg Naturhistorische Sammlungen Dresden, etc., which are active and promising.

Furthermore, this research crosses the Stanford University's work and a paper in collaboration with the Anthropological and Archaeological Department is in work in progress.

¹ Thanks to the collaboration with Dr. Claudia Mondelli, Prof. Elti Cattaruzza, Prof. Elisabetta Zendri, Dr. Eleonora Balliana, Prof. Gonella Francesco and Dr. Ralfand Schweins.

5.1. Bibliography

- [1] L. F. Vieira Ferreira, D. P. Ferreira, D. S. Conceição, L. F. Santos, M. F. C. Pereira, T. M. Casimiro, and I. Ferreira Machado, “Portuguese tin-glazed earthenware from the 17th century. Part 2: A spectroscopic characterization of pigments, glazes and pastes of the three main production centers,” *Spectrochim. Acta - Part A Mol. Biomol. Spectrosc.*, vol. 149, pp. 285–294, 2015.
- [2] S. Shoal, “Using FT-IR spectroscopy for study of calcareous ancient ceramics,” *Opt. Mater. (Amst.)*, vol. 24, no. 1–2, pp. 117–122, Oct. 2003.
- [3] B. Fabbri, S. Gualtieri, and S. Shoal, “The presence of calcite in archeological ceramics,” *J. Eur. Ceram. Soc.*, vol. 34, no. 7, pp. 1899–1911, Jul. 2014.
- [4] G. Barone, V. Crupi, F. Longo, D. Majolino, P. Mazzoleni, D. Tanasi, and V. Venuti, “FT-IR spectroscopic analysis to study the firing processes of prehistoric ceramics,” *J. Mol. Struct.*, vol. 993, no. 1–3, pp. 147–150, May 2011.
- [5] C. Lofrumento, A. Zoppi, and E. M. Castellucci, “Micro-Raman spectroscopy of ancient ceramics: a study of Frenchsigillata wares,” *J. Raman Spectrosc.*, vol. 35, no. 89, pp. 650–655, Aug. 2004.
- [6] P. Holakooei, “A multi-spectroscopic approach to the characterization of early glaze opacifiers: Studies on an Achaemenid glazed brick found at Susa, south-western Iran (mid-first millennium BC),” *Spectrochim. Acta. A. Mol. Biomol. Spectrosc.*, vol. 116, pp. 49–56, Dec. 2013.
- [7] L. Damjanović, V. Bikić, K. Šarić, S. Erić, and I. Holclajtner-Antunović, “Characterization of the Early Byzantine Pottery from Caričin Grad (South Serbia) in Terms of Composition and Firing Temperature,” *J. Archaeol. Sci.*, vol. 46, pp. 156–172, Mar. 2014.
- [8] A. Nevin, G. Spoto, and D. Anglos, “Laser spectroscopies for elemental and molecular analysis in art and archaeology,” *Appl. Phys. A*, vol. 106, no. 2, pp. 339–361, Dec. 2011.
- [9] R. Fantoni, L. Caneve, F. Colao, L. Fiorani, A. Palucci, R. Dell’Erba, and V. Fassina, “Laser-induced fluorescence study of medieval frescoes by Giusto de’ Menabuoi,” *J. Cult. Herit.*, vol. 14, no. 3, pp. S59–S65, Jun. 2013.
- [10] V. Lazic, F. Colao, R. Fantoni, A. Palucci, V. Spizzichino, I. Borgia, B. G. Brunetti, and A. Sgamellotti, “Characterisation of lustre and pigment composition in ancient pottery by laser induced fluorescence and breakdown spectroscopy,” *J. Cult. Herit.*, vol. 4, pp. 303–308, Jan. 2003.
- [11] L. Caneve, F. Colao, R. Fantoni, and L. Fiorani, “Scanning lidar fluorosensor for remote diagnostic of surfaces,” *Nucl. Instruments Methods Phys. Res. Sect. A Accel. Spectrometers, Detect. Assoc. Equip.*, vol. 720, pp. 164–167, 2013.
- [12] A. Ceglia, W. Meulebroeck, P. Cosyns, K. Nys, H. Terry, and H. Thienpont, “Colour and Chemistry of the Glass Finds in the Roman Villa of Treignes, Belgium,” *Procedia Chem.*, vol. 8, pp. 55–64, 2013.
- [13] a. Ceglia, W. Meulebroeck, K. Baert, H. Wouters, K. Nys, H. Thienpont, and H. Terry, “Cobalt absorption bands for the differentiation of historical na and ca/k rich glass,” *Surf. Interface Anal.*, vol. 44, no. 2, pp. 219–226, 2012.
- [14] A. Ceglia, W. Meulebroeck, H. Wouters, K. Baert, K. Nys, H. Terry, and H. Thienpont, “Using optical spectroscopy to characterize the material of a 16th c. stained glass window,” in *Proc. SPIE 8422*, 2012, vol. 8422, p. 84220A.
- [15] M. S. Shackley, “Chapter 2. An Introduction to X-Ray Fluorescence (XRF) Analysis in Archaeology,” in *X-Ray Fluorescence Spectrometry (XRF) in Geoarchaeology*, 2011, pp. 7–44.
- [16] L. Pardini, a. El Hassan, M. Ferretti, a. Foresta, S. Legnaioli, G. Lorenzetti, E. Nebbia, F. Catalli, M. a. Harith, D. Diaz Pace, F. Anabitarte Garcia, M. Scuotto, and V. Palleschi, “X-Ray Fluorescence and Laser-Induced Breakdown Spectroscopy analysis of Roman silver denarii,” *Spectrochim. Acta Part B At. Spectrosc.*, vol. 74–75, pp. 156–161, Aug. 2012.
- [17] C. Papachristodoulou, A. Oikonomou, K. Ioannides, and K. Gravani, “A study of ancient pottery by means of X-ray fluorescence spectroscopy, multivariate statistics and mineralogical analysis,” *Anal. Chim. Acta*, vol. 573–574, pp. 347–53, Jul. 2006.
- [18] V. Spizzichino and R. Fantoni, “Laser Induced Breakdown Spectroscopy in archeometry: A review of its application and future perspectives,” *Spectrochim. Acta - Part B At. Spectrosc.*, vol. 99, pp. 201–209, 2014.
- [19] a. Erdem, a. Çilingiroğlu, a. Giakoumaki, M. Castanys, E. Kartsonaki, C. Fotakis, and D. Anglos, “Characterization of Iron age pottery from eastern Turkey by laser- induced breakdown spectroscopy

- (LIBS),” *J. Archaeol. Sci.*, vol. 35, no. 9, pp. 2486–2494, Sep. 2008.
- [20] K. Şerifaki, H. Böke, Y. Şerife, and B. İpekoğlu, “Characterization of materials used in the execution of historic oil paintings by XRD, SEM-EDS, TGA and LIBS analysis,” *Mater. Charact.*, vol. 60, no. 4, pp. 303–311, 2009.
- [21] G. Nirmala and G. Viruthagiri, “FT-IR characterization of articulated ceramic bricks with wastes from ceramic industries,” *Spectrochim. Acta - Part A Mol. Biomol. Spectrosc.*, vol. 126, pp. 129–134, 2014.
- [22] M. Bayazit, I. Isik, and A. Issi, “Investigating the firing technologies of Part-Roman potsherds excavated from Kuriki (Turkey) using thermal and vibrational spectroscopic techniques,” *Vib. Spectrosc.*, vol. 78, pp. 1–11, 2015.
- [23] G. Raja Annamalai, R. Ravisankar, a Rajalakshmi, a Chandrasekaran, and K. Rajan, “Spectroscopic characterization of recently excavated archaeological potsherds from Tamilnadu, India with multi-analytical approach,” *Spectrochim. Acta. A. Mol. Biomol. Spectrosc.*, vol. 133, pp. 112–8, Dec. 2014.
- [24] L. Maritan, C. Mazzoli, V. Michielin, D. M. Bonacossi, M. Luciani, and G. Molin, “The Provenance and Production Technology of Bronze Age and Iron Age Pottery from Tell Mishrifeh/Qatna (Syria),” *Archaeometry*, vol. 47, no. 4, pp. 723–744, 2005.
- [25] M. Á. Cau Ontiveros, G. Montana, E. Tsantini, and L. Randazzo, “Ceramic Ethnoarchaeometry in Western Sardinia: Production of Cooking Ware at Pabillonis*,” *Archaeometry*, no. February, p. n/a-n/a, May 2014.
- [26] G. Artioli, “Scientific methods and cultural heritage,” p. 520, 2010.
- [27] R. Palanivel and S. Meyvel, “Microstructural and microanalytical study - (SEM) of archaeological pottery artefacts,” *Rom. Reports Phys.*, vol. 55, no. 3–4, pp. 333–341, 2010.
- [28] A. Krapukaityt, I. Pakutinskien, S. Tautkus, and A. Kareiva, “SEM and EDX Characterization of Ancient Pottery,” *Lith. J. Phys.*, vol. 46, no. 3, pp. 383–388, 2006.
- [29] K. Domoney, a. J. Shortland, and S. Kuhn, “Characterization of 18Th-Century Meissen Porcelain Using Sem-Eds*,” *Archaeometry*, vol. 54, no. 3, pp. 454–474, Jun. 2012.
- [30] R. Kumar and B. Bhattacharjee, “Porosity, pore size distribution and in situ strength of concrete,” *Cem. Concr. Res.*, vol. 33, no. 1, pp. 155–164, 2003.
- [31] G. Cultrone, E. Sebastián, K. Elert, M. J. de la Torre, O. Cazalla, and C. Rodriguez-Navarro, “Influence of mineralogy and firing temperature on the porosity of bricks,” *J. Eur. Ceram. Soc.*, vol. 24, no. 3, pp. 547–564, Mar. 2004.
- [32] C. Volzone and N. Zagorodny, “Mercury intrusion porosimetry (MIP) study of archaeological pottery from Hualfin Valley, Catamarca, Argentina,” *Appl. Clay Sci.*, vol. 91–92, pp. 12–15, Apr. 2014.
- [33] L. Jacobson, F. C. de Beer, and R. Nshimirimana, “Tomography imaging of South African archaeological and heritage stone and pottery objects,” *Nucl. Instruments Methods Phys. Res. Sect. A Accel. Spectrometers, Detect. Assoc. Equip.*, vol. 651, no. 1, pp. 240–243, Sep. 2011.
- [34] F. Casali, “X-Ray digital radiography and computed tomography for cultural heritage,” *Archeometriai Műhely*, vol. 1, pp. 24–28, 2006.
- [35] L. Salvo, P. Cloetens, E. Maire, S. Zabler, J. . Blandin, J. . Buffière, W. Ludwig, E. Boller, D. Bellet, and C. Jossierond, “X-ray micro-tomography an attractive characterisation technique in materials science,” *Nucl. Instruments Methods Phys. Res. Sect. B Beam Interact. with Mater. Atoms*, vol. 200, pp. 273–286, Jan. 2003.
- [36] L. Salvo, M. Suéry, A. Marmottant, N. Limodin, and D. Bernard, “3D imaging in material science: Application of X-ray tomography,” *Comptes Rendus Phys.*, vol. 11, no. 9–10, pp. 641–649, Nov. 2010.
- [37] J.-Y. Buffière, H. Proudhon, E. Ferrie, W. Ludwig, E. Maire, and P. Cloetens, “Three dimensional imaging of damage in structural materials using high resolution micro-tomography,” *Nucl. Instruments Methods Phys. Res. Sect. B Beam Interact. with Mater. Atoms*, vol. 238, no. 1–4, pp. 75–82, Aug. 2005.
- [38] “ILL:Neutron for Science.” [Online]. Available: <https://www.ill.eu/instruments-support/instruments>.
- [39] T. Reimann, S. Mühlbauer, M. Horisberger, P. Böni, and M. Schulz, “The new neutron grating interferometer at the ANTARES beamline - Design, Principle, and Applications -,” *J. Appl. Crystallogr.*, no. accepted, pp. 1–34, 2016.
- [40] M. Strobl, “General solution for quantitative dark-field contrast imaging with grating interferometers,” *Sci. Rep.*, vol. 4, p. 7243, 2014.
- [41] “Heinz Maier-Leibnitz Zentrum (MLZ). Neutron for Research, Industry and Medicine.” [Online]. Available:

<http://www.mlz-garching.de/antares>.

- [42] G. Ricci, L. Caneve, D. Pedron, N. Holesch, and E. Zendri, “A multi-spectroscopic study for the characterization and definition of production techniques of German ceramic sherds ☆,” *Microchem. J.*, vol. 126, pp. 104–112, 2016.

GLOSSARY

Stoneware: dense and hard ceramic ware with low porosity and fired to high temperatures.

Near-stoneware: art historians and archaeologists define it as a typical ash-glazed light grey ware with visible artificial quartz tempering. invented.

Earthenware: ceramic ware made of slightly porous opaque clay fired at relatively low temperature. Faience, delft and majolica are examples of earthenware.

Glaze: is a glass that has been tuned to melt to the desired degree at the target temperature, have a thermal expansion compatible with the body to which it is attached. Glazes are made from finely ground mixtures of mineral and man-made powders. Glaze can contain other compounds which provide colour, opacity and character desired visually. Glazes are normally suspended in water and are applied to ware by painting, dipping, or spraying. The chemistry of glaze is an aspect most related to the way it is fired.

Engobe: white or coloured slip applied to clay as a coating. The term *slip* is often used interchangeably with this, although slip refers more as a decorative material/process. Engobe is usually applied at the leather hard stage, whereas in tile it is applied to dry pressed ware as a curtain over a continuously moving production line (or as a powder layer during pressing). The engobe must have enough flux to fire-bond and it also must match the firing shrinkage. When glaze is applied over an engobe, it is important that the thermal expansions complement each other. In tile, for example, the thermal expansion of the slip needs to match the body and the glaze expansion be a little lower.

Slip: in ceramics this term can refer to different things: i) a clay slurry poured into molds to be cast into shapes; ii) a mix of clay and other minerals and fluxes that is applied to dry or leather hard ware to produce an enhanced surface, either to increase quality, reduce permeability by water, improve glaze coverage, add a design motif or improve fired hardness; iii) a simple mix of water and clay that is used as a glue to attach leather hard or dry elements together.

Vitrification: is a process which regards the solidification of a melt into a glass rather than a crystalline structure. Glass, clay bodies and glazes vitrify, but in ceramics use of the term focuses most on clay bodies.

Opacifier: is a glaze additive that transforms an otherwise transparent glaze into an opaque one. Common opacifiers are tin oxide and zircon compounds. Opacifiers typically work by simply not

dissolving into the melt, the white suspended particles thus reflect and scatter the light. When opacifiers are added to coloured glazes, the depth of colour is lost.

Flux: is an oxide that lowers the melting or softening temperature of a mix of others. Fluxing oxides interact with other oxides, and normally, the more kinds of fluxes present in a mix the lower its melting temperature is. Examples of fluxing oxides for high temperature glazes are K_2O , Na_2O , CaO , SrO , Li_2O , MgO , ZnO (CaO and MgO are not active at lower temperatures). In glaze chemistry, each of these oxides is an individual with its own optimal percentage and interaction with silica and alumina. Colorants can also be powerful fluxes, as copper, cobalt and manganese all melt very actively in oxidation and reduction conditions. However iron is a strong flux in reduction. Feldspars are an example of a natural mix of refractory and fluxing oxides that, together, melt at a fairly low temperature.

DISSERTATION ABSTRACT

The aim of the PhD research was to define a scientific methodology able to correlate the production techniques and the chemical and physical characteristics of traditional ceramic materials. The methodological approach considered traditional techniques employed in archaeometric research, and the use of innovative methods only recently applied in cultural heritage material investigation, in order to develop an effective and innovative methodology for the study of this kind of materials.

The research was performed at first by studying the relationship between raw material composition, firing temperatures and the final chemical-physical features of raw ceramic samples ad hoc made in laboratory, following traditional methods and using different kinds of raw clay materials and firing temperatures. Subsequently, through the reverse process, potteries of different provenance and age were analysed in order to verify the correlation between the production techniques and the characteristics of the ceramic materials. Archaeological potteries from Torcello, one of the first settled islands on the northern Venetian lagoon, alongside historical ceramic sherds from Central and Eastern German sites, never investigated before, were selected as interesting case studies for the research project.

The ceramic samples were studied and characterized using chemical, physical and petrological techniques, with the joint use of traditional and non-traditional analytical methods. Chemical composition, mineral phases, microstructure, particle packing as well as morphology of pottery depend on the native material composition, technology and conservation state. Considering these distinctive chemical and physical properties, the samples were investigated through a multi-analytical approach by optical and morphological studies (Polarizing Microscopy (OM), Scanning Electron Microscopy (SEM)), chemical characterization (X-ray Diffraction (XRD), Fourier-Transform Infrared Spectroscopy (FT-IR), micro-Raman spectroscopy, X-ray Fluorescence (XRF)) and microstructural analysis by Mercury Intrusion Porosimetry (MIP).

The proposed innovative approach included chemical and morphological analysis, encouraging the use of non-destructive techniques. UV-Vis spectrophotometry, Laser Induced Fluorescence (LIF) and the micro-destructive Laser Induced Breakdown Spectroscopy (LIBS) were applied to deepen the chemical characterization and the production techniques of the ceramic glaze present in the historical potteries. LIF technique was applied to study both the ceramic glaze and matrix composition of the potteries exploiting the mineral luminescence. The results were integrated and combined with those obtained by UV-Vis spectrophotometry, XRF and LIBS, which was able to provide highly sensitive qualitative elemental data. Morphological

studies were carried out by X-ray micro-Computed Tomography (μ -CT), which provided a complementary microstructural investigation of the ceramic pastes respecting the integrity of the artefact. The results were compared with those obtained by MIP.

UV-Vis spectrophotometry, LIF and μ -CT, only recently applied within conservation science but not yet widely employed within archaeology, offer the advantage of being non-destructive with respect to the integrity of the art objects. Despite the fact that LIBS technique is micro-destructive (with a minimal loss of material and order of fractions of micrograms), it appears to be complementary to LIF and its ability to analyze materials in laboratory or in situ conditions is highly appreciated.

The results obtained encourage the application of the laser techniques in archaeological and historical ceramics. Furthermore, X-ray μ -CT permits the implementation of the data previously obtained by MIP and SEM in a non-destructive way, offering the possibility of obtaining imaging of the microstructure and pore distribution and more specifically to investigate the role of close porosity on the material microstructure and the porosity behaviour during the firing processes.

Furthermore, this research has been able to collect innovative results in order to estimate the firing temperature and technology of the ceramic sherds, thus expanding the knowledge upon pottery production in Torcello and in central-Eastern Germany.

ACKNOWLEDGEMENTS

Firstly, I would like to express my sincere gratitude to my advisor Prof. Elisabetta Zendri for her support throughout my Ph.D activity and research. She motivated and encouraged me to follow archaeometry research, which I found being a very interesting and exciting research topic. Furthermore, I thank her for her enthusiasm in research activities, always carried on with smile.

Besides my advisor, I would like to thank the rest of my research group and the guys of Via Torino for their insightful comments and encouragement, as well as, in particular, for their friendship.

My sincere thanks also goes to the precious support of Dr. Luisa Caneve of ENEA Research Centre in Frascati, who provided me the opportunity to join her team and who gave me access to the laboratory and research facilities.

I thank Prof. Danilo Pedron of University of Padova for his time, training and availability. Prof. Gerhard Heide of TU Bergakademie Freiberg, together with Prof. Jan-Michael Lange and Martin Kaden of Senkenberg Museum Dresden for their hospitality and competences during my PhD period in Germany, as well as for the access to the laboratories and facilities. I had really good time in their laboratories and it gave me a wonderful experience abroad. Dr. Stephan Krabath and Nadine Holesch, from Landesamt für Archäologie Sachsen (Archaeological Heritage Office in Saxony), are kindly acknowledged for all the collected German ceramic samples and their archaeological insights as well as Dr. Diego Calaon, from Stanford University, with whom I hope to cooperate in the future.

I would like to thank also Dr. Marianna Kulkova and Dr. Alexander Kulkov of Saint Petersburg University, which trusted this project and allowed me to carry on tomographic measurements with their skills and for inviting me at their beautiful city in which I had great experiences.

I also would like to thank Prof. Elti Cattaruzza, from Ca' Foscari University, for his precious help and comfort.

Arcadia Ricerche in Venice, as well as Prof. Pietro Riello and his team from Ca' Foscari University are acknowledged for their facilities availability.

A huge thanks is for my friends located almost everywhere, and at last but not the least, is mandatory mentioned my family. I would like to thank all of them, in particular my parents and my sister's family for supporting me spiritually throughout my academic career path and my life in general, although distant.